

Pharmacometric analysis of monoclonal antibodies to support clinical decision-making

Inaugural-Dissertation

to obtain the academic degree

Doctor rerum naturalium (Dr. rer. nat.)

submitted to the Department of Biology, Chemistry, Pharmacy
of Freie Universität Berlin

by

Ana-Marija Grišić

from Sremska Mitrovica, SFR Yugoslavia

Berlin 2020

Declaration of Authorship

Except where reference is made in the text, this thesis contains no material published elsewhere or extracted in whole or in part from a thesis presented by me for another degree or diploma. No other person's work has been used without due acknowledgment in the main text of the thesis. This thesis has not been submitted for the award of any other degree or diploma in any other tertiary institution.

Ana-Marija Grišić

The present thesis was conducted from 2016 to 2020 under the supervision of Prof. Dr. Charlotte Kloft at the Institute of Pharmacy, Freie Universität Berlin

1. Reviewer: Prof. Dr. Charlotte Kloft

2. Reviewer: Prof. Dr. Bernd Meibohm

Date of disputation: 23. April 2021

*“(...) a scientist must also be absolutely like a child.
If [s]he sees a thing, [s]he must say that [s]he sees it,
whether it was what [s]he thought [s]he was going to see or not.
See first, think later, then test. But always see first.
Otherwise you will only see what you were expecting.”*

(Douglas Adams, “The Ultimate Hitchhiker’s Guide to the Galaxy”)

Abstract

Monoclonal antibodies (mAbs) are successful treatment options in a variety of therapeutic areas, including cancer and inflammatory diseases. Even though introduction of infliximab (IFX) – the first mAb for inflammatory bowel diseases (IBD) – is considered a revolutionary step in IBD treatment, over the course of time challenges of IFX therapy arose. Given informative clinical data, quantitative approaches, such as pharmacometrics, are increasingly recognised for their potential to provide a deeper mechanistic understanding and contribute to overcoming clinical challenges, thus improving IBD therapy success.

This work aimed to contribute to improving success of IBD treatment and the rational use of IFX. Insights in (1) dynamic exposure-biomarker relationship, (2) clearance mechanisms of mAbs and relevance of study design, and (3) pharmacokinetic (PK) behaviour of IFX in pregnancy are reported.

Within this thesis the first population nonlinear mixed-effects (NLME) PK/PD model that quantitatively describes the IFX dose-exposure-CRP concentration relationship was developed. The model provides mechanistic insights, e.g. on significant factors influencing the IFX PK and the maximum inhibitory effect of IFX on CRP synthesis, and has been employed to assess the standard IFX dosing regimen, whereby potentially advantageous dosing regimens were identified. Moreover, the developed model can be further utilised to support Therapeutic Drug Monitoring and clinical decision-making.

While the quantitative approaches are powerful tools, the methodology alone cannot overcome the limitations of the clinical data used for the model development. Adequately informative data are a prerequisite for a quantitative analysis, highlighting the importance of the clinical study design. Within the herein reported work, this aspect was addressed using cetuximab – an anti-EGFR oncology mAb – as a case study, due to a highly informative dataset available for this drug. Firstly, the most comprehensive NLME PK model of cetuximab was developed, which revealed both an exposure- and a time-dependency of clearance. The model was subsequently utilised to identify clinical study design characteristics relevant for the identification of the mechanistic clearance model. The provided guidelines can be extrapolated for analyses of other mAbs as well. The importance of rich sampling for a detailed PK characterisation is emphasised, and guidance on the methodological aspects of such an analysis (e.g. model selection relative to study design) and choice of exposure metrics used for exposure-response analyses given.

Recognising the need for a more elaborate comprehension of IBD therapy in special populations, a part of the herein disclosed work focused on pregnant IBD patients receiving IFX. In addition to general therapy challenges, pregnancy opens additional clinical questions with respect to both safety and

efficacy of IBD treatment, in pregnant patient and foetus alike. The herein developed population NLME PK model of IFX in pregnancy is the first such model reported. The model provided insights in the impact of pregnancy on IFX PK, revealing a decreased IFX clearance in the second and third trimesters. The need for a consensus on IFX PK target in IBD management is emphasised, as well as the importance of monitoring of anti-drug antibodies regardless of the pregnancy status.

Altogether, these findings provide a better understanding of the pharmacokinetics and pharmacodynamics of IFX in IBD patients and the developed models offer a basis for model-informed precision dosing.

Zusammenfassung

Monoklonale Antikörper (mAb) gehören zu den etablierten Arzneimitteltherapien für Indikationen wie Onkologie und Entzündungserkrankungen. Die Einführung von Infliximab (IFX) – dem ersten mAb zur Behandlung chronisch-entzündlicher Darmerkrankungen (IBD) – stellte eine Revolution in der Behandlung von IBD dar, die allerdings von einigen Komplikationen begleitet wird. Quantitative Ansätze wie die Pharmakometrie können ein tieferes mechanistisches Verständnis ermöglichen, um die Therapieherausforderungen zu bewältigen und die IBD-Therapie zu optimieren.

Ziel dieser Arbeit war dazu beizutragen, den Therapieerfolg in der IBD-Behandlung und den rationalen Einsatz von IFX zu verbessern. Dazu sollen Erkenntnisse in (1) den dynamische Expositions-Biomarker-Zusammenhang, (2) die Eliminationsmechanismen von mAbs sowie die Relevanz des Studiendesigns hierfür und (3) die Pharmakokinetik (PK) von IFX während der Schwangerschaft erarbeitet werden.

Das entwickelte PK/pharmakodynamische (PD) Populationsmodell ist das erste Modell, das die Zusammenhänge zwischen der IFX-Dosis, der Exposition und der Konzentration des C-reaktive Proteins (CRP) quantitativ charakterisiert. Das Modell bietet mechanistische Einblicke, wie z.B. wesentliche Faktoren, die die IFX-PK beeinflussen und den maximalen inhibitorischen Effekt von IFX auf die CRP Synthese, und wurde genutzt, um das standardmäßige IFX-Dosierungsschema neu zu bewerten. Dabei wurden potenziell verbesserte Dosierungsschemata identifiziert. Das entwickelte Modell kann für das Therapeutische Drug Monitoring sowie als Basis für klinische Entscheidungen genutzt werden.

Die erarbeiteten quantitativen Ansätze sind auf aussagekräftige und informative klinische Daten angewiesen. Daher wurde in dieser Arbeit auch die Relevanz des klinischen Studiendesigns für die pharmakometrische Analyse erforscht. Dafür wurde Cetuximab – ein anti-EGFR mAb gegen Tumorerkrankungen – aufgrund der umfangreicheren Datenverfügbarkeit als Modellarzneistoff gewählt. Das entwickelte Modell ist das erste PK-Populationsmodell für Cetuximab, das sowohl die Expositions- als auch die Zeitabhängigkeit der Cetuximab-Elimination systematisch untersucht. Das Modell wurde danach angewandt, um die entscheidenden Merkmale eines klinischen Studiendesigns, die für die Bestimmung des mechanistischen Eliminationsmodells relevant sind, zu identifizieren. Die Empfehlungen können ebenso auf Populationsanalysen von anderen mAbs extrapoliert werden. Die Wichtigkeit eines umfangreichen Samplings für eine detaillierte PK-Charakterisierung wurde besonders hervorgehoben, und es wurden Hinweise zu methodischen Aspekten einer solchen Analyse und zur Auswahl von Expositionsmetriken gegeben, die für Expositions-Wirkungs-Analysen verwendet werden.

In Speziellen Patientengruppen ist es erforderlich, ein besseres Verständnis für die IBD-Therapie zu gewinnen. Daher lag der Fokus in einem weiteren Teil dieser Arbeit auf schwangeren IBD-Patientinnen, die IFX erhalten. Neben den allgemeinen therapeutischen Herausforderungen führt eine Schwangerschaft zu zusätzlichen klinischen Fragen hinsichtlich der Sicherheit und Wirksamkeit der IBD-Behandlung, sowohl bei der schwangeren Patientin als auch beim Fötus. Das hier entwickelte Populationsmodell, das die IFX PK in der Schwangerschaft charakterisiert, ist das erste derartige Modell. Das Modell ergab neue Einblicke in die Auswirkungen der Schwangerschaft auf die IFX PK und zeigte, dass die Elimination von IFX im zweiten und dritten Trimenon vermindert war. Darüber hinaus zeigte diese Arbeit den Bedarf eines Konsensus über die IFX PK-Zielkonzentration sowie die Bedeutung des Monitorings von Anti-IFX-Antikörpern, unabhängig vom Schwangerschaftsstatus.

Insgesamt wurde im Rahmen dieser Arbeit ein verbessertes Verständnis über die PK und PD von IFX in IBD-Patienten geschaffen. Die entwickelten Modelle bieten die Grundlage für ein sogenanntes „Model-informed precision dosing“, ein modellbasiertes Therapeutisches Drug Monitoring.

Table of contents

Abstract.....	i
Zusammenfassung.....	iii
Table of contents.....	v
Abbreviations.....	vii
List of publications	ix
1 Introduction and fundamentals.....	1
1.1 Inflammatory bowel diseases: The epidemic on the rise	1
1.1.1 Definition and epidemiology	1
1.1.2 Disease aetiopathogenesis.....	2
1.1.3 Mechanisms of inflammation and biomarkers in IBD.....	3
1.1.4 Signs and symptoms	6
1.2 Biologic therapies in IBD	7
1.2.1 Anti-TNF α mAbs.....	7
1.2.2 Infliximab.....	7
1.3 <i>In silico</i> approach to leverage <i>in vivo</i> data.....	10
1.3.1 Pharmacometric modelling and simulation.....	10
1.3.2 Current modelling knowledge and contributions in IBD.....	12
1.4 Aims and research questions	13
2 Data and methodological approaches	15
2.1 Data.....	15
2.1.1 Clinical study I design (<i>Paper I</i>).....	15
2.1.2 Clinical study II design (<i>Paper II</i>)	16
2.1.3 Clinical study III design (<i>Paper III</i>).....	17
2.1.4 Clinical study IV design (<i>Paper IV</i>).....	18
2.2 Pharmacometric data analyses	19
2.2.1 Fundamentals of pharmacometric modelling.....	19
2.2.2 Characterisation of infliximab pharmacokinetic behaviour and exposure-response relationship and dosing regimen assessment	24
2.2.3 Clearance of monoclonal antibodies: Cetuximab case study	26
2.2.4 Infliximab pharmacokinetics in pregnancy	28
2.3 Software	29
3 Results and Discussion	31
3.1 Pharmacokinetic behaviour of infliximab.....	31
3.2 Disease activity (bio)markers.....	37
3.3 Infliximab exposure-disease activity response relationship.....	39

3.4	Assessment of dosing regimens with respect to CRP remission.....	42
3.5	Clearance of monoclonal antibodies: Cetuximab case study	44
3.6	Effect of pregnancy on infliximab pharmacokinetics	51
4	Conclusions and future perspectives.....	59
5	Literature.....	61
	Appendix.....	81
	Acknowledgements.....	163
	Curriculum Vitae	165

Abbreviations

0.EL	Zero-order elimination
ADA(+/-)	Anti-drug antibody/-ies (positive/negative)
ADR	Approved dosing regimen
AS	Ankylosing spondylitis
AUC	Area under the concentration-time curve
BW	Body weight
CD	Crohn's disease
CDAI	Crohn's disease activity index
C _{IFX}	Infliximab concentration
C _{max}	Maximum concentration
C _{min}	Minimum concentration
CL	Clearance
CMT	Compartment
CRP	C-reactive protein
CWRES	Conditional weighted residuals
EBE(s)	Empirical Bayes Estimate(s)
EGFR	Epidermal growth factor receptor
ELISA	Enzyme-linked immunosorbent assay
EMA	European Medicines Agency
FcRn	Neonatal Fc-receptor
FDA	U.S. Food and Drug Administration
FOCEI	First-order conditional estimation with interaction
GIT	Gastro-intestinal tract
HBI	Harvey-Bradshaw index
IBD	Inflammatory bowel diseases
IFX	Infliximab
Ig	Immunoglobulin
IFN γ	Interferon- γ
IL	Interleukin

IMM	Immunomodulators
i.v.	Intravenous
LCL	Linear clearance
LLOQ	Lower limit of quantification
mAb(s)	Monoclonal antibody/-ies
MMCL	Michaelis-Menten clearance
NLME	Nonlinear mixed-effects
OFV	Objective function value
PA	Psoriatic arthritis
PBPK	Physiologically-based pharmacokinetic
PD	Pharmacodynamic(s)
PK	Pharmacokinetic(s)
Q	Intercompartmental flow
qXw	Every X weeks
QSP	Quantitative systems pharmacology
RA	Rheumatoid arthritis
RAS	Rat sarcoma proto-oncogene
RMSE	Root mean squared error
ROS/RNS	Reactive oxygen/nitrogen species
RSE	Relative standard error
RUV	Residual unexplained variability
SSE	Stochastic simulation and estimation
TMDD	Target mediated drug disposition
(tm/s)TNF α	(Transmembrane/soluble) tumour necrosis factor- α
TVARCL	Time-varying linear clearance
UC	Ulcerative colitis
V1	Central volume of distribution
V2	Peripheral volume of distribution
VPC	Visual predictive check

List of publications

This thesis is based on the following papers, which are referred to in the text by their Roman numerals:

I **A.M. Griscic**, A. Eser, W. Huisinga, W. Reinisch, C. Kloft. Quantitative relationship between infliximab exposure and inhibition of C-reactive protein synthesis to support inflammatory bowel disease management. *British Journal of Clinical Pharmacology*. DOI: 10.1111/bcp.14648 (2020).

II H. Edlund*, **AM. Griscic***, C. Steenholdt, M.A. Ainsworth, J. Brynskov, W. Huisinga, C. Kloft. Absence of relationship between Crohn's disease activity index or C-reactive protein and infliximab exposure calls for objective Crohn's disease activity measures for the evaluation of treatment effects at treatment failure. *Therapeutic Drug Monitoring*. 41(2):235-242 (2019).

III **A.M. Griscic**, A. Khandelwal, M. Bertolino, W. Huisinga, P. Girard, C. Kloft. Semimechanistic clearance models of oncology biotherapeutics and impact of study design: Cetuximab as a case study. *CPT: Pharmacometrics & Systems Pharmacology*. 9(11):628-638 (2020).

IV **A.M. Grišić***, M. Dorn-Rasmussen*, B. Ungar, J. Brynskov, J.F.K.F Ilvemark, N. Bolstad, D.J. Warren, M.A. Ainsworth, W. Huisinga, S. Ben-Horin, C. Kloft[#], C. Steenholdt[#]. Infliximab clearance decreases in second and third trimesters of pregnancy in inflammatory bowel disease. *United European Gastroenterology Journal*. DOI: 10.1177/2050640620964619 (2020).

Reprints were made with permission from the respective publishers.

1 Introduction and fundamentals

1.1 Inflammatory bowel diseases: The epidemic on the rise

1.1.1 Definition and epidemiology

Inflammatory bowel diseases (IBD) are a group of inflammatory diseases of the gastro-intestinal tract (GIT), including Crohn's disease (CD) and ulcerative colitis (UC), affecting approximately 4 million people around the world [1]. The most significant differences between CD and UC (Figure 1.) are location and extent of the inflammation, as well as genetic predisposition and risk factors. In UC, the inflammation begins in the rectum and continuously spreads upwards, in the most severe case (pancolitis) affecting the whole colon. In contrast to UC, the inflammation in CD is discontinuous and can affect any part of the GIT, from mouth to anus. Furthermore, the inflammation in UC is restricted to the mucosa (the epithelial lining of the gut), while in CD it is transmural, affecting deeper layers of the bowel wall as well, and can be present throughout the full thickness of the wall [2-7].

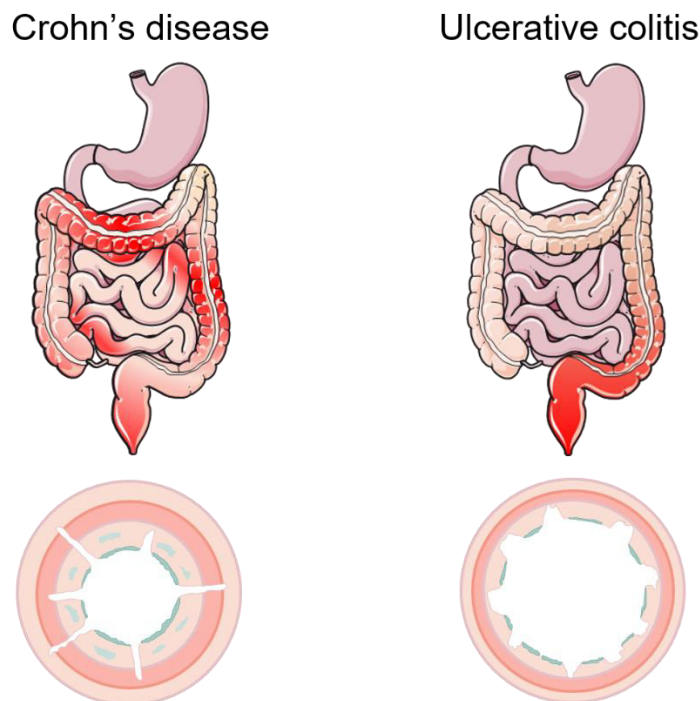


Figure 1. Two main types of IBD: Crohn's disease and ulcerative colitis. Upper part: illustration of location and (dis)continuity of inflammation (red); Lower part: depiction of bowel cross-sections illustrating the extent of inflammation - transmural in Crohn's disease and limited to the mucosa in ulcerative colitis. Parts of the figure were taken and adjusted from Servier Medical Art (<https://smart.servier.com>, Creative Commons Attribution 3.0 Unported License; last access on: 26 Jun 2019).

The IBD area is an epitome of the great imprint that the rapid development of modern society and science are leaving on the fields of medicine and pharmacy. With the development of novel diagnostic techniques, the diagnosis and assessment of the severity of IBD saw a notable improvement in the past decades [8,9]; and understanding of the mechanisms underlying IBD is constantly deepening [10]. The recent advances that have brought about a revolution in IBD treatment through the discovery of novel therapeutic concepts and drugs, are discussed below [11]. Moreover, Therapeutic Drug Monitoring – regular measuring of blood concentration of a drug in order to maintain the drug concentration within a target range and when indicated inform dosing individualisation - in IBD has improved (e.g. through development of treatment algorithms), contributing to an improved overall disease management [12]. However, not all trends related to IBD have been positive. The past decades also recorded a constant rise in IBD incidence and prevalence in the world, especially in North America and Europe [1]. This trend might in part root from the modern lifestyle, as suggested by the hypotheses that environmental factors and lifestyle (e.g. diet) contribute to the increasing number of IBD patients [1], exemplified by a higher incidence in urban populations. Interestingly, moving from the country of origin to another country has been found to be accompanied by a change in the IBD incidence in the following generations - pointing to the role of environmental factors. Finally, stress has been directly related to IBD risk as well [1].

1.1.2 Disease aetiopathogenesis

Even though many aetiological factors have been identified, up to now the cause and the cascade of immunological events in IBD remain unexplained. The root of the disease seems to be genetically predefined dysregulated intestinal mucosal immune response against commensal gut flora that causes the inflammation. This inflammation is characterised by the granulocyte and macrophage infiltration of the gut and an increased release of pro-inflammatory cytokines, chemokines and reactive oxygen and nitrogen species (ROS/RNS) intermediated by monocytes, macrophages and T cells [2, 3,13].

The disruption in the intestinal permeability has been described as one of the crucial events in the IBD development [14]. Thereby, a contact between the enteric flora and the immune system is enabled, as well as loss of electrolytes and water into the gut, leading to leak flux diarrhoea [15]. The structural and functional changes of the barrier comprise tight junction changes, apoptosis of epithelial cells, lesions (erosions and ulcers), and transcytosis [2,15]. However, the question whether the barrier disruptions are a cause or a consequence of IBD has not been fully elucidated. Earlier research suggested that oxidative stress leads to the barrier disruptions, by maintaining the active inflammation and further ROS generation [2]. Contrarily, recent research speaks in favour of the barrier disruption as a prerequisite for the IBD development. A study that used the “gut inflammation-on-a-chip” approach to mimic mouse colitis model showed that one of the early events in IBD, i.e. oxidative stress generation by mononuclear cells (mainly monocytes), requires the barrier disruption [16]. Hypothetically, it is possible that the

disrupted barrier initiates the oxidative stress, which in turn leads to maintenance and further disruption of the barrier. Further research is needed to address these questions and unify the contradictory findings. Mechanistically, the barrier disruptions are thought to originate from an elevated presence of cytokines, especially tumour necrosis factor- α (TNF α) and interferon γ (IFN γ), but certain environmental factors are anticipated to contribute as well. For instance, some dietary factors, such as a high intake of fat and refined sugars, induce low grade inflammation in the gut and can thereby increase the intestinal permeability [14,15].

Once the gut inflammation has developed, it is sustained by infiltration of leukocytes (in particular monocytes) and their differentiation (to macrophages), resulting in cytokine release. The cytokine profile in IBD is pro-inflammatory (as opposed to anti-inflammatory in the healthy gut) that leads to tissue injury and includes TNF α , interleukin (IL)-1 β , IL-12, IL-6 [2,17]. The quantitative analyses have further confirmed the importance of the pro-inflammatory macrophages for the IBD development: Using an *in silico* model that described inflammation in IBD (incl. behaviour of T-cells, macrophages, dendritic, and epithelial cells), it has been demonstrated that even in the presence of an ongoing inflammatory response to the enteric bacteria, epithelial recovery will take place if pro-inflammatory macrophages are absent [18]. Finally, the spectrum of the gut bacteria in IBD is different than that found in the healthy gut, with narrower heterogeneity and additional presence of specific, invasive strains (e.g. special adhesive and invasive *E. coli* in CD) [1,17].

1.1.3 Mechanisms of inflammation and biomarkers in IBD

Critical aspects for a successful treatment of any disease are understanding of the underlying mechanisms and identification of the disease markers that can be used to quantitatively track the disease activity. Due to the complex mechanisms of IBD, the choice of an appropriate disease biomarker has posed itself a challenging task [19-21]. The advantages and disadvantages of the currently used biomarkers relevant for the herein reported work are discussed below.

Tumour necrosis factor-alpha

In healthy individuals, TNF α has regulatory and protective roles. When overexpressed, however, it leads to an inflammatory cascade and is considered the main inflammatory agent in IBD. Its crucial role in IBD has been demonstrated by detection of increased concentrations, both in serum and tissue, in IBD patients, and successful control of the disease with anti-TNF α drugs. Furthermore, serum concentration of TNF α was shown to be predictive of the disease severity [2,14,22-26]. There are two forms of this cytokine: precursor membrane-bound (mainly on cell surface of activated macrophages and lymphocytes) ‘transmembrane’ (tmTNF α) and soluble form (in blood; sTNF α). Both are believed to play a role in IBD, acting via binding to the TNF α -receptors (type 1 and 2), expressed on most of the nucleated cells. Thereby initiated cascade of events results in an apoptotic or inflammatory outcome [2,13,23,26,27]. In addition, through its effects on tight junctions and transcellular passage of luminal

antigens, TNF α directly contributes to the epithelial disruption [15]. Apart from TNF α , TNF α -receptors, which stimulate T-cells and the inflammatory response, are overexpressed in IBD as well [2]. Due to the practicability of its measurement, sTNF α has been in focus, although the past years have revealed the importance of tmTNF α for IBD, when it was found that anti-TNF α drugs that do not bind to tmTNF α (e.g. etanercept) are not effective in IBD [23,28].

C-reactive protein

C-reactive protein (CRP) is a nonspecific inflammatory marker released predominantly upon signals from IL-6, TNF α and IL-1 as part of the acute phase immune response, caused by e.g. trauma, tissue necrosis and inflammation [29-32]. CRP is a sensitive marker: its concentrations rise rapidly, reaching the values as much as 1000-fold above the baseline, and decline fast, with a short life of ca. 19 h. Importantly, the half-life of CRP is constant, not impacted by the underlying disease or CRP concentration itself, making it a robust biomarker for tracking of immune response [31]. Its potential as a biomarker is further reinforced by the fact that none of the currently used therapeutics directly impacts its synthesis [31,32]. Correlation of CRP concentration and IBD severity has been established, though it seems less pronounced in UC than in CD [29,31,32]. This dependence of CRP-disease activity relationship on IBD type is not fully understood and could be due to different disease mechanisms or be a consequence of the disease signs.

Faecal loss of proteins – a common finding in IBD – is a potentially important aspect to be considered with respect to the IBD biomarkers, including CRP. Although present in both disease types, faecal loss of proteins is more common in UC, and bloody diarrhoea [37] is one of the main signs of UC. Based on the reports of faecal loss of monoclonal antibodies (mAbs) through the inflamed IBD gut [3] and the similarity of the size, CRP molecules are expected to be lost faecally as well (Figure 2). In case of a higher incidence and extent of faecal protein loss (including bloody diarrhoea), a higher loss of CRP via faeces is anticipated, resulting in a buffered increase of CRP plasma concentration with increasing disease activity, and thus hindering the disease activity-CRP concentration relationship. It could therefore be postulated that the more common faecal protein loss in UC might in part explain the observed less pronounced relationship between CRP concentration and disease activity compared to CD. This hypothesis has not been addressed thus far, even though clarifying the reasons for the different findings in UC and CD would be beneficial, especially in terms of establishing the relationship between IBD drug exposure and CRP response.

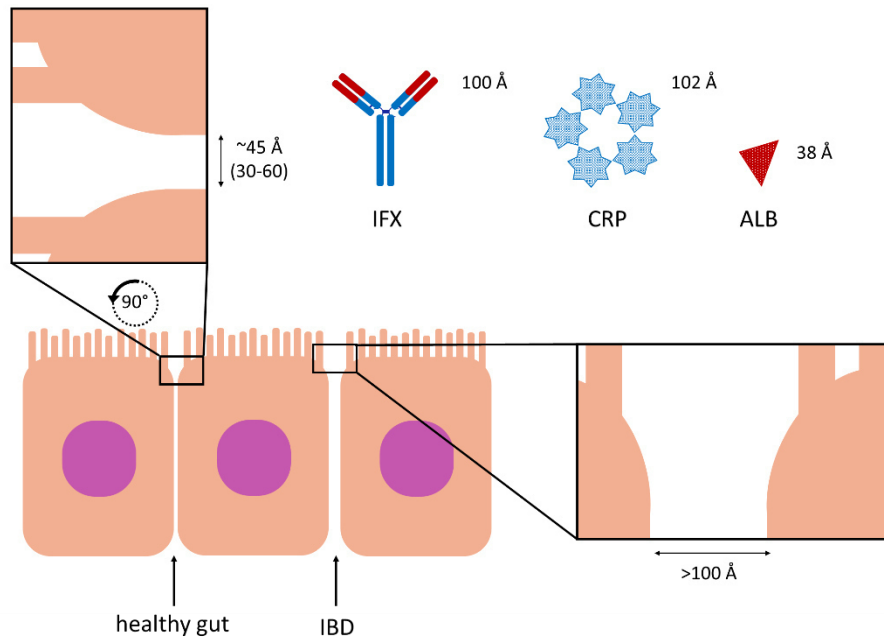


Figure 2. Illustration of faecal loss of macromolecules in healthy gut versus inflammatory bowel diseases [33-36]. ALB: Albumin; CRP: C-reactive protein; IBD: Inflammatory bowel diseases; IFX: Infliximab.

Serum albumin

Albumin is another acute phase protein, whose serum concentration decreases in the acute phase response [38]. Even though its long half-life of ca. 19 days makes it a much less sensitive inflammation marker than CRP, an inverse proportionality has been found between the two [39,40]. It is important to note that the kinetic behaviour of albumin is of much higher complexity than in the case of CRP. Albumin serum concentration is a result of the rate of its synthesis in the liver, its distribution, (fractional) catabolism (in multiple organs, including lower intestine), and exogenous loss, all of which are influenced by multiple factors (e.g. synthesis rate by inflammation, catabolic rate by albumin concentration, exogenous loss by faecal loss) [38,39]. In IBD, albumin concentration is decreased as a result of decreased synthesis, increased catabolism, potentially increased extravasation [38,39], and increased loss via faeces (up to 36 g/day vs. ~1 g/day in healthy individuals) [41,42]. In contrast to CRP, the already lowered serum albumin concentration due to the present inflammation in IBD is theoretically further decreased by the increased faecal loss, thus potentially enhancing the relationship between IBD activity and serum albumin concentration as a biomarker. However, due to the compensatory increase of albumin synthesis [42], this effect might not be significantly pronounced. Whether and to what extent the faecal loss of serum albumin might be relevant in this context has not yet been elucidated. As the fractional catabolic rate of albumin is in a direct relationship with serum albumin concentration (i.e. decreased synthesis leads to decreased catabolism, and *vice versa*), it is improbable that the hypoalbuminemia in IBD be only caused by decreased protein absorption [38,43]. Mechanism of hypoalbuminemia in the inflammation stays controversial, as some studies report

decreased synthesis [44,45] and increased degradation [44], and others even increased synthesis in certain inflammatory conditions [46].

In addition, further confounding factors may be present as well. Since up to 30%-50% of the albumin degradation takes place in different parts of the small intestine (duodenum > jejunum > ileum), massive resections of the small bowel – one of the therapeutic procedures in the IBD treatment – could result in a prolonged albumin survival [47]. Contrarily, gastrointestinal leakage (e.g. bleeding, ulcers) would have an opposite effect on albumin concentrations [47]. Accurate estimation of the albumin loss via faeces (i.e. quantification of faecal albumin) is an additional challenge, due to the proteolytic degradation [42].

Finally, the low serum albumin concentration is not necessarily only a consequence of IBD (and other gastrointestinal diseases), but might also contribute to the disease symptoms. Low albumin concentrations (~20 g/L – 26 g/L [42]) have been associated with diarrhoea, which would on the one hand further aggravate hypoalbuminemia, and on the other contribute to the IBD symptoms and would thereby be measured as IBD activity. A study in critically ill patients found that a cut-off of 26 g/L was predictive of diarrhoea with 100% sensitivity [42].

1.1.4 Signs and symptoms

Regardless of the described differences, CD and UC manifest in very similar symptoms. Patients typically experience diarrhoea, passage of blood, mucus and pus, as well as abdominal pain. An important characteristic of CD is its dynamical nature and specific complications. Namely, one of the properties of CD is its “behaviour”, which may comprise the presence of strictures (narrowing of the intestine) and fistulas (abnormal connection between two organs). The inflammation in CD can change both location and behaviour over time, accompanied by changes in clinical manifestations [2-7]. As a consequence of the disease characteristics and therapy, other symptoms such as anaemia, osteoporosis, pyoderma gangrenosum and erythema nodosum can also develop [5]. In up to a quarter of IBD patients extraintestinal symptoms and complications (uveitis, ankylosing spondylitis, arthritis, myocarditis, iritis, etc.) are present [4].

Clinical activity

The ultimate goal of IBD management is reduction of clinical activity, measured via clinical activity indices (e.g. Harvey-Bradshaw index [HBI] and Crohn’s disease activity index [CDAI] for CD). However, the agreement between clinical activity indices and mucosal inflammation – evaluated using endoscopy – has been found to be unreliable [48,49]. This is not surprising, considering that the clinical activity indices are hugely based on subjective measures and reports of IBD signs and symptoms, such as pain and general well-being. Over time, new indices (e.g. van Hees index) that take into account laboratory data as well have been developed, although their use remains very limited [49,50].

It is important to note that co-existing states might alter activity of IBD, with one particular example being pregnancy. Empirical findings suggest that the net effect of pregnancy on IBD activity is insignificant [51]. From mechanistic perspective, this net effect is the sum of a number of pregnancy-induced changes, some of which could be directly linked to the IBD status. Due to its natural course, pregnancy is accompanied by immunity-related changes, i.e. modifications in the maternal immune system. As a dysregulated immune response is one of the aetiological factors of IBD, this could also influence the disease status. In the first trimester, a strong inflammatory response, needed for the implantation and the formation of the decidua and the placenta, develops. It is characterised by infiltration and accumulation of NK ('natural killer') cells, dendritic cells and macrophages in the decidua. As the foetus enters the phase of rapid growth and development, the anti-inflammatory state is promoted. When the foetal development is completed, a proinflammatory state, crucial for delivery, is induced once again [52,53]. Furthermore, hormone (oestrogen and progesterone)-induced GIT changes, such as smooth muscle dysfunction, are more frequent in women with pre-existing GIT diseases, such as IBD [54]. Finally, the known effects of sex hormones (e.g. decrease in the endoplasmic reticulum stress, increased epithelial cell barrier and wound healing, induction of IL-8 production *in vitro* [55]) might also come into play as the pregnancy-related hormonal changes take place.

1.2 Biologic therapies in IBD

Introduction of biologic therapies in the IBD management has been referred to as “the greatest therapeutic advance in the care of inflammatory bowel disease” [56]. Anti-TNF α mAbs, pioneered by infliximab (IFX), were the first class of biologics to be approved for the IBD treatment. Although other (e.g. anti-integrin and anti-IL-12/23) mAbs followed and many are currently being evaluated, the anti-TNF α drugs are still the most widely used biologics in IBD, with IFX often found preferred [56].

1.2.1 Anti-TNF α mAbs

The anti-TNF α mAbs act mainly by binding TNF α , thus cancelling out its endogenous effects (see 1.1.3). In addition, they express other favourable effects for IBD treatment as well: they promote immunosuppressive regulatory macrophages, thereby inhibiting T-cells and stimulating synthesis of anti-inflammatory cytokines [13]. The full anti-TNF α mAbs, such as IFX, also invoke complement-dependent and antibody-dependent cell-mediated cytotoxicity and lead to apoptosis of activated immune cells; this is not the case with the mAbs lacking Fc-fragments, such as certolizumab pegol [13].

1.2.2 Infliximab

Introduction of IFX – a chimeric IgG1 anti-TNF α mAb – is considered a revolutionising moment in the IBD management. The IFX therapy has been consistently and repeatedly related to clinical remission (assessed by the clinical activity indices) [57-62], biomarker remission (especially CRP and faecal calprotectin) [58,59,63], and endoscopic remission [57,58,64,65]. This led to IFX keeping the status of one of the most widely used anti-TNF α drugs in the IBD management, despite constant inflow of new

therapeutics for this indication and the high incidence of immunogenicity [66]. In addition, IFX has been found to be effective in paediatric IBD patients as well [67-69].

Pharmacokinetics of infliximab

A characteristic that is shared by all mAbs alike is the complex pharmacokinetics (PK) resulting from many pathways a mAb molecule can follow in the organism, which can be disease specific. Relevant PK pathways of IFX are schematically summarised in Figure 3.

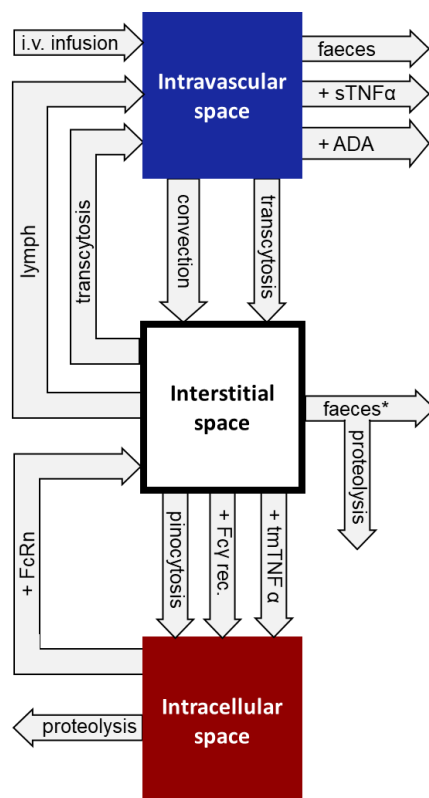


Figure 3. Schematic overview of relevant pharmacokinetic processes of infliximab to and from three relevant spaces: intravascular, interstitial, intracellular. ADA: anti-drug antibodies; Fc γ rec.: Fc γ receptor; FcRn: neonatal Fc receptor; sTNF α : soluble tumour necrosis factor- α ; tmTNF α : transmembrane tumour necrosis factor- α ; *faecal loss in case of increased gut permeability.

As IFX is administered via intravenous (i.v.) infusion, it does not undergo absorption processes. With this route of administration, maximum concentration (C_{max}) is achieved earlier and is higher than in the case of other routes, e.g. subcutaneous administration. An IFX molecule leaves the intravascular space (i.e. blood) by either (1) binding to sTNF α and degradation of the complex [70], (2) forming immune complexes with anti-drug antibodies (ADA) [70,107], (3) faecal loss due to gastrointestinal bleeding, or (4) distribution to the interstitium via convection or transcytosis [70]. These processes occur simultaneously and are affected by many factors, e.g. target abundance, or co-medication with immunomodulators (known to have a suppressive effect on ADA formation [71]), or co-existing state, such as transport into foetus during pregnancy [72]. From the interstitial space a molecule can be carried

back to the blood via the lymph or, at a lesser extent, transcytosis [70]. A molecule can also be excreted to the gut lumen from the intestinal interstitial space, and subsequently excreted from the body or undergo proteolysis [3]. This process depends on the gut permeability and the size of the molecule: smaller molecules (e.g. mAb fragments) are anticipated to be lost at a higher extent. Finally, the molecules can leave the interstitial space by transport into the cells via (1) binding to tmTNF α , (2) binding to Fc γ -receptors, or (3) pinocytosis [70]. Upon pinocytosis, a portion of mAb molecules binds to the neonatal Fc receptor (FcRn) on the cell surface. The IFX molecules undergo proteolysis in lysosomes, or, in case of being bound to FcRn, are recycled back to the interstitium. FcRn is thus a salvaging pathway, that in a pH-dependent manner binds the mAb molecule, protects it from degradation in the cell, and releases it upon exocytosis in the increased pH environment of the interstitium [70]. The FcRn pathway is nonspecific and saturable, making it dependent on the endogenous IgG concentration [73].

The above-mentioned binding of IFX to its target, TNF α , is known as target-mediated drug disposition (TMDD), and is a general characteristic of mAbs. An implication of this PK concept is that as the PK partly depends on the target abundance, and thus IBD severity (pharmacodynamics; PD), there is a bidirectional PK/PD relationship, where not only does the drug impact the disease, but the opposite also holds true [74,75].

Exposure-response relationship

The characterisation of PK/PD relationship of IFX in IBD poses a challenge, due to both the complex PK of IFX described above, and the use of multiple disease markers, some of which also express complex kinetics (e.g. albumin) [76]. Binding of TNF α by IFX neutralises the TNF α -induced cascade of events, leading to an improvement of IBD clinical activity (e.g. reduction in pain and diarrhoea), promotion of mucosal healing, and normalisation of disease (bio)markers (e.g. CRP, albumin). This is further complicated by the bidirectional PK/PD relationship outlined above (Figure 4).

Therapy challenges

Typical dosing regimen of IFX comprises 5 mg/kg IFX doses on weeks 0, 2, and 6 (“induction phase”) and every 8 weeks (q8w) thereafter (“maintenance phase”). Although the efficacy of IFX in IBD has been established [57-65], the IFX therapy still meets challenges posing obstacles to a successful IBD therapy. Namely, \sim 1/3 of patients do not respond to IFX therapy from the very beginning of the treatment (“primary non-responders”), whereas in \sim 1/2 of primary responders the response gradually fades over time (“secondary non-responders”) [77]. The primary non-response is likely due to different, i.e. non-TNF α -driven, underlying disease mechanisms, with potential contribution of underexposure during induction phase. The secondary loss of response is postulated to, at least partly, originate from lower IFX exposure and the formation of ADA [78]. Due to the protein nature of IFX, ADA develop as

a part of the typical reaction of the organism to the foreign protein. The ADA molecules bind IFX to form immune complexes, increasing thereby elimination of IFX and leading to decreased IFX exposure and reduced efficacy. Additional challenges are met in special populations, exemplified by the dilemma whether to discontinue IFX therapy in later trimesters of pregnancy in pregnant IBD patients in order to minimise the foetal exposure, or to continue the IFX therapy throughout the pregnancy in order to maximise the chances of maintaining therapeutic IFX levels, and thus disease remission, in the patient.

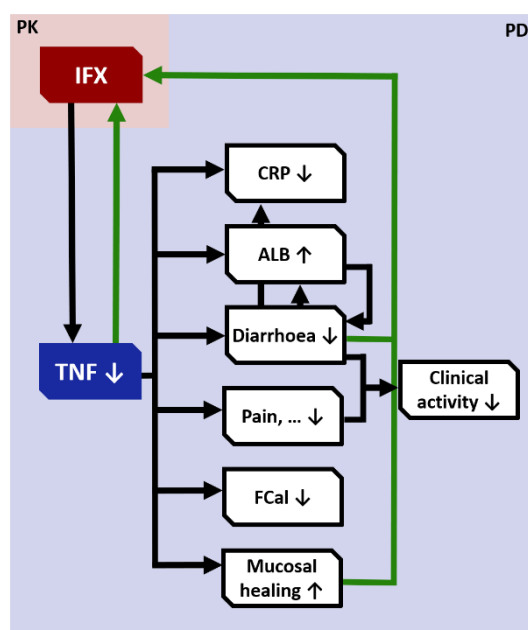


Figure 4. Illustration of highly intertwined PK and PD events in IFX treatment of IBD. The black arrows represent the events initiated by IFX administration, whereas the green arrows represent the effect of PD on IFX PK. ALB: Albumin concentration; CRP: C-reactive protein concentration; FCal: Faecal calprotectin concentration; IFX: infliximab concentration; TNF: Tumour necrosis factor- α concentration.

1.3 *In silico* approach to leverage *in vivo* data

1.3.1 Pharmacometric modelling and simulation

Pharmacometrics is defined as “the science of developing and applying mathematical and statistical methods to characteri[s]e, understand, and predict a drug’s PK, PD, and biomarker-outcomes behavio[u]r” [79]. Together with other quantitative approaches, specifically physiologically-based PK (PBPK) and quantitative systems pharmacology (QSP) modelling and simulations (Figure 5), pharmacometrics (e.g. population analysis) has proved itself a crucial means for gaining knowledge of relevant mechanisms, informing drug development, and assisting in therapeutic decision-making.

In the past years, the impact of pharmacometrics has been increasing, and its value is widely recognised across therapeutic areas, by also both regulatory agencies and pharmaceutical industry [80-82]. From the drug development perspective, pharmacometrics is often used to support the registration of newly developed drugs (including IBD drugs), often informs the choice of the approved dosing regimens of

drugs, and in some cases even obviates the need for clinical trials, for instance in cases of changing the initially approved dosing regimen of a drug [83-85]. From the clinical perspective, the value of pharmacometrics lies in its potential to support post-approval treatment optimisation in the clinical routine, and thereby improve the therapy success [86-89]. This is especially true in certain cases, such as the treatment of special populations (e.g. paediatrics [90], critically ill patients [89]), the Therapeutic Drug Monitoring setting, and for drug dose-exposure-response investigations [91]. Finally, adequate implementation of the concept of individualised dosing (i.e. personalised or precision medicine) relies heavily on modelling and simulation techniques [86].

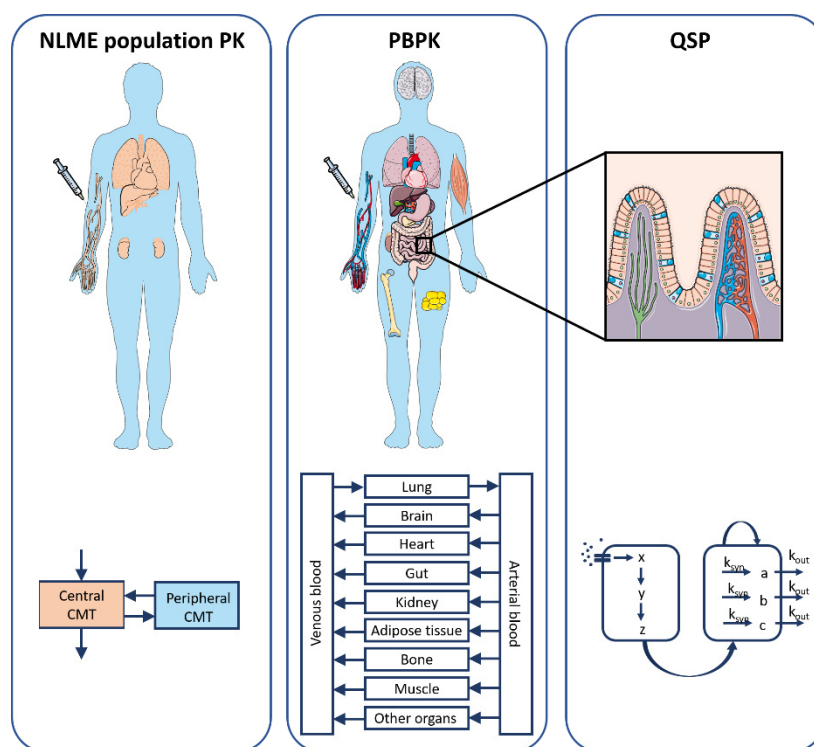


Figure 5. Common classification of modelling and simulation approaches: (1) nonlinear mixed-effects (NLME) population PK modelling, (2) physiologically-based PK (PBPK) modelling, and (3) quantitative systems pharmacology (QSP) methods. The three approaches can be used complementarily to inform drug development and clinical decision making. Parts of the figure were taken and adjusted from Servier Medical Art (<https://smart.servier.com>, Creative Commons Attribution 3.0 Unported License; last access on: 26 Jun 2019). CMT: Compartment; NLME: Nonlinear mixed-effects; PBPK: Physiologically-based pharmacokinetic modelling; QSP: Quantitative systems pharmacology.

Pharmacometric analyses comprise application of modelling techniques on clinical data with the goal to “integrate data, knowledge, and mechanisms to aid in arriving at rational decisions regarding drug use and development” [92]. Of special interest is a compartmental, population approach – the nonlinear mixed-effects (NLME) modelling approach – whereby a model is fitted to the entirety of available data simultaneously, and typical trends (population parameters, “fixed effects”) and variability (“random effects”) between and within individuals are estimated. A NLME model usually comprises three submodels: (1) a structural model that describes the typical profile of the analysed population, (2) a

statistical model that quantifies the variability at different levels (e.g. within a patient, across patients, across occasions), and (3) a covariate model that enables explaining (a part of) the variability by predictive patient-, disease-, and therapy-related factors, i.e. covariates [93]. The pharmacometric aspects relevant for herein presented work are given in *Methods* section of the thesis.

1.3.2 Current modelling knowledge and contributions in IBD

A number of quantitative studies have focused on IBD, with some of them significantly contributing to the understanding of the disease mechanisms and therapeutic decision-making. While unveiling of the disease mechanisms and therapeutic targets has benefited most from QSP models (which have identified inhibitory effects of IL-10 on inflammatory macrophages [18] – a believed mode of action of anti-TNF α mAbs [95], linked the cytokines to the clinical efficacy endpoints [96], and provided insights in mono- and combination therapies [97,98]), empirical/mechanism-motivated population models are most often employed to analyse clinical data and directly derive inferences about the therapy management.

To this end, multiple population PK models have been developed for drugs used in IBD [99-108]. These models enabled identification of subpopulations at risk of therapy failure, and provide a means for more individualised therapy decisions. For instance, they revealed that development of ADA, a higher disease activity and a higher body weight increase elimination of IFX, thereby predisposing these populations to IFX underexposure. Integration of PBPK and population approaches has been undertaken as well, notably to translate knowledge of adult PK to paediatrics, providing predictions of ADA dynamics as well [109]. Furthermore, the superiority of model-based dosing in terms of maintaining target concentration of IFX in patients with IBD has been demonstrated using simulations [110].

The scope of the empirical semi-mechanistic models of IBD drugs is more recently being broadened to PD aspects as well. Dreesen et al. applied NLME modelling approach to compare different exposure targets in regard to the prediction of mucosal healing in UC. They used the model to derive a target exposure at week 12 of therapy that predicts mucosal healing in 70% of the patients. Thus, these results provide a basis for improved outcomes in IBD patients receiving IFX therapy [64]. Furthermore, a population PK/PD model relating IFX exposure to faecal calprotectin concentration and mucosal healing in Crohn's disease patients was recently reported [108]. That study reported a high variability in biomarker response, arguing towards monitoring of the biomarker in addition to IFX concentration.

While increasing presence of modelling and simulation in the IBD area is evident, exploiting the quantitative approaches to their fullest extent to integrate all available knowledge and translate into versatile clinical tools ultimately improving clinical outcomes remains a goal for the future. In addition to the above given examples, modelling and simulation bears the potential for shedding a light on and predicting immunogenicity to the therapeutic mAbs and factors that influence it, identifying drug exposure targets related to disease (bio)markers, or support unveiling, predicting and preventing loss of response to the therapy so often encountered in IBD patients.

1.4 Aims and research questions

The overall objective of this work was to contribute to the improvement of success of IBD treatment and the rational use of IFX in the therapy of IBD. This complex objective was split into the following subobjectives:

- Characterisation of systemic IFX exposure in IBD and identification of factors leading to underexposure – addressed in *Paper I*;
- Characterisation of relationship between IFX exposure and IBD activity in a general IBD patient population and patients with treatment failure – addressed in *Papers I and II*, to:
 - identify disease activity marker(s) that can be quantitatively related to IFX exposure,
 - mechanistically describe and quantify the effect of IFX exposure on IBD activity,
 - determine the maximum effect of IFX on the disease activity marker and corresponding IFX exposure,
 - investigate alternative dosing regimens leading to adequate therapy;
- Investigation and understanding of the impact of study design on identifiability of mAb clearance models – addressed in *Paper III*;
- Identification and quantification of potential pregnancy-induced changes of IFX exposure and assessment of the current IFX dosing strategy in pregnancy – addressed in *Paper IV*.

2 Data and methodological approaches

2.1 Data

Clinical data for the analyses reported in *Papers I-IV* were provided as elaborated below and summarised in **Table 1**.

Table 1. Overview of all analysed clinical data.

	<i>Paper I</i>	<i>Paper II</i>	<i>Paper III</i>	<i>Paper IV</i>
Drug	Infliximab	Infliximab	Cetuximab	Infliximab
Trial type	Investigator-initiated, single-centre	Single-blinded, multicentre, randomised	Ph1 trial: Phase I, open-label EVEREST: Phase I/II, open-label, randomised	Bi-centre prospective, investigator-initiated
n _{patients}	121	47	226 (Ph1: 62; EVEREST: 164)	19
n _{PK samples}	388	152 from 68 patients*	3821	172
Treatment schedule(s)	Based on clinical decisions	5 mg/kg IFX q4w	Ph1 trial: - Arm A: Cetuximab ADR - Arm B: Cetuximab 400, 500, 600, or 700 mg/m ² q2w monotherapy, from week 7 co-therapy with FOLFIRI EVEREST: Cetuximab ADR + irinotecan first 3 weeks, afterwards: - Group A: Cetuximab ADR - Group B: Cetuximab dose escalation (by 50 mg/m ² weekly, up to 500 mg/m ² /week) - Group C: Cetuximab ADR + irinotecan	5 mg/kg q8w 5 mg/kg q6w 10 mg/kg q6w
PK sampling schedule(s)	C _{min} and mid-interval	C _{min} pre-intervention and at week 12 and 20	Ph1: C _{min} throughout the trial; In addition, at the end of the first cetuximab infusion and over the dosing interval starting on day 29: end of infusion and at 4, 24, 48, 96, 168, 240, and 336 h after the start of infusion in Arm B EVEREST: C _{min} throughout the trial; In addition: - Group A and C: end of infusion and 6, 24, 48, 72, 168h after the start of the infusion - Group B: From each dose level 5 patients over the dosing interval starting at the second dose of the dose level	C _{min}
IFX assay	ELISA	HMSA	ELISA	IF-ELISA
ADA assay	HMSA	HMSA	-	ADS ELISA

*The previously published PK model [107] was developed using data (152 PK samples) from 68 patients, 47 of which were subsequently included in the analysis reported in *Paper II*.

ADA: Anti-drug antibodies; ADR: approved dosing regimen (initial 400 mg/m², subsequent 250 mg/m²); C_{min}: Minimum infliximab concentration; HMSA: Homogeneous liquid-phase mobility shift assay; (IF-/ADS-)ELISA: (Immunofluorometric/Automated drug-sensitive) Enzyme-linked immunosorbent assay; FOLFIRI: co-therapy with irinotecan (180 mg/m²), 5-fluorouracil (180 mg/m² bolus and 46-h 2400 mg/m² infusion) and folic acid (2-h 400 mg/m² infusion); IFX: Infliximab; PK: Pharmacokinetic; qXw: every X weeks.

2.1.1 Clinical study I design (*Paper I*)

Clinical data were collected as part of an investigator-initiated trial at the University Hospital of the Medical University of Vienna. The study included 121 IBD patients (89 with CD, 31 with UC and 1 patient with undetermined IBD type) receiving maintenance (>6 weeks) IFX therapy. Absolute IFX doses ranged from 100 to 1300 mg (median 400 mg). As part of Therapeutic Drug Monitoring, 388

blood samples were obtained, mainly at minimum concentration ('trough', C_{\min}) levels and at the middle of the dosing interval in the period 2010-2012. Relevant PK/PD-related and covariate data were obtained: serum concentration of IFX, ADA, CRP and albumin, body weight, smoking status, sex, disease duration, HBI, number of surgeries, disease location, behaviour, age at diagnosis per Montreal classification for CD and disease severity per Montreal classification for UC, IFX dosing, and co-therapy information.

Concentrations of IFX and ADA that were provided for the analysis had been quantified using IDK monitor[®] enzyme-linked immunosorbent assay (ELISA; Immunodiagnostik AG, Bensheim, Germany [111]), and a homogeneous liquid-phase mobility shift assay (Prometheus[®] Anser[®] ADA, Prometheus Laboratories Inc., San Diego, California [112]), respectively.

2.1.2 Clinical study II design (*Paper II*)

Data comprised a subset of the dataset collected as part of a "parent" 12-week, single-blinded, multicentre, randomised clinical trial, with a 20-week follow-up period. The parent trial population comprised CD patients previously on maintenance IFX treatment (5 mg/kg q5w-q8w) who experienced treatment failure. The treatment failure was defined as CDAI \geq 220 and/or presence of \geq 1 draining perianal fistula. The trial comprised two arms, receiving either IFX (5 mg/kg) at an intensified dosing frequency of q4w (arm A), or personalised IFX treatment informed by circulating IFX and ADA concentration, according to a treatment algorithm (arm B; *Paper II*). The blood sampling was performed at the time of screening (before the first trial dose) and at study weeks 12 and 20. In addition, presence of ADA, disease activity as per CDAI, CRP concentration, and patient-related covariate data were collected throughout the study (at weeks 0, 4, 8, 12, and 20).

The analysis reported in *Paper II* was performed on a subset of the parent trial population, selected to minimise confounding factors. The subset (n=47) included patients treated with 5 mg/kg IFX at q4w dosing frequency. The patients in whom IFX treatment was ceased were included up to 4 weeks after the last IFX dose. For the patients who were switched to another dosing frequency at the end of the study period (week 12) all subsequent (past week 12) assessments were excluded. Furthermore, for investigations related to CDAI four additional patients who had fistulising disease activity only were excluded, for the reasons of previous reports of inappropriateness of CDAI for disease activity assessment in fistulising disease [113]. These patients were however included in investigations related to CRP concentrations.

Concentrations of IFX and ADA that were provided for the analysis had been quantified using a homogenous mobility shift assay [112], whereby unbound IFX and total (unbound + IFX-bound) ADA concentrations were measured.

2.1.3 Clinical study III design (*Paper III*)

Data were compiled from two multicentre clinical trials (Figure 6) in patients ($n_{\text{patients}}=226$, $n_{\text{samples}}=3821$) with advanced rat sarcoma proto-oncogene (RAS) wild-type metastatic colorectal cancer on treatment with cetuximab, as detailed below. Full study descriptions are reported elsewhere [114,115].

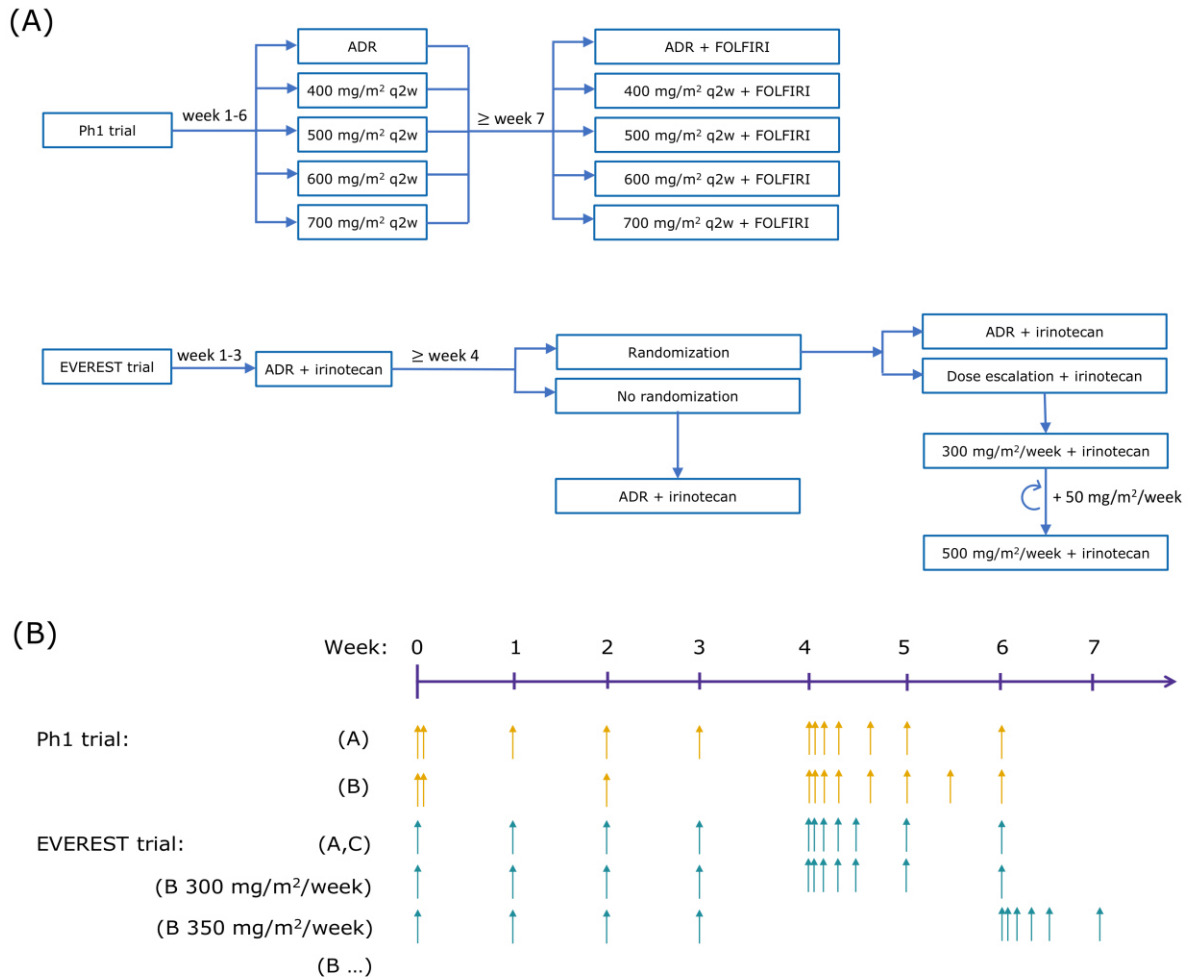


Figure 6. Overview of the dosing and PK sampling schemes from the clinical studies analysed in *Paper III*. (A) Dosing algorithm; (B) Pharmacokinetic sampling schedule.

The *Ph1 trial* [114] was a phase I, open-label trial in which PK and PD of cetuximab were evaluated. During initial 6 weeks, the patients, assigned to two arms, received i.v. cetuximab as monotherapy. The patients in the arm A received cetuximab as per approved dosing regimen (ADR), comprising initial 400 mg/m² infusion and subsequent weekly 250 mg/m² infusions. The patients in the arm B were further assigned to 4 treatment groups, comprising cetuximab doses of 400, 500, 600, and 700 mg/m² q2w. From week 7 on, all patients in addition to cetuximab started FOLFIRI treatment, which comprised co-therapy with irinotecan (180 mg/m²), 5-fluorouracil (180 mg/m² bolus and 46-h 2400 mg/m² infusion)

and folic acid (2-h 400 mg/m² infusion). Throughout the duration of the trial PK samples were taken at C_{min} levels. Additional PK samples were collected at the end of the first cetuximab infusion and over the dosing interval starting on day 29: at the end of infusion and at 4, 24, 48, 96, and 168 hours after the start of infusion in arm A, and at the end of infusion and at 4, 24, 48, 96, 168, 240, and 336 hours after the start of infusion in arm B.

The *EVEREST* trial [115] was a phase I/II, open-label, randomised, controlled trial that evaluated PK and PD of cetuximab dose escalation. All patients were co-treated with cetuximab (ADR) and irinotecan for the first 3 weeks. Subsequently, the patients were assigned to 3 treatment groups, dependent on fulfilment of randomisation criteria. The patients who had neither required irinotecan discontinuation nor experienced skin reaction of grade >1 or any other cetuximab-related toxicity of grade >2 were deemed eligible for randomisation. The eligible patients were thereafter treated with either cetuximab ADR (group A) or underwent cetuximab dose escalation (group B). The dose escalation comprised increasing cetuximab dose by 50 mg/m² per week, up to the maximum dose of 500 mg/m²/week. The patients who were not eligible for randomisation (group C) continued the cetuximab ADR-irinotecan co-treatment. Throughout the duration of the trial, PK samples were taken at C_{min} levels. Additional PK samples in groups A and C were collected at the end of infusion and 6, 24, 48, 72, and 168 hours after the start of infusion. Additional dense sampling in group B was obtained from 5 patients from each dose level over the dosing interval starting on the second dose of the dose level. In both trials, the patients were treated until disease progression or an unacceptable adverse event.

2.1.4 Clinical study IV design (*Paper IV*)

Data were collected as part of a bicentre prospective clinical study that included all pregnant IBD patients treated with IFX until 2018 at the Copenhagen University Hospital Herlev, Denmark, and Sheba Medical Hospital, Israel. Patients (n_{patients}=19, n_{pregnancies}=23, n_{samples}=172) with at least one biobanked blood sample during pregnancy were included. The patients were at maintenance therapy at the time of conception, receiving IFX doses of 5 mg/kg q8w, 5 mg/kg q6w, 5 mg/kg q10w, or 10 mg/kg q8w. During pregnancy, the absolute dose administered to each patient remained the same as prior to pregnancy, i.e. based on the pre-pregnancy body weight. The samples were taken at C_{min} levels before, during and after pregnancy, and stored at -80°C until their analysis. For quantification of IFX an immunofluorometric ELISA was employed on the automated dissociation-enhanced lanthanide fluorescent immunoassay platform (AutoDELFI; PerkinElmer, Turku, FIN [116]). In addition to the PK measurements, covariate information was collected as well, including disease activity assessment (HBI for CD, and Simple Clinical Colitis Activity index or partial Mayo Score for UC), ADA status, body weight, concomitant medication, serum albumin concentration, platelet and white blood cell count. The presence of ADA was assessed in samples with IFX concentration ≤5 µg/mL using an AutoDELFI automated drug-sensitive ELISA that measures unbound neutralising ADA

concentration. All samples were analysed simultaneously under blinded conditions at the Dept. of Medical Biochemistry, Oslo, Norway.

2.2 Pharmacometric data analyses

In all papers (*Papers I-IV*) graphical and statistical data analyses were performed as a first step, in order to gain insights into the data and investigate potential trends of interest. Subsequently, pharmacometric PK(/PD) models were developed in *Papers I, III* and *IV* using the NLME approach [93], as elaborated below.

2.2.1 Fundamentals of pharmacometric modelling

A general analysis workflow as applicable in all below described analyses is shown in Figure 7. Briefly, after the clinical data (see 2.1) was collected at the clinical sites, the datasets were formatted to a software-specific input file format. Subsequently, exploratory analyses were performed and, if indicated, PK(/PD) NLME model development was initiated. All investigated models were evaluated (e.g. goodness of fit, precision, etc.). Once the most adequate (“final”) model was identified, an extensive assessment of the model performance was undertaken, to challenge and confirm/disprove the adequacy of the model. Thus, the model development was an iterative procedure, whereby the learnings from the evaluation step were used to update the model, and the evaluation was repeated. After the final model had been developed, simulations based on this model were performed, to answer further research questions.

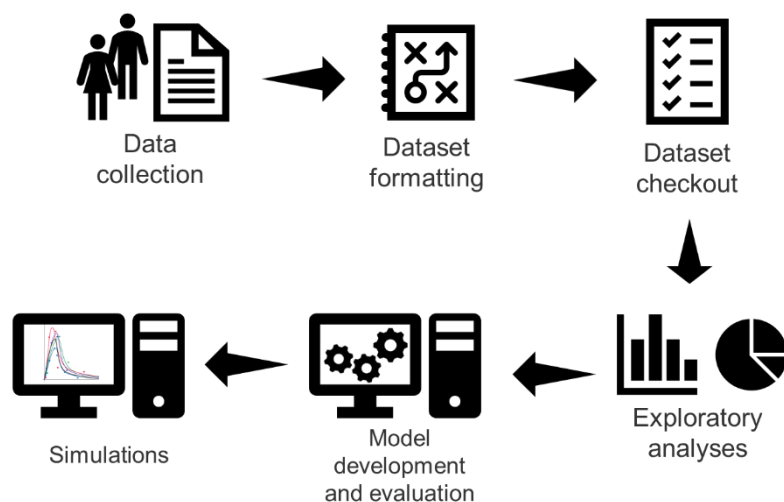


Figure 7. Main steps of the general pharmacometrics analysis workflow.

Dataset management: Formatting and checkout

The clinical data collected was recorded in a so-called ‘raw’ format, and formatting and cleaning the dataset was oftentimes necessary prior to the analysis. The formatting requirements posed by NONMEM® (ICON Plc, Ireland) – the software used in all herein reported pharmacometric analyses – include, but are not limited to: chronological ordering of (dosing, sampling, or other) events, inclusion

Data and methodological approaches

of required information (e.g. columns containing: identifier for each patient in the dataset, dependent variable, flag for missing dependent variable, flag for values below lower limit of quantification [LLOQ], event compartment). As the next step, a dataset checkout was performed, in order to (1) confirm whether the software-specific data structure had been achieved, and (2) assess plausibility and completeness by identifying incomplete or missing values and measurements <LLOQ of the bioanalytical assay; e.g. if frequency of dependent variable measurements <LLOQ of the analytical assay was $\leq 10\%$ these samples were flagged and excluded from the modelling dataset [117]. The dataset management was performed using R and RStudio, and NONMEM-ready datasets were saved in comma-separated values (csv) format.

Exploratory analyses

Once the final dataset was created, exploratory analyses were performed, comprising graphical and statistical exploration of the data, in order to summarise the data (e.g. distributions), and detect potential trends of interest in the data and test for their significance (e.g. correlation between variables). Common investigations included, but were not limited to, relationship between dependent variable (e.g. drug concentration) and independent variable (e.g. time), relationship between dependent variable and covariates, and correlation between covariates.

Nonlinear mixed-effects model development

As briefly mentioned in the *Introduction* (see 1.3.1), the NLME approach [93] enables analysis of data from all individuals in a population simultaneously by using nonlinear function to describe the relationships between the dependent variable and model parameters/independent variable. The resulting model is defined in terms of (“mixed”) fixed- and random-effects parameters, which are constant and vary among individuals, respectively. A typical NLME model consists of three main parts: (1) the structural submodel, (2) the statistical submodel, and (3) the covariate submodel.

The **structural submodel** defines behaviour in the *typical* individual in the population, e.g. in a PK model the typical drug concentration-time profile in the population:

$$Y_{ij} = f(\phi_i, x_{ij})$$

, where Y_{ij} denotes the observed dependent variable of the i^{th} individual at the j^{th} observation, f the nonlinear function (i.e. the structural model), ϕ_i vector of model parameters (e.g. clearance [CL], volume of distribution) of length k , and x_{ij} study design variables (e.g. administered dose).

The **statistical submodel** quantifies the variability at different levels and thus together with the structural model defines *individual* behaviour, e.g. individual drug concentration-time profiles of the patients in a population. Commonly, a statistical submodel comprises between-patient variability and residual unexplained variability (RUV), although other levels of variability (e.g. between-occasion

variability) can be implemented as well. The **between-patient variability** in a parameter (e.g. CL) captures the deviations of the individual parameter value (i.e. empirical Bayes or maximum *a posteriori* estimate; EBE) from the typical model parameter value in the population. Due to the nature of the data, the model parameters in NLME models are often assumed to be log-normally distributed (and thus non-negative), and the between-patient variability is then modelled using an exponential relationship [93]:

$$\phi_{ik} = \theta_k \cdot e^{\eta_{ik}}, \eta_k \sim \mathcal{N}(0, \omega_k^2)$$

, where ϕ_{ik} denotes the k^{th} model parameter of the i^{th} individual, θ_k typical value of the parameter, η_k vector of random-effects parameters of all the individuals in the population, η_{ik} individual random-effect parameter value, and ω_k^2 variance of the estimated random-effects parameter. For easier interpretation, the variance of estimated random-effect parameters is usually reported as coefficient of variation (CV%) [93]:

$$CV\% = \sqrt{e^{\omega_k^2} - 1} \cdot 100\% .$$

The **RUV** captures the deviation of the observations from the model predictions; e.g. in case of a PK model the difference between the observed and the model predicted drug concentration. The RUV model is most often represented via additive, proportional or combined additive and proportional function. The combined model is defined as follows:

$$Y_{ij} = f(\phi_i, x_{ij}) \cdot (1 + \varepsilon_{proportional,ij}) + \varepsilon_{additive,ij}$$

$$\varepsilon_{proportional} \sim \mathcal{N}(0, \sigma_{proportional}^2)$$

$$\varepsilon_{additive} \sim \mathcal{N}(0, \sigma_{additive}^2)$$

, where Y_{ij} denotes the observed dependent variable, $f(\phi_i, x_{ij})$ the model prediction, $\varepsilon_{proportional,ij}$ and $\varepsilon_{additive,ij}$ proportional and additive RUV parameters for the i^{th} individual at the j^{th} observation, respectively, $\varepsilon_{proportional}$ and $\varepsilon_{additive}$ vectors of proportional and additive RUV parameters for all observations of all individuals in the population, $\sigma_{proportional}$ and $\sigma_{additive}$ variance of proportional and additive RUV parameters, respectively.

Of note, between-patient variability in RUV [118] can also be defined, e.g. on the total (combined model) RUV:

$$Y_{ij} = f(\phi_i, x_{ij}) + (f(\phi_i, x_{ij}) \cdot \varepsilon_{proportional,ij} + \varepsilon_{additive,ij}) \cdot e^{\eta_{RUV,i}}, \eta_{RUV} \sim \mathcal{N}(0, \omega_{RUV}^2)$$

, where Y_{ij} denotes the observed dependent variable, $f(\phi_i, x_{ij})$ the model prediction, $\varepsilon_{proportional,ij}$ and $\varepsilon_{additive,ij}$ proportional and additive RUV parameters for the i^{th} individual at the j^{th} observation,

η_{RUV} vector of random-effects parameters of all the individuals in the population, $\eta_{RUV,i}$ individual random-effect parameter value, and ω_{RUV}^2 variance of the estimated random-effects parameter.

Finally, the **covariate submodel** defines relationships between structural parameters and one or more covariates (e.g. body weight, sex). In the herein reported work, the covariate model development comprised three steps: (1) pre-selection based on mechanistic plausibility and trends identified in the exploratory analysis, (2) univariate covariate modelling, and (3) step-wise modelling, whereby the covariates were added to the model in the order of decreasing impact on the model fit (i.e. objective function value [OFV]) and afterwards eliminated if removal of a covariate had no substantial impact on the model fit. While many different mathematical relationships can be used for this purpose, e.g. depending on the nature of the covariate, physiological anticipation, parametrisation and ease of interpretation, only the ones relevant for the work conducted within this thesis are given in the following:

- Continuous covariates, power relationship:

$$g(\theta_{ik}, cov_i) = \theta_k \cdot \left(\frac{cov_i}{cov_{median}} \right)^{\theta_{cov}}$$

- Categorical covariates, fractional change model:

$$g(\theta_{ik}, cov_i) = \begin{cases} \theta_k, & \text{for } cov_i = a \\ \theta_k \cdot (1 + \theta_{cov}), & \text{for } cov_i = b \end{cases}$$

- Categorical covariates, binary power relationship:

$$g(\theta_{ik}, cov_i) = \theta_k \cdot \theta_{cov}^{cov_i}, cov_i \in \{0,1\}$$

, where g denotes the covariate function, θ_{ik} value of the k^{th} fixed-effects parameter of the i^{th} individual, cov_i the covariate value in the i^{th} individual, θ_k typical value of the k^{th} fixed-effects parameter, cov_{median} median value of the covariate in the population, θ_{cov} the covariate-effect parameter (e.g. exponent in power relationship), a and b unique possible values of a categorical, dichotomous covariate.

Parameter estimation

For the estimation of the (both fixed-effects and random-effects) model parameters that best fit the observed data, the maximum likelihood estimation approach was used, whereby a set of parameters that maximises the likelihood of observing the observed data given the model is identified [93,119]. This is, for convenience reasons, accomplished by minimising the objective function (OF), defined as:

$$OF = -2 \cdot \log (\mathcal{L}(\theta, \omega^2, \sigma^2 | Y))$$

, where θ denotes the vector of fixed-effects parameters, ω^2 and σ^2 variances of random-effects parameters, and Y vector of the observed data. When comparing nested models, comparison of the OFV is one of the criteria to identify the model with a better fit (i.e. lower OFV).

As for most NLME models analytical computation of the likelihood is not possible, the OFV is approximated using numerical methods. In the NLME parameter estimation software NONMEM® many estimation methods are available for this purpose, including approximation methods that use simplified functions to approximate the likelihood, specifically first-order conditional estimation with interaction (FOCEI), of importance for the work described herein. In FOCEI method, the mode of joint density (i.e. the most likely values of between-patient variability random effects $[\eta]$) and the first-order approximation of variances of η 's are considered. Thereby, between-patient variability is accurately evaluated, and within-patient variability is evaluated via linear approximation [119].

In the cases when the observed data is sparse, the information contained in the data might not be informative enough to inform (precise) estimation of one or more parameters in the model. When prior information (e.g. estimates and their uncertainty from a previously developed model) that is deemed appropriate are available, the frequentist prior approach [120] can be used to further inform and thereby stabilise the estimation of these parameters. This idea – to account for previous knowledge about a topic investigated – is the central point of the Bayesian statistics, where a prior distribution of a parameter value is combined with the data in order to obtain a new, posterior distribution. A limitation of using prior knowledge is that the choice of prior will clearly influence the results, i.e. the posterior distribution and final parameter estimates. The major difference between the Bayesian approach and the frequentist prior approach is that in the Bayesian statistics the parameters are considered to be random, whereas in the frequentist prior approach only the form of the parameter distribution is considered and no assumption that the distribution governs the randomness in the parameter is made. As explained above, an estimate of a parameter p is usually obtained by minimising the OF with respect to p . If an additional rich dataset were available for an analysis in addition to the sparse dataset, one could simply analyse the pooled data. In that case, the objective function O would be:

$$O = O_S + O_R$$

, where O_S and O_R denote the OF based on the sparse and rich data, respectively.

Instead of pooling the data (e.g. if the rich dataset is not readily available), a prior model developed using the rich data can be used in place of the rich data itself. For any value of a parameter p , OF from the prior model O_P can be computed. The O_P thus represents the prior information about the value of p from the rich data and is used as an approximation of O_R :

$$O_R \approx O_P$$

$$O = O_S + O_P$$

During the minimisation procedure, as different values of p are considered, the further the value is from the minimum of O_p , the larger the O_p will be, and the less likely it is that this value is the minimum of the OF. Thus, O_p is referred to as “penalty”. If there were no information in the sparse data whatsoever, then $O_S \rightarrow 0$ and $O \rightarrow O_p$ [120].

Model evaluation

The process of identifying the model that best fits the data is an iterative one between model estimation and model evaluation, whereby the changes in the model are informed by the results of model evaluation step. The selection criteria most relevant for this work included: plausibility of parameter estimates, estimation precision (e.g. relative standard error [RSE] and confidence interval), shrinkage of individual parameters towards the typical values [121], goodness-of-fit plots, log-likelihood profiling [122], visual predictive checks (VPC) [123]. The goodness-of-fit plots included, but were not limited to: plots of observations vs individual and population predictions, conditional weighted residuals (CWRES) [124] versus independent variable and population predictions, distributions of random-effects and EBEs.

Simulations as an application of a model

Once a model that best describes the data has been developed, the model can be further utilised to perform simulations and thereby address further research questions and investigate “what if” scenarios (e.g. what if the drug was administered at a different dosing frequency). Deterministic simulations are based on fixed-effects parameters and do not account for random-effects parameters, thus representing the typical behaviour. Stochastic (Monte Carlo) simulations account for both fixed-effects and random-effects parameters (e.g. between-subject variability), thus providing information on the variability as well. In addition, the stochastic simulation and estimation (SSE) approach automatised in PsN [125] was used in this work. The SSE is a useful tool in cases when multiple models are to be investigated in a simulation setting: A number of simulated datasets is generated using a reference model, and subsequently the reference and alternative models are fitted to the simulated data and statistical measures and OFV outputted.

Details on the pharmacometric approaches applied to each project are given in the following section.

2.2.2 Characterisation of infliximab pharmacokinetic behaviour and exposure-response relationship and dosing regimen assessment

PK model

In *Paper I*, to compensate for the sparse nature of the analysed data and support the parameter estimation, prior information from the IFX PK model developed by Fasanmade et al. [100] was utilised

using the frequentist prior approach. RUV was described with a combined model and between-patient variability in RUV [118], thereby allowing RUV to vary among the patients.

PK/PD model development

In *Papers I and II* relationships between IFX exposure and IBD activity measures were addressed. Graphical analyses were performed as described above and, as indicated by these results, in *Paper I* PK/PD model development was undertaken with CRP concentration as an IBD activity marker.

The PK/PD model relating IFX to CRP concentration was implemented via a sequential modelling approach: after the final PK model was developed, the EBEs were passed to the continuous PD model (instead of simultaneously fitting PK and PD data). Based on the pharmacological mechanisms and immunological sequence of events, the IFX effect-induced CRP concentration changes were anticipated not to be instantaneous, and thus an indirect effect, turnover PD model [92] was employed [126]:

$$E_{base} = \frac{k_{in}}{k_{out}}$$

, where E_{base} denotes baseline steady-state level of the effect, and k_{in} and k_{out} rate constants for the biomarker production and removal, respectively.

The IFX impact was implemented via an inhibitory effect on CRP synthesis and E_{max} relationship [126]:

$$E = \frac{E_{max} \cdot C_{drug}}{EC_{50} + C_{drug}}$$

, where E denotes the drug effect, C_{drug} the drug concentration, and EC_{50} the concentration of the drug at half-maximal effect (i.e. when E is 50% E_{max}).

To stabilise the estimation of the random-effects parameters of the PD model, the frequentist prior approach was employed.

In order to present a clinically relevant and intuitive measure of the drug's potency, IFX concentration at 90% of the maximum effect (EC_{90}) was calculated as follows [127]:

$$E = 0.9 \cdot E_{max}$$

$$0.9 \cdot E_{max} = \frac{E_{max} \cdot C_{drug}}{EC_{50} + C_{drug}}$$

More general:

$$E = \frac{F[\%]}{100[\%]} \cdot E_{max}$$

$$\frac{F[\%]}{100[\%]} \cdot E_{max} = \frac{E_{max} \cdot C_{drug}}{EC_{50} + C_{drug}}$$

$$F[\%] = \frac{C_{drug}}{EC_{50} + C_{drug}} \cdot 100[\%]$$

By solving for C_{drug} :

$$F[\%] \cdot (EC_{50} + C_{drug}) = C_{drug} \cdot 100[\%]$$

$$F[\%] \cdot EC_{50} = C_{drug} \cdot (100[\%] - F[\%])$$

$$\therefore C_{drug} = \frac{F[\%]}{100[\%] - F[\%]} \cdot EC_{50}$$

, where E denotes $F\%$ of the maximum drug effect, E_{max} the maximum drug effect, EC_{50} the concentration of the drug at half-maximal effect (i.e. for $F=50\%$), C_{drug} drug concentration.

Assessment of standard dosing regimen of IFX

To assess the standard and alternative dosing regimens of IFX in terms of CRP remission achievement, stochastic simulations ($n=1000$) were performed using the final PK/PD model, accounting for the most influential covariates identified. The investigated dosing regimens differed in dosing frequency in the maintenance phase (q4w to q12w), whereas the administered dose (5 mg/kg) and induction phase dosing frequency (weeks 0, 2, and 6) were kept constant, corresponding to the current standard. The CRP remission was defined as $CRP < 5$ mg/L [128].

2.2.3 Clearance of monoclonal antibodies: Cetuximab case study

PK model development

In *Paper III*, the “log-transform both sides” approach [93] was utilised, whereby both the data and the model predictions were ln-transformed. Of note, the model parameters are not transformed and thus retain their initial interpretation. Six different base models were investigated, focusing on the **CL component**:

Linear (LCL) [129]:

$$\frac{dA_1}{dt} = -Q \cdot C_1 + Q \cdot C_2 - CL \cdot C_1$$

Time-varying linear (TVARCL):

$$\frac{dA_1}{dt} = -Q \cdot C_1 + Q \cdot C_2 - CL \cdot e^{\frac{(E_{max,CL} + \eta_{E_{max,CL}}) \cdot t^Y}{t_{50}^Y + t^Y}} \cdot C_1$$

Michaelis-Menten (MMCL) [130]:

$$\frac{dA_1}{dt} = -Q \cdot C_1 + Q \cdot C_2 - \frac{V_{max} \cdot C_1}{K_m + C_1}$$

Parallel LCL and MMCL (LCL+MMCL):

$$\frac{dA_1}{dt} = -Q \cdot C_1 + Q \cdot C_2 - CL \cdot C_1 - \frac{V_{max} \cdot C_1}{K_m + C_1}$$

Parallel TVARCL and MMCL (TVARCL+MMCL):

$$\frac{dA_1}{dt} = -Q \cdot C_1 + Q \cdot C_2 - CL \cdot e^{\frac{(E_{max,CL} + \eta_{E_{max,CL}}) \cdot t^\gamma}{t_{50}^\gamma + t^\gamma}} \cdot C_1 - \frac{V_{max} \cdot C_1}{K_m + C_1}$$

Parallel linear and zero-order (LCL+0.EL) [131]:

$$\frac{dA_1}{dt} = -Q \cdot C_1 + Q \cdot C_2 - CL \cdot C_1 - k_0$$

, where A_1 denotes drug amount in central compartment, C_1 and C_2 drug concentration in central and peripheral compartment, respectively, Q intercompartmental flow, CL linear clearance from central compartment, $E_{max,CL}$ maximum change in time-varying linear CL , $\eta_{E_{max,CL}}$ between-patient variability in $E_{max,CL}$, t_{50} time at which clearance is halved, γ curve shape factor, V_{max} maximal rate of saturable elimination, K_m concentration at half V_{max} , and k_0 zero-order rate constant of elimination from central compartment.

Covariates were investigated for significance using the full fixed-effects modelling approach [132], whereby covariates were pre-selected based on data availability and mechanistic and pharmacological plausibility, and simultaneously implemented in the final base model. The resulting “full covariate model” was fit to the data and each covariate evaluated with respect to its impact on between-patient variability, estimation precision and extent of the effect.

Study design investigations

For further analysis, the four study designs and the six investigated models were compared using the SSE approach. The final base model developed as described above was considered the reference model. A simulation population of 100 virtual patients was generated, with body surface area – relevant for dosing purposes – sampled in such a way to correspond to the clinical database and assumed to be time-constant. Using the reference model and the simulation population, 200 datasets were generated. The six models were fitted to the 200 datasets, and accuracy and bias (root mean squared error; RMSE) [133] in parameter estimates and exposure metrics assessed. This procedure was repeated for the four study designs, followed by comparison.

The four study designs (Figure 8) differed in the number of dosing levels (single vs multiple) and sampling density (rich vs sparse). In all study designs, all virtual patients received an induction dose of 400 mg/m² at infusion rate of 5 mg/min. The subsequent doses were administered at an infusion rate of

10 mg/min. After the induction dose, the virtual patients received the following doses of cetuximab q1w:

- 200, 250, 300, 350, 400, 450, or 500 mg/m² in study designs A and C;
- the approved dose (250 mg/m²) in study designs B and D.

In all virtual patients across the study designs PK samples were taken at C_{min} after each dose until week 12. At week 12 the patients were stratified in 5 sampling groups. In each group PK sampling was performed once monthly for three consecutive months, distributed over the period up to 18 months since study start. In the “rich” study designs (A and B), additional samples were taken after the 5th dose at the end of infusion and 4, 24, 48, 72, and 96 h after the start of the infusion.

		Sampling density	
		Rich	Sparse
Dosing levels	Multiple	Study design A	Study design C
	Single	Study design B	Study design D

Figure 8. Overview of the four investigated study designs.

Investigated exposure metrics were C_{min} and area under the concentration-time curve (AUC) after the second dose and at steady state, where steady state was defined as approximate time when 90% of maximal linear CL decrease had occurred.

2.2.4 Infliximab pharmacokinetics in pregnancy

PK model development

As a first step, a fundamental (“initial”) PK model was developed using only pre-pregnancy data (n_{samples}=94, i.e. 55% of all PK samples). Subsequently, the initial model with the structural PK parameters fixed to the final estimates was fit to the totality of data (i.e. pre-, in- and post-pregnancy), and the potential effects of pregnancy and pregnancy trimester were investigated as covariates. Finally, other covariates of interest were pre-selected based on the data availability (e.g. the range of the covariate values) and exploratory analyses, and investigated in the model.

Simulations to investigate IFX (dis)continuation in pregnancy

Using the final model, deterministic and stochastic simulations were performed in order to demonstrate the concentration-time profiles of typical patients and a patient population, respectively. For stochastic simulations, a simulation population comprising 6000 virtual patients was generated, whereby the patients differed in significant covariates (ADA and pregnancy status) and strategy of IFX

administration during pregnancy (dis-/continuation of IFX in the third trimester). The ADA status (positive/negative) was assigned on the patient level, i.e. as a time-invariant covariate. For pregnant patients, the date of conception corresponded to the second maintenance IFX administration (week 22 of IFX therapy). All patients were assigned to receive an IFX dose corresponding to 5 mg/kg (standard dosing strategy) for a standard 65 kg patient, i.e. 325 mg, at a standard dosing interval (week 0, 2, 6, and q8w thereafter). The simulated exposures were further processed to calculate the percentage of patients reaching three PK targets: 3, 4, and 5 $\mu\text{g/mL}$ at week 62 of therapy – corresponding to week 40 of pregnancy in the pregnant patients. The calculated target achievement was compared relative to ADA status, pregnancy status, and dis-/continuation of IFX in the third trimester.

2.3 Software

Throughout all projects the pre- and post-processing was performed using R (version $\geq 3.2.4$) and RStudio, and modelling and simulation activities using NONMEM[®] (version 7.3, ICON Plc, Ireland), PsN (<https://uopharmacometrics.github.io/PsN/>; in *Paper I and Paper IV* version $\geq 4.7.0$, in *Paper III* version 4.4.8) and Pirana (<https://www.certara.com/software/pirana-modeling-workbench/>). In *Paper III* all estimations were performed on a Linux (version 3.0.101) cluster with SUSE operating system using Sun Grid Engine and the GFortran compiler.

3 Results and Discussion

Pharmacometrics holds a potential to overcome some of the many challenges faced in the management of IBD, from identification of useful biomarkers, to dosing decisions, to therapeutic decisions in special patient populations. As many other mAbs, IFX is dosed on body size-based basis, the assumption being that adjusting for body size (i.e. body weight) will partly compensate for between-patient differences and result in a similar exposure among the patients. In a side project outside of this thesis [134] it has however been demonstrated that body weight-based and flat (same absolute dose for all patients) dosing of IFX resulted in a similar exposure distribution in a patient population. This indicated that a more quantitative, more *individualised*, approach is required for IFX dosing in IBD. The herein reported work provides insights offering support to the clinical management of IBD, including biomarker choice and dosing decisions, in a general patient population, and a special population, i.e. pregnant IBD patients.

3.1 Pharmacokinetic behaviour of infliximab

For the development of the IFX PK model in a general patient population (*Paper I*), 388 PK samples from 121 patients were available. The model that described the data best was a 2-compartment model with linear elimination. To stabilise the estimation of the PK parameters for which the information in the data were insufficient (central volume of distribution V_1 and intercompartmental flow Q), estimates from a published model [100] were used. Initially, the estimation of between-patient variability in V_1 , V_2 , and CL was also informed by prior, however as CL was of interest for covariate investigations, and between-patient variability in CL could be estimated from the data, the use of prior for the random-effects parameters was abandoned, and the variability in V_1 and V_2 instead fixed. For RUV, a mixed additive and proportional model was used. The RUV was “individualised”, i.e. allowed to vary among patients, by introducing the between-patient variability in RUV. On the onset of covariate modelling, the parameters informed by the prior were fixed to their final estimates from the base model. The (time-varying) covariates found to significantly influence IFX CL were ADA status, serum albumin concentration, body weight, and co-medication with immunomodulators. Table 2 (upper part) gives parameter estimates of the final PK model. The equations describing the final model were as follows:

$$CL = CL_{pop} \cdot (1 + \theta_{ADA_CL} \cdot ADA) \cdot \left(\frac{sAlb}{43 \text{ g/L}}\right)^{\theta_{sAlb_CL}} \cdot \left(\frac{BW}{70 \text{ kg}}\right)^{\theta_{BW_CL}} \cdot \theta_{IMM_CL}^{IMM} \cdot e^{\eta_{CL}}$$

$$V_1 = V_{1,pop} \cdot e^{\eta_{V1}}$$

$$V_2 = V_{2,pop} \cdot e^{\eta_{V2}}$$

$$Q = Q_{pop},$$

Results and Discussion

, where CL denotes the individual CL value, CL_{pop} the typical CL of the population, ADA the status of ADA (0 for ADA- and 1 for ADA+), $sAlb$ the serum albumin concentration, BW the body weight, IMM an indicator (0 for absence, 1 for presence) for co-therapy with immunomodulators, η_{CL} the between-patient variability in CL, V_1 the individual volume of central compartment, $V_{1,pop}$ the typical central compartment volume of the population, V_2 the individual volume of peripheral compartment, $V_{2,pop}$ the typical peripheral compartment volume of the population, Q the individual intercompartmental exchange flow, Q_{pop} the typical intercompartmental exchange flow of the population.

Table 2. Parameter estimates of the final PK/PD model relating IFX exposure to CRP synthesis inhibition.

Parameter, unit	Mean (%RSE) [%shrinkage]
<i>PK submodel parameters</i>	
Central volume of distribution V_1 , L	3.67 (-)
Intercompartmental flow Q , L/h	0.0067 (-)
Peripheral volume of distribution V_2 , L	0.956 (11)
CL, L/h	0.0109 (3)
Effect of ADA on CL	0.972 (4)
Effect of Alb on CL	-1.17 (21)
Effect of body weight on CL	0.356 (41)
Effect of IMM co-therapy on CL	0.847 (5)
Between-patient variability in V_1 , %CV	12.8 (-) [83]
Between-patient variability in V_2 , %CV	55.3 (-) [56]
Between-patient variability in CL, %CV	34.9 (8) [6]
Additive RUV in PK, SD ($\mu\text{g/mL}$)	0.478 (21) [17]
Proportional RUV in PK, %CV	24 (14) [17]
Between-patient variability in RUV, %CV	22.2 (18) [46]
<i>PD submodel parameters</i>	
Baseline CRP concentration, mg/L	6.32 (17)
CRP degradation rate constant k_{deg} , h^{-1}	0.0365 (-)
Half-maximal inhibitory concentration IC_{50} , $\mu\text{g/mL}$	2.04 (43)
Maximum effect I_{max} , %	71.9 (9)
Between-patient variability in IC_{50} , %CV	209 (42) [28]
Between-patient variability in baseline CRP concentration, %CV	115 (15) [0]
Proportional RUV in PD, %CV	65.3 (4) [10]

RSE: Relative standard error; PK: Pharmacokinetic(s); V_1 : Central volume of distribution; V_2 : Peripheral volume of distribution; Q: Intercompartmental flow; CL: Clearance; ADA: Anti-drug antibodies concentration; Alb: Serum albumin concentration; IMM: Co-therapy with immunomodulators; RUV: Residual unexplained variability; PD: Pharmacodynamic(s); CRP: C-reactive protein concentration; k_{deg} : CRP degradation rate constant; IC_{50} : Infliximab concentration leading to half-maximal effect; I_{max} : Maximum effect.

During its two decades of usage, IFX has been a subject of many PK modelling studies (Table 3). While there are variations in the reported models, a general agreement exists in the identified model structure and significant covariates, endorsing the herein published PK model as well. The published models were 1- or 2-compartment models, and the significant covariates – albeit differing among models – broadly fall into same mechanism-related categories: body size (body weight, fat-free mass), ADA status, co-medication, and disease activity (albumin, HBI, CRP). The slight differences presumably root from differences in the data availability/sparsity, and investigated population-specific characteristics.

Table 3. Overview of previously published population PK(/PD) models of IFX in IBD, ordered chronologically.

Reference	Indication	Structural PK model	Covariates	PD variable: model
Furuya et al. [135]	CD	1-CMT linear model	-	TNF α -inflammation (CDAI): turnover TNF α model with IFX-binding and subsequent effect on inflammation
Fasanmade et al. [99]	UC	2- CMT linear model	CL ~ albumin, ADA, sex V_1 ~ BW and sex	-
Fasanmade et al. [100]	CD, incl. paediatrics	2- CMT linear model	CL ~ BW, ADA, albumin, concomitant immunomodulators V_1, V_2, Q ~ BW	-
Dotan et al. [104]	IBD	2- CMT linear model	CL ~ BW, albumin, ADA V_1, V_2, Q ~ BW	-
Aubourg et al. [136]	CD	2- CMT linear model	V_1 ~ BW V_1, CL ~ sex	-
Buurman et al. [102]	IBD	2- CMT linear model	CL ~ ADA, sex, period (induction/maintenance) V_1 ~ HBI	-
Ternant et al. [137]	CD	1- CMT linear model	CL ~ CRP and Fc γ receptor 3A genotype V_1 ~ BW	Time to relapse (CDAI>250 or 150<CDAI<250 with 70-point increase from baseline over 2 consecutive weeks): Cox proportional-hazard model

Results and Discussion

Reference	Indication	Structural PK model	Covariates	PD variable: model
Edlund et al. [107]	CD	2- CMT linear model	CL ~ BW, ADA V ₁ , V ₂ , Q ~ BW	-
Passot et al. [138]	IBD, RA, PA, AS, incl. pediatrics	1- CMT linear model	CL ~ disease, BW, sex, concomitant methotrexate V ~ BW, sex, age≤15y	-
Brandse et al. [139]	IBD	2- CMT linear model	CL ~ ADA, BW, albumin	ADA: time-to-event/bidirectional IFX-ADA interaction
Eser et al. [103]	IBD	2- CMT linear model	CL ~ BW, ADA, albumin V ₁ , V ₂ , Q ~ BW	-
Kevans et al. [140]	UC	2- CMT linear model	CL ~ BW, albumin, ADA, time V ₁ , V ₂ , Q ~ BW	Clinical response at week 14 and corticosteroid-free (Mayo) remission rate at week 54 of therapy: Graphical analysis
Petitcollin et al. [141]	Pediatric CD	1- CMT linear model	CL ~ time (as an ADA surrogate), albumin	Paediatric CDAI remission: Survival, i.e. Kaplan-Meier/multivariate Cox proportional-hazard analysis
Petitcollin et al. [142]	IBD	1- CMT linear model	CL ~ time, BW, CRP, IBD type, dose, disease activity for UC (Mayo score), azathioprine cotreatment	Time to relapse: Multivariate Cox proportional-hazard model
Ternant et al. [143]	IBD, spondyloarthritis (AS and PA), RA, incl. pediatrics	1- CMT linear model	CL ~ BW, sex, disease, concomitant methotrexate V ~ BW, sex, disease, age<15y	-
Berends et al. [144]	UC	2- CMT linear model	CL ~ ADA, albumin	TNFα: TMDD-QSS model
Dreesen et al. [64]	UC	1- CMT linear model	CL ~ albumin, CRP and fat-free mass V ~ concomitant corticosteroids, pancolitis at baseline	Mucosal healing (Mayo endoscopic subscore): logistic regression model with IFX-mucosal healing interaction
Kimura et al. [145]	IBD	2- CMT linear model	-	Inflammation: IFX-TNFα binding-inflammation suppression model

Reference	Indication	Structural PK model	Covariates	PD variable: model
Vande Casteele et al. [146]	UC	Taken from Fasanmade et al. [99]	Taken from Fasanmade et al. [99]	Mayo endoscopic score: Linear relationship with baseline IFX CL and IFX concentrations; multivariable logistic regression model
Bauman et al. [147]	Pediatric IBD	2- CMT linear model	CL ~ BW, albumin, erythrocyte sedimentation rate, ADA	-
Dreesen et al. [108]	CD	2-CMT linear model	CL ~ faecal calprotectin, albumin, CDAI, ADA	Faecal calprotectin: E _{max} turnover model Endoscopic remission: 1 st order Markov model

ADA: Anti-drug antibodies; AS: Ankylosing spondylitis; BW: Body weight; CD: Crohn's disease; CDAI: Crohn's disease activity index; CL: Clearance; CMT: Compartment; IBD: Inflammatory bowel diseases; IFX: Infliximab; PA: Psoriatic arthritis; PD: Pharmacodynamic(s); PK: Pharmacokinetic(s); Q: Intercompartmental flow; RA: Rheumatoid arthritis; TMDD-QSS: Quasi-steady-state approximation of target-mediated drug disposition; TNF α : Tumour necrosis factor- α ; UC: Ulcerative colitis; V: Volume of distribution; V₁: Central volume of distribution; V₂: Peripheral volume of distribution.

In the herein described analysis, the presence of ADA was identified as a covariate with the highest impact on IFX CL, with approximately 2-fold (97%) higher CL in patients who developed ADA (ADA+), compared to the ADA negative (ADA-) patients. The ADA develop as a natural response of an organism to a foreign (therapeutic) protein, and the observed depletion of IFX exposure by ADA presence was anticipated. Mechanistically, the development of ADA can affect both PK and the effect of IFX. The ADA molecules binding to active sites of IFX molecule ("neutralising ADA") hinder its efficacy by disabling binding to its target, i.e. TNF α . Furthermore, the formed IFX-ADA complexes are promptly cleared from the blood, contributing to the higher CL of IFX [148]. The development of ADA is influenced by different factors intensifying or hindering this process, some of which have been identified. For instance, compared to episodic treatment, an uninterrupted, continued IFX treatment (i.e. without "drug holidays"), as well as concomitant use of azathioprine or methotrexate, is related to a lower risk of ADA development [3,13,74,149]. Of note, the analytical assay for ADA quantification employed in this study captured both drug-bound and -unbound (i.e. total) ADA molecules of all immunoglobulin (Ig) subtypes. The Ig profile in an immune response changes over time in the process referred to as Ig class switching, steered by cytokines secreted by T cells [150,151]. The Ig class switching is expected to take place in the case of ADA as well, since ADA represent an immune response to a drug. On the course of the process, the Ig constant regions change from IgM (in primary response) to IgD, IgE, IgA and/or one of four IgG isotypes (IgG3, IgG1, IgG2 and finally IgG4) [152]. In short, naïve B lymphocytes produce IgM and IgD antibodies as part of the primary immunological response. If T helper (T_h) cell-mediated signalling occurs, the switching process is initiated [150,151]. The cytokines activate the transcription of the constant heavy chain genes that encode the Ig class to be

Results and Discussion

secreted [150]. The switching occurs in a defined order of Ig classes/subclasses (IgM, IgD → IgG3 → IgG1 → IgA1 → IgG2 → IgG4 → IgE → IgA2), due to location (i.e., order) of exons encoding them [153]. The switching begins approximately 6 days after activation by T cell-dependent antigen *in vivo* [151]. In the late immune response the dominant Ig classes are the ones that do not fix (and therefore do not activate) the complement, i.e. IgG2 and IgG4, serving as the organism's way of restricting the inflammation and damage [152,154]. In fact, IgG4 is known to be the main Ig class after repeated or long-term exposure to an antigen and thus also in the case of immunity against therapeutic proteins [154], as was already demonstrated for adalimumab [155]. This is important to consider since the assays for ADA quantification measure different molecular species, e.g. by binding the ADA molecules by different number of bonds. For instance, some assays (e.g., ELISA) do not capture monovalent antibodies. Since IgG4 are functionally monovalent [156,157] and this Ig class is expected to be dominant in late immune response, this should be accounted for when choosing the assay for ADA determination in the patients. A study on beekeepers exposed frequently and repeatedly to bee stings showed that during the first 6 months of the exposure IgG1 class was the most abundant. Over time, the IgG1 contribution decreased and IgG4 increased, until IgG4 became the most numerous, accounting for up to >90% of the response. Another observation from the referenced study was that except for avoiding detection in precipitating assays, IgG4 molecules additionally interfered with immune precipitation of IgG1; namely, mixing of early (IgG1-governed) and late (IgG4) serum resulted in negative results [157,158]. In general, the production of pro-inflammatory IgG1 molecules is induced within 7 days after the initiation of the immune response, their number reaches maximum after 1-2 weeks and they disappear after 2-3 weeks; whereas IgG4 are induced after months or even years of exposure. The count of IgG4 increases similarly to IgG1, but the IgG4/IgG1 ratio changes from being constant at the beginning to increase in favour of IgG4 [156,159]. With respect to the drugs dosed at longer dosing intervals, Ig concentrations might decline over time after each drug administration (i.e. immunisation), hence potentially resulting in an ADA concentration-time profile analogous to a drug (in this case IFX). Lastly, the fact that, as functionally monovalent antibodies, IgG4 might not affect IFX in exactly the same manner as bivalent IgG1 classes, should be considered as well. Therefore, there is a need for a consensus in the scientific community on what ADA class(es) and subclass(es) should be monitored as predictors of the IFX therapy success and the loss of response.

Apart from the ADA status, concomitant therapy with immunomodulators was also identified as another significant covariate influencing IFX CL, with ~15% lower CL in patient who received immunomodulators compared to the ones that were not co-treated. Immunomodulators, such as methotrexate, have been in use for IBD long before the introduction of IFX and are known to contribute to disease stabilisation [160]. Thus, the mechanism underlying the effect of immunomodulators on IFX CL might be in part due to the IFX-independent therapeutic effect of these drugs, and subsequent relative reduction in disease activity and reduced IFX elimination through TMDD or other disease-

induced elimination pathways (e.g. GIT bleeding). In addition, immunomodulators hinder the development of ADA, and thereby presumably decrease IFX CL through ADA-binding. The latter mechanism would however be expected to be accounted for by ADA status as a covariate in the model.

In this analysis, potential effect of serum albumin and CRP concentrations on the IFX PK was investigated as well. Although albumin and CRP concentrations are both surrogates for IBD activity, tend to be correlated, and have shown correlation with IFX exposure, only the effect of albumin on IFX CL could be quantified with sufficient precision in this analysis and was thus retained in the model: IFX CL was found to decrease with increasing albumin concentration. It is important to note that, while albumin is considered a biomarker for IBD activity, its catabolism is highly correlated with the catabolism of IgG molecules [70], thus making albumin simultaneously a marker for the nonspecific CL of IFX. Finally, IFX CL increased with increasing body weight, assumingly related to the non-specific CL pathways.

3.2 Disease activity (bio)markers

One of the biggest challenges in the management and monitoring of IBD activity is identification of the most appropriate disease activity (bio)marker, making the clear goal of IBD treatment – clinical remission – difficult to quantify and monitor. A myriad of measures are used to assess IBD activity, from objective ones like endoscopy, to less specific ones like biomarkers, to complex, mostly symptoms-weighted scales like disease activity indices. Due to the high invasiveness of the procedure, endoscopy is unlikely to become a routine measure for IBD activity monitoring, thus bringing the biomarkers into the spotlight [161]. An appropriate disease marker should reflect both the effects of the drug and the current disease activity [162]. However, thus far no clear guidance on the advantage of clinical usage of one biomarker over the others has been made available and further investigations on the identification of the best marker for the IBD monitoring are warranted. A part of the herein reported work focused on investigations and comparison of routinely measured (bio)markers of IBD activity.

In *Paper II*, CRP and CDAI were assessed and compared as disease markers in patients with IFX treatment failure (i.e. non-responders). The IFX PK exposure metrics (AUC and C_{\min} for each dosing interval and cumulative AUC and mean C_{\min} from the 12 weeks of the study) were estimated from a previously developed PK model [107]. As response variables, CDAI values and CRP concentrations, their change from baseline and last visit, and response and remission outcomes at week 12 were investigated. The two disease activity markers were found to be only very weakly correlated, implying that at least one of them does not represent a true measure of the disease activity and/or that there is a potential time delay in their changes. Neither CDAI nor CRP were consistently and significantly related to any of the investigated exposure metrics, although trends of somewhat lower C_{\min} and AUC in non-responders were identified. In the case of CDAI, this finding is less surprising, since CDAI is by definition a subjective marker (e.g. accounting for abdominal pain and a patient's general well-being)

Results and Discussion

and fails to link it to endoscopic or biomarker data have been reported previously [20,48,163,164]. In fact, CDAI is no longer accepted by regulatory authorities (FDA and EMA) as a primary efficacy endpoint for CD trials [165]. This lack of exposure-response relationship for both CRP and CDAI could be ascribed to the fact that both investigated markers are nonspecific, especially from the perspective of anti-TNF α drug monitoring, and an ideal marker should be both disease- and drug-specific. However, these findings could potentially be due to the investigated population as well, for instance the fact that CDAI was part of the study inclusion criteria, and CRP concentrations being <LLOQ in almost 40% of the patients.

Since in non-responders the relationship between IFX and either CRP or CDAI response could not be established (*Paper II*), as the next step an evaluation of disease activity (bio)markers in a broader IBD population was undertaken (*Paper I*). In the study reported in *Paper I*, three disease activity measures were assessed: serum albumin and CRP concentration in all IBD patients, and HBI for CD patients. The exploratory analysis (Table 4) showed a statistically significant correlation between serum albumin and CRP concentrations, whereas HBI was not significantly correlated with either of the two biomarkers. Correlation of all three markers with IFX concentration was investigated as well. Similarly, HBI was the only marker that was not statistically significantly related to IFX, while albumin and CRP concentrations showed significant correlation (p -value $<10^{-4}$ and $<10^{-9}$, respectively). As HBI is, similar to CDAI, a subjective disease activity measure, these findings seem to support mutual correlation between the more objective markers (albumin and CRP) and emphasise the subjectivity of HBI. The correlation with IFX concentration was both the strongest and the most statistically significant in the case of CRP (Figure 9).

Table 4. Correlation among different disease activity markers and between disease activity markers and IFX concentration.

	Variable 1	Variable 2	Spearman's rank correlation ρ	p-value
Disease activity markers	albumin	CRP	-0.513 ^c	$2 \cdot 10^{-16}$
	CRP	HBI	0.093 ^a	0.181
	albumin	HBI	-0.161 ^a	0.022
C_{IFX} and disease activity markers	C _{IFX}	CRP	-0.347 ^b	$2 \cdot 10^{-10}$
	C _{IFX}	albumin	0.237 ^b	$2 \cdot 10^{-5}$
	C _{IFX}	HBI	-0.193 ^a	0.003

a: very weak correlation; b: weak correlation; c: moderate correlation.

C_{IFX}: Infliximab concentration; CRP: C-reactive protein; HBI: Harvey-Bradshaw Index.

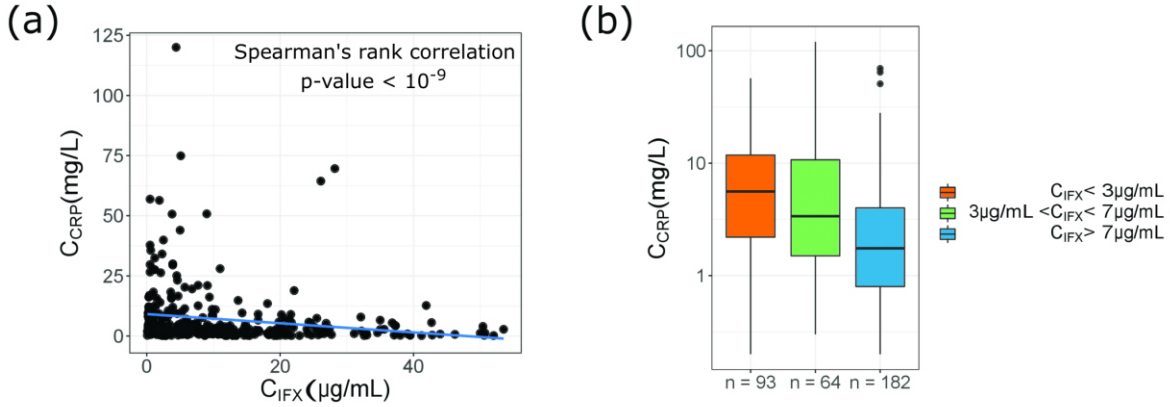


Figure 9. Relationship between infliximab (IFX) and C-reactive protein (CRP) concentration. (a) CRP concentration over IFX concentration; (b) Simplified representation, where IFX concentrations are stratified in 3 groups: ≤ 3 $\mu\text{g/mL}$, $3-7$ $\mu\text{g/mL}$, and >7 $\mu\text{g/mL}$ [78].

3.3 Infliximab exposure-disease activity response relationship

Based on the exploratory graphical and statistical analysis, in this population (see 2.1.1) CRP was found to be the disease activity marker best related to IFX exposure. Thus, as the next step, quantitative characterisation of IFX exposure-CRP concentration response relationship was undertaken (*Paper I*).

For the development of the PK/PD model, the sequential modelling approach was employed. Thereby, the individual parameters estimates (EBEs) from the PK model were extracted and the PK model parameters were fixed in the PK/PD model, while only the PD submodel was fit to the data. The PD model comprised a CRP turnover model, with an inhibitory effect of IFX on CRP synthesis described using an E_{\max} model, parametrised as follows:

$$\frac{dCRP}{dt} = k_{syn} \cdot \frac{I_{max} \cdot C_{IFX}}{IC_{50} \cdot e^{\eta_{IC50}} + C_{IFX}} - k_{deg} \cdot CRP(t)$$

$$k_{syn} = CRP_{baseline} \cdot e^{\eta_{CRPbaseline}} \cdot k_{deg}$$

, where CRP denotes CRP concentration, k_{syn} the zero-order CRP synthesis rate constant, I_{max} is the maximum effect (maximum percentage of CRP synthesis that can be inhibited by IFX), C_{IFX} the concentration of IFX, IC_{50} the concentration of IFX that leads to 50% of the maximum effect, k_{deg} the CRP degradation rate constant, $CRP_{baseline}$ the CRP concentration at baseline, η_{IC50} and $\eta_{CRPbaseline}$ between-patient variability in IC_{50} and baseline CRP concentration, respectively.

While the fixed-effects parameters of the PD submodel were precisely estimated, the estimation of the between-patient variability terms was supported by the frequentist prior approach. In the absence of prior quantitative knowledge on IFX-CRP relationship in IBD, the prior parameter estimates were taken from a PK/PD model of adalimumab in rheumatoid arthritis previously published by Ternant et al. [166]. Considering the similarity of the drugs and the fact that the two parameters in question were

Results and Discussion

between-subject variability in baseline CRP concentration and IC_{50} value, this model was deemed appropriate. Due to the need for use of a prior for precise estimation of the between-patient variability, covariate investigations were approached with caution and comprised graphical (EBEs vs. covariates plots) and statistical analysis, and implementation in the model in a uni- and multivariate manner. None of the investigated covariate models was stable or precisely estimated, and thus none of the investigated covariates (e.g. diagnosis, time since diagnosis, smoking status, number of surgeries, age at diagnosis) were retained in the final model. The parameter estimates of the final model are given in Table 2 (lower part), while Figure 10 shows the final graphical PK/PD model and VPCs for the PK and PD submodel.

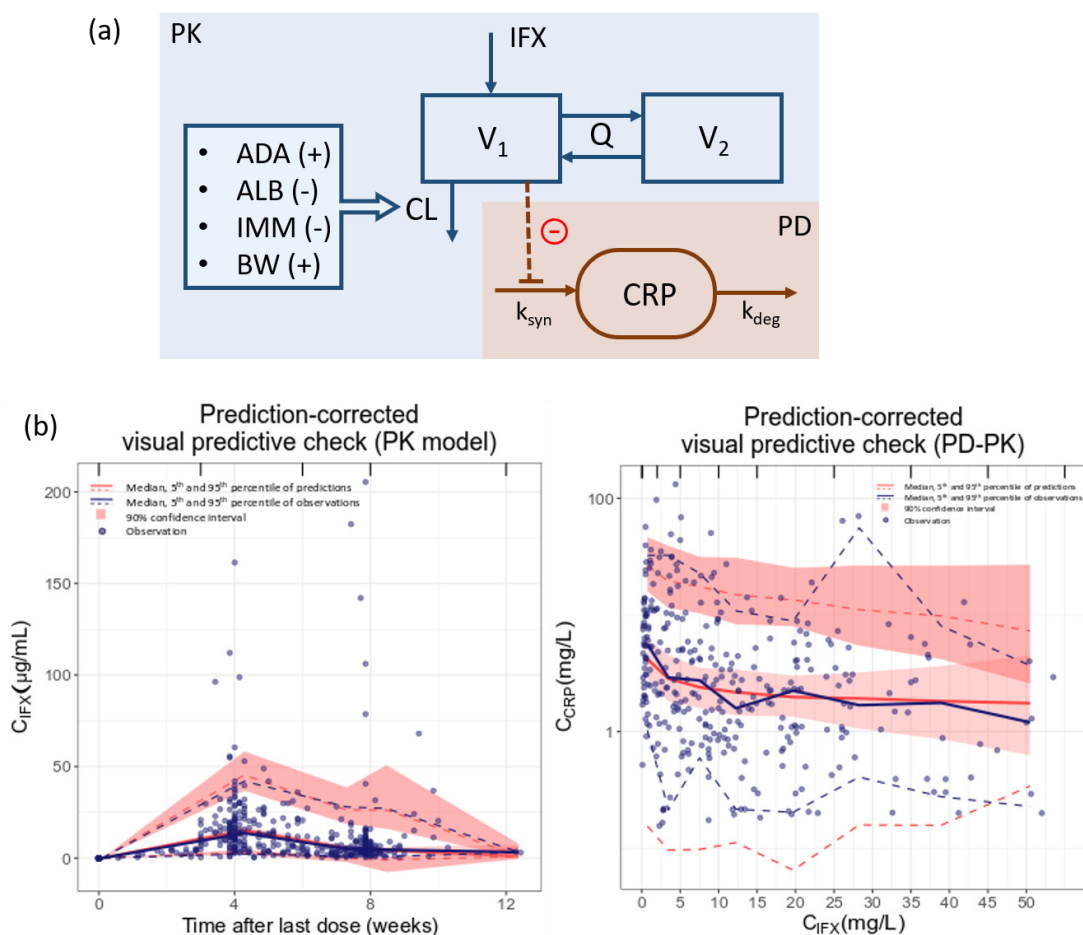
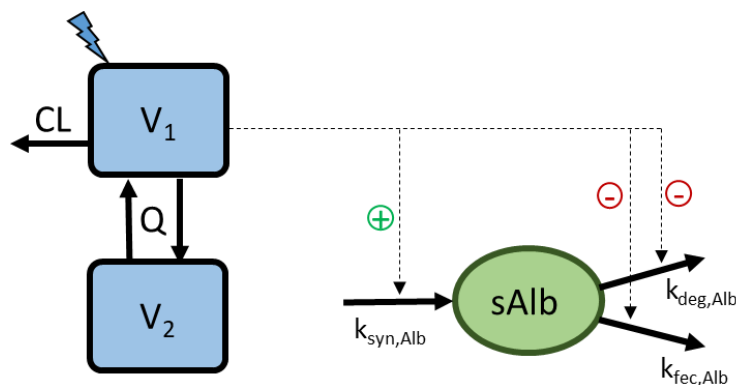


Figure 10. (a) Final graphical PK/PD model; (b) Prediction-corrected visual predictive check for the PK (left panel) and PD model (right panel). Blue dots denote observations, blue and red lines median (full line) and 5th and 95th percentile (dashed) of observations and simulations, respectively, shaded areas represent 90% confidence interval around median, 5th and 95th percentile of simulations. ADA: Anti-drug antibodies; ALB: Albumin; BW: Body weight; C_{IFX} : Infliximab concentration; CRP: C-reactive protein; IFX: Infliximab; IMM: Co-medication with immunomodulators; k_{deg} : CRP degradation rate constant; k_{syn} : CRP synthesis rate constant; PD: Pharmacodynamic(s); PK: Pharmacokinetic(s); Q : Intercompartmental flow; V_1 : Central volume of distribution; V_2 : Peripheral volume of distribution.

As an IBD biomarker, CRP concentration has certain advantages compared to the other routinely monitored biomarkers: it highly correlates to endoscopic findings [167], has high sensitivity and short reaction time (~19 h half-life), and its kinetic behaviour is well understood and independent of the present disease/health state [31]. These characteristics also provide some advantages when modelling CRP as a PD variable. Conveniently, the half-life of CRP is constant and unaffected by the IBD drugs or the disease itself, and thus the degradation rate constant did not require estimation, but could be fixed to the value corresponding to the CRP half-life, i.e. 0.0365 h^{-1} . Considering that IFX does not inhibit the synthesis of CRP directly, but through a cascade of events initiated by IFX-binding of TNF α and subsequent, and thus time-delayed, lower CRP synthesis, the indirect synthesis inhibition E_{max} model was assumed. Baseline (at the time of the first IFX administration) CRP concentration was estimated to be 6.32 mg/L (0.632 mg/dL), which was found plausible taking both published baseline CRP values (mean baseline CRP 1.88 mg/dL in patients with moderate to severe CD, with ~1/3 below 0.5 mg/dL [128]), and an in-house IBD database (baseline CRP median (range) 0.61 (0.02-10.25) mg/dL, n=76) as references for comparison. A high dispersion of individual baseline CRP concentration values (~115%CV, 5th-95th percentile range based on 1000 simulations: 1.503-28.4 mg/L) further supports the plausibility of this estimation, as it was anticipated in a diverse patient population as the one herein investigated. The model estimated the maximum possible degree of CRP synthesis inhibition by IFX to be ~72%, implying that ~28% of CRP synthesis cannot be inhibited by IFX, regardless of the administered dose. This is in accordance with mechanistic expectations, since TNF α is not a sole immunological initiator of CRP synthesis [31], and therefore even with a complete neutralisation of TNF α , CRP synthesis is not necessarily fully inhibited. Concentration of IFX leading to 50% of the maximum inhibition was estimated to be 2.04 $\mu\text{g/mL}$ – a value close to the commonly used PK C_{min} targets [78], while an IFX concentration of 18.4 $\mu\text{g/mL}$ was required to achieve 90% of the maximum inhibition. The between-patient variability in IC_{50} was estimated with a high precision to be very high (~209% CV), similar to the one recently reported for faecal calprotectin [108], potentially indicating a high difference in the inhibition of CRP synthesis even among the patients with a similar IFX exposure. As a clinically relevant consequence, in this case monitoring of CRP concentration would be arguably advantageous over monitoring the drug concentrations alone.

After the IFX exposure-CRP synthesis inhibition model had been developed, expansion of this model to include serum albumin as an additional biomarker, as well as development of a separate PK/PD IFX-albumin model were attempted. Taking into account the complex PK behaviour of albumin (see 1.1.3), a theoretical model of IFX effect on albumin was postulated (Figure 11). Since the data on the faecal loss of albumin were not available, the model was further simplified to remove this parameter (equation in Figure 11). This model and more simplified versions were investigated, both on top of the previously developed IFX-CRP model and as a separate IFX-albumin PK/PD model. None of the investigated models could be successfully fit to the data. This is likely due to the complexity of this model and the

sparsity of the available data, but potentially also endorses the weaker relationship between IFX and serum albumin compared to the IFX-CRP relationship, as discussed above.



$$\frac{dAlb}{dt} = k_{syn,Alb} \cdot \left(1 + \frac{S_{max,Alb} \cdot C_{IFX}}{SC_{50,Alb} + C_{IFX}} \right) - k_{deg,Alb} \cdot \left(1 - \frac{I_{max,Alb} \cdot C_{IFX}}{IC_{50,Alb} + C_{IFX}} \right) \cdot Alb$$

Figure 11. Assumed graphical PK/PD model of IFX PK (blue boxes) and its effects on albumin (green box), and equation of the simplified model. V_1 : Central volume of distribution; V_2 : Peripheral volume of distribution; Q : Intercompartmental flow; CL : Clearance; $k_{syn,Alb}$ denotes the albumin synthesis rate constant, $k_{deg,Alb}$ the albumin degradation rate constant, $S_{max,Alb}$ the maximum effect (stimulation) of IFX on albumin synthesis, $SC_{50,Alb}$ the concentration of IFX that leads to 50% of the maximum effect on synthesis, $I_{max,Alb}$ the maximum effect (inhibition) of IFX on albumin degradation, $IC_{50,Alb}$ the concentration of IFX that leads to 50% of the maximum effect on degradation, Alb serum albumin concentration, and $k_{fec,Alb}$ loss of albumin via faeces.

3.4 Assessment of dosing regimens with respect to CRP remission

The standard and alternative dosing regimens were evaluated by performing simulations from the developed IFX-CRP PK/PD model. As changing the dosing interval of IFX had been demonstrated to be advantageous over alterations of the administered dose [168], the investigated alternative dosing regimens differed from the standard dosing regimen only in the dosing interval, which varied from q4w to q12w. As ADA presence and co-medication with immunomodulators were identified as major covariates, they were taken into account in the simulations. Main results of these investigations are shown in Figure 12: The distribution of time to loss of CRP remission (“non-remission”; defined as CRP concentration > 5 mg/L) for ADA+ and ADA- patients with (upper panel) and without (lower panel) co-therapy with immunomodulators for all simulated dosing intervals is shown in Figure 12a; whereas a simplification, showing only median times to CRP non-remission, is presented in Figure 12b. In the figure, the number of patients experiencing loss of CRP remission at any point during a dosing interval is given below the corresponding boxes. More than 50% of ADA+ patients treated with the standard dosing interval (q8w) experienced CRP non-remission, independent of the co-therapy with immunomodulators. Concomitant immunomodulator use decreased this number in both ADA+ (from 74% in absence to 55% in presence of concomitant immunomodulators) and ADA- patients (from 10% in absence to 5% in presence of concomitant immunomodulators). While ADA- patients that are co-treated with immunomodulators, might not require intensification of dosing interval, for patients who

are ADA+ and/or do not receive immunomodulators, a shorter dosing interval is recommended: A better dosing regimen in terms of achieving CRP remission in ADA+ patients would be q6w and q5w in the cases with and without immunomodulators co-treatment, respectively, and for ADA- patients that do not receive immunomodulators q7w. The substantial impact of immunomodulators co-therapy on the IBD activity is in alignment with previous clinical reports of benefits of IFX-immunomodulators co-therapy, both in adults [71] and paediatrics [169], and might be due to a mix of effects [56], such as reduction of ADA production [71], or their independent therapeutic effect on IBD activity [170].

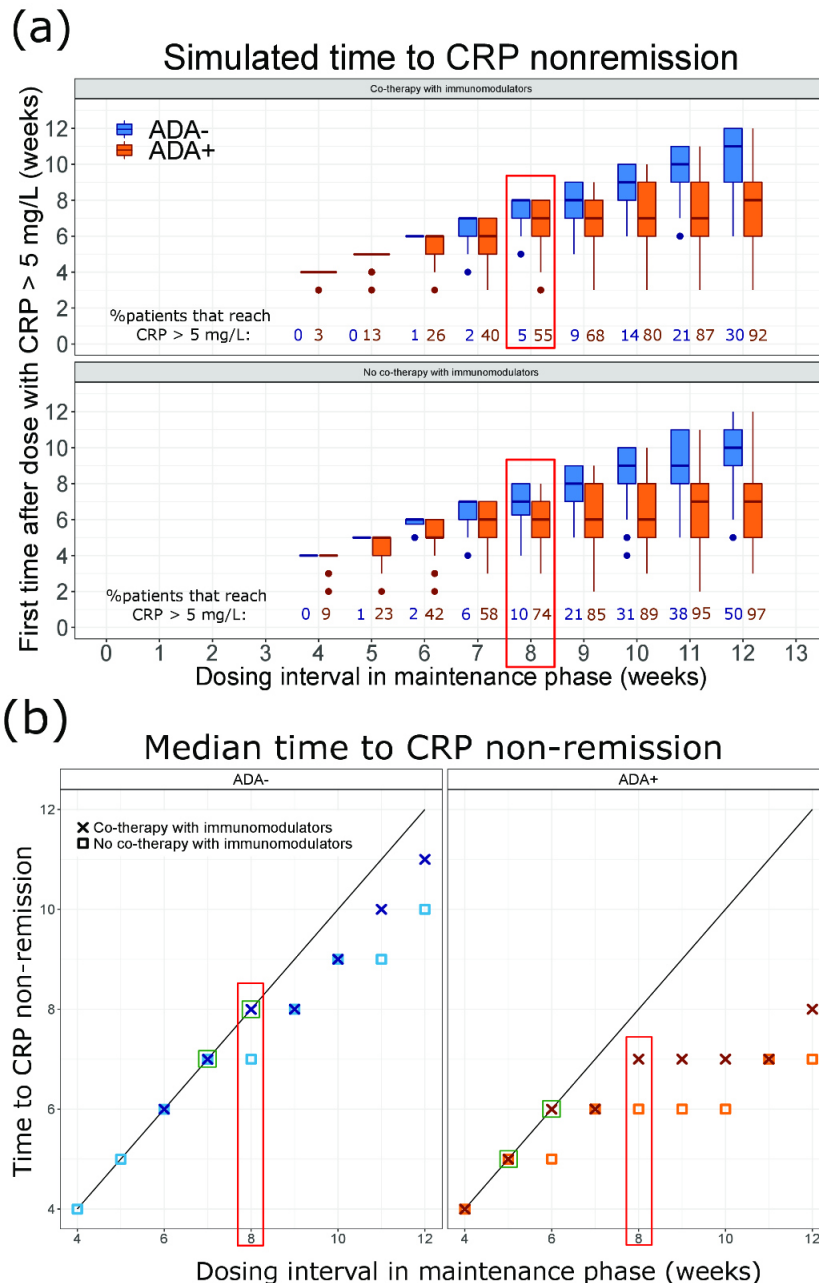


Figure 12. Evaluation of the standard and alternative infliximab (IFX) dosing regimens with respect to C-reactive protein (CRP) suppression via stochastic simulations ($n=1000$) of patients that differ only in anti-drug antibody (ADA) status. For the simulations, variability in the PK submodel parameters was considered. (a) Distribution of timepoints in weeks after 5th dose when CRP concentration reached 5 mg/L (“CRP non-remission”) as box-

Results and Discussion

whisker plot over simulated IFX dosing intervals, stratified by ADA status and co-therapy with immunomodulators. Note that the virtual patients that do not experience CRP concentrations above 5 mg/L (i.e. without loss of CRP remission) are not included in the plot. Proportions of patients experiencing CRP nonremission (shown below each box) are higher in cases of ADA development and absence of co-therapy with immunomodulators; (b) Simplification showing only the median time after the 5th dose when CRP concentration reached CRP nonremission stratified by ADA development and immunomodulatory co-therapy. In presence of co-therapy with immunomodulators, the standard IFX dosing interval of every 8 weeks (q8w) corresponds to median time to CRP nonremission in ADA- patients, whereas for ADA+ patients reduction to q6w is to be recommended. In absence of co-therapy with immunomodulators, for ADA- patients dosing interval of q7w corresponds to median time to CRP nonremission, whereas for ADA+ patients further reduction to dosing interval of q5w should be preferred. Red frame: standard IFX dosing regimen every 8 weeks.

3.5 Clearance of monoclonal antibodies: Cetuximab case study

PK model development

A complex PK behaviour characteristic for mAbs, including TMDD, non-specific elimination and potential time-variance, presumably requires highly informative data to be mechanistically described. A general limitation observed throughout the herein reported work, as well as in previously published modelling and simulation analyses in the IBD area, was sparsity and thus limited informativeness of the analysed data. In order to provide a better understanding of the impact of data, i.e. clinical study design the data originate from, on the results of modelling analyses, the following analysis was performed. For this type of investigations, a sufficiently rich dataset containing highly informative data was essential, which was acquired by pooling two clinical trials of cetuximab (Erbix[®]; Merck KGaA, Darmstadt, Germany), an oncology anti-epidermal growth factor receptor (EGFR) mAb. Cetuximab was deemed an appropriate case study drug, not only due to the availability of the rich data, but also because of the fact that previously published PK models of cetuximab [129-131] show disagreement in CL models, warranting further investigation.

As a first step, a PK model was developed based on the totality of the available data, with focus on the CL model. The parameter estimates for the six investigated models are given in Table 5, while Figure 13 shows the goodness-of-fit plots. A 2-compartment model with parallel Michaelis-Menten and linear CL that changes exponentially over time (MMCL+TVARCL model) performed best in describing the data. As anticipated, addition of body surface area (via power function with exponent fixed to 0.75 and 1 for effect on CL and volumes of distribution, respectively) was found to significantly decrease OFV and slightly reduce between-patient variability and RUV. Thereafter, age, sex, RAS mutation status, creatinine CL, dose group, co-medication with irinotecan or 5-fluorouracil/folic acid, and serum concentrations of amphiregulin, epidermal growth factor, IL-8, transforming growth factor- α , and vascular endothelial growth factor, and Eastern Cooperative Oncology Group performance status were

pre-selected and assessed as covariates on CL using full fixed-effects modelling approach. None of these covariates were found to be statistically or clinically relevant.

Table 5. Comparison of the six investigated nonlinear mixed-effects base models of cetuximab, that differ in captured clearance (CL) mechanisms: linear CL (LCL), time-varying linear CL (TVARCL), nonlinear Michaelis-Menten CL (MMCL), parallel nonlinear and linear CL (MMCL + LCL), parallel nonlinear and time-varying linear CL (MMCL + TVARCL), and parallel linear and zero-order elimination (LCL + 0.EL).

	LCL	TVARCL	MMCL	MMCL + LCL	MMCL + TVARCL	LCL + 0.EL
LCL, L/h (RSE%)	0.0222 (3)	0.0262 (3)	-	0.0153 (4)	0.0174 (5)	0.0206 (-)
V ₁ , L (RSE%)	3.84 (3)	3.67 (3)	3.75 (3)	3.71 (2)	3.65 (3)	3.82 (-)
Q, L/h (RSE%)	0.0188 (17)	0.0282 (12)	0.0332 (19)	0.0323 (4)	0.0368 (5)	0.0216 (-)
V ₂ , L (RSE%)	3.38 (12)	1.65 (11)	2.67 (8)	3.25 (6)	2.65 (4)	3.31 (-)
K _M , mg/L (RSE%)	-	-	283 (26)	9.81 (5)	13.3 (21)	-
V _{max} , mg/h (RSE%)	-	-	9.48 (17)	0.882 (5)	0.861 (5)	-
I _{max} , % (RSE%)	-	-19.6 (16)	-	-	-23.1 (20)	-
T ₅₀ , weeks (RSE%)	-	7.26 (15)	-	-	20.5 (29)	-
γ (RSE%)	-	2.54 (24)	-	-	1 FIX	-
K ₀ , mg/h (RSE%)	-	-	-	-	-	0.0472 (-)
η _{LCL} , CV% (RSE%)	38.3 (6)	36.6 (6)	-	37.9 (8)	36.1 (23)	39.4 (-)
[Shr%]	[6]	[6]	-	[19]	[23]	[8]
η _{V1} , CV% (RSE%)	26.8 (11)	27.3 (10)	26.4 (15)	25.9 (11)	26.2 (10)	27.4 (-)
[Shr%]	[31]*	[31]	[32]	[32]	[32]	[32]
η _{V2} , CV% (RSE%)	103.9 (13)	84.1 (9)	83.4 (17)	61.2 (9)	61.3 (14)	104.4 (-)
[Shr%]	[27]	[39]	[29]	[27]	[32]	[29]
η _{Vmax} , CV% (RSE%)	-	-	30.5 (9)	43.6 (10)	48.8 (12)	-
[Shr%]	-	-	[6]	[34]*	[12]*	-
η _{Tmax} , CV% (RSE%)	-	25.2 (11)	-	-	51.5 (18)	-
[Shr%]	-	[29]	-	-	[35]	-
η _{K0} , CV% (RSE%)	-	-	-	-	-	150.3 (-)
[Shr%]	-	-	-	-	-	[57]
Additive RUV, mg/L (RSE%)	9.44 (11)	7.79 (12)	8.14 (13)	5.85 (12)	4.85 (22)	8.65 (-)
Proportional RUV, CV% (RSE%)	23.1 (5)	22.8 (4)	23.4 (5)	24.0 (4)	23.5 (4)	22.9 (-)

0.EL, zero-order elimination; AIC, Akaike information criterion; η, between-patient variability; γ, curve shape factor; K₀, zero-order rate constant of elimination from central compartment; K_M, Michaelis-Menten rate constant; LCL, linear clearance; I_{max}, maximum change in time-varying clearance; MMCL, Michaelis-Menten clearance; Q, intercompartmental exchange rate; RSE, relative standard error; RUV, residual unexplained variability; Shr, shrinkage; T₅₀, time at which clearance is halved; TVARCL, time-varying linear clearance; V₁, central volume of distribution; V₂, peripheral volume of distribution; V_{max}, maximum rate of saturable elimination.

The final (MMCL+TVARCL) PK model comprised parallel nonlinear and time-varying linear CL, implying both exposure- and time-dependency. The baseline linear CL of 0.0174 L/h decreased exponentially to a mean maximal decrease of ~18% (155 %CV) with a half-time of ~5 months. Half of the maximal rate of nonlinear CL of 0.861 mg/h was reached at cetuximab concentration of 13.3 mg/L. As TMDD (represented via MMCL) results from drug-target binding, the contribution of TMDD to overall CL depends on the mAb concentration. In this study, at very low drug concentrations, where the assumption $C_{\text{cetuximab}} \ll K_m$ is reasoned, the nonlinear CL was approximately 4x higher than baseline linear CL (Figure 14).

Results and Discussion

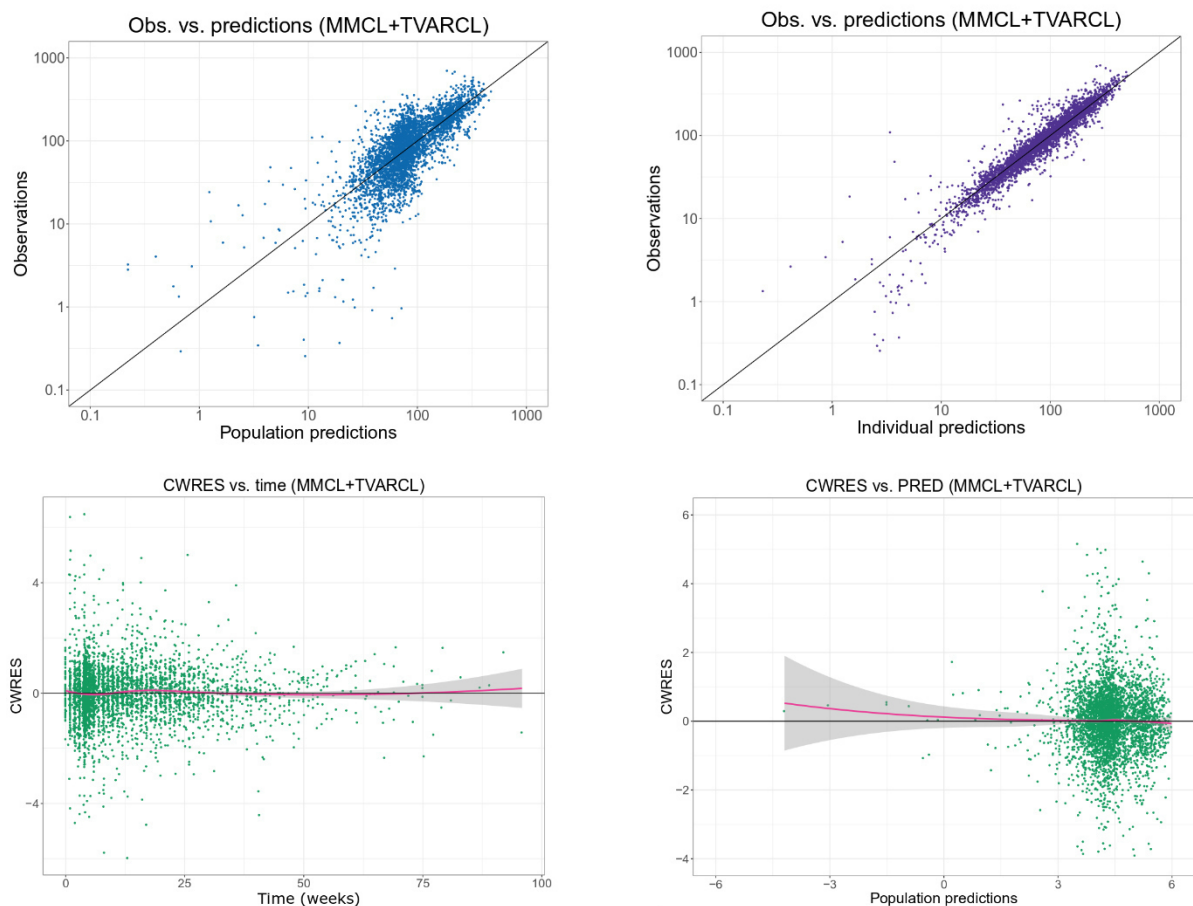


Figure 13. Goodness-of-fit plots for the final cetuximab PK base model.

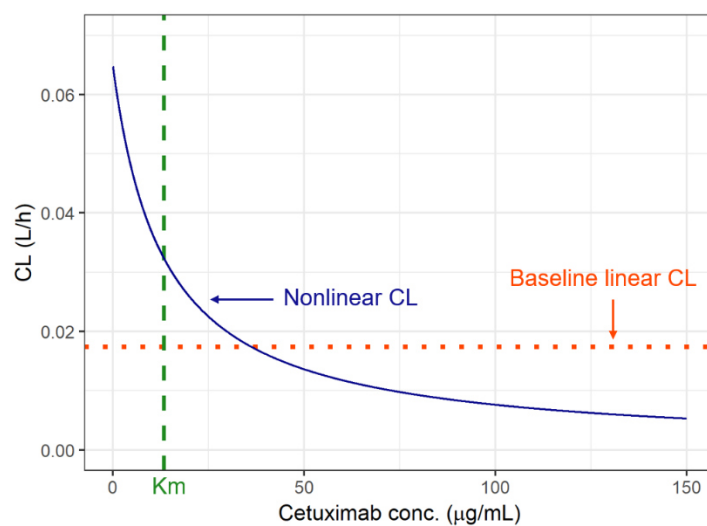


Figure 14. Illustration of the contribution of the nonlinear CL (target-mediated drug disposition) to cetuximab CL: At very low cetuximab concentrations ($C_{\text{cetuximab}} \ll K_m$) the nonlinear CL was approximately 4x higher than baseline linear CL. CL: Clearance; K_m : Concentration at half-maximal rate of saturable elimination.

Such a model with three CL components – linear, nonlinear and time-effect – has not been reported before. In the studies by Azzopardi et al. [131] and Dirks et al. [130] the cetuximab elimination was best described by LCL+0.EL and MMCL model, respectively. The latter study identified no time-dependency of the cetuximab CL, contrary to the herein reported findings. A potential explanation for this disagreement might lie in the differences in the investigated populations or the study designs. Namely, the median follow-up in the study analysed by Dirks et al. was approximately 6 weeks, significantly shorter than in the herein analysed population (~23 weeks), which might have been insufficient to inform identification of the time change of CL.

While the nonlinear CL of mAbs is a well-established and mechanistically sound concept [70,171,172], the time-dependency is a recent, yet not fully understood one, so far mainly reported in context of oncology mAbs [173-176]. To shed some light on the mechanisms of the time effect (Figure 15), the magnitude of CL change was compared between responders (the patients with complete or partial response) and non-responders (the patients with stable or progressive disease) [173,175,177]. In both patient groups, an initial decrease of CL was observed, however it was of higher extent in responders than non-responders, consistent with the previously reported studies. A study by Krippendorff et al. [178] demonstrated that administration of an anti-EGFR drug leads to an initial decrease in target activation due to drug-target binding, and a subsequent increase as drug exposure decreases. This is anticipated for both responders and non-responders. In responders, the decline continues, while in non-responders the increased disease burden becomes predominant, resulting in eventual CL increase in non-responders. Overall, this effect of the disease status on PK is likely due to a mix of mechanisms, that are hypothesised to include cancer-related cachexia [176], i.e. a higher protein turnover rate due to inflammation [70]. Over time, in responders the disease state improves, leading to normalisation of the protein turnover, and thereby a decrease in nonspecific, linear, elimination of the mAb.

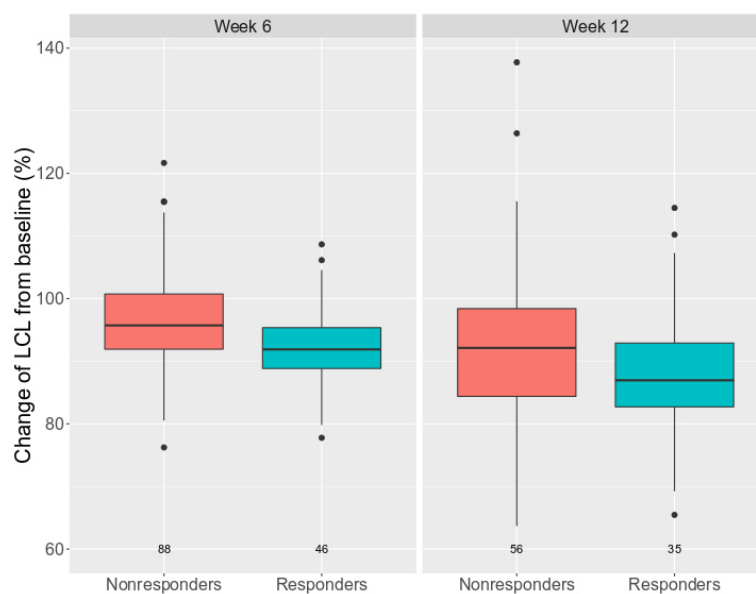


Figure 15. Change of linear CL from baseline at weeks 6 and 12, stratified by post-treatment response.

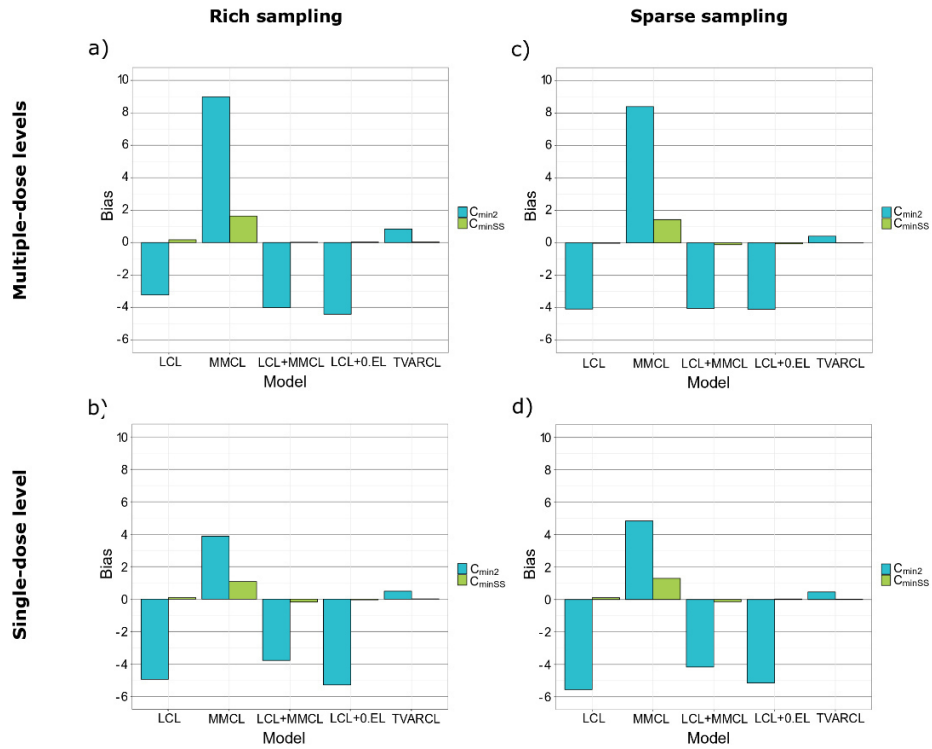
Study design investigations

“Models are representations of a ‘system’” [92], i.e. reality – in pharmacometric analyses of systems described by the collected clinical data. Thus, it is implied that a model’s “resolution”, i.e. the complexity and mechanistic detail that can be captured by the model, is fully dependent on the data. The first part of this analysis demonstrated this, by enabling development of the most complex CL model yet published for cetuximab through a rich dataset, e.g. in terms of the number of included patients, the range of investigated dose levels, and the density of the PK sampling in the population. In the second part of the analysis, the characteristics of a clinical dataset (number of dose levels [single vs. multiple dose levels] and sampling density [rich vs. sparse sampling]) relevant for characterisation of a mAb CL model were further assessed in order to evaluate and inform clinical study designs.

The first approach herein applied was comparison of bias [133] in parameter estimates of the final (MMCL+TVARCL, i.e. reference) model across the four above described study designs (*Paper III*). To this end, in the case of single-dose level and/or in particular sparse sampling, the bias increased, especially in parameters related to nonlinear, Michaelis-Menten CL. This is in accordance with mechanistic expectations, since the nonlinear CL is saturated at a high drug exposure, and thus heavily dependent on presence of lower drug exposure which might not be well captured with single dose level data. Furthermore, sparse sampling will unquestionably be less informative for the parameter estimation in general, including the Michaelis-Menten CL parameters, even in presence of multiple dose levels.

The second approach investigated was “multi-dimensional” – performed across the four study designs and different (‘true’ MMCL+TVARCL and alternative) CL models, and through assessment how these differences reflect on the most often used exposure metrics (C_{\min} and AUC early in the treatment and at steady state). The effect of study design was of a higher extent for bias than RMSE (i.e. accuracy; Figure 16, Figure 17). In general, a greater and clearer impact of the sampling density was observed compared to the number of dose levels. Furthermore, the effect of study design differed among different exposure metrics. Focusing on the seemingly more relevant study design characteristic, i.e. the sampling density, the impact was found to be of a lesser extent for bias in C_{\min} than for bias in AUC. This can be explained by the higher complexity of AUC, which takes into account exposure over a time period, than C_{\min} , which focuses on a single time point equally informed by all study designs. Additional sampling apart from the end of a dosing interval, particularly near C_{\max} , is necessary to properly inform AUC. Interestingly, bias in both metrics and for all compared models was overall lower in the case of single dose level, compared to multiple dose level designs. The best alternative to the true model depended on the exposure metric, but was in most cases TVARCL model, which disregards the nonlinear CL component. This is further in agreement with the above reported finding of the nonlinear CL parameters of the true, MMCL+TVARCL, model being the most sensitive to the study design changes. When it comes to the comparison of exposure metrics, C_{\min} at steady state was found to be the most robust.

Panel I



Panel II

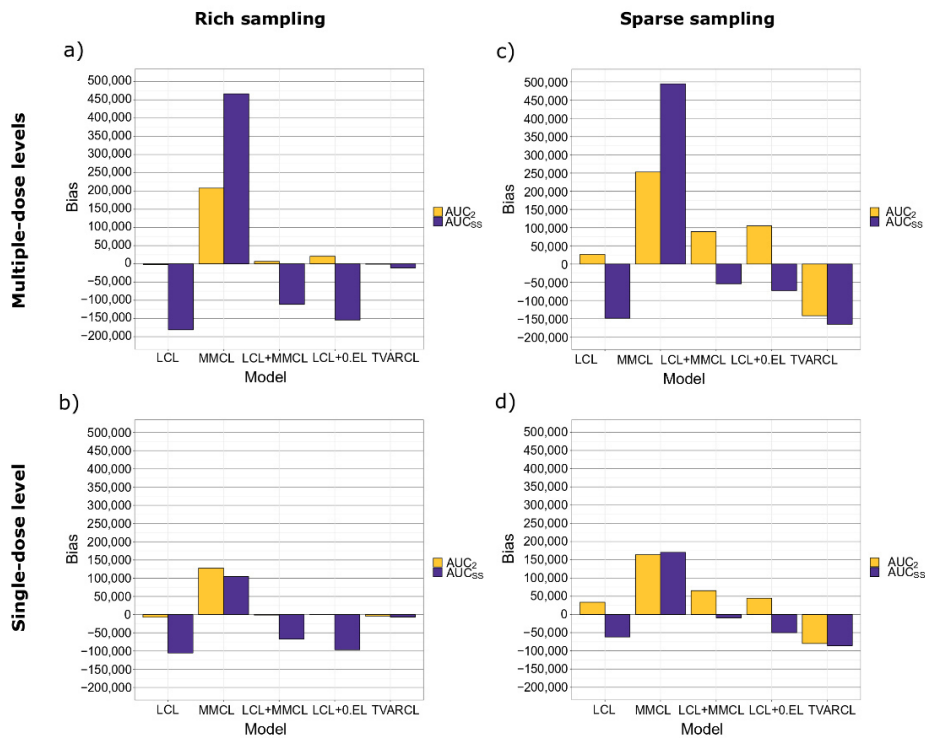
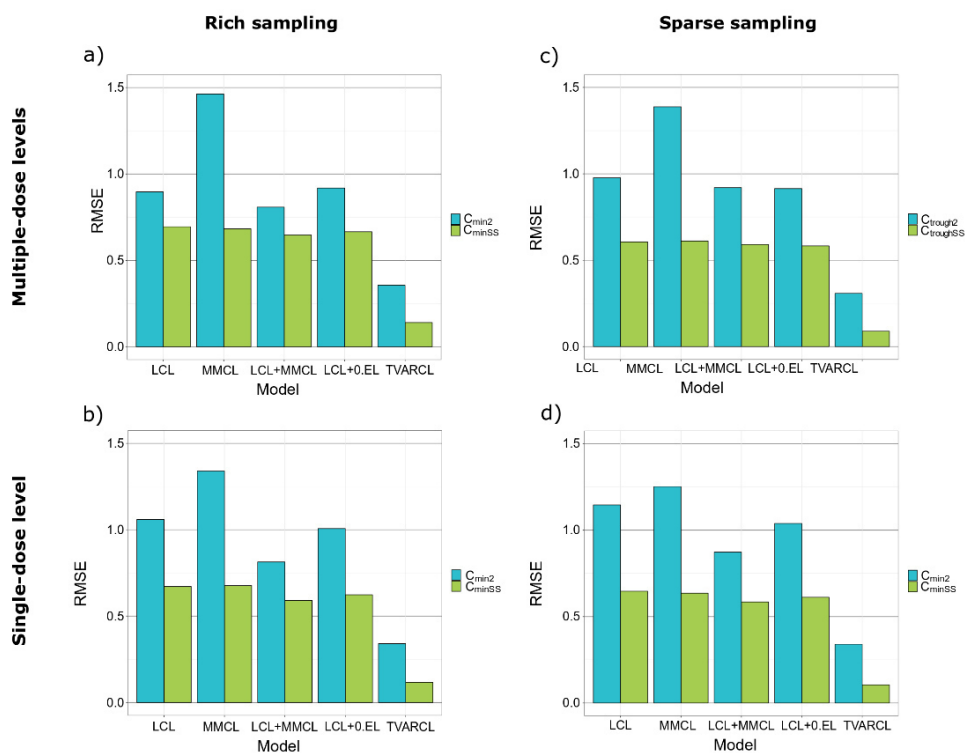


Figure 16. Bias in minimum concentration (Panel I) and area under the concentration-time curve (Panel II) after the second ($C_{min,2}$, AUC_2) dose and at steady state ($C_{min,SS}$, AUC_{SS}) compared to reference MMCL + TVARCL model. (a) Study design A: multiple-dose levels and rich sampling; (b) Study design B: single-dose level and rich sampling; (c) Study design C: multiple-dose levels and sparse sampling; (d) Study design D: single-dose level and sparse sampling. 0.CL, zero-order clearance; LCL, linear clearance; MMCL, Michaelis-Menten clearance; TVARCL, time-varying linear clearance.

Results and Discussion

Panel I



Panel II

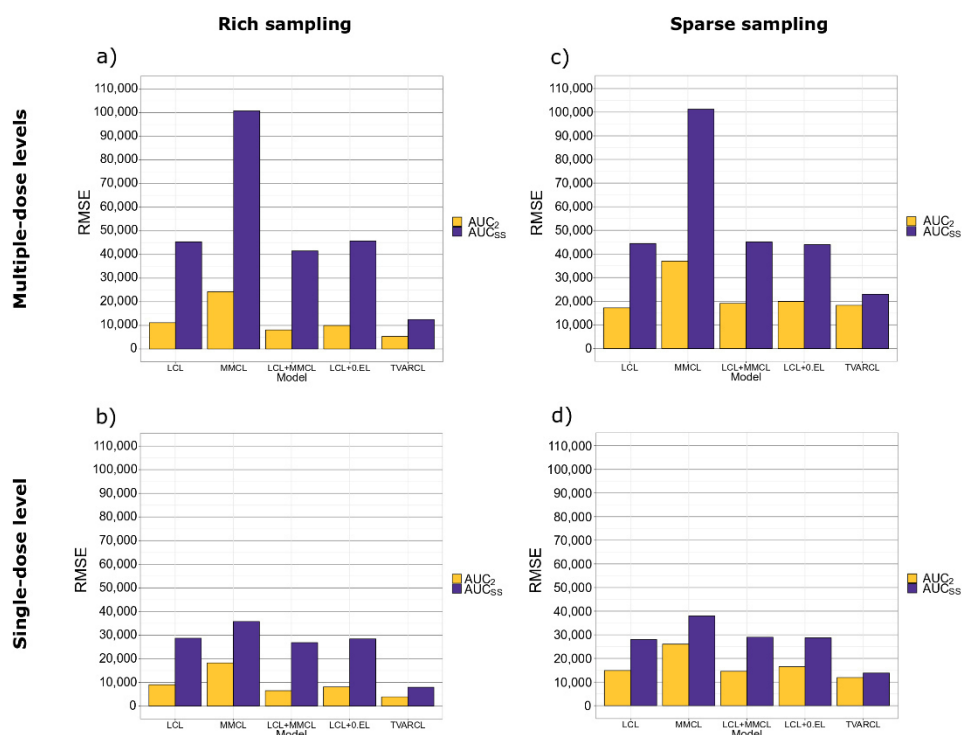


Figure 17. Accuracy in minimum concentration (Panel I) and are under the concentration-time curve (Panel II) after the second ($C_{min,2}$, AUC_2) dose and at steady state ($C_{min,SS}$, AUC_{SS}) compared to reference MMCL + TVARCL model. (a) Study design A: multiple dose levels and rich sampling; (b) Study design B: single dose level and rich sampling; (c) Study design C: multiple dose levels and sparse sampling; (d) Study design D: single dose level and sparse sampling. 0.CL, zero-order clearance; LCL, linear clearance; MMCL, Michaelis-Menten clearance; RMSE, root mean squared error; TVARCL, time-varying linear clearance.

3.6 Effect of pregnancy on infliximab pharmacokinetics

In special populations, such as children or pregnant women, PK of mAbs is expected to be altered due to physiological and mechanistic reasons [179]. The anti-TNF α drugs belong to pregnancy category B according to the FDA, meaning that whether they can cause harm to a foetus or not is not yet known and that there is no documented human toxicity. In other words, according to the FDA, it is justified to administer drugs from this group to a pregnant patient if undoubtedly needed [180,181]. Various authority bodies, institutions and organisations classify IFX differently in regard to the safety of its use during pregnancy and their recommendations are rather inconsistent. In the European Crohn's and Colitis Organization guidelines IFX is labelled as "probably safe" [52]; the Australian TGA classifies the drug in category C, among the drugs that, based on their pharmacological effects, have been shown to cause or have potential to cause harmful (potentially reversible) effects on the foetus, without causing malformations [182]. With respect to this, a clinical strategy for reduction of the foetal exposure is ceasing the IFX therapy in the third trimester, since IFX crosses the placenta most efficiently during later pregnancy trimesters [183,184]; however, the decision on whether to continue the therapy or not is made on an individual basis [183,185].

Studies assessing the PK of mAbs during pregnancy are very scarce, with only one report comparing the PK of IFX in presence and absence of pregnancy [186], excluding papers discussing possible general pregnancy-induced PK changes. Due to the lack of IFX (and mAbs in general) clinical data from pregnant patients, most aspects of mAbs PK/PD in pregnancy remain unexplained [52]. Theoretically, the pregnancy could affect mAb PK and/or PD in several ways. It is well known that IgG molecules cross the placenta throughout the second and the third trimesters of pregnancy. At the very beginning of the pregnancy, the transfer is negligible, because the continuous and compact FcRn-free inner layer of cells (cytotrophoblast) prevents penetration of IgG. By the end of the first trimester FcRn is increasingly present in the outer cell layer of the placenta (syncytiotrophoblast). Over time, the syncytiotrophoblast expands and the cytotrophoblast layer becomes discontinuous. As a consequence, the area for IgG transport grows, access to foetal vessel endothelium is enabled, and IgG molecules are internalised into the syncytiotrophoblast by endocytosis. In the endosome, the FcRn can bind the IgG molecules and release them at the basal membrane, which has neutral pH. The IgG can then pass through the basal lamina directly to the foetal vessel endothelium, thanks to the vasculosyncytial zones present in the terminal villi, in which sinusoids of foetal capillaries lie beside the syncytiotrophoblast (not separated by stromal cells) [52,184,187,188].

Overall, the rate of the transplacental transport increases exponentially with pregnancy duration and reaches its maximum around the 28th gestational week [189]. Due to the active transport and a long half-life, the IFX concentration in the neonates is often higher than in the maternal blood. This "trapping"

Results and Discussion

phenomenon has been supported by studies that report IFX concentration in the umbilical cord blood to be 98%-400% of the maternal level. Furthermore, the drug is detectable in the neonates for up to 9 months after delivery [184,185,187,190-193]. Another potential effect of pregnancy is immunity related. Namely, pregnancy is accompanied by modifications of the maternal immune system. As a dysregulated immune response is one of the aetiological factors of IBD, this could also influence the disease status and IFX therapy. In the first trimester, a strong inflammatory response, needed for implantation and formation of the decidua and the placenta, develops. It is characterised by infiltration and accumulation of NK cells, dendritic cells and macrophages in the decidua. As the foetus enters the phase of rapid growth and development, an anti-inflammatory state is promoted. Finally, when the foetal development is over, once again a proinflammatory state, crucial for the delivery, is induced [52,53]. Apart from these immunological changes, the TNF α concentration increases throughout the pregnancy, reaching maximum at the onset of the labour [184]. This could be one of the mechanisms of potential IFX PK/PD changes, since TMDD contributes to the IFX elimination and with an increased target concentration this effect could be of importance. Another characteristic of pregnancy consists of body water changes, that could cause alterations in the IFX distribution. In pregnancy, blood flow and volume are increased. Plasma volume can rise for up to 50% (increase of ~1200-1600 mL compared to pre-pregnancy values) and extracellular volume increases by 30%-50%. These differences could theoretically influence PK/PD of IFX, especially since volume of distribution of IFX is limited to intravascular and extracellular fluid [52,54,194]. Due to the fact that IFX is dosed based on body weight, it is difficult to predict the overall effect without clinical data. One proposed hypothesis is that in pregnancy higher doses are required, because volume of central compartment of IFX increases proportionally to body weight [52]. Furthermore, if the above mentioned potential alterations indeed lead to differences in IFX concentrations in pregnancy, it could also reflect on frequency and extent of development of ADA, that in turn would further affect the IFX elimination, as ADA-mediated elimination is one of important elimination pathways of the drug [52]. Finally, hormone (oestrogen and progesterone)-induced GIT changes, such as smooth muscle dysfunction, are more frequent in women with pre-existing GIT diseases, including IBD [54].

The importance and effects of TNF α for the human foetus are not fully understood, but it is known that TNF α takes part in protection of the embryo from birth defects. This role of TNF α raises concerns about the use of the anti-TNF α drugs during pregnancy, since inhibiting TNF α and its protective effects could theoretically increase the risk of birth anomalies. At the same time, approximately 30% of women with IBD experience disease flares during pregnancy. The flares themselves carry a risk of adverse birth outcomes, with high TNF α concentrations being associated with an increased risk of infections during pregnancy, more frequent foetal growth retardations and spontaneous abortions [52,184,195]. Since IFX does not cross-react with other species, only developmental toxicity studies in cynomolgus monkey have been performed. These studies showed no teratogenic effect [180,183,184]. The safety of use of

the anti-TNF α drugs in the human pregnancy has been assessed previously, but there are large discrepancies between conclusions of different studies, ranging from “safe” [52,181,183,190,191,196], to “inconclusive” [184], to “not safe” [189]. Overall, taking into account the risks of an uncontrolled disease on both the pregnant patient and the foetus, it seems that the benefits of IFX use in the pregnancy outweigh the risks. The possible IFX-induced effects on the child’s immunity (i.e. a possibility of immunosuppression) should however be taken into account, even though the data so far suggest that a serious immune deficit is highly unlikely. According to the guidelines, live-virus vaccines are considered contraindicated in patients receiving biological therapy, whereas in the newborns that were exposed to IFX *in utero* the vaccines should be postponed until IFX in the infant becomes undetectable [187,192].

The analysis reported in *Paper IV* investigated IFX PK in pregnancy based on routinely collected PK samples from pregnant IBD patients. Of 23 pregnancies documented, 2 miscarriages and 1 birth with a congenital abnormality were recorded, while other 20 pregnancies ended with healthy births. These results seem in accordance with the above mentioned findings, however due to the limited size of the population no further analysis or inferences regarding IFX safety in pregnancy were made.

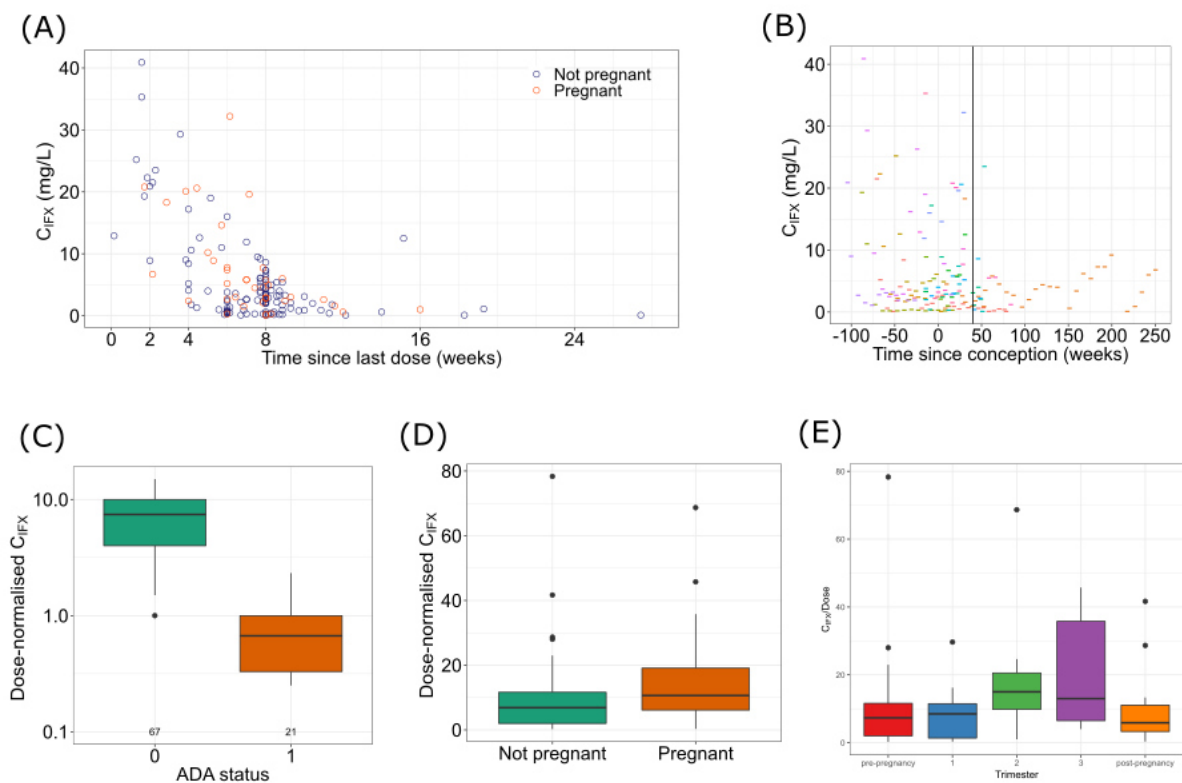


Figure 18. Exploratory analysis: Infliximab concentration (C_{IFX}) since last dose (A) and since conception (B); and dose-normalised C_{IFX} per ADA status (C), pregnancy status (D), and per trimester (E).

In accordance with the trends observed during statistical and graphical analyses (Figure 18), the population PK analysis identified changes of IFX CL in pregnancy. The model that described the data

Results and Discussion

best (Figure 19) was a 1-compartment model with linear elimination, and ADA and (the second and the third) trimester of pregnancy as covariates on CL. Table 6 shows respective parameter estimates of the model. The presence of ADA resulted in a 69% increase of IFX CL. No CL change was detected in the first trimester of pregnancy, whereas a decrease of 12% was identified in the second and the third trimesters. An attempt was made to segregate the changes in the second and the third trimester, but, although a trend (11% and 15% decrease, respectively) was observed, acceptably precise estimation could not be achieved, likely due to the sparseness of the sampling and absence of IFX dosing in the third trimester. Pre-selected covariates (body weight, co-therapy with immunomodulators, diagnosis, serum albumin concentration, platelet and white blood cell counts) were investigated on top of ADA and trimester effect, but none were found to have a significant impact on IFX CL. Finally, the development of ADA was not observed to be impacted by pregnancy (Table 7).

Table 6. Parameter estimates of the final PK model of IFX in pregnancy.

Clearance, L/d	0.608 ^a
Volume of distribution, L	18.2 ^a
Effect of ADA on clearance ^b	0.685 ^a
Effect of 2 nd /3 rd trimester on clearance ^b	-0.121 (56)
Interpatient variability in clearance, CV% (RSE%) [Shrinkage]	30.7 (28) [23]
Interpatient variability in volume of distribution, CV% (RSE%) [Shrinkage]	53.3 (30) [23]
Residual unexplained variability, µg/mL (RSE%) [Shrinkage]	0.371 (13) [6]

^aparameter value fixed to the final estimate from the initial model;

^bthe covariate effects on clearance were defines as: $CL = CL_{typical} \cdot (1 + Effect\ of\ ADA\ on\ clearance) \cdot (1 + Effect\ of\ \frac{2^{nd}}{3^{rd}}\ trimester\ on\ clearance)$

Table 7. Incidence of ADA in different periods of the study (pre-, post-pregnancy, and in each trimester).

	n _{samples,total}	n _{samples,ADA+}	ADA+ (%)	p-value* (vs. pre-pregnancy)
Total	137	41	29.9	-
Pre-pregnancy	91	24	26.4	-
1 st trimester	17	8	47.1	0.15
2 nd trimester	13	4	30.8	1.00
3 rd trimester	4	2	50	0.64
Post-pregnancy	12	3	25	1.00

*p-value as per Yates chi-squared test

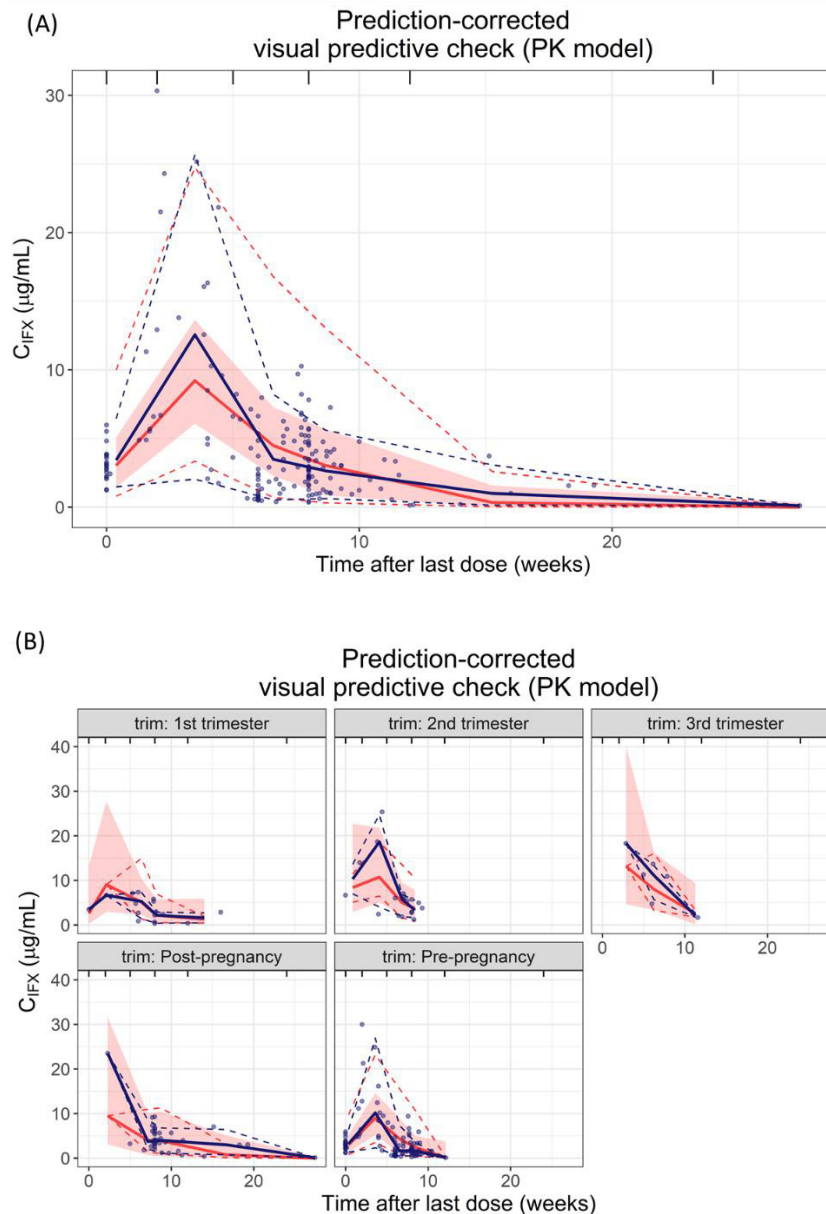


Figure 19. Prediction-corrected visual predictive check for the final pharmacokinetic (PK) model of infliximab in pregnancy for all data (A) and per (non)pregnancy phase (B). Full lines are median and dashed lines 5th and 95th percentile of observations (blue lines) and simulations (red lines); red dashed areas denote the 90% confidence interval around the median of the simulated data; blue dots denote observations.

These findings are in accordance with the report of Seow et al. [186] that previously addressed IFX PK in pregnancy. The herein reported analysis was designed to identify and quantify potential pregnancy-related IFX PK changes, however the mechanisms underlying these phenomena remain unclear. It is known that the placental syncytiotrophoblast sheds into the maternal circulation [197-200], from approximately the 6th week of pregnancy [198,200] until delivery. Furthermore, viability and certain level of “left-over” functionality of the shed cell parts have been identified [201,202], although FcRn has not been investigated in this context. One potential hypothesis is that the FcRn on shed

syncytiotrophoblast parts might maintain some level of functionality, thus prolonging the half-life of IFX in the maternal circulation upon shedding (Figure 20). Another relevant aspect might be the change in the endogenous IgG concentration. Namely, the endogenous IgG concentration is known to gradually decrease over pregnancy – potentially as a part of the immunosuppressive effect of pregnancy, reaching the lowest concentrations in the third trimester [203,204]. Since the relationship between the IgG concentration and IgG half-life is inversely proportional (due to the saturability of FcRn), and the fact that endogenous and exogenous (e.g. IFX) IgG molecules share the same kinetic pathways, an increase in half-life of both endogenous and therapeutic IgG is anticipated. Of note, therapeutic mAbs, even at the highest therapeutic concentrations, have a negligible contribution to the total IgG concentration [205]. Further studies are warranted to dissect the mechanisms of pregnancy-induced mAb PK changes.

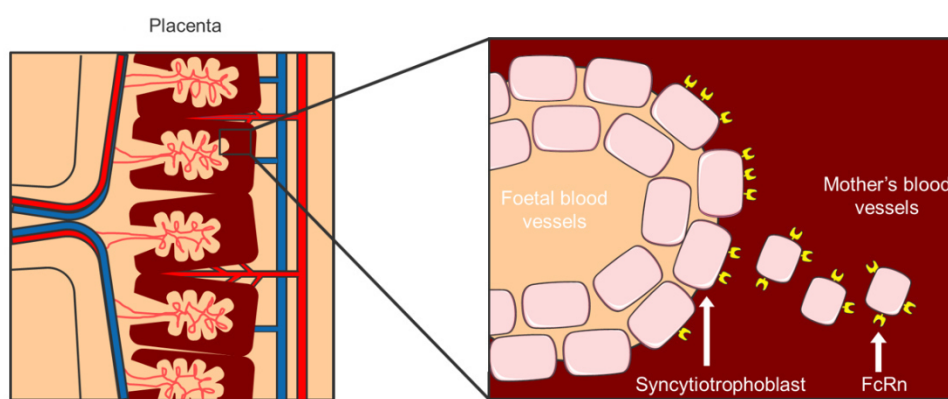


Figure 20. Illustration of one of the hypothesised mechanisms of prolonged IFX half-life in pregnancy: shedding of the FcRn-carrying syncytiotrophoblast into maternal circulation.

In the second part of the herein reported analysis, the developed PK model was applied to assess implications of the IFX discontinuation in terms of exposure achieved in the pregnant patients. As different IFX PK targets have been described in the literature, three cut-offs (3, 4, and 5 $\mu\text{g/mL}$) were investigated, in order to assess the sensitivity of the findings to PK target changes, and thus potential relevance of a consensus on target C_{\min} in the clinical setting. Figure 21 provides comparison of the typical IFX concentration-time profiles, and Table 8 achievement of the three PK targets, for simulated ADA+ and ADA- patients under three treatment settings: in absence of pregnancy, in continuous IFX therapy throughout the pregnancy, and in pregnancy with IFX therapy discontinuation in the third trimester.

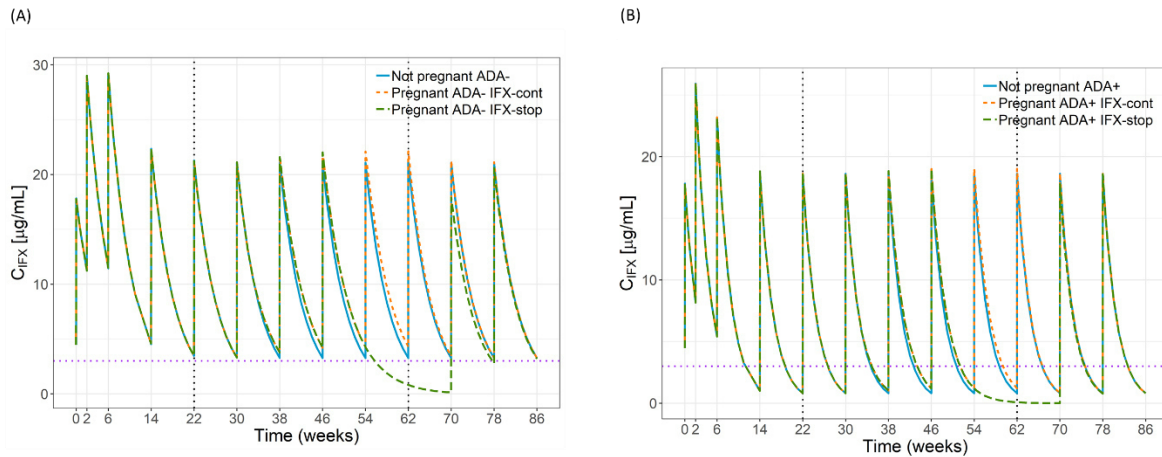


Figure 21. Simulated typical IFX concentration-time profiles in absence of pregnancy, and during pregnancy with (IFX-stop) and without IFX therapy discontinuation (IFX-cont): (A) without, and (B) with anti-drug antibody formation. Dotted vertical lines represent pregnancy period; dotted horizontal line denotes a PK target of 3 µg/mL.

Regardless of the PK target, discontinuation of IFX therapy in the third trimester led to a significant decrease of the percentage of both ADA+ and ADA- patients reaching the target. The significant impact of ADA found in the pre-modelling analysis and in the PK model thus clearly reflected on the PK target achievement under all three investigated treatment settings. Finally, the simulations demonstrated the effect of the second and third trimesters of pregnancy, with an increased target achievement in the pregnant compared to the non-pregnant patients. This finding might provide a partial explanation for the recently reported [206] increased risk of flares in the case of IFX discontinuation in pregnancy. The same study reported a similar risk of complications when IFX is continued and discontinued, supporting safety of IFX therapy throughout the pregnancy from maternal perspective.

Table 8. Attainment of PK target (3, 4 or 5 µg/mL) for ADA+ and ADA- patients in absence of pregnancy ('Non-pregnant'), continuation of IFX maintenance therapy throughout the entire pregnancy ('Pregnant, IFX cont. '), and pausing during the third trimester of pregnancy ('Pregnant, IFX-discont. ').

	Non-pregnant	Pregnant, IFX cont.	Pregnant, IFX-discont.
ADA-	%n _{>3µg/mL} = 51	%n _{>3µg/mL} = 65	%n _{>3µg/mL} = 30
	%n _{>4µg/mL} = 39	%n _{>4µg/mL} = 52	%n _{>4µg/mL} = 19
	%n _{>5µg/mL} = 28	%n _{>5µg/mL} = 41	%n _{>5µg/mL} = 11
ADA+	%n _{>3µg/mL} = 11	%n _{>3µg/mL} = 17	%n _{>3µg/mL} = 3
	%n _{>4µg/mL} = 5	%n _{>4µg/mL} = 9	%n _{>4µg/mL} = 1
	%n _{>5µg/mL} = 2	%n _{>5µg/mL} = 3	%n _{>5µg/mL} = 1

Results and Discussion

With respect to the disease activity in the investigated population, a trend of a decreased activity in pregnancy starting already in the first trimester and an increased disease activity in the first months after delivery was observed, especially for CD patients (measured by HBI), whereas the trends were less clear in UC (measured by Simple Clinical Colitis Activity Index). While it could be hypothesised that the increased postpartal CD activity might be related to the low/absent IFX exposure due to the therapy discontinuation in the third trimester, the limited sample size in the herein analysed dataset hindered any concrete inferences or further analysis.

4 Conclusions and future perspectives

Within this thesis substantial steps were taken to acquire a deeper mechanistic understanding of PK and PD of IFX in the IBD patients, provide a basis for model-informed clinical decision-making and support the rational use of IFX in IBD. Specifically, insights in (1) a dynamic exposure-biomarker relationship, (2) CL mechanisms of mAbs and relevance of study design characteristics, and (3) the PK behaviour of IFX in pregnancy are reported.

The developed PK/PD model – the first model describing IFX dose-exposure-CRP concentration relationship – enabled precise estimation of the maximum effect of IFX on CRP synthesis and the respective IFX concentration. The model-based simulations revealed that to achieve CRP remission shortening of the IFX dosing interval, dependent on ADA status and absence/presence of co-therapy with immunomodulators, is necessary. The model can be further utilised for further comparisons of different dosing regimens of IFX in a general IBD patient population and to support Therapeutic Drug Monitoring and clinical decision-making. This model also provides a basis for more elaborate IFX PK/PD models; for instance, if data would be available, the model could be broadened to include additional IBD (bio)markers (e.g. faecal calprotectin), or utilised in an integrated multi-level way in combination with other approaches (e.g. PBPK or systems biology modelling) to deepen the understanding of IFX exposure-response relationship, improve predictions of the treatment outcome and contribute to the overall treatment success. As ADA status was consistently identified as a crucial factor on IFX exposure, further understanding of relevance of different ADA IgG subtypes is warranted. In addition, a model of ADA formation could identify predictors of ADA development, and thus potentially inform clinical decisions for prevention of their development.

The PK model of cetuximab comprises the most detailed cetuximab CL characterisation reported, and the investigations of study design provide a guideline for future clinical studies for pharmacometric analyses. Identifiability of the true CL model of mAbs was found to heavily depend on the underlying data. While analysed IFX clinical data often does (due to clinical therapeutic decisions) comprise multiple dose levels, the sampling is usually sparse (only at C_{\min}), and clinical trials with rich sampling might enable the ‘true’ characterisation of IFX PK. Moreover, the observed differences in sensitivity of the exposure metrics (C_{\min} and AUC) highlight the value of dynamic models – such as the IFX-CRP PK/PD model developed as a part of this work – which contain information on the whole PK profile of a drug over time, instead of focusing on one exposure metric. In case such a dynamic model is not available and the data might be too limited to inform the true model, the choice of the exposure metric to be used in the exposure-response analysis should be made in advance, and considered during the PK model development (i.e. choice of alternative simplified models).

Conclusions and future perspectives

The developed PK model of IFX in pregnancy – the first such model reported – suggested that pregnancy is accompanied by a decrease in the IFX elimination. Solely from the PK target attainment perspective, continuation of IFX therapy throughout the pregnancy was found advantageous over discontinuation in the third trimester. Further studies addressing the mechanisms of the pregnancy-induced changes, including the CL alterations observed within this work, would facilitate a deeper understanding of the underlying physiological processes and enable mechanism-based predictions of disease activity in pregnancy, further informing the need for therapy adjustments in this period. Furthermore, the herein reported findings call for an identification and a consensus on the PK target of IFX and emphasise the importance of ADA status monitoring regardless of the pregnancy status. Expansion of this model to include a disease activity (bio)marker or to a more extensive PK model (e.g. by linking to a PBPK mAb pregnancy model) could shed more light on the IFX PK mechanisms in pregnancy and maternal and foetal IFX exposure. Finally, further investigations of safety of IFX use in pregnancy for the foetus are warranted.

In summary, the work performed within this thesis contributes to a better understanding of the PK and PD of IFX in IBD patients. Furthermore, it provides novel information for future studies and pharmacometric analyses, as well as for clinical management of IBD in general IBD patient population, and in pregnant IBD patients.

5 Literature

- [1] A.N. Ananthakrishnan. Epidemiology and risk factors for IBD. *Nat. Rev. Gastroenterol. Hepatol.*, 12: 205-217 (2015).
- [2] F. Biasi, G. Leonarduzzi, P.I. Oteiza, G. Poli. Inflammatory bowel disease: Mechanisms, redox considerations, and therapeutic targets. *Antioxid. Redox Signal.*, 19: 1711-1747 (2013).
- [3] J.F. Brandse, G.R. van den Brink, M.E. Wildenberg, D. van der Kleij, T. Rispens, J.M. Jansen, R.A. Mathot, C.Y. Ponsioen, M. Löwenberg, G.R.A.M. D’Haens. Loss of infliximab into feces is associated with lack of response to therapy in patients with severe ulcerative colitis. *Gastroenterol.*, 149: 350-355 (2015).
- [4] D.C. Baumgart, W.J. Sandborn. Inflammatory bowel disease: Clinical aspects and established and evolving therapies. *Lancet.*, 369: 1641-1657 (2007).
- [5] D.C. Baumgart, W.J. Sandborn. Crohn’s disease. *Lancet.*, 380: 1590-1605 (2012).
- [6] R.J. Xavier, D.K. Podolsky. Unravelling the pathogenesis of inflammatory bowel disease. *Nature.*, 448: 427-434 (2007).
- [7] J. Satsangi, M.S. Silverberg, S. Vermeire, J.-F. Colombel. The Montreal classification of inflammatory bowel disease: Controversies, consensus, and implications. *Gut.*, 55: 749-753 (2006).
- [8] M. Naganuma, N. Hosoe, T. Kanai, H. Ogata. Recent trends in diagnostic techniques for inflammatory bowel disease. *Korean J. Intern. Med.*, 30: 271-278 (2015).
- [9] E.V. Loftus. Emerging diagnostic methods in inflammatory bowel disease. *Gastroenterol. Hepatol. (N.Y.)*, 3: 284-286 (2007).
- [10] D.Q. Shih, S.R. Targan, D. McGovern. Recent advances in IBD pathogenesis: Genetics and immunobiology. *Curr. Gastroenterol. Rep.*, 10: 568-575 (2008).
- [11] M. Duijvestein, R. Battat, N. Vande Casteele, G.R. D’Haens, W.J. Sandborn, R. Khanna, V. Jairath, B.G. Feagan. Novel therapies and treatment strategies for patients with inflammatory bowel disease. *Curr. Treat. Options Gastroenterol.*, 16: 129-146 (2018).
- [12] F.I. Scott, G.R. Lichtenstein. Advances in therapeutic drug monitoring of biologic therapies in inflammatory bowel disease: 2015 in review. *Curr. Treat. Options Gastroenterol.*, 14: 91-102 (2016).

Literature

- [13] I. Ordas, D.R. Mould, B.G. Feagan, W.J. Sandborn. Anti-TNF monoclonal antibodies in inflammatory bowel disease: Pharmacokinetics-based dosing paradigms. *Clin. Pharmacol. Ther.*, 91: 635-646 (2012).
- [14] A. Michielan, R. D’Inca. Intestinal permeability in inflammatory bowel disease: Pathogenesis, clinical evaluation, and therapy of leaky gut. *Mediators Inflamm.*, 2015: 628157 (2015).
- [15] J. Mankertz, J.-D. Schulzke. Altered permeability in inflammatory bowel disease: Pathophysiology and clinical implications. *Curr. Opin. Gastroenterol.*, 23: 379-383 (2007).
- [16] W. Shin, H.J. Kim. Intestinal barrier dysfunction orchestrates the onset of inflammatory host-microbiome cross-talk in a human gut inflammation-on-a-chip. *Proc. Natl. Acad. Sci. U. S. A.*, 115: E10539-E10547 (2018).
- [17] A. Buisson, M.-A. Bringer, N. Barnich, E. Vazeille. Macrophages versus *Escherichia coli*: A decisive fight in Crohn’s disease. *Inflamm. Bowel Dis.*, 22: 2943-2955 (2016).
- [18] K. Wendelsdorf, J. Bassaganya-Riera, R. Hontecillas, S. Eubank. Model of colonic inflammation: Immune modulatory mechanisms in inflammatory bowel disease. *J. Ther. Biol.*, 21: 1225-1239 (2010).
- [19] J.D. Falvey, T. Hoskin, B. Meijer, A. Ashcroft, R. Walmsley, A.S. Day, R.B. Gearry. Disease activity assessment in IBD: Clinical indices and biomarkers fail to predict endoscopic remission. *Inflamm. Bowel Dis.*, 21: 824-831 (2015).
- [20] H.N. Iskandar, M.A. Ciorba. Biomarkers in inflammatory bowel disease: Current practices and recent advances. *Transl. Res.*, 19: 313-325 (2012).
- [21] A.J. Walsh, R.V. Bryant, S.P.L. Travis. Current best practice for disease activity assessment in IBD. *Nat. Rev. Gastroenterol. Hepatol.*, 13: 567-579 (2016).
- [22] B.R.R. de Mattos, M.P.G. Garcia, J.B. Nogueira, L.N. Paiatto, C.G. Albuquerque, C.L. Souza, L.G.R. Fernandes, W.M. da Silva Cunha Tamashiro, P.U. Simioni. Inflammatory bowel disease: An overview of immune mechanisms and biological treatments. *Mediators Inflamm.*, 2015: 493012 (2015).
- [23] P.E. Dube, S. Punit, D.B. Polk. Redeeming an old foe: Protective as well as pathophysiological roles for tumor necrosis factor in inflammatory bowel disease. *Am. J. Physiol. Gastroenterol. Liver Physiol.*, 308: G161-G170 (2015).
- [24] M. Maeda, N. Watanabe, H. Neda, N. Yamauchi, T. Okamoto, H. Sasaki, Y. Tsuji, S. Akiyama, N. Tsuji, Y. Niitsu. Serum tumor necrosis factor activity in inflammatory bowel disease. *Immunopharmacol. Immunotoxicol.*, 14: 451-461 (1992).
- [25] A.J. Yarur, A. Jain, D.A. Sussman, J.S. Barkin, M.A. Quintero, F. Princen, R. Kirkland, A.R. Deshpande, S. Singh, M.T. Abreu. The association of tissue anti-TNF drug levels with serological and

endoscopic disease activity in inflammatory bowel disease: The ATLAS study. *Gut.*, 65: 249-255 (2016).

[26] T. Horiuchi, H. Mitoma, S. Harashima, H. Tsukamoto, T. Shimoda. Transmembrane TNF- α : Structure, function and interaction with anti-TNF- α agents. *Rheumatol.*, 49: 1215-1228 (2010).

[27] J.R. Bradley. TNF-mediated inflammatory disease. *J. Pathol.*, 214: 149-160 (2008).

[28] M.F. Neurath. Cytokines in inflammatory bowel disease. *Nat. Rev. Immunol.*, 14: 329-342 (2014).

[29] E.A. Fagan, R.F. Dyck, P.N. Maton, H.J. Hodgson, V.S. Chadwick, Aviva Petrie, M.B. Pepys. Serum levels of C-reactive protein in Crohn's disease and ulcerative colitis. *Eur. J. Clin. Inv.*, 12: 351-359 (1982).

[30] B. Galve-de Rochemonteix, K. Wiktorowicz, I. Kushner, J.-M. Dayer. C-reactive protein increases productions of IL-1 α , IL-1 β , and TNF- α , and expression of mRNA by human alveolar macrophages. *J. Leukoc. Biol.*, 53: 439-445 (1993).

[31] S. Vermeire, G. Van Assche, P. Rutgeerts. C-reactive protein as a marker for inflammatory bowel disease. *Inflam. Bowel Dis.*, 10: 661-665 (2004).

[32] M. Henriksen, J. Jahnsen, I. Lygren, N. Stray, J. Sauar, M.H. Vatn, B. Moum, the IBSEN Study Group. C-reactive protein: A predictive factor and marker of inflammation in inflammatory bowel disease. Results from a prospective population-based study. *Gut.*, 57: 1518-1523 (2008).

[33] A. Tojo, S. Kinugasa. Mechanisms of glomerular albumin filtration and tubular reabsorption. *Int. J. Nephrol.*, 2012: 481520 (2012).

[34] Y.H. Tan, M. Liu, B. Nolting, J.G. Go, J. Gervay-Hague, G. Liu. A nanoengineering approach for investigation and regulation of protein immobilization. *ACS Nano.*, 2: 2374-2384 (2008).

[35] A.K. Shrive, G.M. Cheetham, D. Holden, D.A. Myles, W.G. Turnell, J.E. Volanakis, M.B. Pepys, A.C. Bloomer, T.J. Greenhough. Three dimensional structure of human C-reactive protein. *Nat. Struct. Biol.*, 3: 346-354 (1996).

[36] C. Zihni, C. Mills, K. Matter, M.S. Balda. Tight junctions: From simple barriers to multifunctional molecular gates. *Nat. Rev. Mol. Cell Biol.*, 17: 564-580 (2016).

[37] R. Panaccione. Mechanisms of inflammatory bowel disease. *Gastroenterol. Hepatol.*, 9: 529-532 (2013).

[38] B.R. Don, G. Kaysen. Serum albumin: Relationship to inflammation and nutrition. *Semin. Dial.*, 17: 432-437 (2004).

Literature

- [39] B.H.C.M.T. Prinsen, M.G.M. de Sain-van der Velden. Albumin turnover: Experimental approach and its application in health and renal diseases. *Clin. Chim. Acta.*, 347: 1-14 (2004).
- [40] S. Ishida, I. Hashimoto, T. Seike, Y. Abe, Y. Nakaya, H. Nakanishi. Serum albumin levels correlate with inflammation rather than nutrition supply in burns patients: A retrospective study. *J. Med. Invest.*, 61: 361-368 (2014).
- [41] J. L. Throop, M.E. Kerl, L.A. Cohn. Albumin in health and disease: Protein metabolism and function. *Compend. Contin. Educ. Pract. Vet.*, 1: 932-939 (2004).
- [42] T. Peters. All about albumin: Biochemistry, genetics, and medical applications. Academic Press, San Diego, 1st ed. (1995).
- [43] G.A. Kaysen. Serum albumin concentration in dialysis patients: Why does it remain resistant to therapy? *Kidney Int.*, 64: S92-S98 (2003).
- [44] H.J. Moshage, J.A.M. Janssen, J.H. Franssen, J.C.M. Hafkenscheid, S.H. Yap. Study of the molecular mechanism of decreased liver synthesis of albumin in inflammation. *J. Clin. Invest.*, 79: 1635-1641 (1987).
- [45] G.A. Kaysen, J.A. Dubin, H.-G. Müller, L.M. Rosales, N.W. Levin, W.E. Mitch, the HEMO study group. Inflammation and reduced albumin synthesis associated with stable decline in serum albumin in hemodialysis patients. *Kidney Int.*, 65: 1408-1415 (2004).
- [46] G.A. Kaysen, J.A. Dubin, H.-G. Müller, W.E. Mitch, L.M. Rosales, N.W. Levin, the HEMO study group. Relationships among inflammation nutrition and physiologic mechanisms establishing albumin levels in hemodialysis patients. *Kidney Int.*, 62: 2240-2249 (2002).
- [47] S.J. Winawer, T. Herskovic, R. Goldsmith, S.A. Broitman, N. Zamcheck. Albumin survival in patients with massive small-bowel resection. *Am. J. Dig. Dis.*, 12: 753-760 (1967).
- [48] L. Peyrin-Biroulet, W. Reinisch, J.-F. Colombel, G.J. Mantzaris, A. Kornbluth, R. Diamond, P. Rutgeerts, L.K. Tang, F.J. Cornillie, W.J. Sandborn. Clinical disease activity, C-reactive protein normalisation and mucosal healing in Crohn's disease in the SONIC trial. *Gut.*, 63: 88-95 (2014).
- [49] L.G.M. Jørgensen, L. Fredholm, P.H. Petersen, H. Hey, P. Munkholm, I. Brandslund. How accurate are clinical activity indices for scoring of disease activity in inflammatory bowel disease (IBD)? *Clin. Chem. Lab. Med.*, 43: 403-411 (2005).
- [50] L. Peyrin-Biroulet, J. Panes, W.J. Sandborn, S. Vermeire, S. Danase, B.G. Faegan, H.-F. Colombel, S.B. Hanauer, B. Rycroft. Defining disease severity in inflammatory bowel disease: Current and future directions. *Clin. Gastroenterol. Hepatol.*, 14: 348-354 (2016).

- [51] J.G. Hashash, S. Kane. Pregnancy and inflammatory bowel disease. *Gastroenterol. Hepatol.*, 11: 96-102 (2015).
- [52] R.H. Stone, J. Hong, H. Jeong. Pharmacokinetics of monoclonal antibodies used for inflammatory bowel diseases in pregnant women. *J. Clin. Toxicol.*, 4: 209 (2014).
- [53] G. Mor, I. Cardenas, V. Abrahams, S. Guller. Inflammation and pregnancy: The role of the immune system at the implantation site. *Ann. N. Y. Acad. Sci.*, 1221: 80-87 (2011).
- [54] P. Soma-Pillay, C. Nelson-Piercy, H. Tolppanen, A. Mebazaa. Physiological changes in pregnancy. *Cardiovasc. J. Afr.*, 27: 89-94 (2016).
- [55] J. van der Giessen, C.J. van der Woude, M.P. Peppelenbosch, G.M. Fuhler. A direct effect of sex hormones on epithelial barrier function in inflammatory bowel disease models. *Cells.*, 19: 261 (2019).
- [56] S. Paramsothy, A.K. Rosenstein, S. Mehandru, J.-F. Colombel. The current state of the art for biological therapies and new small molecules in inflammatory bowel disease. *Mucosal. Immunol.*, 11: 1558-1570 (2018).
- [57] C.H. Seow, A. Newman, S.P. Irwin, A.H. Steinhart, M.S. Silverberg, G.R. Greenberg. Trough serum infliximab: A predictive factor of clinical outcome for infliximab treatment in acute ulcerative colitis. *Gut.*, 59: 49-54 (2010).
- [58] K. Papamichael, S. Rakowsky, C. Rivera, A.S. Cheifetz, M.T. Osterman. Association between serum infliximab trough concentrations during maintenance therapy and biochemical, endoscopic, and histologic remission in Crohn's disease. *Inflamm. Bowel Dis.*, 24: 2266-2271 (2018).
- [59] M.G. Ward, B. Warner, N. Unsworth, S.-W. Chuah, C. Brownclarke, S. Shieh, M. Parkes, J.D. Sanderson, Z. Arkir, J. Reynolds, P.R. Gibson, P.M. Irving. Infliximab and adalimumab drug levels in Crohn's disease: Contrasting associations with disease activity and influencing factors. *Aliment. Pharmacol. Ther.*, 46: 150-161 (2017).
- [60] D. Tighe, S. Smith, A. O'Connor, N. Bresin, B. Ryan, D. McNamara. Positive relationship between infliximab and adalimumab trough levels at completion of induction therapy with clinical response rates, at a tertiary referral center. *JGH Open.*, 1: 4-10 (2017).
- [61] F. Cornillie, S.B. Hanauer, R.H. Diamond, J. Wang, K.L. Tang, Z. Xu, P. Rutgeerts, S. Vermeire. Postinduction serum infliximab trough level and decrease of C-reactive protein level are associated with durable sustained response to infliximab: A retrospective analysis of the ACCENT I trial. *Gut.*, 63: 1721-1727 (2014).

Literature

- [62] M.P. Martinez-Montiel, B. Casis-Herce, G.J. Gomez-Gomez, A. Masedo-Gonzales, C. Yela-San Bernardino, C. Piedracoba, G. Castellano-Tortajada. Pharmacologic therapy for inflammatory bowel disease refractory to steroids. *Clin. Exp. Gastroenterol.*, 8: 257-269 (2015).
- [63] A. Carlsen, R. Omdal, K.Ø. Leitaø, K. Isaksen, A.K. Hetta, L.N. Karlsen, L. Aabakken, N. Bolstad, D. Warren, K.E.A. Lundin, T. Grimstad. Subtherapeutic concentrations of infliximab and adalimumab are associated with increased disease activity in Crohn's disease. *Therap. Adv. Gastroenterol.*, 11: 1756284818759930 (2018).
- [64] E. Dreesen, R. Faelens, G. Van Assche, M. Ferrante, S. Vermeire, A. Gils, T. Bouillon. Optimising infliximab induction dosing for patients with ulcerative colitis. *Br. J. Clin. Pharmacol.*, 85: 782-795 (2019).
- [65] A. Koga, T. Matsui, N. Takatsu, Y. Takada, M. Kishi, Y. Yano, T. Beppu, Y. Ono, K. Ninomiya, F. Hirai, T. Nagahama, T. Hisabe, Y. Takaki, K. Yao, H. Imaeda, A. Andoh. Trough level of infliximab is useful for assessing mucosal healing in Crohn's disease: A prospective cohort study. *Intest. Res.*, 16: 223-232 (2018).
- [66] K.T. Park, A. Sin, M. Wu, D. Bass, J. Bhattacharya. Utilization trends of anti-TNF agents and health outcomes in adults and children with inflammatory bowel diseases: A single-center experience. *Inflamm. Bowel Dis.*, 20: 1242-1249 (2014).
- [67] B. Ungar, Y. Glidai, M. Yavzori, O. Picard, E. Fudim, A. Lahad, Y. Haberman, D.S. Shouval, I. Weintraub, R. Eliakim, S. Ben-Horin, B. Weiss. Association between infliximab drug and antibody levels and therapy outcome in pediatric inflammatory bowel diseases. *J. Pediatr. Gastroenterol. Nutr.*, 67: 507-512 (2018).
- [68] H. Rolandsdotter, P. Marits, U. Sundin, A.-C. Wikström, U.L. Fagerberg, Y. Finkel, M. Eberhardson. Serum-infliximab trough levels in 45 children with inflammatory bowel disease on maintenance treatment. *Int. J. Mol. Sci.*, 18: 575-586 (2017).
- [69] J. Ohem, O. Hradsky, K. Zarubova, I. Copova, P. Bukovska, R. Prusa, K. Malickova, J. Bronksy. Evaluation of infliximab therapy in children with Crohn's disease using trough levels predictors. *Dig. Dis.*, 36: 40-48 (2018).
- [70] J.T. Ryman, B. Meibohm. Pharmacokinetics of monoclonal antibodies. *CPT Pharmacometrics Syst. Pharmacol.*, 6: 576-588 (2017).
- [71] A.S. Strik, G.R. van den Brink, C. Ponsioen, R. Mathot, M. Löwenberg, G.R. D'Haens. Suppression of anti-drug antibodies to infliximab or adalimumab with the addition of an immunomodulator in patients with inflammatory bowel disease. *Aliment. Pharm. Ther.*, 45: 1128-1134 (2017).

- [72] P. Palmeira, C. Quinello, A.L. Silveira-Lessa, C.A. Zago, M. Carneiro-Sampaio. IgG placental transfer in healthy and pathological pregnancies. *J. Immun. Res.*, 2012: 985646 (2012).
- [73] S. Fuhrmann, C. Kloft, W. Huisinga. Impact of altered endogenous IgG on unspecific mAb clearance. *J. Pharmacokinet. Pharmacodyn.*, 44: 351-374 (2017).
- [74] R. J. Keizer, A.D.R. Huitema, J.H.M. Schellens, J.H. Beijnen. Clinical Pharmacokinetics of Therapeutic Monoclonal Antibodies. *Clin. Pharmacokinet.*, 49: 493-507 (2010).
- [75] L. Liu. Pharmacokinetics of monoclonal antibodies and Fc-fusion proteins. *Protein Cell.*, 9: 15-32 (2018).
- [76] J. Kim, W.L. Hayton, J.M. Robinson, C.L. Anderson. Kinetics of FcRn-mediated recycling of IgG and albumin in human: Pathophysiology and therapeutic implications using a simplified mechanism-based model. *Clin. Immunol.*, 122: 146-155 (2007).
- [77] U. Wong, R.K. Cross. Primary and secondary nonresponse to infliximab: Mechanisms and countermeasures. *Expert Opin. Drug Metabol. Toxicol.*, 13: 1039-1046 (2017).
- [78] N. Vande Castele, M. Ferrante, G. Van Assche, V. Ballet, G. Compennolle, K. Van Steen, S. Simoens, P. Rutgeerts, A. Gils, S. Vermeire. Trough concentration of infliximab guide dosing for patients with inflammatory bowel disease. *Gastroenterol.*, 148: 1320-1329 (2015).
- [79] P.J. Williams, E.I. Ette. *Pharmacometrics: Impacting drug development and pharmacotherapy*. In: *Pharmacometrics: The science of quantitative pharmacology*. John Wiley & Sons, Hoboken, New Jersey. (2006).
- [80] J.Y. Lee, C.E. Garnett, J.V.S. Gobburu, V.A. Bhattaram, S. Brar, J.C. Earp, P.R. Jadhav, K. Krudys, L.J. Lesko, F. Li, J. Liu, R. Madabushi, A. Marathe, N. Mehrotra, C. Tornøe, Y. Wang and H. Zhu. Impact of pharmacometric analyses on new drug approval and labelling decisions: A review of 198 submissions between 2000 and 2008. *Clin Pharmacokinet.* 50(10):627-635(2011).
- [81] European Medicines Agency. 2014 Activity report of the modelling and simulation working group (MSWG). https://www.ema.europa.eu/en/documents/report/2014-activity-report-modelling-simulation-working-group_en.pdf (last access: 24 March 2019). (2014).
- [82] EFPIA MID3 Workgroup: S.F. Marshall, R. Burghaus, V. Cosson, S.Y.A. Cheung, M. Chenel, O. DellaPasqua, N. Frey, B. Hamren, L. Harnisch, F. Ivanow, T. Kerbusch, J. Lippert, P.A. Milligan, S. Rohou, A. Staab, J.L. Steimer, C. Tornøe, S.A.G. Visser. Good practices in model-informed drug discovery and development: Practice, application, and documentation. *CPT: Pharmacometrics Syst. Pharmacol.*, 5: 93-122 (2016).

Literature

- [83] V.A. Bhattaram, B.P. Booth, R.P. Ramchandani, B.N. Beasley, Y. Wang, V. Tandon, J.Z. Duan, R.K. Baweja, P.J. Marroum, R.S. Uppoor, N.A. Rahman, C.G. Sahajwalla, J.R. Powell, M.U. Mehta, J.V.S. Gobburu. Impact of pharmacometrics on drug approval and labeling decisions: A survey of 42 new drug applications. *AAPS J.*, 7: E503-E512 (2005).
- [84] V.A. Bhattaram, C. Bonapace, D.M. Chilukuri, J.Z. Duan, C. Garnett, J.V.S. Gobburu, S.H. Jang, L. Kenna, L.J. Lesko, R. Madabushi, Y. Men, J.R. Powell, W. Qiu, R.P. Ramchandani, C.W. Tornoe, Y. Wang, J.J. Zheng. Impact of pharmacometric reviews on new drug approval and labeling decisions – a survey of 21 drug applications submitted between 2005 and 2006. *Clin Pharmacol Ther.*, 81: 213-221 (2007).
- [85] European Medicines Agency. Assessment report: Solymbic. https://www.ema.europa.eu/en/documents/assessment-report/solymbic-epar-public-assessment-report_en.pdf (last access: 15 June 2020). (2017).
- [86] A.S. Darwich, K. Ogungbenro, A.A. Vinks, J.R. Powell, J.-L. Reny, N. Marsousi, Y. Daali, D. Fairman, J. Cook, L.J. Lesko, J.S. McCune, C. Knibbe, S.N. de Wildt, J.S. Leeder, M. Neely, A.F. Zuppa, P. Vicini, L. Aarons, T.N. Johnson, J. Boiani, A. Rostami-Hodjegan. Why has model-informed precision dosing not yet become common clinical reality? Lessons from the past and a roadmap for the future. *Clin. Pharmacol. Ther.*, 101: 646-656 (2017).
- [87] I.K. Minichmayr, J.A. Roberts, O.R. Frey, A.C. Roehr, C. Kloft, A. Brinkmann. Development of a dosing nomogram for continuous-infusion meropenem in critically ill patients based on a validated population pharmacokinetic model. *J. Antimicrob. Chemother.*, 73: 1330-1339 (2018).
- [88] A. Henrich, M. Joerger, S. Kraff, U. Jaehde, W. Huisinga, C. Kloft, Z.P. Parra-Guillen. Semimechanistic bone marrow exhaustion pharmacokinetic-pharmacodynamic model for chemotherapy-induced cumulative neutropenia. *J. Pharmacol. Exp. Ther.*, 362: 347-358 (2017).
- [89] L. Ehmann, M. Zoller, I.K. Minichmayr, C. Scharf, W. Huisinga, J. Zander, C. Kloft. Development of a dosing algorithm for meropenem in critically ill patients based on a population pharmacokinetic/pharmacodynamic analysis. *Int. J. Antimicrob. Agents.*, 54: 309-317 (2019).
- [90] R. Michelet, J.V. Bocxlaer, A. Vermeulen. PBPK in preterm and term neonates: A review. *Curr. Pharm. Des.*, 23: 5943-5954 (2017).
- [91] J.F. Standing. Understanding and applying pharmacometric modelling and simulation in clinical practice and research. *Br. J. Clin. Pharmacol.*, 83: 247-254 (2017).
- [92] D.R. Mould, R.N. Upton. Basic concepts in population modeling, simulation, and model-based drug development. *CPT Pharmacometrics Syst. Pharmacol.*, 1: e6 (2012).

- [93] D.R. Mould, R.N. Upton. Basic concepts in population modeling, simulation, and model-based drug development – Part 2: Introduction to pharmacokinetic modeling methods. *CPT Pharmacometrics Syst. Pharmacol.*, 2: e38 (2013).
- [94] S. Stuebler, C. Kloft, W. Huisinga. Systems biology model of the mucosal immune system. Population Approach Group Europe (PAGE), Stockholm, Sweden, 11-14 June 2019. [www.page-meeting.org/?abstract=8861], 2019.
- [95] P.J. Koelink, F.M. Bloemendaal, B. Li, L. Westera, E.W.M. Vogels, M. van Roest, A.K. Gloudemans, A.B. van't Wout, H. Korf, S. Vermeire, A.A. Te Velde, C.Y. Ponsioen, G.R. D'Haens, J.S. Verbeek, T.L. Geiger, M.E. Wildenberg, G.R. van den Brink. Anti-TNF therapy in IBD exerts its therapeutic effect through macrophage IL-10 signaling. *Gut.*, 69: 1053-1063 (2020).
- [96] V. Ramakrishnan, P.Lu, J. McBride, F. Fuh, A. Lekkerkerker, M. Tang, A. Leber, R. Hontecillas, A. Quartino, J.Y. Jin, J. Bassaganya-Riera, S. Ramanujan, K. Gadkar. A quantitative systems pharmacology model to describe the immunopathogenesis of inflammatory bowel disease and guide drug development decisions. *J. Pharmacokinet. Pharmacodyn.*, 45: S85 (2018).
- [97] V. Balbas-Martinez, L. Ruiz-Cerdá, I. Irurzun-Arana, I. González-García, A. Vermeulen, J.D. Gómez-Mantilla, I.F. Trocóniz. A systems pharmacology model for inflammatory bowel disease. *PLoS One.*, 13: e0192949 (2018).
- [98] G. Dwivedi, L. Fitz, M. Hegen, J. Harrold, A. Heatherington, C. Li. A multiscale model of intraleukin-6-mediated immune regulation in Crohn's disease and its application in drug discovery and development. *CPT: Pharmacometrics Syst. Pharmacol.*, 3: e89 (2014).
- [99] A.A. Fasanmade, O.J. Adedokun, J. Ford, D. Hernandez, J. Johanns, C. Hu, H.M. Davis, H. Zhou. Population pharmacokinetics analysis of infliximab in patients with ulcerative colitis. *Eur. J. Clin. Pharmacol.*, 65: 1211-1228 (2009).
- [100] A.A Fasanmade, O.J. Adedokun, M. Blank, H. Zhou, H.M. Davis. Pharmacokinetic properties of infliximab in children and adults with Crohn's disease: A retrospective analysis of data from 2 phase III clinical trials. *Clin. Ther.*, 33: 946-964 (2011).
- [101] D. Ternant, A. Aubourg, C. Magdelaine-Beuzelin, D. Degenne, H. Watier, L. Picon, G. Paintaud. Infliximab pharmacokinetics in inflammatory bowel disease. *Ther. Drug Monit.*, 30: 523-529 (2008).
- [102] D.J. Buurman, J.M. Maurer, R.J. Keizer, J.G.W. Kosterink, G. Dijkstra. Population pharmacokinetics of infliximab in patients with inflammatory bowel disease: Potential implications for dosing in clinical practice. *Aliment. Pharmacol. Ther.*, 42: 529-539 (2015).

Literature

- [103] A. Eser, C. Primas, S. Reinisch, H. Vogelsang, G. Novacek, D.R. Mould, W. Reinisch. Prediction of individual serum infliximab concentrations in inflammatory bowel disease by a Bayesian dashboard system. *J. Clin. Pharmacol.*, 58: 790-802 (2018).
- [104] I. Dotan, Y. Ron, H. Yanai, S. Becker, S. Fishman, L. Yahav, M.B. Yehoyada, D.R. Mould. Patient factors that increase infliximab clearance and shorten half-life in inflammatory bowel disease: A population pharmacokinetic study. *Inflamm. Bowel Dis.*, 20: 2247-2259 (2014).
- [105] J.R. Wade, G. Parker, G. Kosutic, B.G. Feagen, W.J. Sandborn, C. Laveille, R. Oliver. Population pharmacokinetic analysis of certolizumab pegol in patients with Crohn's disease. *J. Clin. Pharmacol.*, 55: 866-874(2015).
- [106] S.E. Berends, A.S. Strik, J.C. Van Selm, M. Löwenberg, C.Y. Ponsioen, G.R. D'Haens, R.A. Mathot. Explaining interpatient variability in adalimumab pharmacokinetics in patients with Crohn's disease. *Ther. Drug Monit.*, 40: 202-211(2018).
- [107] H. Edlund, C. Steenholdt, M.A. Ainsworth, E. Goebgen, J. Brynskov, O.O. Thomsen, W. Huisinga, C. Kloft. Magnitude of increased infliximab clearance imposed by anti-infliximab antibodies in Crohn's disease is determined by their concentration. *AAPS J.*, 19: 223-233(2017).
- [108] E. Dreesen, S. Berends, D. Laharie, G. D'Haens, S. Vermeire, A. Gils, R. Mathot. Modelling of the relationship between infliximab exposure, faecal calprotectin and endoscopic remission in patients with Crohn's disease. *Br. J. Clin. Pharmacol.* doi: 10.1111/bcp.14364 (2020).
- [109] P.R.V. Malik, A.N. Edginton. Physiologically-based pharmacokinetic modeling vs. allometric scaling for the prediction of infliximab pharmacokinetics in pediatric patients. *CPT Pharmacometrics Syst. Pharmacol.*, 8: 835-844 (2019).
- [110] J. Wojciechowski, R.N. Upton, D.R. Mould, M.D. Wiese, D.J.R. Foster. Infliximab maintenance dosing in inflammatory bowel disease: An example for in silico assessment of adaptive dosing strategies. *AAPS J.*, 19: 1136-1147 (2017).
- [111] N.A. Kennedy, G.A. Heap, H.D. Green, B. Hamilton, C. Bewshea, G.J. Walker, A. Thomas, R. Nice, M.H. Perry, S. Bouri, N. Chanchlani, N.M. Heerasing, P. Hendy, S. Lin, D.R. Gaya, J.R. Fraser Cummings, C.P. Selinger, C.W. Lees, A.L. Hart, M. Parkes, S. Sebastian, J.C. Mansfield, P.M. Irving, J. Lindsay, R.K. Russell, T.J. McDonald, D. McGovern, J.R. Goodhand, T. Ahmad, UK Inflammatory Bowel Disease Pharmacogenetics Study Group. Predictors of anti-TNF treatment failure in anti-TNF-naive patients with active luminal Crohn's disease: A prospective, multicentre, cohort study. *Lancet Gastroenterol. Hepatol.*, 4: 341-353 (2019).
- [112] S.L. Wang, L. Ohrmund, S. Hauenstein, J. Salbato, R. Reddy, P. Monk, S. Lockton, N. Ling, S. Singh. Development and validation of a homogeneous mobility shift assay for the measurement of

infliximab and antibodies-to-infliximab levels in patient serum. *J. Immunol. Methods*, 382: 177-188 (2012).

[113] R. Sostegni, M. Daperno, N. Scaglione, A. Lavagna, R. Rocca, A. Pera. Review article: Crohn's disease: Monitoring disease activity. *Aliment. Pharmacol. Ther.*, 17 Suppl2: 11-17 (2003).

[114] J. Taberner, F. Ciardiello, F. Rivera, E. Rodriguez-Braun, F.J. Ramos, E. Martinelli, M.E. Vega-Villegas, S. Roselló, S. Liebscher, O. Kisker, T. Macarulla, J. Baselga, A. Cervantes. Cetuximab administered once every second week to patients with metastatic colorectal cancer: A two-part pharmacokinetic/pharmacodynamic phase I dose-escalation study. *Ann. Oncol.*, 21: 1537-1545 (2010).

[115] E. Van Cutsem, S. Tejpar, D. Vanbeckevoort, M. Peeters, Y. Humblet, H. Gelderblom, J.B. Vermorken, F. Viret, B. Glimelius, E. Gallerani, A. Hendlisz, A. Cats, M. Moehler, X. Sagaert, S. Vlassak, M. Schlichting, F. Ciardiello. Inpatient cetuximab escalation in metastatic colorectal cancer according to the grade of early skin reactions: The randomized EVEREST study. *J. Clin. Oncol.*, 30: 2861-2868 (2012).

[116] K.K. Jørgensen, I.C. Olsen, G.L. Goll, M. Lorentzen, N. Bolstad, E.A. Haavardsholm, K.E.A. Lundin, C. Mørk, J. Jahnsen, T.K. Kvien, NOR-SWITCH study group. Switching from originator infliximab to biosimilar CT-P13 compared with maintained treatment with originator infliximab (NOR-SWITCH): a 52-week, randomised, double-blind, non-inferiority trial. *Lancet*, 389: 2304-2316 (2017).

[117] X.S. Xu, A. Dunne, H. Kimko, P. Nandy, A. Vermeulen. Impact of low percentage of data below the quantification limit on parameter estimates of pharmacokinetic models. *J. Pharmacokinet. Pharmacodyn.*, 38: 423-432 (2011).

[118] M.O. Karlsson, E.N. Jonsson, C.G. Wiltse, J.R. Wade. Assumption testing in population pharmacokinetic models: Illustrated with an analysis of moxonidine data from congestive heart failure patients. *J. Pharmacokinet. Biopharm.*, 26: 207-246 (1998).

[119] R.J. Bauer, NONMEM tutorial part II: Estimation methods and advanced examples. *CPT Pharmacometrics Syst. Pharmacol.*, 8: 538-556 (2019).

[120] P.O. Gislekog, M.O. Karlsson, S.L. Beal. Use of prior information to stabilize a population data analysis. *J. Pharmacokinet. Pharmacodyn.*, 29: 473-505 (2002).

[121] R.M. Savic, M.O. Karlsson. Importance of shrinkage in empirical Bayes estimates for diagnostics: Problems and solutions. *AAPS J.*, 11: 558-569 (2009).

[122] L. Lindbom, P. Pihlgren, N. Jonsson. PsN-toolkit – A collection of computer intensive statistical methods for non-linear mixed effect modeling using NONMEM. *Comput. Methods Programs Biomed.* 79: 241-257 (2005).

Literature

- [123] M. Bergstrand, A.C. Hooker, J.E. Wallin, M.O. Karlsson. Prediction-corrected visual predictive checks for diagnosing nonlinear mixed-effects models. *AAPS J.*, 13: 143-151 (2011).
- [124] A.C. Hooker, C.R. Staats, M.O. Karlsson. Conditional weighted residuals (CWRES): A model diagnostic for the FOCE method. *Pharm. Res.*, 24: 2187-2197 (2007).
- [125] L. Lindbom, J. Ribbing, E.N. Jonsson. Perl-speaks-NONMEM (PsN)—a Perl module for NONMEM related programming. *Comput. Method Programs Biomed.*, 75: 85-94 (2004).
- [126] R.N. Upton, D.R. Mould. Basic concepts in population modeling, simulation, and model-based drug development: Part 3—Introduction to pharmacodynamic modeling methods. *CPT Pharmacometrics Syst. Pharmacol.*, 3: e88 (2014).
- [127] H. Motulsky, A. Christopoulos. Fitting models to biological data using linear and nonlinear regression: A practical guide to curve fitting. Oxford University Press, New York. (2004).
- [128] W. Reinisch, Y. Wang, B.J. Oddens, R. Link. C-reactive protein, an indicator for maintained response or remission to infliximab in patients with Crohn's disease: A post-hoc analysis from ACCENT I. *Aliment. Pharmacol. Ther.*, 35: 568-576 (2012).
- [129] P. Girard, A. Kovar, B. Brockhaus, M. Zuehlsdorf, M. Schlichting, A. Munafo. Tumor size model and survival analysis of cetuximab and various cytotoxics in patients treated for metastatic colorectal cancer. Population Approach Group Europe (PAGE), Glasgow, Scotland, 11-14 June 2013. [<https://www.page-meeting.org/default.asp?abstract=2902>], 2013.
- [130] N.L. Dirks, A. Nolting, A. Kovar, B. Meibohm. Population pharmacokinetics of cetuximab in patients with squamous cell carcinoma of the head and neck. *J. Clin. Pharmacol.*, 48: 267-278 (2008).
- [131] N. Azzopardi, T. Lecomte, D. Ternant, M. Boisdrion-Celle, F. Piller, A. Morel, V. Gouilleux-Gruart, C. Vignault-Desvignes, H. Watier, E. Gamelin, G. Paintaud. Cetuximab pharmacokinetics influences progression-free survival of metastatic colorectal cancer patients. *Clin. Cancer Res.*, 17: 6329-6337 (2011).
- [132] M. Gastonguay. Full covariate models as an alternative to methods relying on statistical significance for inferences about covariate effects: A review of methodology and 42 case studies. Population Approach Group Europe (PAGE), Athens, Greece, 7-10 June 2011. [https://www.page-meeting.org/pdf_assets/1694-GastonguayPAGE2011.pdf], 2011.
- [133] B.A. Walther, J.L. Moore. The concepts of bias, precision and accuracy, and their use in testing the performance of species richness estimators, with a literature review of estimator performance. *Ecography*. 28: 815-829 (2005).

- [134] A.-M. Griscic, W. Huisinga, W. Reinisch, C. Kloft. Dosing infliximab in Crohn's disease: Is adjustment for body size justified? *J. Crohn. Colitis*, 11: S325-S326 (2017).
- [135] Y. Furuya, T. Ozeki, R. Takayanagi, H. Yokoyama, K. Okuyama, Y. Yamada. Theory based analysis of anti-inflammatory effect of infliximab on Crohn's disease. *Drug Metab. Pharmacokinet.*, 22: 20-25 (2007).
- [136] A. Aubourg, L. Picon, T. Lecomte, T. Bejan-Angoulvant, G. Paintaud, D. Ternant. A robust estimation of infliximab pharmacokinetic parameters in Crohn's disease. *Eur. J. Clin. Pharmacol.*, 71: 1541-1542 (2015).
- [137] D. Ternant, Z. Berkane, L. Picon, V. Gouilleux-Gruart, J.-F. Colombel, M. Allez, E. Louis, G. Paintaud. Assessment of the influence of inflammation and FCGR3A genotype on infliximab pharmacokinetics and time to relapse in patients with Crohn's disease. *Clin. Pharmacokinet.*, 54: 551-562 (2015).
- [138] C. Passot, D. Mulleman, T. Bejan-Angoulvant, A. Aubourg, S. Willot, T. Lecomte, L. Picon, P. Goupille, G. Paintaud, D. Ternant. The underlying inflammatory chronic disease influences infliximab pharmacokinetics. *mAbs*, 8: 1407-1416 (2016).
- [139] J.F. Brandse, D. Mould, O. Smeeke, Y. Ashruf, S. Kuin, A. Strik, G.R. van den Brink, G.R. D'Haens. A real-life population pharmacokinetic study reveals factors associated with clearance and immunogenicity of infliximab in inflammatory bowel disease. *Inflamm. Bowel Dis.*, 23: 650-660 (2017).
- [140] D. Kevans, S. Murthy, D.R. Mould, M.S. Silverberg. Accelerated clearance of infliximab is associated with treatment failure in patients with corticosteroid-refractory acute ulcerative colitis. *J. Crohn. Colitis*, 12: 662-669 (2018).
- [141] A. Petitcollin, O. Leuret, C. Tron, F. Lemaitre, M.-C. Verdier, G. Paintaud, G. Bouguen, S. Willot, E. Bellissant, D. Ternant. Modeling immunization to infliximab in children with Crohn's disease using population pharmacokinetics: A pilot study. *Inflamm. Bowel Dis.*, 24: 1745-1754 (2018).
- [142] A. Petitcollin, C. Brochard, L. Siproudhis, C. Tron, M.-C. Verdier, F. Lemaitre, C. Lucidarme, G. Bouguen, É. Bellissant. Pharmacokinetic parameters of infliximab influence the rate of relapse after de-escalation in adults with inflammatory bowel diseases. *Clin. Pharmacol. Ther.*, 106: 605-615 (2019).
- [143] D. Ternant, C. Passot, A. Aubourg, P. Goupille, C. Desvignes, L. Picon, T. Lecomte, D. Mulleman, G. Paintaud. Model-based therapeutic drug monitoring of infliximab using a single serum trough concentration. *Clin. Pharmacokinet.*, 57: 1173-1184 (2018).

Literature

- [144] S.E. Berends, T.J. van Steeg, M.J. Ahsman, S. Singh, J.F. Brandse, G.R.A.M. D'Haens, R.A.A. Mathot. Tumor necrosis factor-mediated disposition of infliximab in ulcerative colitis patients. *J. Pharmacokinet. Pharmacodyn.*, 46: 543-551 (2019).
- [145] K. Kimura, A. Yoshida, F. Katagiri, R. Rakayanagi, Y. Yamada. Prediction of clinical effects of infliximab administered for inflammatory bowel disease based on pharmacokinetic and pharmacodynamic modeling. *Biopharm. Drug Dispos.*, 40: 250-261 (2019).
- [146] N. Vande Casteele, J. Jeyarajah, V. Jairath, B.G. Faegan, W.J. Sandborn. Infliximab exposure-response relationship and thresholds associated with endoscopic healing in patients with ulcerative colitis. *Clin. Gastroenterol. Hepatol.*, 17: 1814-1821 (2019).
- [147] L.E. Bauman, Y. Xiong, T. Mizuno, P. Minar, T. Fukuda, M. Dong, M.J. Rosen, A.A. Vinks. Improved population pharmacokinetic model for predicting optimized infliximab exposure in pediatric inflammatory bowel disease. *Inflamm. Bowel Dis.* 26: 429-439 (2020).
- [148] A.C. Moss, V. Brinks, J.F. Carpenter. Review article: Immunogenicity of anti-TNF biologics in IBD – the role of patient, product and prescriber factors. *Aliment. Pharmacol. Ther.*, 38: 1188-1197 (2013).
- [149] C. Steenholdt, M.A. Ainsworth, M. Tovey, T.W. Klausen, O.O. Thomsen, J. Brynskov, K. Bendtzen. Comparison of techniques for monitoring infliximab and antibodies against infliximab in Crohn's disease. *Ther. Drug Monit.*, 35: 530-538 (2013).
- [150] C.M. Snapper, J.J. Mond. Towards a comprehensive view of immunoglobulin class switching. *Immunol. Today*, 14: 15-17 (1993).
- [151] J. Stavnezer. Immunoglobulin class switching Cytokines direct switching by regulating germline transcription. *Curr. Opin. Immunol.*, 8: 199-205 (1996).
- [152] M.C. Van Zelm. B cells take their time: Sequential IgG class switching over the course of an immune response? *Immunol. Cell Biol.*, 92: 645-646 (2014).
- [153] J.C.A. Janeway, P. Travers, M. Walport, M.J. Shlomchik (Eds.). *Immunobiology: The immune system in health and disease*. Garland Science, New York, 5th ed. (2001).
- [154] G. Vidarsson, G. Dekkers, T. Rispen. IgG subclasses and allotypes: From structure to effector functions. *Front. Immunol.*, 5: 520 (2014).
- [155] P.A. Van Schouwenburg, C.L. Krieckaert, M. Nurmohamed, M. Hart, T. Rispen, L. Aarden, D. Wouters, G.J. Wolbink. IgG4 production against adalimumab during long term treatment of RA patients. *J. Clin. Immunol.*, 32: 1000-1006 (2012).

- [156] R.C. Aalberse, R. van der Gaag, J. van Leeuwen. Serologic aspects of IgG4 antibodies. I. Prolonged immunization results in an IgG4-restricted response. *J. Immunol.*, 130: 722-726 (1983).
- [157] R.C. Aalberse, J. Schuurman. IgG4 breaking the rules. *Immunology*, 105: 9-19 (2002).
- [158] J.S. van der Zee, P. van Swieten, R.C. Aalberse. Inhibition of complement activation by IgG4 antibodies. *Clin. Exp. Immunol.*, 64: 415-422 (1986).
- [159] J. Swierstra, S. Debets, C. de Vogel, N. Lemmens-den Toom, N. Verkaik, N. Ramdani-Bouguessa, M.F. Jonkman, J.M. van Dijk, A. Fahal, A. van Belkum, W. van Wamel. IgG4 subclass-specific responses to *Staphylococcus aureus* antigens shed new light on host-pathogen interaction. *Infect. Immun.*, 83: 492–501 (2015).
- [160] H.H. Herfarth, M.D. Kappelman, M.D. Long, K.L. Isaacs. Use of methotrexate in the treatment of inflammatory bowel diseases (IBD). *Inflamm. Bowel Dis.* 22: 224-233 (2016).
- [161] S. Vermeire, G. Van Assche, P. Rutgeerts. Laboratory markers in IBD: Useful, magic, or unnecessary toys? *Gut.* 55: 426-431 (2006).
- [162] U.S. Food and Drug Administration. Guidance for industry and FDA staff: Qualification process for drug development tools. <https://c-path.org/wp-content/uploads/2014/01/FDA-releases-guidance-for-drug-development-tool-qualification.pdf> (last access 15 June 2020). (2014).
- [163] I. Angriman, M. Scarpa, R. D'Incà, D. Basso, C. Ruffolo, L. Polese, G.C. Sturniolo, D.F. D'Amico, M. Plebani. Enzymes in feces: Useful markers of chronic inflammatory bowel disease. *Clin. Chim. Acta.*, 381: 63-68 (2007).
- [164] R. Modigliani, J.-Y. Mary, J.-F. Simon, A. Cortot, J.C. Soule, J.P. Gendre, E. Rene. Clinical, biological, and endoscopic picture of attacks of Crohn's disease. Evolution on prednisolone. *Groupe d'Etude Thérapeutique Des Affections Inflammatoires Digestives. Gastroenterology.*,98: 811-818 (1990).
- [165] D. Bojic, K. Bodger, S. Travis. Patient reported outcome measures (PROMs) in inflammatory bowel disease: New data. *J Crohn Colitis*, 11: S576-S585 (2017).
- [166] D. Ternant, E. Ducourau, P. Fuzibet, C. Vignault, H. Watier, T. Lequerré, X. Le Loët, O. Vittecoq, P. Goupille, D. Mulleman, G. Paintaud. Pharmacokinetics and concentration-effect relationship of adalimumab in rheumatoid arthritis. *Br. J. Clin. Pharmacol.* 79: 286-297 (2015).
- [167] M. Jürgens, J.M.M. John, I. Cleynen, F. Schnitzler, H. Fidder, W. van Moerkercke, V. Ballet, M. Noman, I. Hoffman, G. van Assche, P.J. Rutgeerts, K. van Stehen, S. Vermeire. Levels of C-reactive protein are associated with response to infliximab therapy in patients with Crohn's disease. *Clin. Gastroenterol. Hepatol.*, 9: 421-427 (2011).

Literature

- [168] H. Andersson, A. Eser, W. Huisinga, W. Reinisch, C. Kloft. Recommendations for dose adjustments of infliximab in Crohn's disease patients with higher clearance. 5th American Conference on Pharmacometrics (ACoP), Las Vegas, Nevada, USA, 12-15 Oct 2014. *J Pharmacokinet Pharmacodyn.* 2014; 41(Suppl.): S27.
- [169] J. Cheng, Z. Hamilton, M. Smyth, C. Barker, D. Israel, K. Jacobson. Concomitant therapy with immunomodulator enhances infliximab durability in pediatric inflammatory bowel disease. *Inflamm. Bowel Dis.* 23: 1762-1773 (2017).
- [170] C.A. Siegel, B.E. Sands. Review article: Practical management of inflammatory bowel disease patients taking immunomodulators. *Aliment. Pharmacol. Ther.*, 22: 1-16 (2005)
- [171] C. Kloft, E.-U. Graefe, P. Tanswell, A.M. Scott, R. Hofheinz, A. Amelsberg, M.O. Karlsson. Population pharmacokinetics of sibrotuzumab, a novel therapeutic monoclonal antibody, in cancer patients. *Invest. New Drugs*, 22: 39-52 (2004).
- [172] K. Kuester, A. Kovar, C. Lüpfer, B. Brockhaus, C. Kloft. Refinement of the population pharmacokinetic model for the monoclonal antibody matuzumab: external model evaluation and simulations. *Clin. Pharmacokinet.*, 48: 477-487 (2009).
- [173] C. Liu, J. Yu, H. Li, J. Liu, Y. Xu, P. Song, Q. Liu, H. Zhao, J. Xu, V.E. Maher, B.P. Booth, G. Kim, A. Rahman, Y. Wang. Association of time-varying clearance of nivolumab with disease dynamics and its implications on exposure response analysis. *Clin. Pharmacol. Ther.*, 101, 657-666 (2017).
- [174] J. Wilkins, B. Brockhaus, S. Wang, H. Dai, B. Neuteboom, S. Brar, C. Bello, A. Khandelwal, P. Girard. Population pharmacokinetic analysis of avelumab in different cancer types. In: Abstracts for American conference on pharmacometrics 2017 (ACoP8). *J. Pharmacokinet. Pharmacodyn.*, 44 (Supl 1): 11-143 (2017).
- [175] P.G. Baverel, V.F.S. Dubois, C.Y. Jin, Y. Zheng, X. Song, X. Jin, P. Mukhopadhyay, A. Gupta, P.A. Dennis, Y. Ben, P. Vicini, L. Roskos, R. Narwal. Population pharmacokinetics of durvalumab in cancer patients and association with longitudinal biomarkers of disease status. *Clin. Pharmacol. Ther.*, 103: 631-642 (2018).
- [176] G. Bajaj, X. Wang, S. Agrawal, M. Gupta, A. Roy, Y. Feng. Model-based population pharmacokinetic analysis of nivolumab in patients with solid tumors. *CPT Pharmacometrics Syst. Pharmacol.*, 6: 58-66 (2017).
- [177] Y. Wang, B. Booth, A. Rahman, G. Kim, S.M. Huang, I. Zineh. Toward greater insight on pharmacokinetics and exposure-response relationship for therapeutic biologics in oncology drug development. *Clin. Pharmacol. Ther.*, 101: 582-584 (2017).

- [178] B.F. Krippendorff, D.A. Oyarzun, W. Huisinga. Predicting the F(ab)-mediated effect of monoclonal antibodies in vivo by combining cell-level kinetic and pharmacokinetic modelling. *J. Pharmacokinet. Pharmacodyn.*, 39: 125-139 (2012).
- [179] H. Edlund, J. Melin, Z.P. Parra-Guillen, C. Kloft. Pharmacokinetics and pharmacokinetic-pharmacodynamic relationships of monoclonal antibodies in children. *Clin. Pharmacokinet.*, 54: 35-80 (2015).
- [180] U.S. Food and Drug Administration. Medication guide Remicade®. https://www.accessdata.fda.gov/drugsatfda_docs/label/2011/103772s5281MedG.pdf (last access: 15 June 2020). (2011).
- [181] L. Puig, D. Barco, A. Alomar. Treatment of psoriasis with anti-TNF drugs during pregnancy: Case report and review of the literature. *Dermatology*, 220: 71-76 (2010).
- [182] Therapeutic Goods Administration. Prescribing medicines in pregnancy database. <https://www.tga.gov.au/prescribing-medicines-pregnancy-database> (last access: 15 June 2020).
- [183] O.H. Nielsen, E. V Loftus Jr., T. Jess. Safety of TNF-alpha inhibitors during IBD pregnancy: a systematic review. *BMC Med*, 11: 174 (2013).
- [184] R.M. Marchioni, G.R. Lichtenstein. Tumor necrosis factor- α inhibitor therapy and fetal risk: A systematic literature review. *World J. Gastroenterol.*, 19: 2591-2602 (2013).
- [185] M.C. Soh, L. MacKillop. Biologics in pregnancy - for the obstetrician. *Obstet. Gynaecol.*, 18: 25-32 (2016).
- [186] C.H. Seow, Y. Leung, N. Vande Castele, E. Ehteshami Afshar, D. Tanyingoh, G. Bindra, M.J. Stewart, P.L. Beck, G.G. Kaplan, S. Ghosh, R. Panaccione. The effects of pregnancy on the pharmacokinetics of infliximab and adalimumab in inflammatory bowel disease. *Aliment. Pharmacol. Ther.*, 45: 1329-1338 (2017).
- [187] N. Djokanovic, C. Klieger-Grossmann, A. Pupco, G. Koren. Safety of infliximab use during pregnancy. *Reprod. Toxicol.*, 32: 93-97 (2011).
- [188] N.E. Simister. Placental transport of immunoglobulin G. *Vaccine*, 21: 3365-3369 (2003).
- [189] J.D. Carter, A. Ladhani, L.R. Ricca, J. Valeriano, F.B. Vasey. A safety assessment of tumor necrosis factor antagonists during pregnancy: A review of the food and drug administration database. *J. Rheumatol.*, 36: 635-641 (2009).
- [190] Z. Shihab, N.D. Yeomans, P. De Cruz. Anti-tumour necrosis factor alpha therapies and inflammatory bowel disease pregnancy outcomes: A meta-analysis. *J. Crohn. Colitis.*, 10: 979-988 (2016).

Literature

- [191] M. Bortlik, N. Machkova, D. Duricova, K. Malickova, L. Hrdlicka, M. Lukas, P. Kohout, O. Shonova, M. Lukas. Pregnancy and newborn outcome of mothers with inflammatory bowel disease exposed to anti-TNF α therapy during pregnancy: Three-centre study. *J. Crohn. Colitis*, 48: 951-958 (2013).
- [192] K.L. Hyrich, S.M.M. Verstappen. Biologic therapies and pregnancy: The story so far. *Rheumatology (Oxford)*, 53: 1377-1385 (2014).
- [193] U. Mahadevan, D.C. Wolf, M. Dubinsky, A. Cortot, S.D. Lee, C.A. Siegel, T. Ullman, S. Glover, J.F. Valentine, D.T. Rubin, J. Miller, M.T. Abreu. Placental transfer of anti-tumor necrosis factor agents in pregnant patients with inflammatory bowel disease. *Clin. Gastroenterol. Hepatol.*, 11: 286-292 (2013).
- [194] D.C. Campbell. Physiological changes of pregnancy. *Semin. Anesth. Perioper. Med. Pain*, 19: 149-156 (2000).
- [195] F.M. Habal, V. Kapila. Inflammatory bowel disease and pregnancy: Evidence, uncertainty and patient decision-making. *Can. J. Gastroenterol.*, 23: 49-53 (2009).
- [196] A. Aratari, G. Margagnoni, M. Koch, C. Papi. Intentional infliximab use during pregnancy for severe steroid-refractory ulcerative colitis. *J. Crohn. Colitis*, 5: 262 (2011).
- [197] H.G. Frank. Placental development. In: R.A. Polin, S.H. Abman, D.H. Rowitch, W.E. Benitz, W.W. Fox (eds.). *Fetal and neonatal physiology*. Elsevier Inc., 5th ed. (2017).
- [198] P. Pantham, K.J. Askelund, L.W. Chamley. Trophoblast deportation part II: A review of the maternal consequences of trophoblast deportation. *Placenta*, 32: 724-731 (2011).
- [199] A.E. Covone, D. Mutton, P.M. Johnson, M. Adinolfi. Trophoblast cells in peripheral blood from pregnant women. *Lancet*, 13: 841-843 (1984).
- [200] L.W. Chamley, Q. Chen, J. Ding, P.R. Stone, M. Abumaree. Trophoblast deportation: Just a waste disposal system or antigen sharing? *J. Reprod. Immunol.* 88: 99-105 (2011).
- [201] C. Gardiner, D.S. Tannetta, C.A. Simms, P. Harrison, C.W.G. Redman, I.L. Sargent. Syncytiotrophoblast microvesicles released from pre-eclampsia placentae exhibit increased tissue factor activity. *PLoS One*. 6: e26313 (2011).
- [202] M. Tong, L.W. Chamley. Placental extracellular vesicles and feto-maternal communication. *Cold Spring. Harb. Perspect. Med.*, 29: a023028 (2015).
- [203] M.A. Khirwadkar, J.R. Kher. Study of serum immunoglobulins in normal pregnancy. *Indian J. Physiol. Pharmacol.*, 35: 69-70 (1991).

[204] F.S. Amah-Tariah, V.D. Dapper, O.J. Olorunfemi, E.A. Osunwoke. Serum immunoglobulin changes in pregnancy complicated with pre-eclampsia and diabetes in Nigerian women. *J. Dent. Med. Sci.*, 15: 83-88 (2016).

[205] W. Wang, E.Q. Wang, J.P. Balthasar. Monoclonal antibody pharmacokinetics and pharmacodynamics. *Clin. Pharmacol. Ther.*, 84: 548-558 (2008).

[206] M. Luu, E. Benzenine, M. Doret, C. Michiels, A. Barkun, T. Degend, C. Quantin, M. Bardou. Continuous anti-TNF α use throughout pregnancy: Possible complications for the mother but not for the fetus. A retrospective cohort on the French National Health Insurance Database (EVASION). *Am. J. Gastroenterol.*, 113: 1669-1677 (2018).

Appendix

Manuscript I

Equity Ratio Statement

Title of the manuscript:

“Quantitative relationship between infliximab exposure and inhibition of C-reactive protein synthesis to support inflammatory bowel diseases management”

Journal British Journal of Clinical Pharmacology
Volume 87, Issue 5, Pages 2374-2384 (2021)

Authorship First author

Status Published

DOI: <https://doi.org/10.1111/bcp.14648>

Reprinted with permission from British Journal of Clinical Pharmacology.

Own contribution


- Data set modification and checkouts
- All modelling and simulation activities, including PK-PD model development, model evaluation, and simulations
- Interpretation of the results, including literature research related to interpretation of the results and creation of the manuscript
- Drafting of all parts of the manuscript
- Creation of all figures and tables
- Adaptation of the manuscript according to the reviewers’ and editor’s comments

Ana-Marija Grišić
(Doctoral candidate, first author)

Prof. Dr. Charlotte Kloft
(Supervisor)

ORIGINAL ARTICLE

Quantitative relationship between infliximab exposure and inhibition of C-reactive protein synthesis to support inflammatory bowel disease management

Ana-Marija Griscic^{1,2}  | Alexander Eser³ | Wilhelm Huisinga⁴ | Walter Reinisch³ | Charlotte Kloft¹

¹Department of Clinical Pharmacy & Biochemistry, Institute of Pharmacy, Freie Universitaet Berlin, Germany

²Graduate Research Training Program PharMetrX, Germany

³Department for Gastroenterology and Hepatology, Medical University of Vienna, Austria

⁴Institute of Mathematics, University of Potsdam, Germany

Correspondence

Charlotte Kloft, Freie Universität Berlin, Institute of Pharmacy, Kelchstr. 31, 12169 Berlin, Germany.

Email: charlotte.kloft@fu-berlin.de

Aim: Quantitative and kinetic insights into the drug exposure-disease response relationship might enhance our knowledge on loss of response and support more effective monitoring of inflammatory activity by biomarkers in patients with inflammatory bowel disease (IBD) treated with infliximab (IFX). This study aimed to derive recommendations for dose adjustment and treatment optimisation based on mechanistic characterisation of the relationship between IFX serum concentration and C-reactive protein (CRP) concentration.

Methods: Data from an investigator-initiated trial included 121 patients with IBD during IFX maintenance treatment. Serum concentrations of IFX, antidrug antibodies (ADA), CRP, and disease-related covariates were determined at the mid-term and end of a dosing interval. Data were analysed using a pharmacometric nonlinear mixed-effects modelling approach. An IFX exposure-CRP model was generated and applied to evaluate dosing regimens to achieve CRP remission.

Results: The generated quantitative model showed that IFX has the potential to inhibit up to 72% (9% relative standard error [RSE]) of CRP synthesis in a patient. IFX concentration leading to 90% of the maximum CRP synthesis inhibition was 18.4 µg/mL (43% RSE). Presence of ADA was the most influential factor on IFX exposure. With standard dosing strategy, ≥55% of ADA+ patients experienced CRP non-remission. Shortening the dosing interval and co-therapy with immunomodulators were found to be the most beneficial strategies to maintain CRP remission.

Conclusions: With the generated model we could for the first time establish a robust relationship between IFX exposure and CRP synthesis inhibition, which could be utilised for treatment optimisation in IBD patients.

KEYWORDS

C-reactive protein remission, inflammatory bowel disease, infliximab dosing

The authors confirm that the Principal Investigator for this paper is Walter Reinisch and that he had direct clinical responsibility for patients.

This is an open access article under the terms of the Creative Commons Attribution-NonCommercial-NoDerivs License, which permits use and distribution in any medium, provided the original work is properly cited, the use is non-commercial and no modifications or adaptations are made.

© 2020 The Authors. British Journal of Clinical Pharmacology published by John Wiley & Sons Ltd on behalf of British Pharmacological Society

1 | INTRODUCTION

The inflammatory bowel diseases (IBDs), Crohn's disease and ulcerative colitis, comprise a complex variety of diseases characterised by chronic intestinal inflammation that may lead to irreversible damage and are associated with poor quality of life. While the control of IBDs has previously been of limited success, introduction of **antitumour necrosis factor α** (TNF α) monoclonal antibodies, such as **infliximab** (IFX), adalimumab and golimumab, brought about a notable advancement.¹ However, loss of response to the approved dosing regimen posits major challenges and introduced the need for Therapeutic Drug Monitoring (TDM), which finds clinical translations mostly with IFX.¹

Furthermore, the choice of the most appropriate treatment target to be tackled and effective monitoring biomarkers in IBD is itself a complex task. Measures of clinical remission² are subjective and thus not appropriate for exploring exposure-response relationships of drugs, whereas the more objective assessment of endoscopic disease activity is less apt for long-term disease monitoring due to invasiveness. C-reactive protein (CRP) concentration has been found to be a suitable surrogate marker due to its correlation with endoscopy³ and favourable kinetic behaviour.⁴

The relationship between serum concentrations of IFX and various disease outcomes has previously been investigated.^{5–10} However, there is a lack of quantitative and kinetic knowledge of those relationships. A pharmacometric framework, using the quantitative pharmacokinetic/pharmacodynamics (PK/PD) population approach,¹¹ in comparison with a static relationship relating exposure and response only at fixed time points, describes the time course of both drug exposure and IBD activity, and additionally enables quantifying the variability between patients in the investigated population, and identifying and quantifying factors that impact drug exposure or disease activity.

The aim of this study was to derive recommendations for dose adjustment and treatment optimisation based on mechanistic and kinetic characterisation of the relationship between IFX dosing, IFX serum concentration and CRP concentration.

2 | METHODS

2.1 | Study design

The data analysed in this study originated from an investigator-initiated trial performed at the University Hospital of the Medical University of Vienna. The study was conducted in accordance with ethical standards and was approved the institutional review board of the Medical University of Vienna. Written informed consent prior to inclusion was obtained from all patients.

Adult patients ($n = 121$) diagnosed with IBD (89 with Crohn's disease, 31 with ulcerative colitis (UC) and one patient with undetermined IBD type) in maintenance IFX treatment were included in the study, regardless of CRP concentration; patients with obvious conditions associated with increased CRP concentration (particularly infectious conditions) were excluded. The patients received IFX at

What is already known about this subject

- Clearance of infliximab (IFX) is subjected to high inter-individual variability, prompting the need for Therapeutic Drug Monitoring (TDM) to counteract loss-of-response in inflammatory bowel diseases (IBD).
- C-reactive protein (CRP) is routinely measured as a biomarker to monitor the activity of IBD.
- Quantitative and kinetic knowledge of the relationship between IFX exposure and disease response is scarce.

What this study adds

- A population pharmacokinetic/pharmacodynamic model describing the inhibitory effects of IFX on CRP synthesis was developed.
- High variability in IFX effect suggests that CRP monitoring should be included in the clinical decision making.
- Based on simulations from the model, dosing adjustments are suggested to support achieving continuous CRP remission.

absolute doses ranging from 100 to 1300 mg (median 400 mg; 1–11 mg/kg, median 5.6 mg/kg) at dosing intervals ranging from 3 to 12 weeks (median 8 weeks). Blood samples ($n = 388$) were taken at C_{\min} (minimum or trough concentration) and at the middle of the dosing interval as part of Therapeutic Drug Monitoring in the period 2010–2012. Serum concentrations of IFX, antidrug antibodies (ADA), CRP, albumin and other relevant laboratory values were determined. In addition, potentially relevant patient-related (body weight, smoking status, sex), disease-related (diagnosis, disease duration as well as Harvey-Bradshaw index, number of surgeries, disease location, behaviour and age at diagnosis per Montreal classification for Crohn's disease and disease severity per Montreal classification for ulcerative colitis) and therapy-related (dosing, premedication with corticosteroids, co-therapy with immunomodulators) characteristics were recorded.

Concentrations of IFX were determined using the IDK monitor enzyme-linked immunosorbent assay (Immunodiagnostik AG, Bensheim, Germany¹²) and concentrations of ADA by a homogeneous liquid-phase mobility shift assay (Prometheus Anser ADA, Prometheus Laboratories Inc., San Diego, California, USA¹³), with a threshold for positive ADA (ie, lower limit of quantification) of 3.13 U/mL.

2.2 | PK/PD model development by pharmacometric analysis

Prior to PK/PD model development, statistical and graphical analyses were performed. Thereafter the data were analysed using the

nonlinear mixed-effects modelling approach.¹⁴ For model development, the software tools NONMEM (version 7.3, ICON Plc, Ireland) and PsN (version 4.7.0) were employed, while R (version 3.3) and RStudio (version 1.1.447) were used for pre- and post-processing. The modelling process consisted of three main parts: (a) development of the base model characterising IFX PK, (b) covariate analysis aiming to identify patient-, disease- or therapy-specific factors significantly influencing IFX exposure and (c) development of a PK/PD model that quantifies the kinetic relationship between IFX exposure and disease activity as measured by CRP concentrations. The details of the modelling steps are given in the Supporting Information. Briefly, the crucial aspects were as follows:

- The *base model* comprises a structural submodel that predicts the PK of IFX in a typical individual of the patient population and a statistical submodel which quantifies between- and within-patient variability in the PK profiles.
- The *covariate model* enables identification of patient, disease or therapy factors that relevantly affect the PK profile, thus enabling individualisation of the IFX concentration-time profile according to these relevant factors.
- In the course of *PK/PD model development*, the effect of IFX on CRP was implemented via sequential PK/PD modelling, ie, after the PK model including covariates was developed the IFX concentration predicted for each individual (based on the so-called empirical Bayesian estimates of the PK parameters) were used for PD model development.¹⁵ To account for the time delay in changes of CRP concentration induced by IFX, indirect effect models were chosen.¹⁵ The quality and predictive performance of the ultimate PK/PD model was assessed by a recommended approach, the prediction-corrected visual predictive check ($n = 1000$ simulations).¹⁶

2.3 | Assessment of standard dosing strategy

The developed PK/PD model was utilised to evaluate the current dosing strategy in terms of CRP remission (defined as $\text{CRP} < 5 \text{ mg/L}$)¹⁷ and this strategy was compared to potential alternative dosing strategies to select the most beneficial dosing approach(es). Stochastic simulations ($n = 1000$) were performed for a typical IBD patient and patients differing in the most influential covariate factors identified. As it has previously been shown that changing the dosing interval is superior to changes in administered dose with respect to adjustment of IFX exposure,¹⁸ the standard dosing regimen (5 mg/kg at weeks 0, 2, 6 and every 8 weeks (q8w) afterwards) was compared to alternative dosing regimens that differed in dosing intervals. The investigations were focused on maintenance phase since no clinical data from the induction phase was available in the dataset underlying the developed model. Dosing intervals investigated ranged from every 4 (q4w) to every 12 weeks (q12w). For recommending alternative IFX dosing regimens, the time after IFX dosing when CRP concentration reached values $\geq 5 \text{ mg/L}$ (CRP nonremission) was calculated for each regimen and compared for ADA+ and ADA- patients across the investigated

dosing intervals in the presence and absence of co-therapy with immunomodulators.

3 | RESULTS

3.1 | PK/PD model development by pharmacometric analysis

The details of the model development process and outcomes are given in the Supporting Information. Altogether, 388 blood samples scattered over the entire dosing interval after IFX dosing from 121 patients were available for PK analysis (Table 1). Table 2 and Figure 1 give characteristics of measurements, demonstrating two sampling periods in this study: (a) from 2 to 6 weeks (mid-term) and (b) from 6 to 10 weeks (end of interval). The IFX concentration-time profiles were adequately characterised by the developed two-compartment PK model with linear elimination (Figure 2). Subsequently, four significant covariates (Supporting Information Figure S3) on clearance (CL) were identified: The development of ADA in a patient increased IFX CL by 97%, leading to an accelerated half-life and reduced exposure of IFX, whereas co-therapy with immunomodulators decreased IFX CL by 15.3%. Furthermore, low serum albumin concentration and high body weight were related to increased CL and thus decreased IFX exposure. Based on bootstrap (Supporting Information Figure S2), albumin concentration of 33 g/L was in almost 100% of cases related to increase in CL of $>20\%$ compared to the reference value. The extent of the effect of body weight was more modest, with both high (96 kg) and low (50 kg) values related to $<20\%$ change in CL compared to the reference value.

The developed PK model adequately described the measured IFX data (Supporting Information Figure S1). Volumes of distribution and intercompartmental exchange capacity values were in the range of typical PK parameters for monoclonal antibodies (mAbs; Supporting Information Table S1). Clearance in this study was 0.0126 L/h for the typical patient, having a body weight of 70 kg and serum albumin concentration of 43 g/L, that did not develop ADA and was not cotreated with immunomodulators. All covariates were considered time-varying, implying that CL changed over time with the covariates in each individual patient. Potential additional time-variance of CL on top of covariate effects could not be identified. From the covariates identified as significant, ADA presence had by far the highest impact: patients developing ADA (ADA+) revealed an approximately 2-fold higher CL compared to ADA- patients (Supporting Information Figure S2).

The concentration of CRP was determined in 339 blood samples. The graphical analysis indicated that there was a strong relation between IFX and CRP concentrations (Figure 3): CRP increased with decreasing IFX concentration (Figure 3A). Using the IFX threshold concentrations described in the literature (3 and 7 $\mu\text{g/mL}$), this trend was also clearly visible on stratification into three groups: IFX underexposed, within the target range and overexposed (Figure 3B). This was confirmed by statistical comparison: the relationship between

TABLE 1 Summary of patient characteristics at the time of first study day

Categorical characteristics	Number of patients (%)
Sex (n = 121)	
Male	62 (51.2)
Female	59 (48.8)
Smoking (n = 118)	
Nonsmoker	41 (34.7)
Smoker	46 (39.0)
Ex-smoker	31 (26.3)
Diagnosis (n = 121)	
Crohn's disease	88 (72.7)
Ulcerative colitis	32 (26.4)
Indeterminable IBD	1 (0.9)
Age at diagnosis of Crohn's disease (n = 88)	
≤16 years	11 (12.5)
17-40 years	65 (73.9)
>40 years	12 (13.6)
Crohn's disease location (n = 88)	
Ileal	10 (11.3)
Colonic	21 (23.9)
Ileocolonic	57 (64.8)
Crohn's disease behaviour (n = 87)	
Nonstricturing, nonpenetrating	30 (34.5)
Stricturing	25 (28.7)
Penetrating	32 (36.8)
Ulcerative colitis severity (n = 32)	
Mild	2 (6.25)
Moderate	9 (28.1)
Severe	21 (65.6)
Number of surgeries (n = 118)	
0	85 (72.0)
1	20 (17.0)
2	10 (8.5)
3	3 (2.5)
Continuous characteristics	Median (minimum, maximum)
Body weight (kg)	70 (47, 115)
Height (cm)	171 (155, 190)
Body mass index (kg/m ²)	23.2 (14.5, 41.7)

IBD, irritable bowel disease.

IFX and disease activity measures was highest for CRP (Spearman's rank correlation: 2×10^{-10} , 2×10^{-5} and 0.003 for CRP, albumin and Harvey-Bradshaw index, respectively). Correlation between CRP and serum albumin concentrations was significant ($P < 10^{-10}$), contrary to the correlation between CRP and Harvey-Bradshaw index ($P > .1$).

Leveraging mechanistic knowledge on the immunological CRP kinetics, an inhibition of CRP synthesis by IFX exposure was assumed and realised in the PK/PD model.⁴ To explore a potential difference in CD and UC subpopulation regarding serum CRP concentrations, multiple approaches were undertaken: the exploratory analysis prior to modelling identified no difference in CRP concentration range after first or previous dose between CD and UC, the relation between IFX and CRP was statistically significant (P value $< 10^{-4}$) in both subpopulations and during model development no effect of IBD type was identified on baseline CRP and/or drug efficacy (IC_{50}). The PK/PD model that adequately described (Supporting Information Figure S4) the relationship between IFX exposure and CRP concentration comprised an indirect response E_{max} model (Figure 2) that accounted for time delay in CRP change induced by IFX. The degradation rate constant of CRP was fixed to correspond to a reported half-life of 19 hours (0.0365 h^{-1}) to avoid identification issues.²⁰ The generated quantitative and kinetic model showed that IFX has the potential to inhibit up to 72% of CRP synthesis in a patient (Figure 4A). IFX concentration leading to 50% of the maximum CRP synthesis inhibition was $2.04 \mu\text{g/mL}$ and IFX concentration leading to 90% of the maximum CRP synthesis inhibition was $18.4 \mu\text{g/mL}$. The time point when these values were reached was naturally dependent on covariates defining the PK profile, as demonstrated in Figure 4B. The baseline CRP concentration could be estimated to be 6.32 mg/L for the typical individual, with high between-patient variability (coefficient of variation; CV) of 115% CV (5th-95th percentile range based on 1000 simulations: $1.50\text{-}28.4 \text{ mg/L}$). Similarly, between-patient variability in IFX concentration leading to half-maximum effect was found to be very high (209% CV; Figure 4C,D). None of the investigated covariates (eg diagnosis, sex, smoking status, age at diagnosis, Crohn's disease behaviour, Crohn's disease location, Montreal classification of ulcerative colitis severity, number of surgeries, baseline body weight, time since diagnosis at first IFX infusion) explained a significant part of the variability.

3.2 | Assessment of standard dosing strategy

To evaluate the standard and alternative dosing regimens, simulations were performed for a typical patient for nine different dosing intervals (q4w-q12w). Figure 5A shows the distribution of time to loss of CRP remission ($\text{CRP} > 5 \text{ mg/L}$) for ADA+ and ADA- patients with (upper panel) and without (lower panel) co-therapy with immunomodulators in dependence of the dosing interval. The numbers below the boxes show the number of patients that experienced $\text{CRP} > 5 \text{ mg/L}$ at any point during a dosing interval: With the standard dosing regimen in the maintenance phase (q8w), more than half of ADA+ patients experience CRP nonremission, regardless of immunomodulator use. However, co-therapy with immunomodulators significantly decreased the proportion of patients experiencing CRP nonremission from 74% to 55%. In Figure 5B, median times to loss of CRP remission per dosing interval were extracted. To increase the number of patients that accomplish CRP remission over the whole dosing interval, a dosing

TABLE 2 Summary of blood samples ($n_{\text{total}} = 388$, $n_{\text{mid-interval}} = 202$, $n_{\text{end-interval}} = 177$) characteristics

Categorical characteristics	Number of total samples (%)	Number of mid-interval samples (%)	Number of trough samples (%)
Concomitant therapy with immunomodulators			
Yes	68 (17.5)	31 (15.3)	25 (14.0)
No	320 (82.5)	172 (84.7)	154 (86.0)
Antidrug antibodies			
Yes	82 (21.1)	41 (20.3)	41 (23.2)
No	306 (78.9)	161 (79.7)	136 (76.8)
Continuous characteristics			
	Median (minimum, maximum)	Median (minimum, maximum)	Median (minimum, maximum)
Absolute dose administered [mg]	400 (100, 1,300)
Concentration of IFX ($\mu\text{g/mL}$) ($n = 388$)	8.30 (0.10, 53.5)	13.8 (0.10, 52.0)	4.30 (0.10, 24.0)
Concentration of CRP (mg/L) ($n = 339$)	2.70 (0.20, 120)	2.80 (0.20, 120)	2.35 (2.00, 50.8)
Concentration of Alb (g/L) ($n = 312$)	42.9 (25.3, 51.6)	43.0 (25.3, 50.8)	42.7 (25.8, 51.6)
Harvey-Bradshaw index ($n = 236$)	2 (0, 19)	2 (0, 18)	2 (0, 19)

Note. Mid-interval samples were defined as samples taken between week 2 and week 6 after dose, end-of-interval (trough) samples were defined as samples taken between week 6 and week 10 after dose.

Abbreviations: Alb, serum albumin; CRP, C-reactive protein; IFX, infliximab.

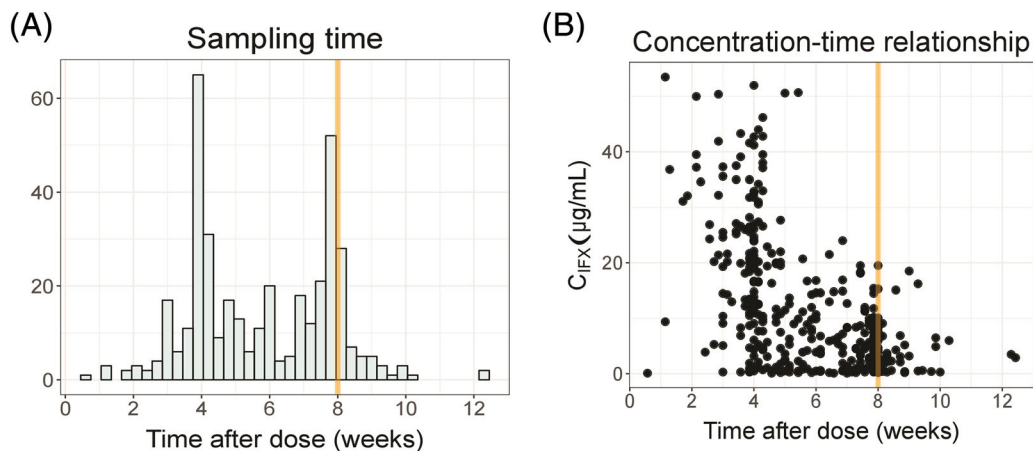


FIGURE 1 Overview of available measurements of infliximab (IFX) concentration in the investigated patient population. (A) Distribution of sampling times over dosing interval. The samples were mainly taken at C_{min} (trough) levels and at the middle of the dosing interval. The different dosing intervals arose from clinical decisions. (B) Concentration of IFX over time after last dose. Note that the dataset informs only the later phase of the concentration-time profile. The vertical orange line designates the standard dosing interval of 8 weeks (q8w). C_{IFX} , measured IFX concentration

interval shorter than the standard regimen would be required in both ADA+ and ADA- patient subpopulations: To this end, in the absence of co-therapy with immunomodulators, dosing intervals superior to q8w would be q7w and q5w for ADA- and ADA+ patients, respectively (Figure 5B). Furthermore, co-therapy with immunomodulators obviates the need for dosing interval reduction in ADA- patients and shortens the needed dosing interval to q6w in ADA+ patients.

4 | DISCUSSION

To the best of the authors' knowledge, this is the first time that a population model that characterises the relationship of IFX PK to CRP concentration as a time-varying variable in IBD has been reported:

This analysis characterised IFX exposure and its inhibition of CRP synthesis, and thereby enabled quantification of relevant PK and PD parameters, including variability in IFX exposure and response in the population. Patients who develop ADA and have low albumin, high BW and/or are not co-treated with immunomodulators were identified as subpopulations vulnerable to IFX underexposure. Furthermore, the model-based investigations indicate that shortening of the standard maintenance phase dosing interval dependent on ADA status should be considered to increase the number of patients maintaining CRP remission.

Despite its long presence in IBD management, therapy with IFX still faces challenges calling for further optimisation, from immunogenicity, to variable induction drug response, to loss of response to the therapy over time. The relationship between IFX exposure and CRP

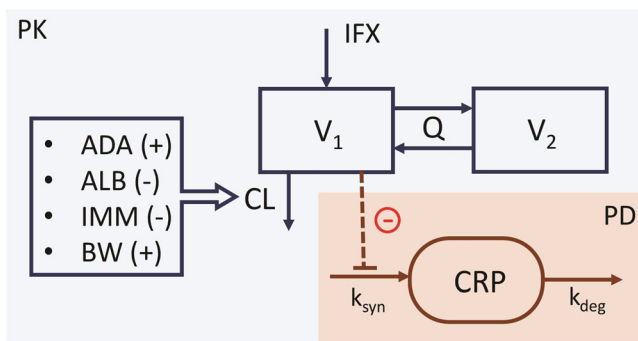


FIGURE 2 Graphical representation of the final pharmacokinetic/pharmacodynamics (PK/PD) model. Infliximab (IFX) PK is described by a two-compartment model with linear elimination. Antidrug antibody status, serum albumin concentration, co-therapy with immunomodulators and body weight were identified to impact the drug clearance (CL). The effect of IFX on C-reactive protein (CRP) was best characterised via the indirect drug effect modelling approach, whereby the plasma concentration of IFX was related to inhibition of CRP synthesis. ADA, antidrug antibodies; ALB, serum albumin concentration; BW, body weight; CL, clearance; CRP, C-reactive protein; IFX, infliximab; IMM, co-therapy with immunomodulators; k_{deg} , rate constant of CRP degradation; k_{syn} , rate constant of CRP synthesis; Q, intercompartmental exchange capacity; V_1 , volume of central compartment; V_2 , volume of peripheral compartment

concentration has so far not been characterised in a quantitative and mechanism-based way. Pharmacometric approaches enable a quantitative, kinetic and mechanistic insight into the underlying PK and PD/immunological pathways to be obtained. The developed models can be used to support clinical decisions as part of TDM, advocated by several national societies for the maintenance period of anti-TNF α therapy.

The first part of this analysis characterised the PK of IFX in IBD patients on maintenance phase treatment, including evaluation of factors that significantly contribute to the variability in IFX PK. In our

analysis, the covariates that significantly impacted CL in the investigated population were ADA status, co-therapy with immunomodulators, serum albumin concentration and body weight. Previously published IFX PK models show a high level of agreement with respect to identified covariates (eg, body size, disease activity markers, ADA, co-medication) and our findings are also in good agreement with these reports.²¹⁻²⁹ In contrast to most of the previously developed models, all covariates in the present analysis were implemented as time-varying variables, thus implying a realistic change of IFX CL over time relative to the covariate values in individual patients. By incorporating the change over time in covariate values (in contrast to baseline covariate values only), more information from a covariate-parameter relationship from the data is used.

Mechanistically, the development of ADA affects both the PK and IFX effects. ADA molecules binding to active sites of the IFX molecule hinder its efficacy by disabling binding to its target, TNF α . Furthermore, the IFX-ADA complexes formed are promptly cleared from blood, contributing to higher CL of IFX.³⁰ Despite differences in assays available for ADA detection/quantification, especially the lower limit of quantification, resulting in varying definitions of ADA positivity in different analyses, ADA have consistently been found to impact IFX CL. The assay used in this study quantified total (both drug-bound and unbound) ADA concentration, with a cut-off for ADA positivity of 3.13 U/mL. In this analysis, an approximately 2-fold higher IFX CL was found in patients who developed ADA compared to patients who did not. The ADA status was, however, not found to impact the drug efficacy in our model. Another important factor that influences IFX CL is serum albumin concentration, as confirmed by our analysis as well. Serum albumin is likely related to IFX CL via two mechanisms: (a) as a marker of disease state and increased protein turnover in inflammation and (b) as a marker of the neonatal Fc-receptor (FcRn) activity (lower albumin concentration indicative of lower FcRn activity, resulting in higher IFX CL), potentially explaining why albumin was the disease activity marker predictive of IFX CL

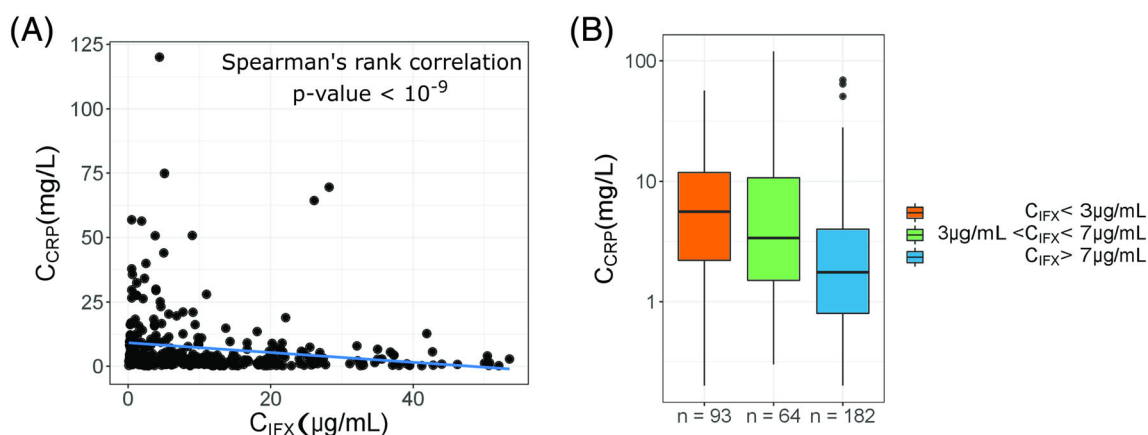


FIGURE 3 Relation between infliximab (IFX) exposure (ie, plasma concentration) and C-reactive protein (CRP) concentration. (A) Concentration of CRP over IFX concentration. The blue line represents linear regression. (B) Simplified comparison of the IFX-CRP relationship. Concentrations of IFX were stratified in three groups: ≤ 3 $\mu\text{g/mL}$, between 3 and 7 $\mu\text{g/mL}$, and > 7 $\mu\text{g/mL}$.¹⁹ The numbers indicate the number of observations each group comprises. A decrease in CRP concentration from the group with lowest IFX exposure to the group with highest is observed. C_{CRP} , measured CRP concentration; C_{IFX} , measured IFX concentration

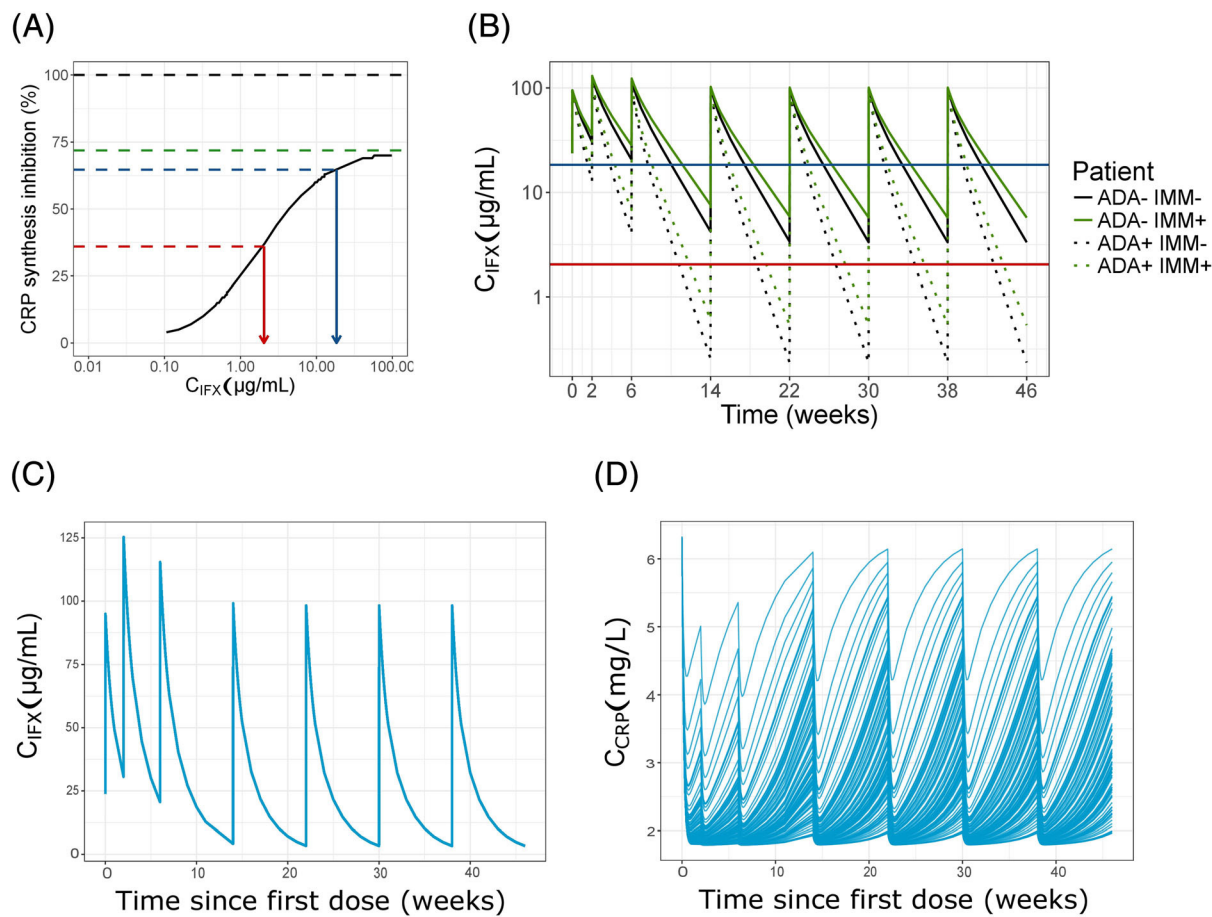


FIGURE 4 Illustration of infliximab (IFX) concentration (C_{IFX})-effect (C-reactive protein [CRP] synthesis inhibition)-time relationships. (A) IFX exposure-CRP synthesis inhibition curve and IFX potency. Red and blue arrows designate the IFX concentrations corresponding to 90% (18.4 $\mu\text{g/mL}$) and 50% (2.04 $\mu\text{g/mL}$) of the maximum CRP synthesis inhibition effect of ~72% (dashed green line), respectively. (B) Time after dose when IFX concentration falls below the 90% (blue line) and 50% (red line) effect concentrations for ADA- (solid lines) and ADA+ (dotted lines) patients without (black lines) and with (green lines) immunomodulator co-therapy. (C) and (D) Visualisation of high unexplained between-patient variability in IFX concentrations leading to a half-maximum effect on CRP concentration (IC_{50} value). Stochastic simulations were performed whereby variability in IC_{50} was considered. (C) IFX concentration-time profile in a reference individual. (D) Corresponding potential CRP concentration profiles. The plot demonstrates that due to high between-patient variability that could not be explained with any covariates, even for a patient with a known PK profile and baseline CRP concentration it is not possible to predict a single corresponding CRP profile, but rather a (rather wide) range of potential CRP profiles. ADA, antidrug antibodies; C_{CRP} , measured CRP concentration; C_{IFX} , measured IFX concentration; IMM, co-therapy with immunomodulators

rather than CRP. Furthermore, our analysis revealed a direct relationship between body weight and IFX CL, as well as an inverse relationship between co-therapy with immunomodulators and CL (see below). This analysis also investigated the potential impact of other covariates (eg, disease, sex), but none of them had a significant effect on CL. Given the similar proportion of male and female patients, our results suggest that dosing recommendations for both sexes must not be different.

Of the myriad measures used to assess activity of IBD, biomarkers currently represent adjunctive treatment targets primarily aimed for disease monitoring.³¹ This study focused on CRP due to its favourable characteristics: (a) correlation with endoscopy,³ (b) high sensitivity and short half-life ($t_{1/2}$ = approximately 19 h), and (c) well-known kinetic behaviour that does not differ between healthy and diseased individuals.⁴

One of the aims of this work was to investigate the PK/PD relationship between IFX exposure and IBD activity measures. In this analysis, disease activity measures were CRP and serum albumin concentrations, and the Harvey-Bradshaw index for patients with Crohn's disease. For UC, disease severity was assessed according to the Montreal classification and disease activity by the partial Mayo score; however, due to the low number of patients with UC, sub-analyses in this group were not performed. As $TNF\alpha$ is the main initiator of immunological cascade resulting in CRP synthesis, lower levels of $TNF\alpha$ lead to lower CRP synthesis (Figure 2). Since IFX does not inhibit CRP synthesis directly, a certain time-delay between maximum IFX exposure and maximum inhibition of CRP synthesis is expected. In the PK/PD model, this time-delay was incorporated as IFX inhibition of CRP synthesis via the indirect response modelling approach. The model estimated that up to approximately 72% of

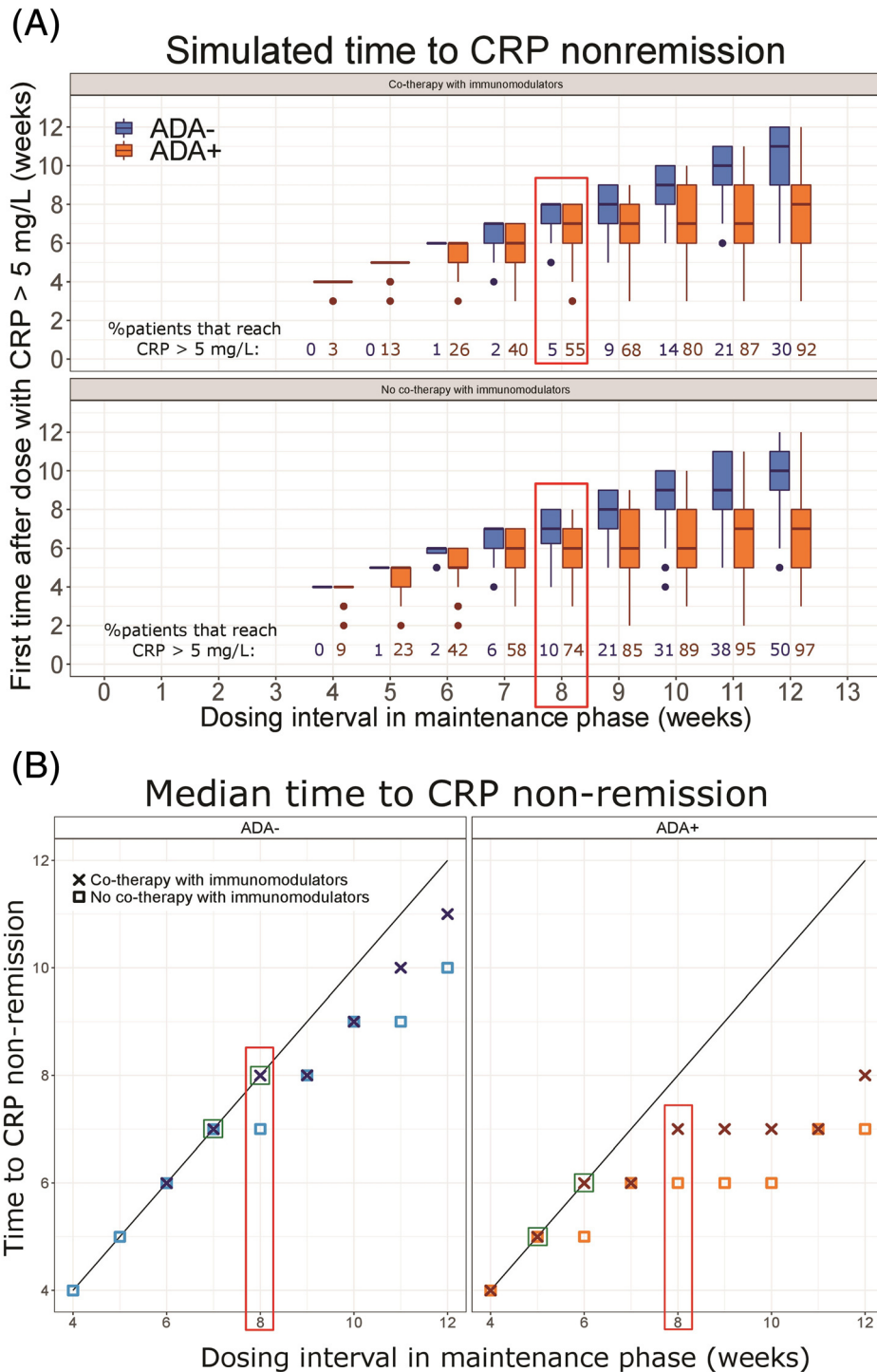


FIGURE 5 Evaluation of the standard and alternative infliximab (IFX) dosing regimens with respect to C-reactive protein (CRP) suppression via stochastic simulations ($n = 1000$) of patients that differ only in antidrug antibody status. For the simulations, variability in the PK submodel parameters was considered. (a) Distribution of time points in the weeks after the fifth dose when CRP concentration reached 5 mg/L (CRP nonremission) as box-whisker plot over simulated IFX dosing intervals, stratified by antidrug antibody (ADA) status and co-therapy with immunomodulators. Note that the virtual patients that do not experience CRP concentrations above 5 mg/L (ie, without loss of CRP remission) are not included in the plot. Proportions of patients experiencing CRP nonremission (shown below each box) are higher in cases of ADA development and absence of co-therapy with immunomodulators. (b) Simplification showing only the median time after the fifth dose when CRP concentration reached CRP nonremission stratified by ADA development and immunomodulatory co-therapy. In the presence of co-therapy with immunomodulators, the standard IFX dosing interval of every 8 weeks (q8w) corresponds to median time to CRP nonremission in ADA- patients, whereas for ADA+ patients reduction to q6w is to be recommended. In the absence of co-therapy with immunomodulators, for ADA- patients a dosing interval of q7w corresponds to the median time to CRP nonremission, whereas for ADA+ patients further reduction to a dosing interval of q5w should be preferred. Red frame, standard IFX dosing regimen every 8 weeks

CRP synthesis can be inhibited by IFX (Figure 4A). In other words, the IFX effect is saturable and CRP synthesis cannot be 100% inhibited by IFX: Regardless of how high IFX concentrations are achieved within an individual, approximately a quarter of CRP synthesis cannot be inhibited. This finding, now quantified, is in good accordance with previous knowledge, since $\text{TNF}\alpha$ is not the only immunological initiator of CRP synthesis.⁴ Concentration of IFX leading to half-maximum effect was 2.04 $\mu\text{g}/\text{mL}$, which approximately corresponds to PK targets previously described in the literature.¹⁹ The corresponding IFX concentration leading to 90% of the maximum effect was 18.4 $\mu\text{g}/\text{mL}$. As, depending on their covariates, different patients might have different PK profiles, the time after a dose when IFX concentration falls below an effective level might differ as well. This is illustrated in Figure 4B: a typical ADA⁻ patient drops below the 90% effect IFX concentration before week 4 in the absence of co-therapy with immunomodulators and after week 4 in the presence of the co-therapy. The IFX concentration never falls below the 50% effect concentration in this subpopulation. In contrast, ADA⁺ patients fall below the 90% effect concentration threshold around week 2, regardless of immunomodulators use, ie, approximately or more than 2x faster than the ADA⁻ patient. Thus, in ADA⁺ patients the 90% effect concentration is achieved during only one quarter of the dosing interval. The beneficial co-therapy with immunomodulators, however, delays crossing the 50% effect concentration threshold in ADA⁺ patients from 5 to 6 weeks. From the clinical perspective, a very important finding of this analysis is the high between-patient variability in IC_{50} value of IFX for the effect on CRP ($\sim 209\%$ CV). One hypothesis to explain the identified high between-patient variability in IC_{50} is the fact that CRP is a far downstream biomarker with respect to IFX binding to $\text{TNF}\alpha$. A similar finding was recently obtained for faecal calprotectin in a report of an IFX-faecal calprotectin PK/PD model.³² This indicates that there is a potentially high individual difference in effect (ie, inhibition of CRP synthesis) among patients even in cases of the same IFX exposure (Figure 4C,D). Practically, this implies that monitoring of disease activity measures, such as CRP concentration, might be advantageous over solely monitoring IFX concentration. Further investigations in the direction of identifying covariates that contribute to this high variability are warranted.

In our data, no long-term inhibitory effect of IFX on CRP was observed, ie, stopping IFX therapy leads to increase in disease activity, regardless of the time after IFX therapy initiation. Contrarily, clinical experience suggests that some patients will remain in a state of remission even if IFX therapy is ceased after a certain period.^{33,34} In our data, samples were collected from a large number of patients, but spread over different ranges of time after first dose and with a relatively short follow-up time. This might contribute to the lack of identification of long-term disease suppression. If long-term data is available and this cumulative IFX effect was identified, it could be added to the PK/PD model.

We acknowledge that our study has certain limitations. As sampling in the first weeks of the dosing interval is scarce, the dataset informs only the later phase of the IFX concentration-time profile.

This limitation manifests itself through the fact that the central volume of distribution and intercompartmental exchange capacity could not be estimated from the data alone, in contrast to clearance and peripheral volume of distribution. The frequentist prior approach enabled this limitation of the real-world clinical data situation to be overcome.³⁵ While the sampling scheme (ie, two samples per dosing interval) resulted in appreciable ranges of all variables (eg, IFX, CRP, ALB, covariates) due to the TDM nature of the dataset, the CRP concentration at the time of the first IFX infusion was not available for most patients. Our generated model, however, was able to estimate the plausible baseline CRP value very precisely. In addition, measurement of further factors, eg, genotyping and assessment of faecal loss of IFX, CRP and albumin, would enable investigation of their potential effect on the PK and PK/PD. For instance, besides the two known mechanisms of the albumin-IFX relationship (ie, the inverse relationship between serum albumin concentration and IBD activity, and the shared PK pathways of albumin and IFX, especially the FcRn salvage pathway), faecal loss might be an additional contributor. Finally, limitations of CRP as a disease marker (eg, lack of specificity) have to be acknowledged; investigation of additional disease markers would add to this knowledge and help further inform the choice of the most appropriate marker. This was accounted for in the developed PK/PD model by a finding of maximum CRP synthesis inhibition lower than 100%, whereby non- $\text{TNF}\alpha$ inducers of CRP synthesis are implied. Altogether, the heterogeneity of the patient population (covering broad ranges of the measured values) and the informative sampling time points (including an additional sample to the one taken just before the next IFX dose, i.e. trough) enabled the described IFX exposure-response relationship to be captured.

Pharmacometric nonlinear mixed-effects modelling analysis of PK/PD relationships enables characterisation of the analysed patient population over time in a continuous manner, at the same time providing insight into the variability between patients and relevant covariates. One of the advantages of this modelling approach is that after successful model development and evaluation, the model can be employed to test different hypotheses via simulations. This is illustrated by the *in silico* substudy we carried out. As the presence of ADA was found to lead to a very high influence on IFX CL and thus IFX exposure, we investigated how this impact reflects on CRP. To this end, simulations were performed for ADA⁺ and ADA⁻ virtual IBD patients to assess different dosing intervals (q4w-q12w) and the impact of co-therapy with immunomodulators. The desired target was defined as CRP concentration $< 5 \text{ mg}/\text{L}$ over the whole dosing interval (CRP remission). To assess the target attainment, simulations ($n = 1000$) were performed for each investigated dosing interval and (a) the percentage of patients with undesired outcome, ie, that reach $\text{CRP} > 5 \text{ mg}/\text{L}$ (CRP nonremission) and (b) the time after the fifth dose when the CRP concentration crossed and exceeded the target value were recorded. As shown in Figure 5A, when a standard dosing regimen (q8w) was simulated without co-therapy with immunomodulators, 10% of ADA⁻ and as much as 74% of ADA⁺ patients experienced CRP values higher than 5 mg/L. These

proportions were lower in the presence of immunomodulators (5% and 55% for ADA- and ADA+ patients, respectively). The median time to loss of CRP remission (Figure 5B) suggests that ADA- patients accomplish continuous CRP remission with standard dosing interval q8w when they are co-treated with immunomodulators. On the other hand, in ADA+ patients a reduction of dosing interval would be required to q5w and q6w in the absence and presence of immunomodulators co-therapy, respectively.

In this study, we report the first PK/PD model relating IFX exposure to inhibition of CRP synthesis in IBD patients. Increased CL of IFX was related to development of ADA, low serum albumin, high body weight and absence of co-therapy with immunomodulators. The developed PK/PD model identified high variability in effect on CRP for the same IFX exposure, which could not be explained with evaluated covariates, suggesting individual CRP measurements should be monitored and included in the decision of a patient's dosing regimen. Based on simulations from the developed PK/PD model, concrete ADA status- and immunomodulatory co-therapy-dependent dosing adjustments of current standard dosing strategies are suggested to support achieving continuous CRP remission in these patients. Finally, the developed model enables simulation of any type of dosing regimen change (eg, dose change) and provides a framework for development of a dashboard system²⁸ that could directly support therapeutic decision making, with respect to achieving both IFX and CRP targets.

Nomenclature of targets and ligands

Key protein targets and ligands in this article are hyperlinked to corresponding entries in <http://www.guidetopharmacology.org>, the common portal for data from the IUPHAR/BPS Guide to PHARMACOLOGY, and are permanently archived in the Concise Guide to PHARMACOLOGY 2019/20.³⁶

ACKNOWLEDGEMENT

Open access funding enabled and organized by Projekt DEAL.

COMPETING INTERESTS

A.M.G. declares no conflicts of interest. A.E. has served as a speaker, consultant and advisory board member for Abbvie, MSD, Takeda, Ferring and Astro Pharma; no other disclosures apply. C.K. and W.H. have received research funding from an industry consortium (AbbVie Deutschland GmbH & Co. KG, Boehringer Ingelheim Pharma GmbH & Co. KG, Grünenthal GmbH, F. Hoffmann-La Roche Ltd, Merck KGaA and SANOFI) to support the PharMetrX PhD program. W.R. has served as a speaker for Abbott Laboratories, Abbvie, Aesca, Aptalis, Astellas, Centocor, Celltrion, Danone Austria, Elan, Falk Pharma GmbH, Ferring, Immundiagnostik, Mitsubishi Tanabe Pharma Corporation, MSD, Otsuka, PDL, Pharmacosmos, PLS Education, Schering-Plough, Shire, Takeda, Therakos, Vifor and Yakult; as a consultant for Abbott Laboratories, Abbvie, Aesca, Amgen, AM Pharma, AOP Orphan, Arena Pharmaceuticals, Astellas, Astra Zeneca, Avaxia, Roland Berger GmbH,

Bioclinica, Biogen IDEC, Boehringer-Ingelheim, Bristol-Myers Squibb, Cellerix, Chemocentryx, Celgene, Centocor, Celltrion, Covance, Danone Austria, Elan, Eli Lilly, Ernest & Young, Falk Pharma GmbH, Ferring, Galapagos, Genentech, Gilead, Grünenthal, ICON, Index Pharma, Inova, Janssen, Johnson & Johnson, Kyowa Hakko Kirin Pharma, Lipid Therapeutics, LivaNova, Mallinckrodt, Medahead, MedImmune, Millenium, Mitsubishi Tanabe Pharma Corporation, MSD, Nash Pharmaceuticals, Nestle, Nippon Kayaku, Novartis, Ocera, Otsuka, Parexel, PDL, Periconsulting, Pharmacosmos, Philip Morris Institute, Pfizer, Procter & Gamble, Prometheus, Protagonist, Provention, Robarts Clinical Trial, Sandoz, Schering-Plough, Second Genome, Seres Therapeutics, Setpointmedical, Sigmoid, Takeda, Therakos, Tigenix, UCB, Vifor, Zealand, Zyngenia and 4SC; as an advisory board member for Abbott Laboratories, Abbvie, Aesca, Amgen, AM Pharma, Astellas, Astra Zeneca, Avaxia, Biogen IDEC, Boehringer-Ingelheim, Bristol-Myers Squibb, Cellerix, Chemocentryx, Celgene, Centocor, Celltrion, Danone Austria, Elan, Ferring, Galapagos, Genentech, Grünenthal, Inova, Janssen, Johnson & Johnson, Kyowa Hakko Kirin Pharma, Lipid Therapeutics, MedImmune, Millenium, Mitsubishi Tanabe Pharma Corporation, MSD, Nestle, Novartis, Ocera, Otsuka, PDL, Pharmacosmos, Pfizer, Procter & Gamble, Prometheus, Sandoz, Schering-Plough, Second Genome, Setpointmedical, Takeda, Therakos, Tigenix, UCB, Zealand, Zyngenia, and 4SC; and has received research funding from Abbott Laboratories, Abbvie, Aesca, Centocor, Falk Pharma GmbH, Immundiagnostik and MSD. C.K. reports grants from Diurnal Ltd and the Innovative Medicines Initiative-Joint Undertaking (DDMoRe) outside the submitted work.

CONTRIBUTORS

A.E. and W.R. conceived and designed the study and provided the data for the analysis. A.M.G. conducted the analysis and drafted the manuscript. C.K. and W.H. provided methodological support. All authors were involved in interpretation of results and critical revision of the manuscript. All authors approved the final version of the manuscript.

DATA AVAILABILITY STATEMENT

Research data are not shared.

ORCID

Ana-Marija Grisic  <https://orcid.org/0000-0002-1093-6879>

REFERENCES

1. Hemperly A, Castele NV. Clinical pharmacokinetics and pharmacodynamics of infliximab in the treatment of inflammatory bowel disease. *Clin Pharmacokinet*. 2018;57(8):929-942.
2. Peyrin-Biroulet L, Panés J, Sandborn WJ, et al. Defining disease severity in inflammatory bowel diseases: current and future directions. *Clin Gastroenterol Hepatol*. 2016;14(3):348-354.
3. Jürgens M, John JMM, Cleynen I, et al. Levels of C-reactive protein are associated with response to infliximab therapy in patients with Crohn's disease. *Clin Gastroenterol Hepatol*. 2011;9(5):421-427.
4. Vermeire S, Van Assche G, Rutgeerts P. C-reactive protein as a marker for inflammatory bowel disease. *Inflamm Bowel Dis*. 2004;10(5):661-665.

5. Bortlik M, Duricova D, Malickova K, et al. Infliximab trough levels may predict sustained response to infliximab in patients with Crohn's disease. *J Crohns Colitis*. 2013;7(9):736-743.
6. Carlsen A, Omdal R, Leitao KØ, et al. Subtherapeutic concentrations of infliximab and adalimumab are associated with increased disease activity in Crohn's disease. *Ther Adv Gastroenterol Mar*. 2018;11:1-11.
7. Cornillie F, Hanauer SB, Diamond RH, et al. Postinduction serum infliximab trough level and decrease of C-reactive protein level are associated with durable sustained response to infliximab: a retrospective analysis of the ACCENT I trial. *Gut*. 2014;63(11):1721-1727.
8. Papamichael K, Rakowsky S, Rivera C, Cheifetz AS, Osterman MT. Association between serum infliximab trough concentrations during maintenance therapy and biochemical, endoscopic, and histologic remission in Crohn's disease. *Inflamm Bowel Dis*. 2018;24(10):2266-2271.
9. Levesque BG, Greenberg GR, Zou G, et al. A prospective cohort study to determine the relationship between serum infliximab concentration and efficacy in patients with luminal Crohn's disease. *Aliment Pharmacol Ther*. 2014;39(10):1126-1135.
10. Edlund H, Grasic AM, Steenholdt C, et al. Absence of relationship between CDAI or CRP and infliximab exposure calls for objective Crohn's disease activity measures for the evaluation of treatment effects at treatment failure. *Ther Drug Monit*. 2019;41(2):235-242.
11. Mould DR, Upton RN. Basic concepts in population modeling, simulation, and model-based drug development. *CPT PSP*. 2012;1(9):1-14.
12. Kennedy NA, Heap GA, Green HD, et al. Predictors of anti-TNF treatment failure in anti-TNF-naïve patients with active luminal Crohn's disease: a prospective, multicentre, cohort study. *Lancet Gastroenterol Hepatol*. 2019;4(5):341-353.
13. Wang SL, Ohrmund L, Hauenstein S, et al. Development and validation of a homogeneous mobility shift assay for the measurement of infliximab and antibodies-to-infliximab levels in patient serum. *J Immunol Methods*. 2012;382(1-2):177-188.
14. Mould DR, Upton RN. Basic concepts in population modeling, simulation, and model-based drug development - part 2: introduction to pharmacokinetic modelling methods. *CPT PSP*. 2013;2(4):e38.
15. Upton RN, Mould DR. Basic concepts in population modeling, simulation, and model-based drug development: part 3 - introduction to pharmacodynamics modeling methods. *CPT PSP*. 2014;3(1):e88.
16. Bergstrand M, Hooker AC, Wallin JE, Karlsson MO. Prediction-corrected visual predictive checks for diagnosing nonlinear mixed-effects models. *AAPS J*. 2011;13(2):143-151.
17. Reinisch W, Wang Y, Oddens BJ, Link R. C-reactive protein, an indicator for maintained response or remission to infliximab in patients with Crohn's disease: a post-hoc analysis from ACCENT I. *Aliment Pharmacol Ther*. 2012;35(5):568-576.
18. Andersson H, Eser A, Huisinga W, et al. Recommendations for dose adjustments of infliximab in Crohn's disease patients with higher clearance. 5th American conference on Pharmacometrics (ACoP), Las Vegas, Nevada, USA, 12-15 Oct 2014. *J Pharmacokinet Pharmacodyn*. 2014;41(Suppl):S27-S27.
19. Vande Castele N, Ferrante M, Van Assche G, et al. Trough concentrations of infliximab guide dosing for patients with inflammatory bowel disease. *Gastroenterology*. 2015;148(7):1320-1329.
20. Vigushin DM, Pepys MB, Hawkins PN. Metabolic and scintigraphic studies of radioiodinated human C-reactive protein in health and disease. *J Clin Invest*. 1993;91(4):1351-1357.
21. Ternant D, Aubourg A, Magdelaine-Beuzelin C, et al. Infliximab pharmacokinetics in inflammatory bowel disease patients. *Ther Drug Monit*. 2008;30(4):523-529.
22. Fasanmade AA, Adedokun OJ, Ford J, et al. Population pharmacokinetic analysis of infliximab in patients with ulcerative colitis. *Eur J Clin Pharmacol*. 2009;65(12):1211-1228.
23. Fasanmade AA, Adedokun OJ, Blank M, Zhou H, Davis HM. Pharmacokinetic properties of infliximab in children and adults with Crohn's disease: a retrospective analysis of data from 2 phase III clinical trials. *Clin Ther*. 2011;33(7):946-964.
24. Dotan I, Ron Y, Yanai H, et al. Patient factors that increase infliximab clearance and shorten half-life in inflammatory bowel disease: a population pharmacokinetic study. *Inflamm Bowel Dis*. 2014;20(12):2247-2259.
25. Buurman DJ, Maurer JM, Keizer RJ, et al. Population pharmacokinetics of infliximab in patients with inflammatory bowel disease: potential implications for dosing in clinical practice. *Aliment Pharmacol Ther*. 2015;41(5):529-539.
26. Dreesen E, Vande Castele N, Tops S, et al. Anti-drug antibodies, low serum albumin and high C-reactive protein increase infliximab clearance in patients with inflammatory bowel disease: a population pharmacokinetic study of the TAXIT trial. *PAGE* 25, 2016; Abstr 5873 [www.page-meeting.org/?abstract=5873].
27. Edlund H, Steenholdt C, Ainsworth MA, et al. Magnitude of increased infliximab clearance imposed by anti-infliximab antibodies in Crohn's disease is determined by their concentration. *AAPS J*. 2017;19(1):223-233.
28. Eser A, Primas C, Reinisch S, et al. Prediction of individual serum infliximab concentrations in inflammatory bowel disease by a Bayesian dashboard system. *J Clin Pharmacol*. 2018;58(6):790-802.
29. Bauman LE, Xiong Y, Mizuno T, et al. Improved population pharmacokinetic model for predicting optimized infliximab exposure in pediatric inflammatory bowel disease. *Inflamm Bowel Dis*. 2020;26(3):429-439.
30. Moss AC, Brinks V, Carpenter JF. Review article: immunogenicity of anti-TNF biologics in IBD - the role of patient, product and prescriber factors. *Aliment Pharmacol Ther*. 2013;38(10):1188-1197.
31. Vermeire S, Van Assche G, Rutgeerts P. Laboratory markers in IBD: useful, magic, or unnecessary toys? *Gut*. 2006;55(3):426-431.
32. Dreesen E, Berends S, Laharie D, et al. Modelling of the relationship between infliximab exposure, faecal calprotectin, and endoscopic remission in patients with Crohn's disease. *Br J Clin Pharmacol*. 2020;14(Supplement_1):S052-S053.
33. Hu H, Xiang C, Qiu C, et al. Discontinuation of scheduled infliximab in Crohn's patients with clinical remission: a retrospective single-center study. *Gastroenterology Res*. 2017;10(2):92-99.
34. Louis E, Mary JY, Vernier-Massouille G, et al. Maintenance of remission among patients with Crohn's disease on antimetabolite therapy after infliximab therapy is stopped. *Gastroenterol*. 2012;142(1):63-70.
35. Gisleskog PO, Karlsson MO, Beal SL. Use of prior information to stabilize a population data analysis. *J Pharmacokinet Pharmacodyn*. 2002;29(5-6):473-505.
36. Alexander SPH, Kelly E, Mathie A, et al. The concise guide to pharmacology 2019/20: enzymes. *Br J Pharmacol*. 2019;176(S1):S297-S396.

SUPPORTING INFORMATION

Additional supporting information may be found online in the Supporting Information section at the end of this article.

How to cite this article: Grsic A-M, Eser A, Huisinga W, Reinisch W, Kloft C. Quantitative relationship between infliximab exposure and inhibition of C-reactive protein synthesis to support inflammatory bowel disease management. *Br J Clin Pharmacol*. 2020;1-11. <https://doi.org/10.1111/bcp.14648>

1 **Supplementary**

2

3 **Title:** Quantitative relationship between infliximab exposure and inhibition of C-reactive
4 protein synthesis to support inflammatory bowel diseases management

5

6 **Authors:**

7 Ana-Marija Grasic^{1,2}, Alexander Eser³, Wilhelm Huisinga⁴, Walter Reinisch³, Charlotte Kloft¹

8

9 **Affiliations:**

- 10 1. Dept. of Clinical Pharmacy & Biochemistry, Institute of Pharmacy, Freie Universitaet
11 Berlin, Germany
- 12 2. Graduate Research Training Program PharMetrX, Germany
- 13 3. Dept. for Gastroenterology and Hepatology, Medical University of Vienna, Austria
- 14 4. Institute of Mathematics, University of Potsdam, Germany

15

16 **PK/PD model development by pharmacometric analysis**

17 Throughout the modelling process, model evaluation and comparison included change of
18 objective function value, plausibility and precision of parameter estimation, goodness-of-fit
19 plots, and visual predictive checks.

20 *Base PK model*

21 Due to the sparse nature of the data the frequentist prior approach was used to support PK
22 parameter estimation, as described in Gisleskog et al.¹ The PK model used as prior was
23 originally developed by Fasanmade et al.² The prior model was used to further inform and
24 stabilise estimation of V_1 and Q . Initially, a prior was additionally employed for between-
25 patient variability in V_1 , V_2 and CL , but as variability in CL was well informed by the data
26 alone the prior was removed and between-patient variability in V_1 and V_2 fixed. Residual
27 unexplained variability was described with a mixed additive and proportional error model.
28 To account for potential differences between patients in residual unexplained variability
29 arising from the high diversity of the investigated population, the residual variability was
30 allowed to vary between patients (i.e. between-patient variability in residual unexplained
31 variability was implemented). This change significantly improved the model fit.

32 *PK model parameters*

33 Volume of the central compartment and intercompartmental exchange flow were 3.67 L and
34 0.00671 L/h, respectively. Volume of the peripheral compartment was estimated to be 0.936
35 L. Between-patient variability in central and peripheral volume of distribution was fixed to
36 12.8 and 55.3 %CV, respectively, as explained above. Proportional residual unexplained
37 variability was estimated to be 24.0% CV, whereas additive residual unexplained variability
38 had a standard deviation of 0.478 $\mu\text{g/mL}$. Inclusion of the covariates in the model explained

39 26.7% of the between-patient variability in CL, decreasing it to a final value of 34.9 %CV. In
 40 addition, accounting for covariate effects resulted in a reduction of between-patient
 41 variability in residual unexplained variability from 31.7% to 22.2% CV. The estimated additive
 42 and proportional residual unexplained variability values were low.

Table S1. Final model parameters.

Parameter, unit	Mean (%RSE) [%shrinkage]
<i>PK submodel parameters</i>	
Central volume of distribution V_1 , L	3.67 (-)
Intercompartmental exchange rate Q , L/h	0.0067 (-)
Peripheral volume of distribution V_2 , L	0.956 (11)
Infliximab clearance, L/h	0.0109 (3)
Effect of ADA on CL	0.972 (4)
Effect of Alb on CL	-1.17 (21)
Effect of body weight on CL	0.356 (41)
Effect of IMM co-therapy on CL	0.847 (5)
Between-patient variability in V_1 , %CV	12.8 (-) [83]
Between-patient variability in V_2 , %CV	55.3 (-) [56]
Between-patient variability in CL, %CV	34.9 (8) [6]
Additive RUV in PK, SD ($\mu\text{g/mL}$)	0.478 (21) [17]
Proportional RUV in PK, %CV	24 (14) [17]
Between-patient variability in RUV, %CV	22.2 (18) [46]
<i>PD submodel parameters</i>	
Baseline CRP, mg/L	6.32 (17)
CRP degradation rate constant k_{deg} , h^{-1}	0.0365 (-)
Half-maximal inhibitory concentration IC_{50} , $\mu\text{g/mL}$	2.04 (43)
Maximum effect I_{max} , %	71.9 (9)
Between-patient variability in IC_{50} , %CV	209 (42) [28]
Between-patient variability in baseline CRP, %CV	115 (15) [0]
Proportional RUV in PD, %CV	65.3 (4) [10]

43

44 *Covariate model*

45 For the covariate modelling, the PK parameters informed by prior were fixed to the PK
 46 estimates from the base PK model, and the potential impact of measured covariates on the
 47 PK parameter clearance (CL) was investigated. Initial screening of covariate impact was

48 based on graphical analysis and univariate modelling, and final covariate selection was based
49 on statistical significance of the covariate impact.

50 Impact of covariates included in the model is shown in Figure S2. The plot clearly
51 demonstrates the dominant impact of anti-drug antibody status on CL compared to other
52 covariates

53 The final PK parameter equations are as follows:

$$54 \quad CL = CL_{pop} \cdot (1 + \theta_{ADA_CL} \cdot ADA) \cdot \left(\frac{sAlb}{43 \text{ g/L}}\right)^{\theta_{sAlb_CL}} \cdot \left(\frac{BW}{70 \text{ kg}}\right)^{\theta_{BW_CL}} \cdot \theta_{IMM_CL}^{IMM} \cdot e^{\eta_{CL}}$$

$$55 \quad V_1 = V_{1,pop} \cdot e^{\eta_{V1}}$$

$$56 \quad V_2 = V_{2,pop} \cdot e^{\eta_{V2}}$$

$$57 \quad Q = Q_{pop},$$

58 in which CL denotes the individual CL value, CL_{pop} the typical CL of the population, ADA the
59 status of ADA (0 for ADA- and 1 for ADA+), $sAlb$ the serum albumin concentration, BW the
60 body weight, IMM an indicator for co-therapy with immunomodulators (0 for absence, 1 for
61 presence of co-therapy), η_{CL} the between-patient variability in CL, V_1 the individual volume
62 of central compartment, $V_{1,pop}$ the typical volume of the central compartment of the
63 population, V_2 the individual volume of peripheral compartment, $V_{2,pop}$ the typical volume of
64 the peripheral compartment of the population, Q the individual intercompartmental
65 exchange flow, Q_{pop} the typical intercompartmental exchange flow of the population

66 *PKPD model*

67 Due to the sparse nature of the data the frequentist prior approach was used to support
68 estimation of between-patient variability terms. The PK/PD model used as prior was
69 developed by Ternant et al.³

70 The developed model considered between-patient variability in IFX concentration needed
71 for 50% of maximum effect (IC_{50} value) and in baseline CRP concentration, and proportional
72 residual unexplained variability.

73 The model equation describing change in CRP over time was:

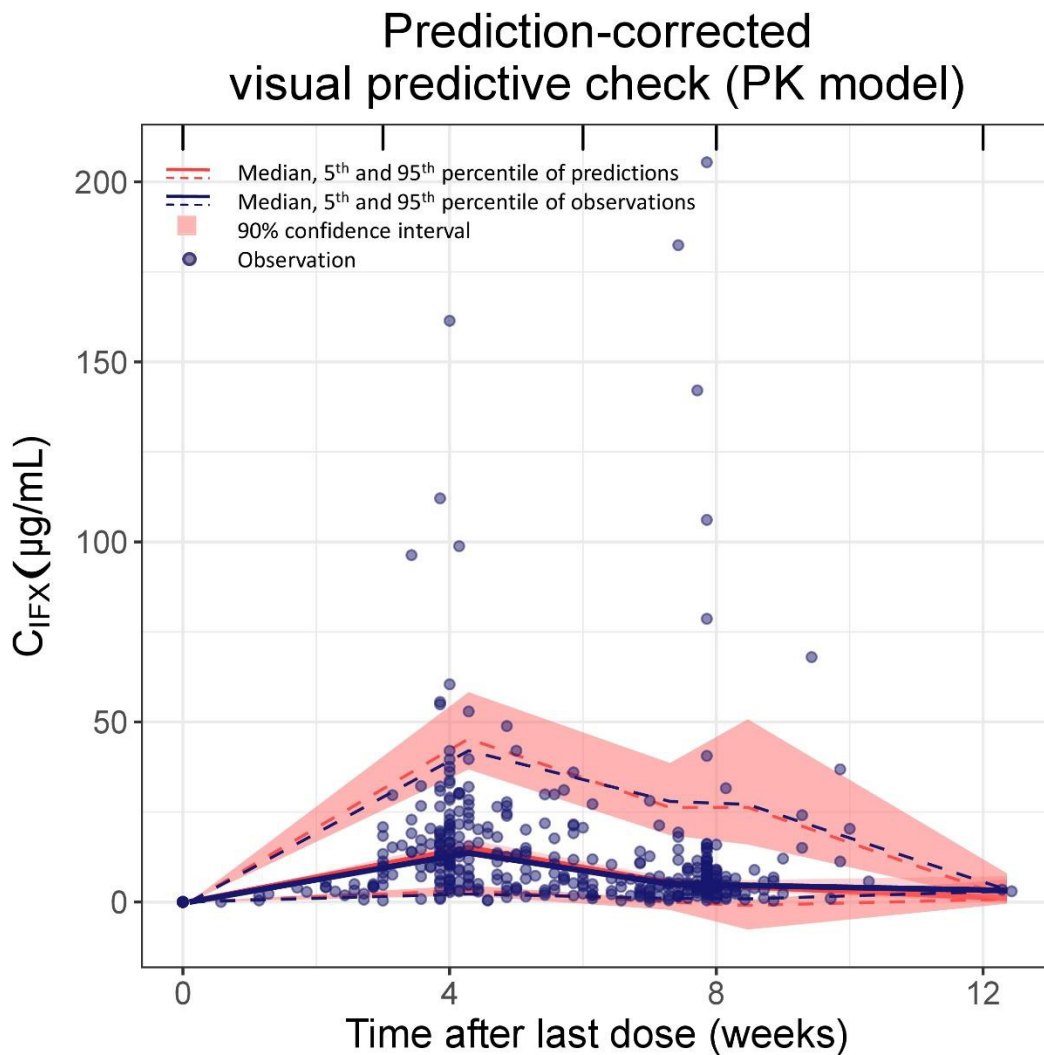
$$74 \frac{dCRP}{dt} = k_{syn} \cdot \frac{I_{max} \cdot C_{IFX}}{IC_{50} \cdot e^{\eta IC_{50}} + C_{IFX}} - k_{deg} \cdot CRP(t), \quad k_{syn} = CRP_{baseline} \cdot e^{\eta CRP_{baseline}} \cdot k_{deg}$$

75 , in which k_{syn} denotes the CRP synthesis rate constant, I_{max} is the maximum effect (maximum
76 percentage of CRP synthesis that can be inhibited by IFX), C_{IFX} the concentration of IFX, IC_{50}
77 the concentration of IFX that leads to 50% of the maximum effect, k_{deg} the CRP degradation
78 rate constant, and η between-patient variability.

79 *References*

- 80 1. Gisleskog PO, Karlsson MO, Beal SL. Use of prior information to stabilize a population
81 data analysis. *J Pharmacokinet Pharmacodyn.* 2002;29(5):473-505.
- 82 2. Fasanmade AA, Adedokun OJ, Blank M, et al. Pharmacokinetic properties of
83 infliximab in children and adults with Crohn's disease: A retrospective analysis of data
84 from 2 phase III clinical trials. *Clin Ther.* 2011;33(7):946-964.
- 85 3. Ternant D, Berkane Z, Picon L, et al. Assessment of the influence of inflammation and
86 FCGR3A genotype on infliximab pharmacokinetics and time to relapse in patients
87 with Crohn's disease. *Clin Pharmacokinet.* 2015;54(5):551-562.

89 **Supplementary figure S1.** Model evaluation: Prediction-corrected visual predictive check for
90 the final PK model. Blue lines represent observations, whereas red lines and surfaces
91 represent model predictions. Full lines are median, dashed lines 5th and 95th percentiles
92 and surfaces 90% confidence intervals. Blue dots are observations. The plot indicates that
93 the model adequately describes the data. C_{IFX} : Measured infliximab concentration. Note that
94 the VPC includes only time points at which observations were available; the full model-based
95 PK profile is illustrated in Figure 4.

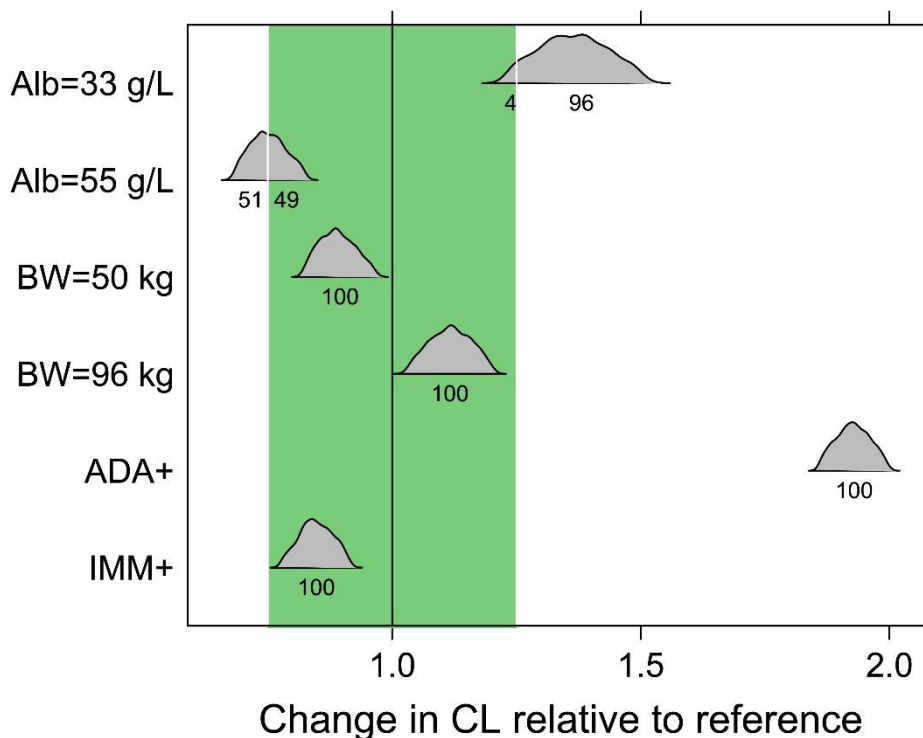


96

97

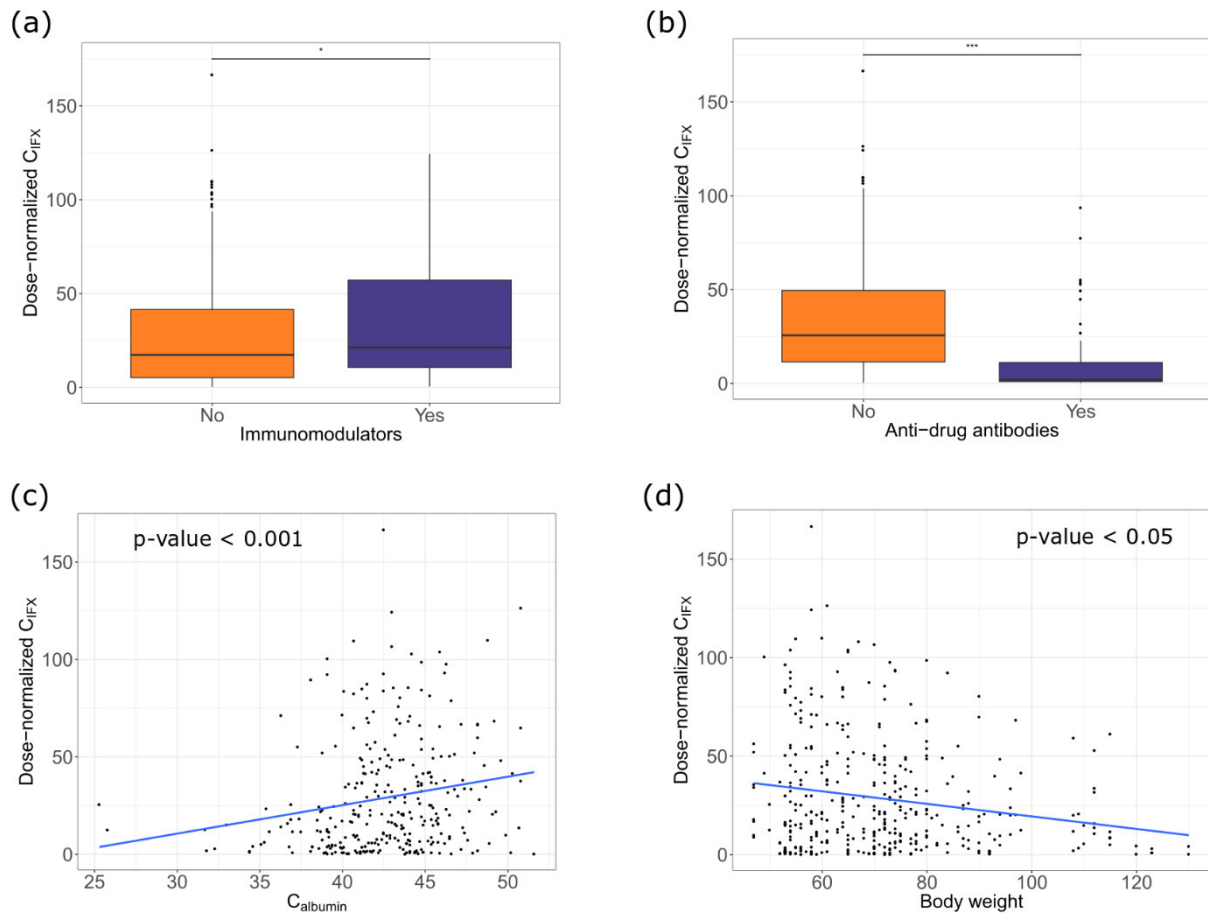
98 **Supplementary figure 2.** Clinical inference of covariates. The x-axis shows change in CL
 99 relative to CL in a reference individual (body weight 70 kg, serum albumin 43 g/L, no anti-
 100 drug antibodies, and no co-therapy with immunomodulators). The y-axis shows relevant
 101 covariates. For the continuous covariates (serum albumin concentration and body weight),
 102 the effect of 5th and 95th percentile of the covariate value in the investigated patient
 103 population is shown. Green surface represents change from CL of $\pm 20\%$ compared to
 104 reference value, as an illustration of the covariate effect extent. The grey areas represent
 105 distributions of the covariate effect based on bootstrap (n=1000). The numbers designate
 106 percentage of the distribution that falls in or out of the $\pm 20\%$ area, respectively. CL:
 107 Clearance; Alb: Serum albumin concentration; BW: Body weight; ADA: Anti-drug antibodies;
 108 IMM: Co-therapy with immunomodulators.

Clinical inference of covariates



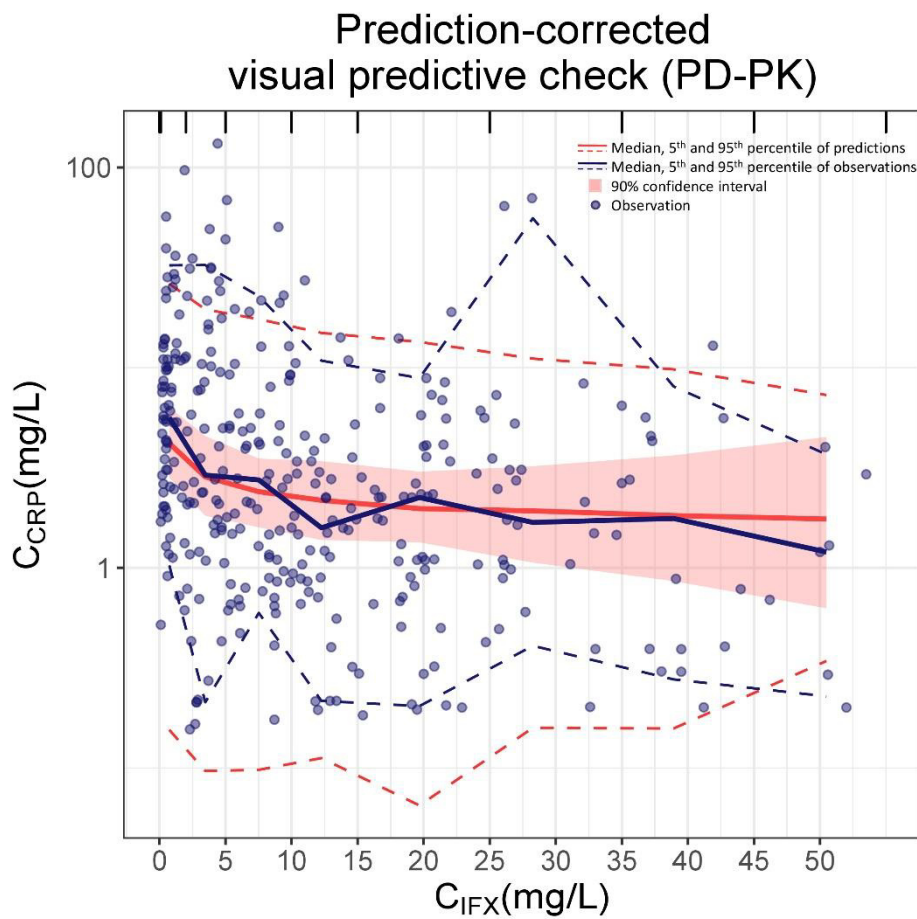
110 **Supplementary figure 3.** Exploratory analysis of relevant covariates on dose-normalised C_{IFX} :
111 (1) co-therapy with immunomodulators, (b) presence of anti-drug antibodies, (c) serum
112 albumin concentration, and (d) body weight. *Wilcoxon p-value < 0.05; *** Wilcoxon p-value <
113 0.001.

114



115

116 **Supplementary figure 4.** Prediction-corrected visual predictive check for the final PK/PD
117 model showing C-reactive protein concentration over infliximab exposure. Blue lines
118 represent measured values, whereas red lines and surfaces represent predictions from the
119 model. Full lines are median, dashed lines 5th and 95th percentiles and surfaces 90%
120 confidence intervals. Blue dots are measurements. The plot indicates that the model
121 adequately describes the relationship between infliximab exposure and CRP concentration.
122 C_{CRP} : Measured C-reactive protein concentration; C_{IFX} : Measured infliximab concentration.



123

124

Manuscript II

Equity Ratio Statement

Title of the manuscript:

“Absence of relationship between Crohn's Disease Activity Index or C-reactive protein and infliximab exposure calls for objective Crohn's disease activity measures for the evaluation of treatment effects at treatment failure”

Journal Therapeutic Drug Monitoring
Volume 41, Issue 2, Pages 235-242 (2019)

Authorship Shared first author

Status Published

DOI: <https://doi.org/10.1097/FTD.0000000000000590>

Due to copyright restrains, this article cannot be reprinted. To access the published version of the article, please refer to the reference given above.

Own contribution

- Interpretation of the results, including literature research related to interpretation of the results and creation of the manuscript
- Drafting of parts of the manuscript, including interpretation and discussion of the results
- Involvement in adaptation of the manuscript according to the reviewers' and editor's comments

Ana-Marija Grišić
(Doctoral candidate, shared first author)

Prof. Dr. Charlotte Kloft
(Supervisor)

Due to copyright permission restrictions, the manuscript (p.107-p.121) has been removed from the electronic version of the dissertation. The manuscript is accessible at:

<https://doi.org/10.1097/FTD.0000000000000590>

Manuscript III

Equity Ratio Statement

Title of the manuscript:

“Semimechanistic clearance models of oncology biotherapeutics and impact of study design: Cetuximab as a case study”

Journal CPT: Pharmacometrics & Systems Pharmacology

Volume 9, Issue 11, Pages 628-638 (2020)

Authorship First author

Status Published

DOI: <https://doi.org/10.1002/psp4.12558>

Reprinted from CPT: Pharmacometrics & Systems Pharmacology journal without changes under the terms of the Creative Commons Attribution License (CC BY-NC-ND 4.0).

Own contribution

- Data set modification and checkouts
- Modelling and simulation activities, including PK model development, model evaluation, and simulations
- Interpretation of the results
- Drafting of all parts of the manuscript
- Creation of all tables and figures for the manuscript
- Adaptations of the manuscript according to the reviewers' and editor's comments

Ana-Marija Grišić

(Doctoral candidate, first author)

Prof. Dr. Charlotte Kloft

(Supervisor)



ARTICLE

Semimechanistic Clearance Models of Oncology Biotherapeutics and Impact of Study Design: Cetuximab as a Case Study

Ana-Marija Griscic^{1,2,3,†}, Akash Khandelwal^{3,*}, Mauro Bertolino³, Wilhelm Huisinga⁴, Pascal Girard^{5,‡} and Charlotte Kloft^{1,‡}

This study aimed to explore the currently competing and new semimechanistic clearance models for monoclonal antibodies and the impact of clearance model misspecification on exposure metrics under different study designs exemplified for cetuximab. Six clearance models were investigated under four different study designs (sampling density and single/multiple-dose levels) using a rich data set from two cetuximab clinical trials (226 patients with metastatic colorectal cancer) and using the nonlinear mixed-effects modeling approach. A two-compartment model with parallel Michaelis–Menten and time-decreasing linear clearance adequately described the data, the latter being related to post-treatment response. With respect to bias in exposure metrics, the simplified time-varying linear clearance (CL) model was the best alternative. Time-variance of the linear CL component should be considered for biotherapeutics if response impacts pharmacokinetics. Rich sampling at steady-state was crucial for unbiased estimation of Michaelis–Menten elimination in case of the reference (parallel Michaelis–Menten and time-varying linear CL) model.

Study Highlights

WHAT IS THE CURRENT KNOWLEDGE ON THE TOPIC?

☑ Characterization of complex clinical pharmacokinetics (PK) of monoclonal antibodies (mAbs) is hindered by limited availability of informative PK data over a wide dose range.

WHAT QUESTION DID THIS STUDY ADDRESS?

☑ This study explored semi-mechanistic clearance (CL) models for mAbs and implications of study design differences on identifiability of the CL models.

WHAT DOES THIS STUDY ADD TO OUR KNOWLEDGE?

☑ This analysis provides a population PK model incorporating both time-varying CL, related to treatment

response, and target-mediated drug disposition (TMDD) component, and stresses the importance of informing the population models with rich data.

HOW MIGHT THIS CHANGE DRUG DISCOVERY, DEVELOPMENT, AND/OR THERAPEUTICS?

☑ Time-variance of CL in addition to TMDD should be considered for biotherapeutics if response impacts PK. Informing PK analyses with rich data (i.e., through pooling data from multiple clinical trials at later stages of drug development) is crucial for reliable metrics derivation for exposure-response relationships.

The emergence of new biologic therapies has led to dramatic improvement in the survival of patients with cancer.¹ However, a fully mechanistic understanding of the behavior of monoclonal antibodies (mAbs) is still lacking, as their distribution and elimination are subject to complex pharmacokinetics (PKs) that may change over time² due to their protein nature with high affinity to their pharmacological target. Therefore, a quantitative description of their PK profile, especially clearance (CL), is a challenging task. The elimination of mAbs is expected to comprise target-mediated drug disposition (TMDD; saturated at higher exposure and nonlinear/linear at lower concentrations) and nonspecific

CL, which may be linear, nonlinear, and/or time-dependent, so both linear and nonlinear clearance are physiologically possible. However, quantification of each of these components in a model is highly dependent on the data (i.e., the sampling scheme and dose range investigated), potentially leading to identification of different models for the same drug.

The mAbs targeting the epidermal growth factor receptor (EGFR) are among the most successful targeted therapies for patients with rat sarcoma proto-oncogene (RAS) wild-type metastatic colorectal cancer (mCRC), one of the most common causes of cancer death worldwide.³

[†]Author was affiliated with each of these participating institutions during the time of the analysis.

[‡]Shared senior authorship.

¹Department of Clinical Pharmacy and Biochemistry, Institute of Pharmacy, Freie Universität Berlin, Berlin, Germany; ²Graduate Research Training Program PharmMetX, Berlin, Germany; ³Merck KGaA, Darmstadt, Germany; ⁴Institute of Mathematics, Universität Potsdam, Potsdam, Germany; ⁵Merck Institute of Pharmacometrics, Merck Serono S.A., Lausanne, Switzerland. *Correspondence: Akash Khandelwal (akash.khandelwal@merckgroup.com)

Received: January 28, 2020; accepted: August 6, 2020. doi:10.1002/psp4.12558

Availability of rich PK data sets for cetuximab (Erbix; Merck KGaA, Darmstadt, Germany) approved in mCRC offered us the opportunity to reconcile the different published population PK models for this mAb, which differ in the elimination model of the compound. The first published model considered only Michaelis–Menten elimination⁴; then, Azzopardi *et al.* proposed a parallel linear and zero-order elimination,⁵ and others found a simple linear elimination.⁶

To explore different semimechanistic CL models for mAbs and investigate implications of study design differences on

identifiability of the CL models, we conducted a population PK analysis on a pooled data set, using cetuximab as a case study. The objectives of this study were to: (1) refine the population PK models of cetuximab in patients with mCRC taking into account the TMDD of the biologic therapy; while also (2) comparing mechanistically plausible CL implementations (including linear, nonlinear, and time-varying CL) and test how response may or may not interfere with PK; and (3) investigate implications of study designs typical for various phases of drug development on the model performance and parameter identifiability.

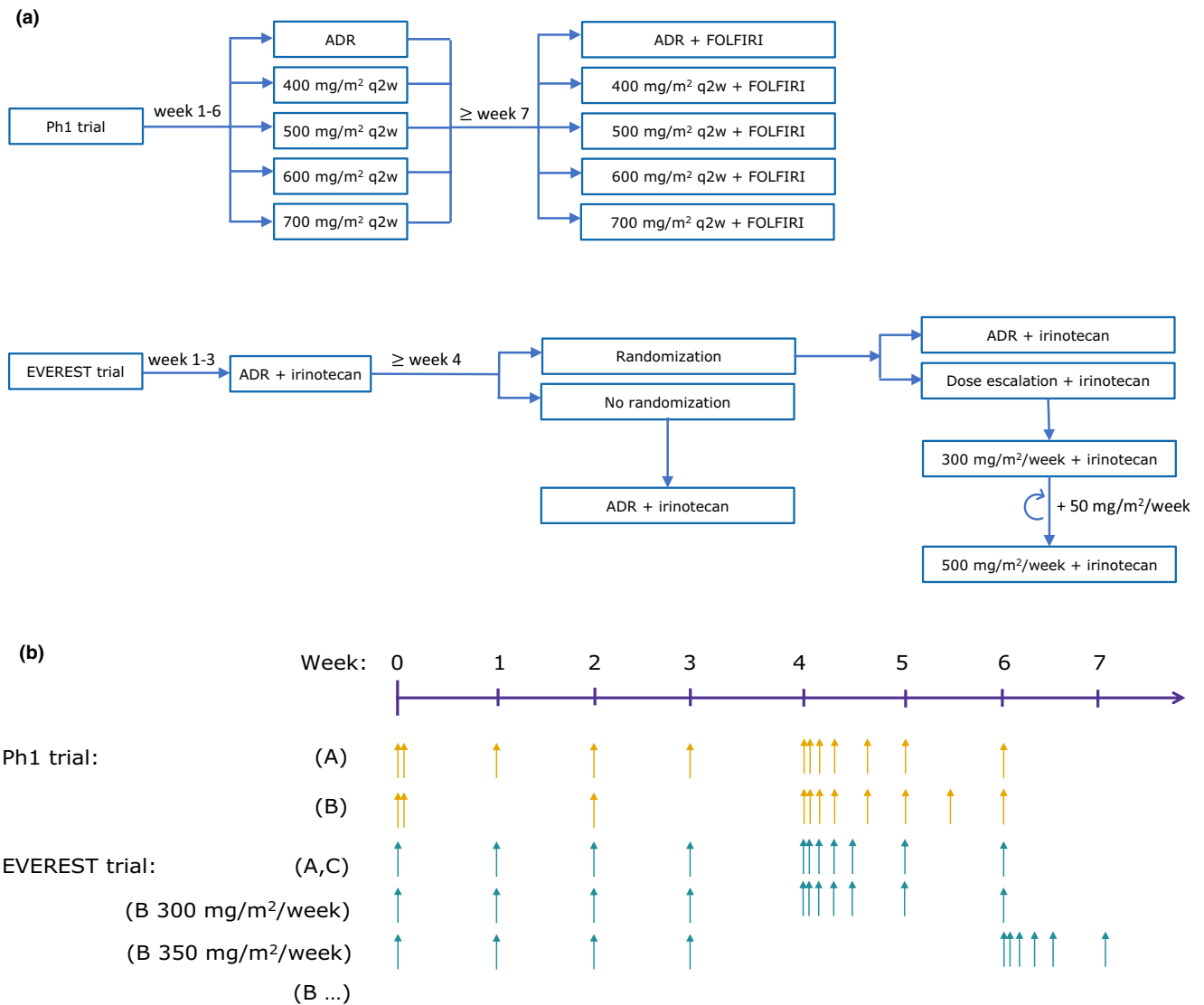


Figure 1 Overview of the analyzed clinical trials: a phase I (PhI) trial⁷ and EVEREST trial.⁸ (a) Dosing algorithm; (b) pharmacokinetic sampling schedule. The PhI trial comprised two arms. In arm A, the patients received the approved dosing regimen (ADR). In arm B, after the initial 2-hour infusion of 400 mg/m², the patients received 2-hour 400 mg/m², 2.5-hour 500 mg/m², 3-hour 600 mg/m², or 3.5-hour 700 mg/m² infusions q2w. In the EVEREST trial, all patients initially received cetuximab ADR in combination with irinotecan; after 3 weeks of treatment the patients eligible for randomization either continued receiving ADR (group A) or underwent dose escalation (group B), whereas the patients not eligible for randomization continued the treatment with ADR (group C). In group B, with each dose increase of 50 mg/m² the dense sampling interval was shifted, denoted as “(B...)” for EVEREST in the figure. For all arms/groups the sampling continued until the patients dropped out of the study or until the study end. ADR, approved dosing regimen for cetuximab (2-hour 400 mg/m², 1-hour 250 mg/m² once weekly); FOLFIRI, co-medication with irinotecan (30–90 minutes of 180 mg/m²) + 5-fluorouracil (180 mg/m² bolus and 2400 mg/m² as infusion over 46 hours) + folic acid (2-hour 400 mg/m²); q2w, every 2 weeks.

METHODS

Clinical trial design and population

The data for this analysis originate from two multicenter clinical trials in patients with advanced mCRC (a phase I (PhI) trial⁷ and EVEREST⁸). The PhI trial was a phase I, open-label, multicenter trial designed to evaluate the PK and pharmacodynamics (PD) of cetuximab. The EVEREST trial was a phase I/II, open-label, randomized, controlled, multicenter trial aiming to evaluate PK and PD of cetuximab dose escalation as well as pharmacogenomic and pharmacogenetic aspects. Full study descriptions are reported elsewhere.^{7,8}

Treatment administration

In the PhI trial, patients received intravenous cetuximab monotherapy for the first 6 weeks, followed by cetuximab-FOLFIRI (folinic acid, 5-fluorouracil, and irinotecan) co-therapy (**Figure 1a**). The patients were assigned to the following treatment groups:

1. Initial 400 mg/m² cetuximab infusion, followed by weekly dose of 250 mg/m² (approved dosing regimen (ADR)) (arm A);
2. Cetuximab dose of 400 mg/m² every 2 weeks (q2w),
3. Cetuximab dose of 500 mg/m² q2w,
4. Cetuximab dose of 600 mg/m² q2w, and
5. Cetuximab dose of 700 mg/m² q2w (arm B)

Starting from week 7, in addition to cetuximab, all patients started FOLFIRI treatment, which comprises irinotecan (180 mg/m²), 5-fluorouracil (180 mg/m² bolus and 46-hour 2400 mg/m² infusion), and folic acid (2-hour 400 mg/m² infusion). The treatment was continued until disease progression or an unacceptable adverse event.

In the EVEREST trial (**Figure 1a**), all patients received cetuximab ADR-irinotecan co-therapy for the first 3 weeks. On the fourth week, patients who had not required irinotecan discontinuation and had not experienced skin reaction of grade > 1 or any other cetuximab-related toxicity of grade > 2 were randomized to continue the ADR (group A) or undergo cetuximab dose escalation (group B). The dose escalation comprised increasing the cetuximab dose by 50 mg/m²/week up to the maximum dose of 500 mg/m²/week. Patients not eligible for randomization continued the cetuximab ADR-irinotecan treatment (group C). The treatment was continued until disease progression or an unacceptable adverse event.

PK assay and sampling

For the PK analysis, the serum cetuximab concentration was measured by an enzyme-linked immunosorbent assay.⁷ **Figure 1b** illustrates the sampling schedules in the two studies.

In the PhI trial, PK samples were taken before and at the end of the first cetuximab infusion, as well as at minimum cetuximab concentrations (C_{\min}) until day 29. For the dosing interval starting on day 29, dense sampling (**Figure 1b**) was performed as follows: patients receiving ADR (arm A) were sampled at the end of infusion and at 4, 24, 48, 96, and 168 hours after the start of infusion, whereas patients in other

treatment groups (arm B) were sampled at the end of infusion and at 4, 24, 48, 96, 168, 240, and 336 hours after the start of infusion. After the dense sampling interval, blood samples were collected at C_{\min} until the end of the study in both arms.

In the EVEREST trial, PK samples were taken before the first dose and at C_{\min} until week 29. In patients on ADR (groups A and C), dense sampling (at the end of infusion and 6, 24, 48, 72, and 168 hours after the start of infusion) was performed over the dosing interval starting on day 29. The patients undergoing dose escalation (group B) were sampled in such a way that five patients from each dose level were intensively sampled for one dosing interval, starting on the second dose of the dose level. After the dense sampling interval, C_{\min} samples were collected from all patients until the end of the study.

Population PK analysis

A population PK model was developed using the nonlinear mixed-effects modeling approach. The data were analyzed using the Stochastic Approximation Expectation Maximization estimation method in NONMEM (version 7.3.0), PsN (version 4.4.8), and Pirana (version 2.9.2), whereas R (version 3.3.2) and RStudio (version 1.1.456) were used for preprocessing and postprocessing of data. The “log-transform both sides” approach was used.

Confirmed by graphical analysis, we used the previously published two-compartment model.^{4,5} We investigated six elimination models from the central compartment: linear clearance (LCL),⁶ linear clearance with exponential change over time (TVARCL),^{9,10} Michaelis–Menten clearance (MMCL),⁴ linear clearance and Michaelis–Menten (MMCL + LCL), linear clearance with exponential change over time and Michaelis–Menten (MMCL + TVARCL), and linear clearance and zero-order (LCL + 0.EL)⁵ clearance (**Figure 2a**). The differential equations for the change of drug amount in the central compartment (parameters part of elimination process marked in bold) were as follows:

$$\text{LCL: } \frac{dA_1}{dt} = -Q \cdot C_1 + Q \cdot C_2 - \mathbf{CL} \cdot C_1 \quad (1)$$

$$\text{TVARCL: } \frac{dA_1}{dt} = -Q \cdot C_1 + Q \cdot C_2 - \mathbf{CL} \cdot e^{\frac{(I_{\max} + \eta I_{\max}) \cdot t^\gamma}{t_{50}^\gamma + t^\gamma}} \cdot C_1 \quad (2)$$

$$\text{MMCL: } \frac{dA_1}{dt} = -Q \cdot C_1 + Q \cdot C_2 - \frac{\mathbf{V}_{\max} \cdot C_1}{K_m + C_1} \quad (3)$$

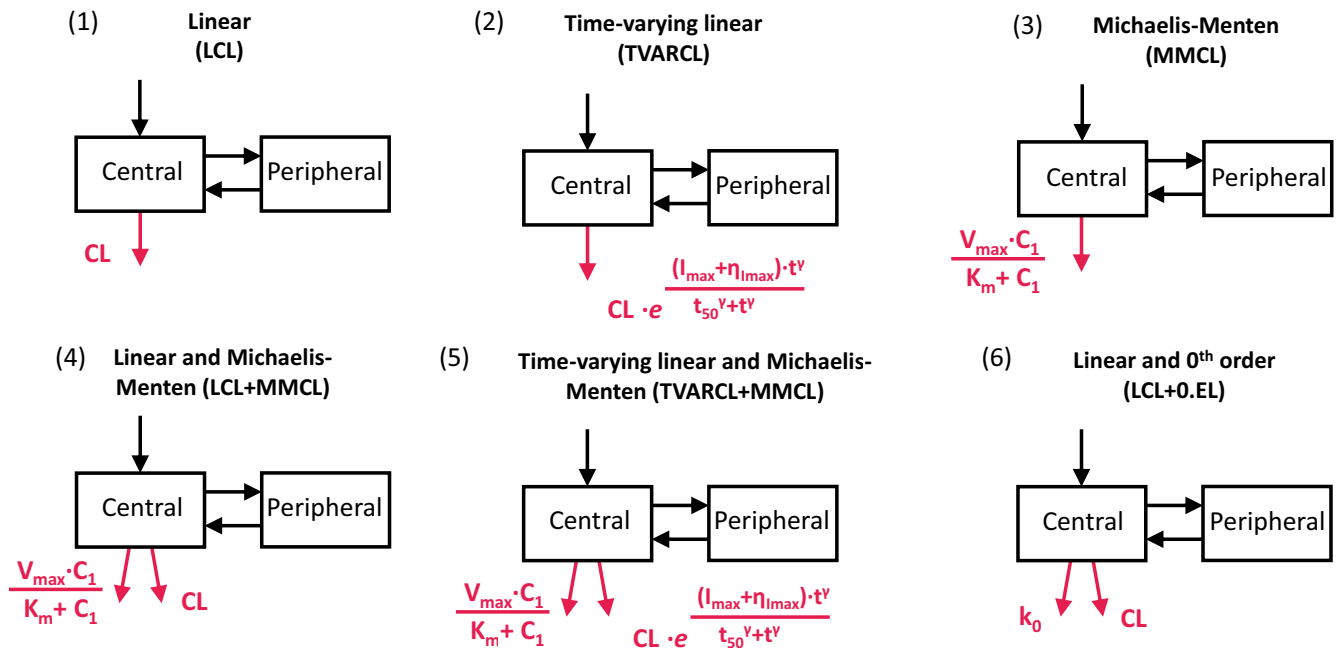
$$\text{MMCL+LCL: } \frac{dA_1}{dt} = -Q \cdot C_1 + Q \cdot C_2 - \mathbf{CL} \cdot C_1 - \frac{\mathbf{V}_{\max} \cdot C_1}{K_m + C_1} \quad (4)$$

$$\text{MMCL+TVARCL: } \frac{dA_1}{dt} = -Q \cdot C_1 + Q \cdot C_2 - \mathbf{CL} \cdot e^{\frac{(I_{\max} + \eta I_{\max}) \cdot t^\gamma}{t_{50}^\gamma + t^\gamma}} \cdot C_1 - \frac{\mathbf{V}_{\max} \cdot C_1}{K_m + C_1} \quad (5)$$

$$\text{LCL+0.EL: } \frac{dA_1}{dt} = -Q \cdot C_1 + Q \cdot C_2 - \mathbf{CL} \cdot C_1 - k_0 \quad (6)$$

where A_1 denotes drug amount in central compartment; A_2 , drug amount in peripheral compartment; C_1 , the concentration

(a)



(b)

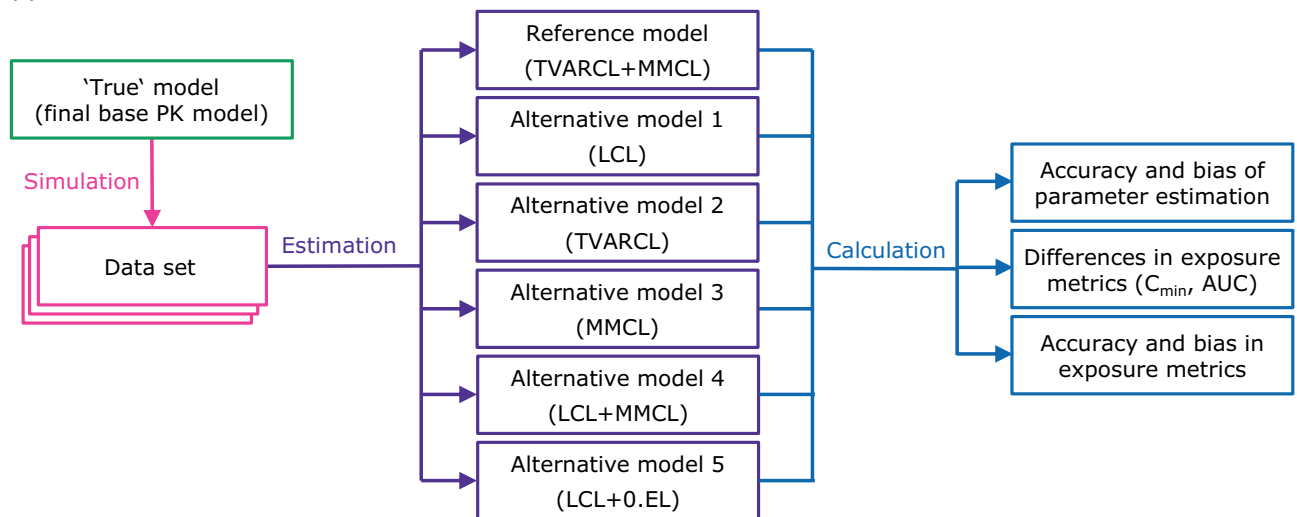


Figure 2 Overview of the analysis workflow. (a) Graphical representation of the investigated base pharmacokinetic (PK) models for cetuximab. (b) Flowchart illustrating the stochastic simulation and estimation (SSE) analysis per study design scenario. The final PK base (reference, “true”) model was used to simulate 200 data sets in the stochastic simulation step. The reference and five alternative models were subsequently fit to the simulated datasets. Thus, altogether $6 \times 200 = 1,200$ model fits were performed. For each model accuracy and bias of parameter estimates, exposure metrics (AUC and C_{min} after the second dose and in steady state), and their bias and accuracy were calculated and compared. The process was repeated for four study designs in total differing in sampling density and number of dose levels. C_1 denotes drug concentration in central compartment; C_2 , drug concentration in peripheral compartment; CL , linear clearance from central compartment; I_{max} , maximum change in time-varying linear clearance; K_m , concentration at half V_{max} ; k_0 , zero-order rate constant of elimination from central compartment; $\eta_{I_{max}}$, between-patient variability in I_{max} ; Q , intercompartmental exchange rate; t_{50} , time at which clearance is halved; V_{max} , maximal rate of saturable elimination; γ , curve shape factor. Parts of the model related to clearance are shown in red.

in central compartment; Q , intercompartmental exchange rate; CL , linear clearance from central compartment; I_{\max} , maximum change in time-varying linear clearance; $\eta_{I_{\max}}$, between-patient variability in I_{\max} ; t_{50} , time at which clearance is halved; γ , curve shape factor; V_{\max} , maximal rate of saturable elimination; K_m , concentration at half V_{\max} ; and k_0 , zero-order rate constant of elimination from central compartment.

The distribution of individual parameter values was assumed to follow a log-normal distribution. For covariate model development, a full fixed-effects modeling approach was used, as proposed by Gastonguay,¹¹ whereby preselected covariates were simultaneously included in the final base model. The criteria for inclusion/exclusion of a covariate comprised statistical relevance (null value not covered by confidence interval) and clinical relevance (difference in baseline linear CL greater than $\pm 25\%$ relative to typical CL value), impact on between-subject variability reduction, and extent of covariate effect on model parameters. Model discrimination was based on plausibility and precision of parameter estimates, the Akaike information criterion (AIC),¹² goodness-of-fit plots, and visual predictive checks.

Study design investigations

In the second part of this analysis, implications of study designs, on the model performance and parameter identifiability were assessed. Using the final base PK model (MMCL + TVARCL) as a reference model, 200 data sets were simulated, each comprising 100 patients, making a total of 20,000 virtual patients. The six investigated models were fit to the simulated data sets under four study-design scenarios, using the stochastic simulation and estimation (SSE) PsN feature,¹³ amounting to a total of 4,800 model fits (Figure 2b).

The body surface area (BSA) of the virtual population of 100 patients was sampled to correspond to the distribution of the clinical database (Table 1) and assumed to be constant over time. In all study designs, all virtual patients received the same initial cetuximab induction dose of 400 mg/m² with infusion rate of 5 mg/min. The infusion rate for subsequent doses was 10 mg/min. The 100 virtual patients were relegated to four study designs (A–D), which differed in sampling density (dense vs. sparse) and dose levels (single vs. multiple-dose levels) and were chosen to correspond to typical trial designs in the initial phases of drug development (A and B) and later (e.g., phase III trials (C and D)). The investigated study designs were as follows:

- Study design A, the virtual patients were stratified in order to ensure that all dose levels were present across the whole range of BSA. The patients were first stratified in four groups corresponding to the BSA quartiles in order to avoid having only low or only high doses in one BSA quartile. To achieve further randomization of the dose distribution, within each group the patients were further randomly stratified to receive 200, 250, 300, 350, 400, 450, or 500 mg/m² every week starting from the second dose. In addition to the C_{\min} sampling described below, additional samples were taken after the fifth dose, at the end of infusion, and 4, 24, 48, 72, and 96 hours after infusion start, corresponding to the clinical trials;

Table 1 Summary of baseline patient characteristics ($n_{\text{patients}} = 226$; $n_{\text{pharmacokinetic samples}} = 3,821$)

	Median (min–max)
Continuous	
Age, years	61 (26–81)
Duration of cetuximab therapy, months	5.8 (0.25–27.3)
Weight, kg	72 (41–132)
Body surface area, m ²	1.85 (1.37–2.70)
Amphiregulin concentration, pg/mL	226 (8.50–5080)
Epidermal growth factor concentration, pg/mL	12.7 (0.61–633)
Interleukin 8 concentration, pg/mL	42.0 (1.76–5650)
Transforming growth factor- α concentration, pg/mL	2.52 (0.404–131)
Vascular endothelial growth factor concentration, pg/mL	278 (46.7–1720)
Creatinine clearance, mL/min	95.5 (31.0–218)
Categorical	
	n (%)
Female	82 (36)
RAS mutation present	81 (36)
ECOG performance status	
0	154 (68)
1	69 (31)
2	3 (1)
RECIST response achieved	63 (28)

ECOG, Eastern Cooperative Oncology Group; RAS, rat sarcoma proto-oncogene; RECIST, Response Evaluation Criteria in Solid Tumors.

- Study design B, the virtual patients were treated according to the approved dosing regimen of cetuximab (250 mg/m² every week; i.e., single dose level). The sampling was performed in the same manner as in study design A;
- Study design C, the virtual patients were treated in the same manner as in study design A, and only C_{\min} samples were taken;
- Study design D, the virtual patients were treated according to the approved dosing regimen of cetuximab (single dose level) and only C_{\min} samples were taken.

Under each study design, all virtual patients were sampled at C_{\min} after each dose for 12 weeks. At week 12, the patients were separated into 5 groups of 20 patients. Each group was sampled once a month for 3 months, until a study duration of 18 months (Figure S1).

To assess the performance across the models, for each investigated study design, clinically relevant exposure metrics (C_{\min} and area under the curve (AUC)) as well as their bias and accuracy were calculated (Supplementary Material), in addition to the standard set of parameters provided by the PsN output (including parameter estimates and their bias and accuracy; Figure 2b). The PK metrics after the second dose and at steady-state (i.e., at the approximate time when 90% of maximal CL decrease has occurred per the reference model (week 60)), were considered. The bias (i.e., mean error) was calculated according to the following equation:

$$\text{Bias} = \frac{1}{N} \cdot \sum_{i=1}^n (\text{est}_i - \text{ref}_i).$$

where N denotes number of simulated trials repetitions (200); n , the number of patients (number of patients in a trial · number of simulated trial repetitions; i.e., $200 \cdot 100 = 20,000$); ref_i , the parameter/exposure metric values of an individual i for the reference PK (MMCL + TVARCL) model; and est_i , the respective values for the alternative models (C_{min} : individual prediction value at defined timepoints), and AUC: integral of central compartment.

RESULTS

PK model comparison

In total, 3,821 PK samples from 226 patients (PhI ($N = 62$) and EVEREST ($N = 164$)) were analyzed. The relevant patient characteristics are given in **Table 1**. Based on AIC computed using Stochastic Approximation Expectation Maximization-importance sampling algorithm, the two-compartment model with parallel Michaelis–Menten and linear clearance that changes exponentially over time (MMCL + TVARCL) outperformed the second best model by 334 points for predicting the serum cetuximab concentration-time profiles in the analyzed population (**Table 2**). By decreasing the value of AIC, we found TVARCL, MMCL + LCL, MMCL, and LCL models, whereas

the worst model was the one assuming elimination as first-order and zero-order mixed processes.

Parameter estimates for the investigated models are presented in **Table 2**. All fixed-effect parameters of the MMCL + TVARCL model showed excellent precision with relative standard error below 30%. Between-patient variability in baseline linear CL, V_1 , V_2 , V_{max} , and I_{max} was ≤ 61.3 coefficient of variation with satisfactory shrinkage. As indicated by goodness-of-fit plots (**Figure S3**), the model describes the clinical data well.

Covariate model

As body size is known to impact the PKs of mAbs,¹⁴ baseline BSA was investigated for influence on baseline CL and volumes of distribution. The most appropriate implementation of baseline BSA was via power function with exponent fixed to 0.75 for CL and 1 for volumes of distribution.¹⁵ The inclusion of BSA decreased objective function value for ~ 60 points, and slightly decreased between-patient variability in baseline CL, V_1 , and V_2 by 8.6%–11.8% (up to 5.4 percentage points, respectively), as well as additive residual unexplained variability (4.85–4.68 $\mu\text{g/mL}$).

Based on biological and clinical relevance, the following covariates were preselected for full fixed-effect covariate

Table 2 Comparison of all investigated base models

	LCL	TVARCL	MMCL	MMCL + LCL	MMCL + TVARCL	LCL + 0.EL
LCL, L/h (RSE%)	0.0222 (3)	0.0262 (3)	-	0.0153 (4)	0.0174 (5)	0.0206 (-)
V_1 , L (RSE%)	3.84 (3)	3.67 (3)	3.75 (3)	3.71 (2)	3.65 (3)	3.82 (-)
Q, L/h (RSE%)	0.0188 (17)	0.0282 (12)	0.0332 (19)	0.0323 (4)	0.0368 (5)	0.0216 (-)
V_2 , L (RSE%)	3.38 (12)	1.65 (11)	2.67 (8)	3.25 (6)	2.65 (4)	3.31 (-)
K_M , mg/L (RSE%)	-	-	283 (26)	9.81 (5)	13.3 (21)	-
V_{max} , mg/h (RSE%)	-	-	9.48 (17)	0.882 (5)	0.861 (5)	-
I_{max} , % (RSE%)	-	-19.6 (16)	-	-	-23.1 (20)	-
T_{50} , weeks (RSE%)	-	7.26 (15)	-	-	20.5 (29)	-
γ (RSE%)	-	2.54 (24)	-	-	1 FIX	-
K_0 , mg/h (RSE%)	-	-	-	-	-	0.0472 (-)
η_{LCL} , CV% (RSE%) [Shr%]	38.3 (6) [6]	36.6 (6) [6]	-	37.9 (8) [19]	36.1 (23) [23]	39.4 (-) [8]
η_{V1} , CV% (RSE%) [Shr%]	26.8 (11) [31]	27.3 (10) [31]	26.4 (15) [32]	25.9 (11) [32]	26.2 (10) [32]	27.4 (-) [32]
η_{V2} , CV% (RSE%) [Shr%]	103.9 (13) [27]	84.1 (9) [39]	83.4 (17) [29]	61.2 (9) [27]	61.3 (14) [32]	104.4 (-) [29]
η_{Vmax} , CV% (RSE%) [Shr%]	-	-	30.5 (9) [6]	43.6 (10) [34]	48.8 (12) [12]	-
η_{Tmax} , CV% (RSE%) [Shr%]	-	25.2 (11) [29]	-	-	51.5 (18) [35]	-
η_{K0} , CV% (RSE%) [Shr%]	-	-	-	-	-	150.3 (-) [57]
Additive RUV, mg/L (RSE%)	9.44 (11)	7.79 (12)	8.14 (13)	5.85 (12)	4.85 (22)	8.65 (-)
Proportional RUV, CV% (RSE%)	23.1 (5)	22.8 (4)	23.4 (5)	24.0 (4)	23.5 (4)	22.9 (-)
AIC (SAEM-IMP)	-6132	-6990	-6534	-6947	-7324	-5990

0.EL, zero-order elimination; AIC, Akaike information criterion; I_{max} , maximum change in time-varying clearance; K_0 , zero-order rate constant of elimination from central compartment; K_M , Michaelis-Menten rate constant; LCL, linear clearance; MMCL, Michaelis-Menten clearance; η , between-patient variability; Q, intercompartmental exchange rate; RSE, relative standard error; RUV, residual unexplained variability; Shr, shrinkage; T_{50} , time at which clearance is halved; TVARCL, time-varying linear clearance; V_1 , central volume of distribution; V_2 , peripheral volume of distribution; V_{max} , maximum rate of saturable elimination; γ , curve shape factor.

The model exhibiting the best performance comprised parallel Michaelis–Menten and time-varying linear clearance (MMCL + TVARCL).

modeling: patient-related factors (age, sex, RAS mutation status, and creatinine clearance), therapy-related factors (dose group and co-medication with irinotecan or 5-fluorouracil/folic acid), and EGFR ligand and other disease-related measurements (serum concentration of amphiregulin, epidermal growth factor, interleukin-8, transforming growth factor- α , vascular endothelial growth factor, and Eastern Cooperative Oncology Group performance status). None of the investigated covariates were statistically or clinically relevant (**Figure S2**), thus the final model comprised only the effect of BSA described above.

Study design investigations

Parameter estimates of the reference model and their bias indicate that across study designs the reference model parameter estimates were the least biased (**Table S2**). However, bias of many parameters increased substantially in case of sparse sampling compared with rich sampling. The highest change is observed for Michaelis–Menten CL parameters, where changing to either single-dose level or sparse sampling resulted in substantial increase in the parameter bias. Median objective function value across model fit repetitions was lowest for the true (MMCL + TVARCL) model, suggesting that this model, in fact, resulted in the best fit from all investigated models, under all study designs. This was further confirmed by the highest percentage of cases. The reference (TVARCL + MMCL) model was chosen as the best based on the AIC value under all study designs; only a slight variation existed among different study designs, which followed the expected pattern: 93% in the case of the most informative study design (multiple dose levels and rich sampling) and 80% for the least informative study design (one dose level and sparse sampling).

As a reference “background” bias comparison, bias in C_{\min} and AUC from the reference model was calculated using simulated datasets as reference (horizontal lines in **Figure 3** and **Figure 4**); as anticipated, this bias was of very low extent. Comparing the five alternatives to the reference MMCL + TVARCL model, bias in C_{\min} at steady-state was consistently lower than bias for C_{\min} after the second dose for all models and across all investigated study designs (**Figure 3**). All alternative models, except for the MMCL model, resulted in a negligible bias in C_{\min} at steady-state. With respect to bias in C_{\min} after the second dose, the TVARCL model exhibited the smallest bias.

In study designs with rich sampling (A and B), bias in AUC after the second dose was consistently lower than bias in AUC at steady-state for all models (**Figure 4**). The TVARCL model resulted in the lowest bias for both exposure metrics. Compared with rich sampling, sparse sampling (study designs C and D) overall resulted in higher bias, especially in AUC after the second dose. Across all study designs and for both AUC metrics, the bias was the highest for the MMCL model. Overall, the impact of study design was more pronounced for bias in AUC than C_{\min} (**Figure S7**).

Altogether, changes in study design altered accuracy of the PK metrics to a lesser extent than bias (**Figure S5** and **Figure S6**). Differences in inaccuracy of C_{\min} across study designs were minimal ($< 1.5 \mu\text{g/mL}$) and can be considered

negligible (**Figure S5**). Study designs with a single-dose level (B and D) resulted in higher accuracy (lower root mean squared error) compared with multiple-dose level designs, regardless of the sampling density.

DISCUSSION

This study revealed that cetuximab CL is best described by parallel nonlinear and linear clearance that changes exponentially over time. Rich sampling at steady-state was crucial for unbiased estimation of Michaelis–Menten elimination in case of the true (MMCL + TVARCL) model (**Table S2**).

New consolidated PK model of cetuximab

Due to the dataset combining rich and sparse data with multiple dose levels collected over more than 2 years, we have been able to identify, to the best of our knowledge for the first time, a complex approximated TMDD model of cetuximab with time varying clearance (MMCL + TVARCL). Cetuximab clearance was best described by a combination of Michaelis–Menten and linear CL components, thus demonstrating both exposure-dependency and time-dependency of cetuximab PK, respectively. The nonlinear CL of a maximum rate of 0.861 mg/h was identified, with 50% of maximum value reached at a drug concentration of 13.3 mg/L. Nonlinear CL at very low cetuximab concentrations ($C \ll K_m$) was approximately four times higher than baseline linear CL (0.0647 vs. 0.0174 L/h, respectively). In parallel, the linear CL component decreased exponentially with mean maximal decrease of $\sim 18\%$ (155% coefficient of variation), reaching 50% of the maximal decrease after ~ 5 months of therapy.

Two previous analyses identified simpler population PK models for cetuximab,^{4,5} likely due to less informative data (i.e., lower number of patients and only one dose level). Azzopardi *et al.*⁵ investigated cetuximab PK in patients with colorectal cancer and found that clearance was best described by the LCL + 0.EL model. Dirks *et al.*⁴ found that the Michaelis–Menten elimination was most appropriate to describe cetuximab clearance in patients with squamous cell carcinoma of the head and neck. They also investigated a potential time change in CL and found that cetuximab elimination was not time-dependent. The disagreement of our findings with the study by Dirks *et al.* might be due to differences in the investigated populations. The median duration of cetuximab treatment was significantly shorter in the study by Dirks *et al.* (6 weeks) compared with our population (~ 23 weeks), which might have resulted in insufficient informativeness of the data with respect to potential time change in CL.

We further found that disregarding either of the two CL components (i.e., considering only the time-varying linear CL or TMDD component) resulted in significantly inferior model performance compared with the model with both clearance components (as identified in the final PK model). For the final (MMCL + TVARCL) model, relative relevance of the different identified clearance components is illustrated in **Figure S4**. The linear pathway contributed to a larger extent to the total cetuximab clearance than the nonlinear one; neglecting the change of clearance over time resulted in minor differences in the cetuximab concentration-time profile of a

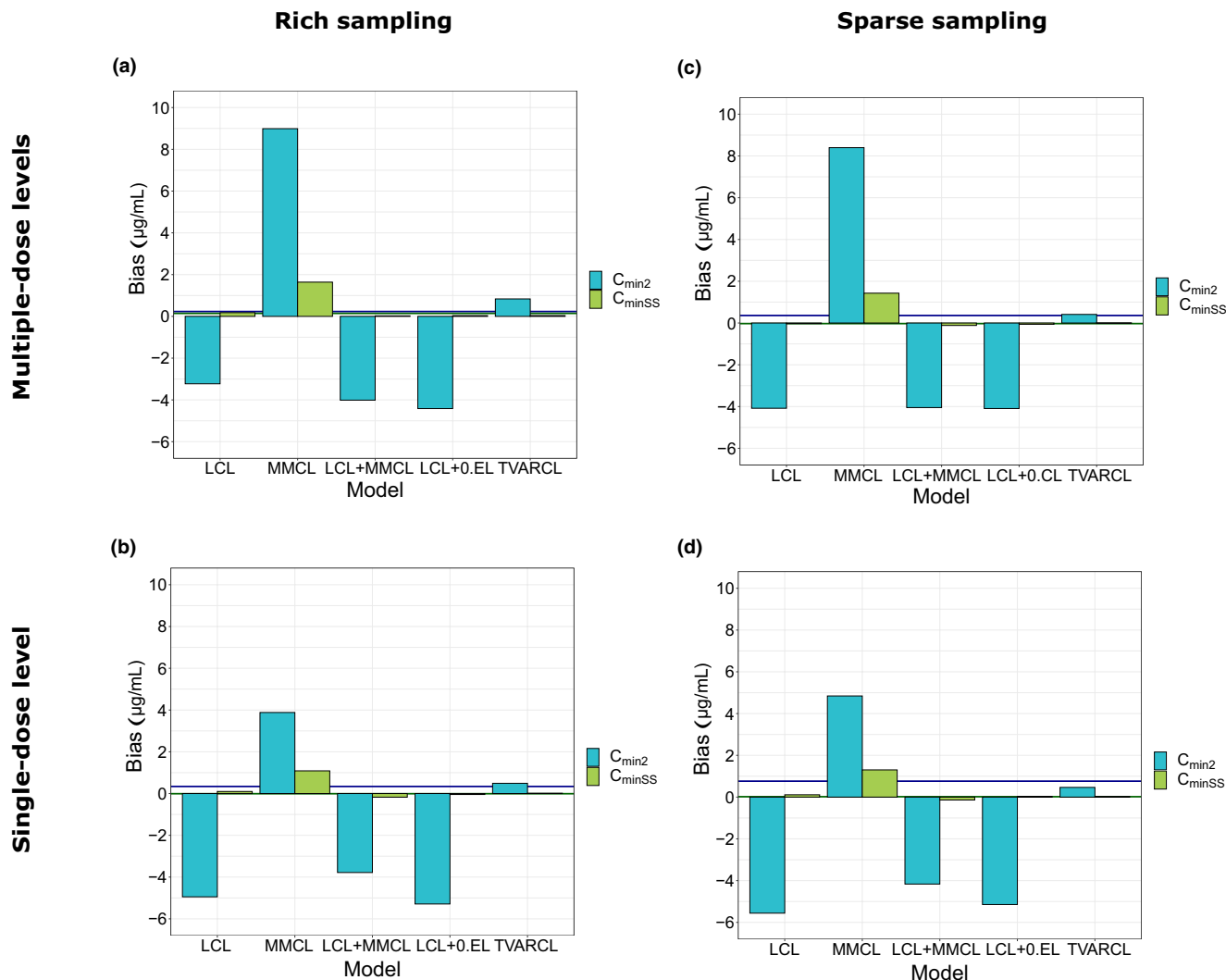


Figure 3 Bias in minimum concentration after the second ($C_{\min 2}$) dose and C_{\min} in steady-state ($C_{\min SS}$) compared with reference MMCL + TVARCL model. (a) Study design A: multiple-dose levels and rich sampling. (b) Study design B: single-dose level and rich sampling. (c) Study design C: multiple-dose levels and sparse sampling. (d) Study design D: single-dose level and sparse sampling. Horizontal lines represent “background” bias for the reference model compared with the simulated observations. 0.EL, zero-order clearance; LCL, linear clearance; MMCL, Michaelis–Menten clearance; TVARCL, time-varying linear clearance

typical patient. For a typical individual after the first dose under ADR, the nonlinear CL at C_{\max} (197 $\mu\text{g/mL}$) was 0.00409, and at C_{\min} (48.3 $\mu\text{g/mL}$) 0.0139 L/h. Furthermore, the change of mAb CL over time has previously been related to disease status in patients with cancer,^{9,16} which is in accordance with our findings as explained below. Thus, the ability to identify the change of CL over time is dependent on disease status change (e.g., initial disease burden and magnitude of change) in the investigated time frame and population (i.e., if an investigated population exhibits no relevant change in disease status, no change in CL over time is expected).

Study design investigations

The capacity to identify a more or less complex model is highly sensitive to the study design. Impact of study design on how well the data informs each model parameter

can be assessed by comparing bias in parameter estimates of the reference model across the study designs.¹⁷ Our results (Table S2) suggest that, in study designs with single-dose levels and/or sparse sampling, the bias in parameters of Michaelis–Menten CL increases the most. This implies that data with only one dose level are less informative for nonlinear CL, which is expected because this CL component is relevant only for the lower exposure range, and might not be captured with only single level dosing. On the other hand, our findings suggest that sparse sampling does not provide enough information to estimate all the parameters, even if multiple-dose level data are available (Table S2).

Both rich and sparse sampling designs were investigated to assess bias and accuracy of parameter estimates and derived exposure metrics. The sampling density was found to be a more influential factor than number of dose levels.

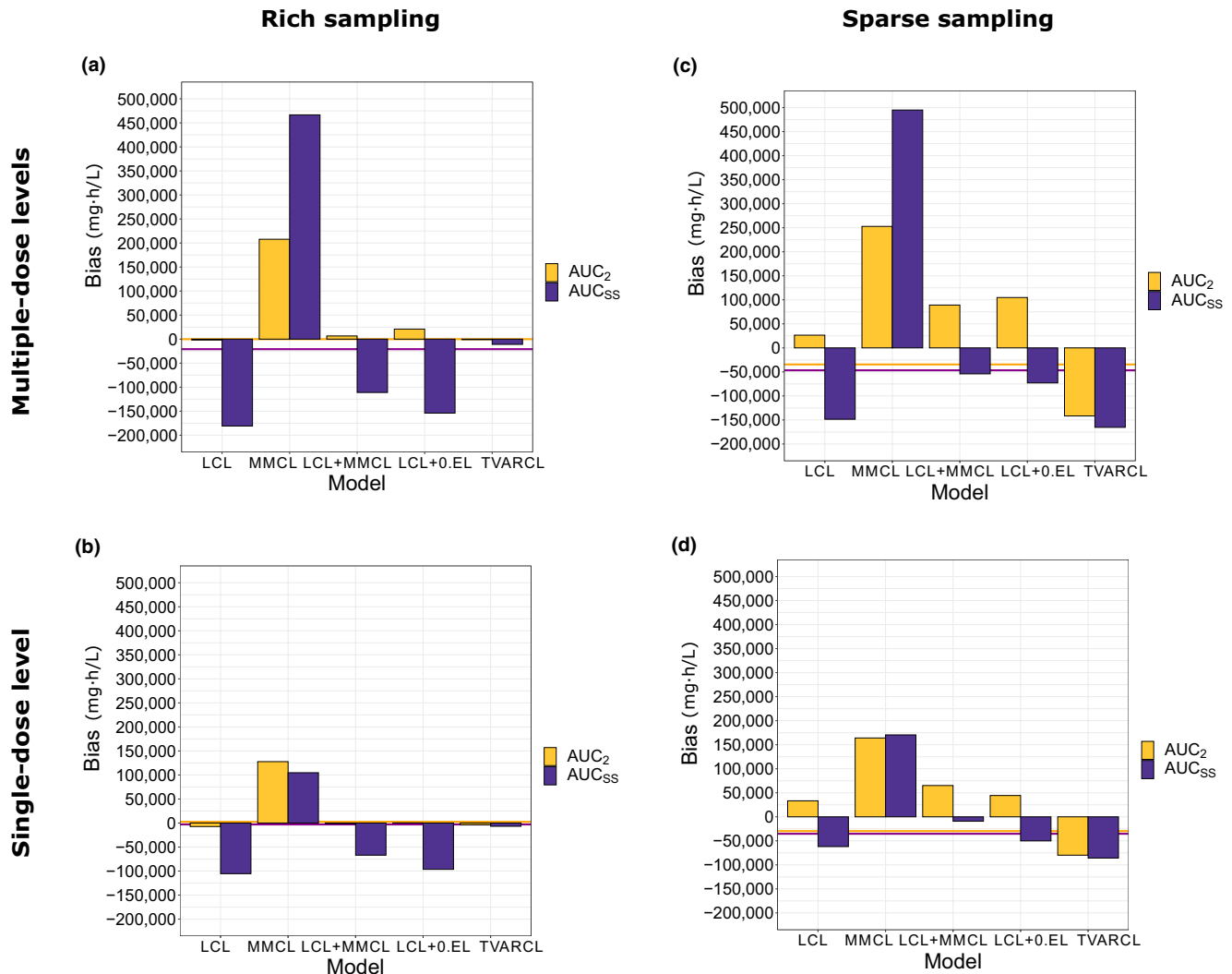


Figure 4 Bias in AUC after the second dose and AUC in steady-state compared with reference MMCL + TVARCL model. (a) Study design A: multiple-dose levels and rich sampling. (b) Study design B: single-dose level and rich sampling. (c) Study design C: multiple-dose levels and sparse sampling. (d) Study design D: single-dose level and sparse sampling. Horizontal lines represent “background” bias for the reference model compared to the individual predictions from the original, reference model, used for simulations. AUC, area under the curve; AUC_{ss}, area under the curve in steady-state; 0.EL, zero-order clearance; LCL, linear clearance; MMCL, Michaelis-Menten clearance; TVARCL, time-varying linear clearance.

Our results indicate that the effect of study design depends on the PK metric considered. For instance, having sparse instead of dense sampling in the TVARCL model resulted in similar (or even slightly decreased) bias in C_{\min} , whereas the bias in AUC increased substantially. This is because the investigated sparse sampling study designs consisted of only C_{\min} samples and thus did not inform the earlier part of the PK curve (especially C_{\max}) essential for AUC calculation. Additional sampling at C_{\max} in addition to C_{\min} samples should reduce the bias in AUC. On the other hand, bias in AUC was lower for all investigated models in single-dose level designs compared with multidose level designs, and a similar trend is observed for bias in C_{\min} .

Altogether, our findings imply that the TVARCL model is the best overall approximation to the true (MMCL + TVARCL) model. In study design A, in which the AUC calculation is

well informed due to rich sampling and the role of nonlinear CL is expected due to low dose levels, the TVARCL model resulted in overprediction of C_{\min} after the second dose. This behavior is mechanistically expected, as the contribution of Michaelis-Menten CL, which is not accounted for in this model, is more important for C_{\min} than the AUC calculation, and it is expected to be more pronounced in the earlier phase of therapy (i.e., after the second dose) before the decrease of linear CL becomes significant and when the accumulation of the drug is not pronounced.

Mechanisms of clearance change

The role of nonlinear CL in disposition of mAbs has been well-established and is mechanistically explained by the presence of TMDD.^{2,18,19} On the other hand, time dependence of PK of mAbs has only recently come into focus and

the understanding of its origin remains hypothetical. Time-dependent elimination has previously been described for mAbs indicated in oncology.^{9,10,16,20}

To investigate potential reasons for the CL change, the time-varying CL component in responders and non-responders to cetuximab therapy was compared. The response was defined as per Response Evaluation Criteria in Solid Tumors (RECIST).²¹ Patients with complete or partial response were classified as responders, whereas patients with stable or progressive disease were classified as nonresponders. The average magnitude of decrease in CL was higher in responders than in nonresponders (**Figure 5**), implying that CL change is related to post-treatment disease status in these patients, in accordance with previously reported findings.^{9,16,22} Mechanistically, the effect of disease status might comprise changes in TMDD (lower target abundance in responders) and/or cancer-related cachexia (lower protein turnover in responders).²⁰ Due to inflammation, the protein turnover rate in patients with cancer is increased compared with that in healthy individuals, as indicated by measures such as decreased albumin concentration.² Decrease over time in disease (and thus inflammatory) status will be reflected in normalization of protein turnover rate, that would, in turn, lead to decrease in nonspecific (linear) elimination of therapeutic proteins, including cetuximab. We identified an initial decrease in cetuximab CL in both groups of patients, although it is of a lower extent in nonresponders than responders (**Figure 5**). Krippendorff *et al.*²³ demonstrated that upon administration of an anti-EGFR drug, there is a steep initial decrease in receptor activation due to blockage by the drug, followed by a gradual increase as drug exposure decreases. At high drug doses, a complete and long-lasting saturation of the target can be accomplished. Regardless of the outcome of the treatment (i.e., whether a patient is a responder or nonresponder), this initial effect is expected to be observed. In responders, further decline in CL over time is expected due to mechanisms elaborated above. However, in nonresponders, the increase in

disease burden would over time prevail, resulting in a net increase in CL.

Exposure-response and therapeutic drug monitoring

The findings of time-dependent change of cetuximab elimination in this study underline the bidirectional PK-PD relationship, which is intuitively anticipated for mAbs. The bidirectional interaction between PK and PD has important implications on assumption of exposure-response causality and thus exposure-response analyses. In traditional exposure-response analyses, a unidirectional exposure-response relationship is assumed (i.e., exposure is considered the independent variable). However, in the presence of the time-dependent changes in elimination that are related to the patient response, this assumption fails to hold true, as response impacts exposure. As a consequence, in this case, the exposure-response relationship is overestimated compared with the true underlying relationship.^{2,22} Thus, in the case of drugs with time-varying elimination, assumptions underlying therapeutic drug monitoring might be shattered. In addition, identifying and accounting for baseline biomarkers for disease status (e.g., cachexia²⁴) would help to overcome these limitations.

In conclusion, a two-compartment model with parallel Michaelis-Menten and linear CL that changes exponentially over time best characterized the PK of cetuximab. The magnitude of decrease in clearance over time is higher for responders than nonresponders, calling for better understanding of exposure-response analyses and therapeutic drug monitoring in the presence of time-varying clearance. Furthermore, the importance of informing the population models with rich data is stressed, supporting analysis of pooled data from multiple trials at later stages of drug development instead of using only sparse data (e.g., in the case of phase III clinical trials).

Supporting Information. Supplementary information accompanies this paper on the *CPT: Pharmacometrics & Systems Pharmacology* website (www.psp-journal.com).

Acknowledgments. The authors would like to acknowledge Anne Drescher for the preparation of the base dataset and preliminary analysis, as well as colleagues from Merck who were involved in the clinical trials and analyses. Medical writing assistance was provided by ClinicalThinking, Inc., Hamilton, NJ, USA, and funded by Merck KGaA, Darmstadt, Germany.

Funding. The clinical trials were funded by Merck KGaA, Darmstadt, Germany.

Conflict of Interest. A.M.G., A.K., and M.B. are employees of Merck KGaA, Darmstadt, Germany. M.B. reports shares. W.H. reports grants from an industry consortium (AbbVie Deutschland GmbH & Co. KG, Boehringer Ingelheim Pharma GmbH & Co. KG, Grünenthal GmbH, F. Hoffmann-La Roche Ltd, Merck KGaA, and Sanofi) for the PharMetriX PhD program. P.G. is an employee of Merck Serono S.A., Lausanne, Switzerland, an affiliate of Merck KGaA, Darmstadt, Germany. C.K. reports grants from an industry consortium (AbbVie Deutschland GmbH & Co. KG, Boehringer Ingelheim Pharma GmbH & Co. KG, Grünenthal GmbH, F. Hoffmann-La Roche Ltd, Merck KGaA, and Sanofi) for the PharMetriX

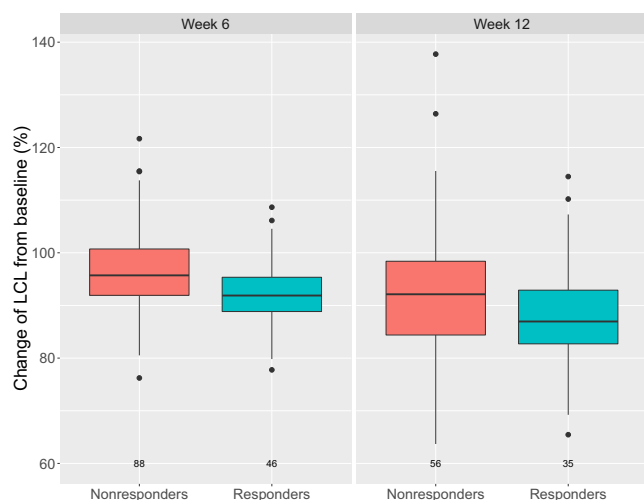


Figure 5 Change of linear clearance (LCL) from baseline at week 6 and week 12 of therapy, stratified by post-treatment response.

PhD program, Diurnal Ltd., and grants from the Innovative Medicines Initiative-Joint Undertaking (“DDMoRe”).

Author Contributions. A.M.G. wrote the manuscript. A.M.G., A.K., W.H., P.G., and C.K. designed the research. A.M.G. and A.K. performed the research. All authors analyzed the data. All authors contributed to review and approval of the manuscript.

- Martini, G. et al. Present and future of metastatic colorectal cancer treatment: a review of new candidate targets. *World J. Gastroenterol.* **23**, 4675–4688 (2017).
- Ryman, J.T. & Meibohm, B. Pharmacokinetics of monoclonal antibodies. *CPT Pharmacometrics Syst. Pharmacol.* **6**, 576–588 (2017).
- World Health Organization: Latest global cancer data. <<https://www.who.int/cancer/PRGlobocanFinal.pdf>> (2018). Accessed November 7, 2019.
- Dirks, N.L., Nolting, A., Kovar, A. & Meibohm, B. Population pharmacokinetics of cetuximab in patients with squamous cell carcinoma of the head and neck. *J. Clin. Pharmacol.* **48**, 267–278 (2008).
- Azzopardi, N. et al. Cetuximab pharmacokinetics influences progression-free survival of metastatic colorectal cancer patients. *Clin. Cancer Res.* **17**, 6329–6337 (2011).
- Girard, P., Kovar, A., Brockhaus, B., Zuehlsdorf, M., Schlichting, M. & Munafo, A. Tumor size model and survival analysis of cetuximab and various cytotoxics in patients treated for metastatic colorectal cancer. The 22nd of the Population Approach Group in Europe; 11–14 June, 2013; Glasgow, Scotland. Abstract 2902. [Google Scholar].
- Taberero, J. et al. Cetuximab administered once every second week to patients with metastatic colorectal cancer: a two-part pharmacokinetic/pharmacodynamic phase I dose-escalation study. *Ann. Oncol.* **21**, 1537–1545 (2010).
- Van Cutsem, E. et al. Inpatient cetuximab escalation in metastatic colorectal cancer according to the grade of early skin reactions: the randomized EVEREST study. *J. Clin. Oncol.* **23**, 2861–2868 (2012).
- Liu, C. et al. Association of time-varying clearance of nivolumab with disease dynamics and its implications on exposure response analysis. *Clin. Pharmacol. Ther.* **101**, 657–666 (2017).
- Wilkins, J. et al. Population pharmacokinetic analysis of avelumab in different cancer types. In Abstracts for American conference on pharmacometrics 2017 (ACoP8). *J. Pharmacokinet. Pharmacodyn.* **44** (suppl. 1), 11–143 (2017).
- Gastonguay, M. Full covariate models as an alternative to methods relying on statistical significance for inferences about covariate effects: a review of methodology and 42 case studies. Poster presented at PAGE 2011, Athens, Greece. Abstract 2229.
- Mould, D.R. & Upton, R.N. Basic concepts in population modeling, simulation, and model-based drug development – Part 2: introduction to pharmacokinetic modeling methods. *CPT Pharmacometrics Syst. Pharmacol.* **2**, e38 (2013).
- Lindbom, L., Ribbing, J. & Jonsson, E.N. Perl-speaks-NONMEM (PsN)—a Perl module for NONMEM related programming. *Comput. Method Programs Biomed.* **75**, 85–94 (2004).
- Dirks, N.L. & Meibohm, B. Population pharmacokinetics of therapeutic monoclonal antibodies. *Clin. Pharmacokinet.* **49**, 633–659 (2010).
- Lobo, E.D. et al. Antibody pharmacokinetics and pharmacodynamics. *J. Pharm. Sci.* **93**, 2645–2668 (2004).
- Baverel, P.G. et al. Population pharmacokinetics of durvalumab in cancer patients and association with longitudinal biomarkers of disease status. *Clin. Pharmacol. Ther.* **103**, 631–642 (2018).
- Walther, B.A. & Moore, J.L. The concepts of bias, precision and accuracy, and their use in testing the performance of species richness estimators, with a literature review of estimator performance. *Ecography* **28**, 815–829 (2005).
- Kloft, C. et al. Population pharmacokinetics of sibrutumab, a novel therapeutic monoclonal antibody, in cancer patients. *Invest. New Drugs* **22**, 39–52 (2004).
- Kuester, K., Kovar, A., Lüpfer, C., Brockhaus, B. & Kloft, C. Refinement of the population pharmacokinetic model for the monoclonal antibody matuzumab: external model evaluation and simulations. *Clin. Pharmacokinet.* **48**, 477–487 (2009).
- Bajaj, G., Wang, X., Agrawal, S., Gupta, M., Roy, A. & Feng, Y. Model-based population pharmacokinetic analysis of nivolumab in patients with solid tumors. *CPT Pharmacometrics Syst. Pharmacol.* **6**, 58–66 (2017).
- Tsuchida, Y. & Therasse, P. Response evaluation criteria in solid tumors (RECIST): new guidelines. *Med. Pediatr. Oncol.* **37**, 1–3 (2001).
- Wang, Y., Booth, B., Rahman, A., Kim, G., Huang, S.M. & Zineh, I. Toward greater insight on pharmacokinetics and exposure-response relationship for therapeutic biologics in oncology drug development. *Clin. Pharmacol. Ther.* **101**, 582–584 (2017).
- Krippendorff, B.F., Oyarzun, D.A. & Huisinga, W. Predicting the F(ab)-mediated effect of monoclonal antibodies in vivo by combining cell-level kinetic and pharmacokinetic modelling. *J. Pharmacokinet. Pharmacodyn.* **39**, 125–139 (2012).
- Lobato, G. C. et al. Associations between baseline serum biomarker levels and cachexia/precachexia in pretreated non-small cell lung cancer (NSCLC) patients. *J. Clin. Oncol.* **37**(15_suppl), 3054 (2019).

© 2020 Merck Healthcare KGaA. *CPT: Pharmacometrics & Systems Pharmacology* published by Wiley Periodicals LLC on behalf of American Society for Clinical Pharmacology and Therapeutics. This is an open access article under the terms of the Creative Commons Attribution-NonCommercial-NoDerivs License, which permits use and distribution in any medium, provided the original work is properly cited, the use is non-commercial and no modifications or adaptations are made.

Supplementary material

1
2
3
4
5
6
7
8
9
10
11
12
13
14
15
16
17
18
19
20
21
22

Methods:

The accuracy was assessed in terms of root mean squared error (RMSE) according to the following equation:

$$RMSE = \sqrt{\frac{1}{N} \cdot \sum_{i=1}^n (est_i - ref_i)^2}$$

where N denotes number of simulation repetitions (200); n , the number of patients (number of patients in a trial · number of trial repetitions); ref_i , the parameter/exposure metric values for the reference PK model; and est_i , the values for the alternative models.

Relative bias was calculated according to the following equation:

$$Relative\ bias = 100\% \cdot \frac{1}{N} \cdot \sum_{i=1}^n \frac{est_i - ref_i}{ref_i}$$

where N denotes number of simulation repetitions (200); n , the number of patients (number of patients in a trial · number of trial repetitions); ref_i , the parameter/exposure metric values for the reference PK model; and est_i , the values for the alternative models.

All estimations were performed on a Linux cluster (version 3.0.101) with a SUSE operating system, using a Sun Grid Engine and the GNU Fortran compiler.

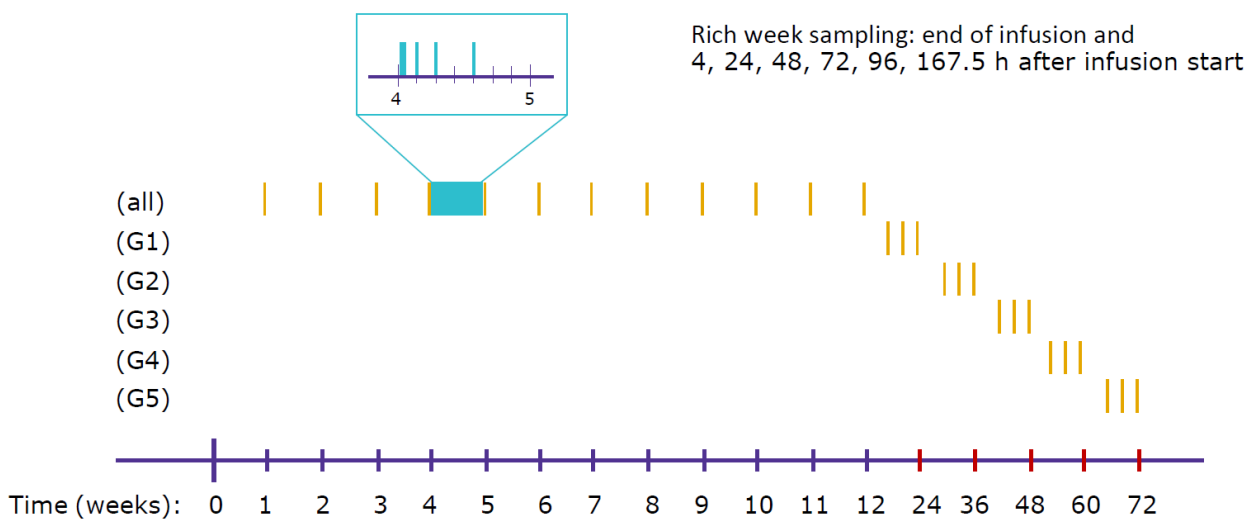
Results:

For the two models incorporating the Michaelis-Menten elimination component the number of model runs with successful minimization was low across all four study designs (for LCL+MMCL and MMCL models, 39.5%-66.5 % and 54.5%-64.0 % of total number of executions, respectively), which could impact the results of the analysis. To exclude this potential impact of the number of model runs included in the analysis (Table S1) and to allow inclusion of models that converged without successful

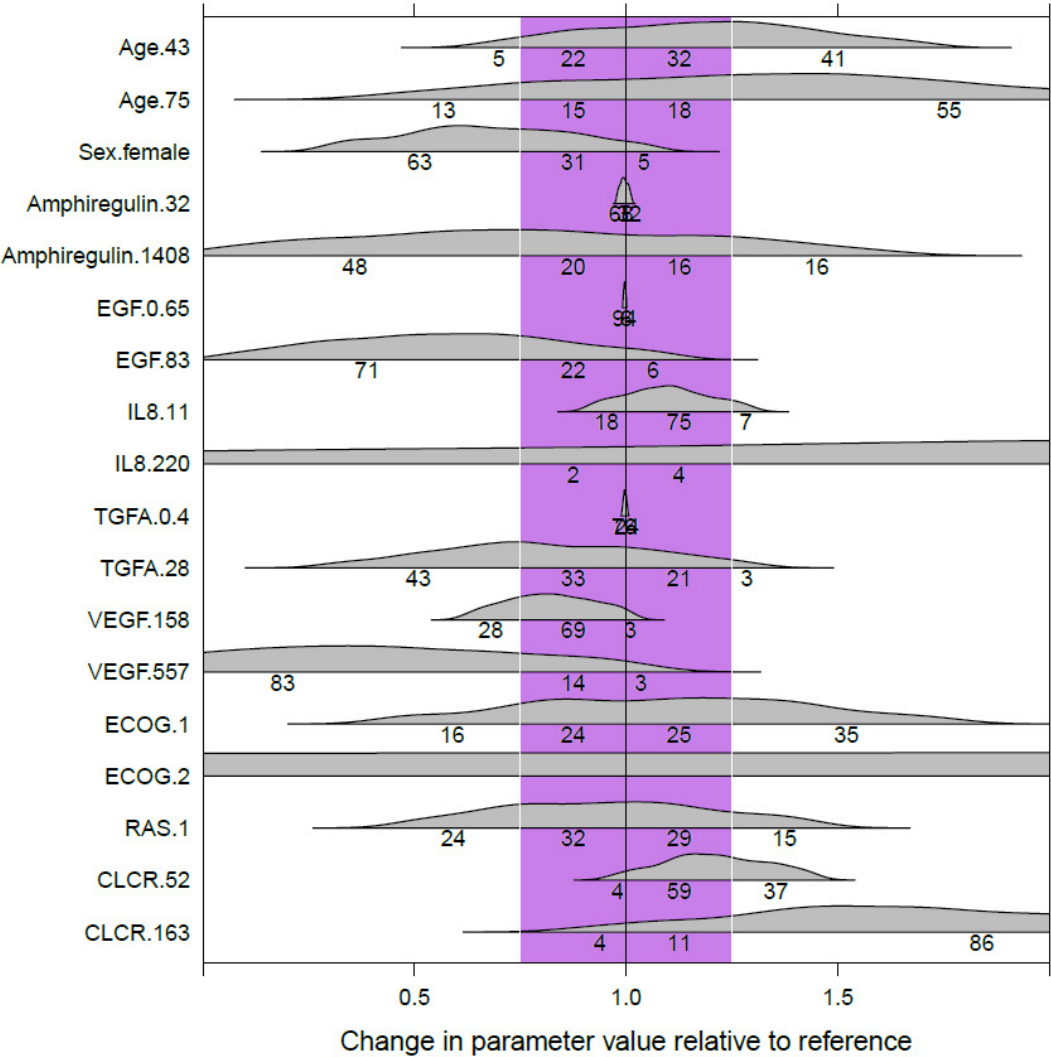
23 minimization, the analysis was repeated on only model runs with successful minimization. The results
24 (data not shown) were analogous, with only minor differences in the bias and RMSE values.

25 **Supplementary Figure Legends**

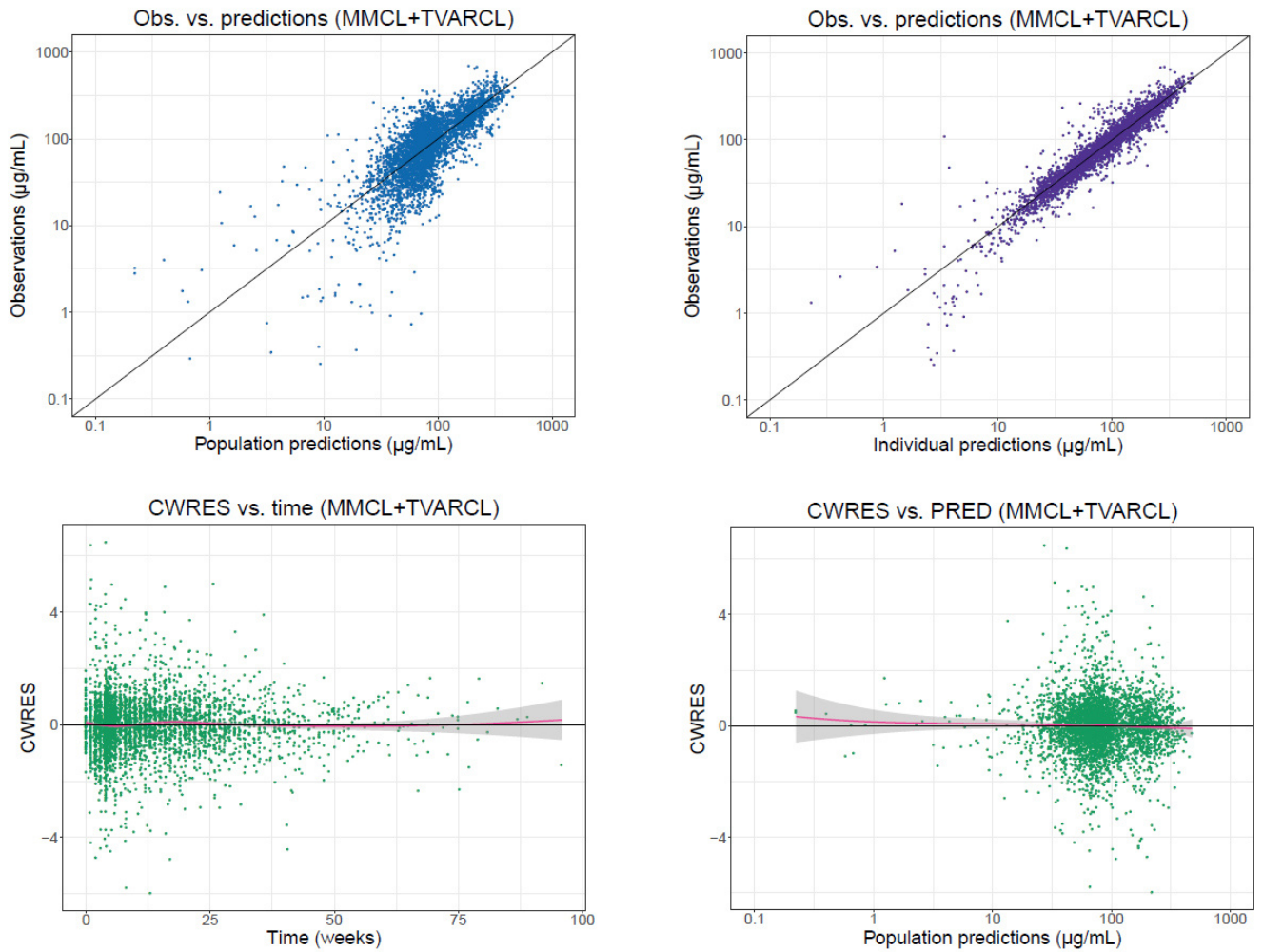
26 **Figure S1.** Pharmacokinetic sampling schedule for the virtual population used for the stochastic
27 simulation and estimation (SSE) analysis. For all patients C_{min} samples were taken after every dose until
28 week 12. At week 12 the patients were divided in 5 groups of 20 patients, and the groups were sampled
29 in such a way that each group was sampled for the duration of 3 months once a month at C_{min} levels.
30 Sampling for group 1 (G1) started at week 12, for group 2 (G2) at week 24, for group 3 (G3) at week
31 36, for group 4 (G4) at week 48, and for group 5 (G5) at week 60. In study design A and C, in addition
32 to the C_{min} samples, dense sampling (at the end of infusion and 4, 24, 48, 72 and 96 h after infusion
33 start) was performed in all patients (blue vertical lines) after the fourth dose.



35 **Figure S2.** Forest plot illustrating clinical inference of covariates on baseline linear clearance (CL)
 36 investigated via full fixed-effects modeling approach. Purple surface represents area of clinical
 37 irrelevance ($\pm 25\%$ change from typical CL value), and grey areas are covariate effect parameter value
 38 distributions based on bootstrap analysis ($n = 1000$). Numbers below the covariate distributions
 39 represent percent of the bootstrapped values that fall under the respective CL change range. Plotted
 40 covariates values (y axis) represent 5th and 95th percentile for continuous or the less frequent category
 41 for categorical covariates in the analyzed population. CLCR, creatinine clearance; ECOG, Eastern
 42 Cooperative Oncology Group score; EGF, epidermal growth factor concentration; IL8, interleukin 8
 43 concentration; TGFA, transforming growth factor- α concentration; VEGF, vascular endothelial growth
 44 factor concentration.

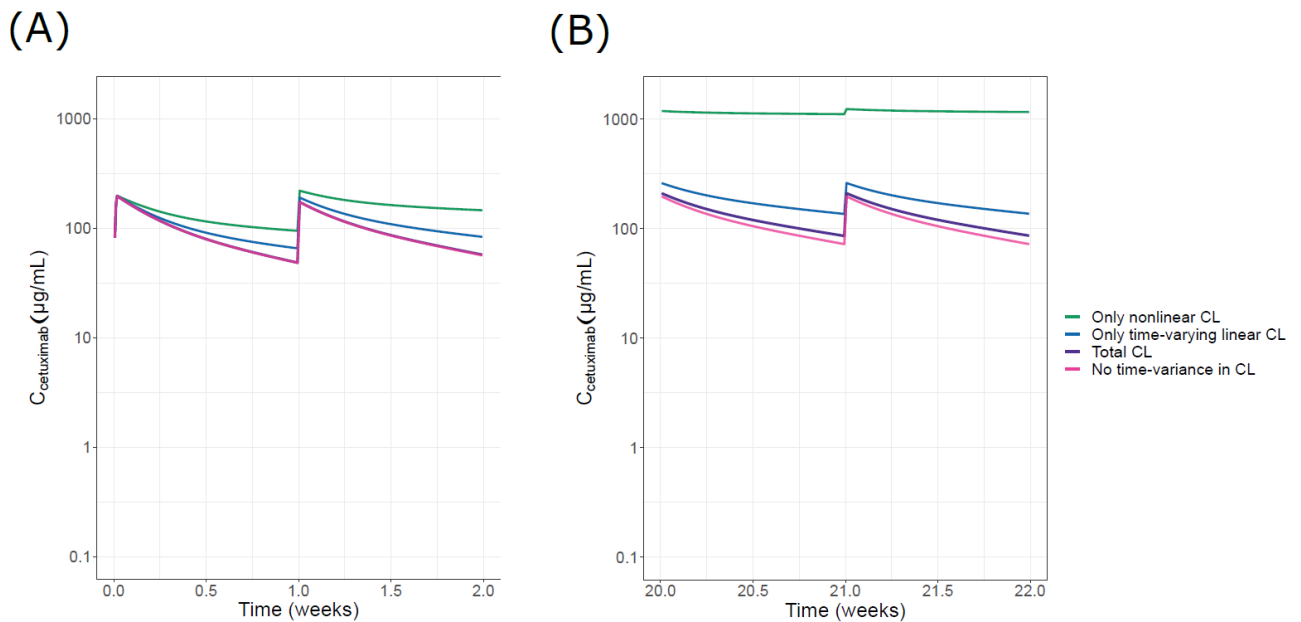


46 **Figure S3.** Goodness-of-fit plots for the final base model indicate good performance of the model with
47 parallel Michaelis-Menten and time-varying clearance (MMCL+TVARCL). CWRES, conditional weighted
48 residuals.

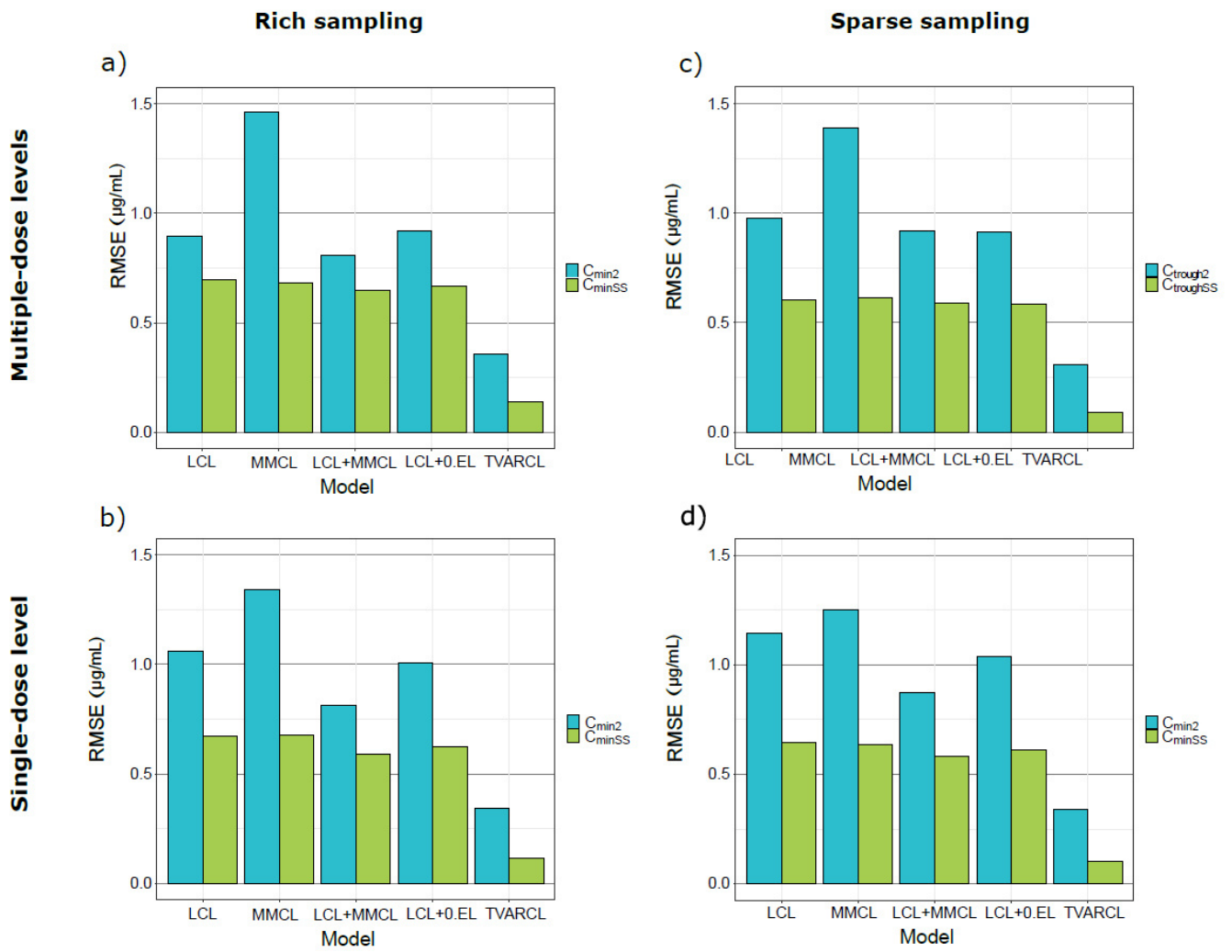


49

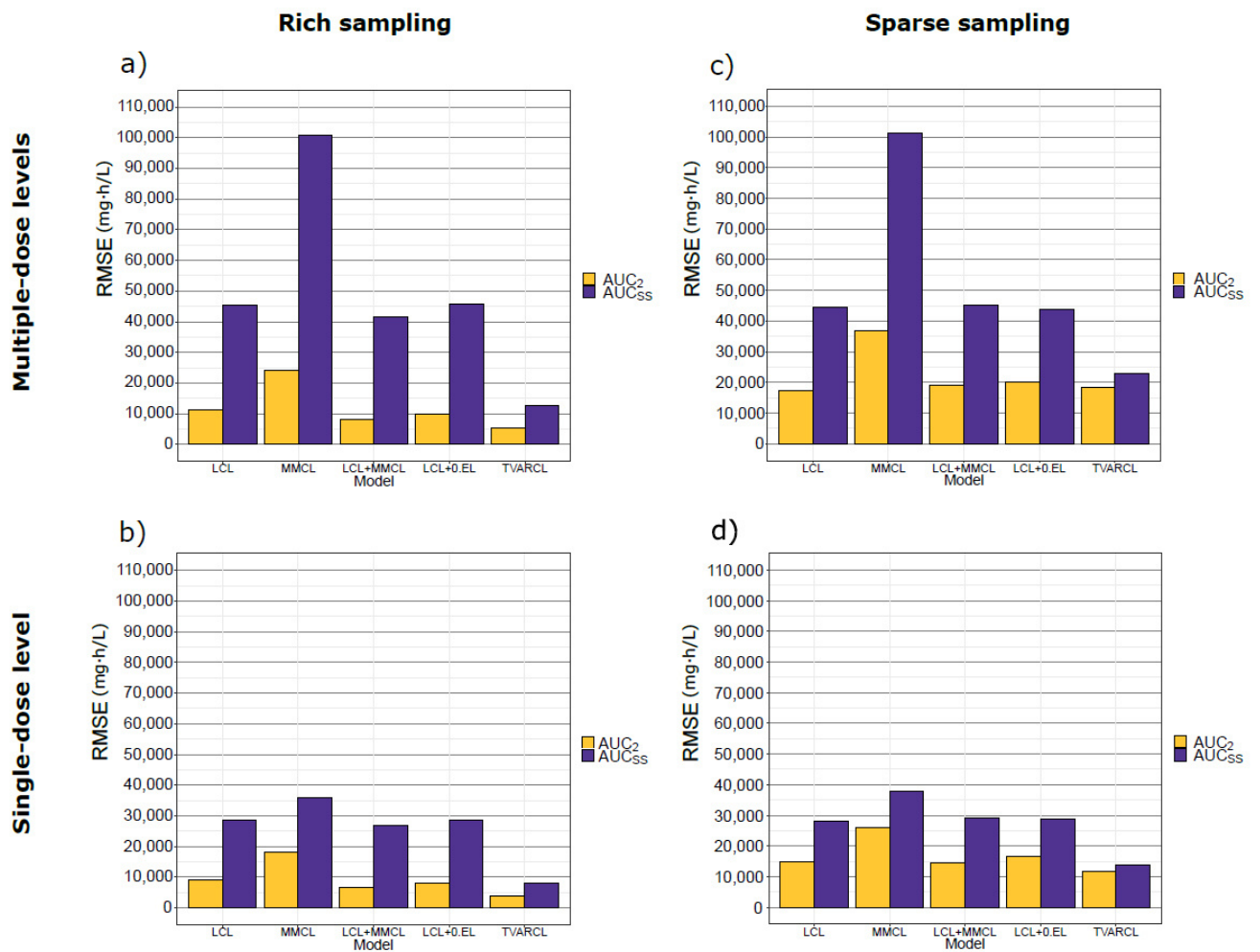
50 **Figure S4.** Relative relevance of different clearance (CL) components identified in the population
51 pharmacokinetic model. Cetuximab concentration-time profiles at the beginning of the treatment (A)
52 and at time of half-maximal change in CL (B) for the identified (“true”) total CL consisting of nonlinear
53 and time-varying linear elimination (“Total CL”), in absence of time-change in linear CL (“No time-
54 variance in CL”), in absence of nonlinear CL (“Only time-varying linear CL”), and in presence of only
55 nonlinear CL (“Only nonlinear CL”). For all presented simulations, typical parameter values (Table 2)
56 from the final model (MMCL+TVARCL) were used, and parameters related to the neglected CL
57 components were excluded.



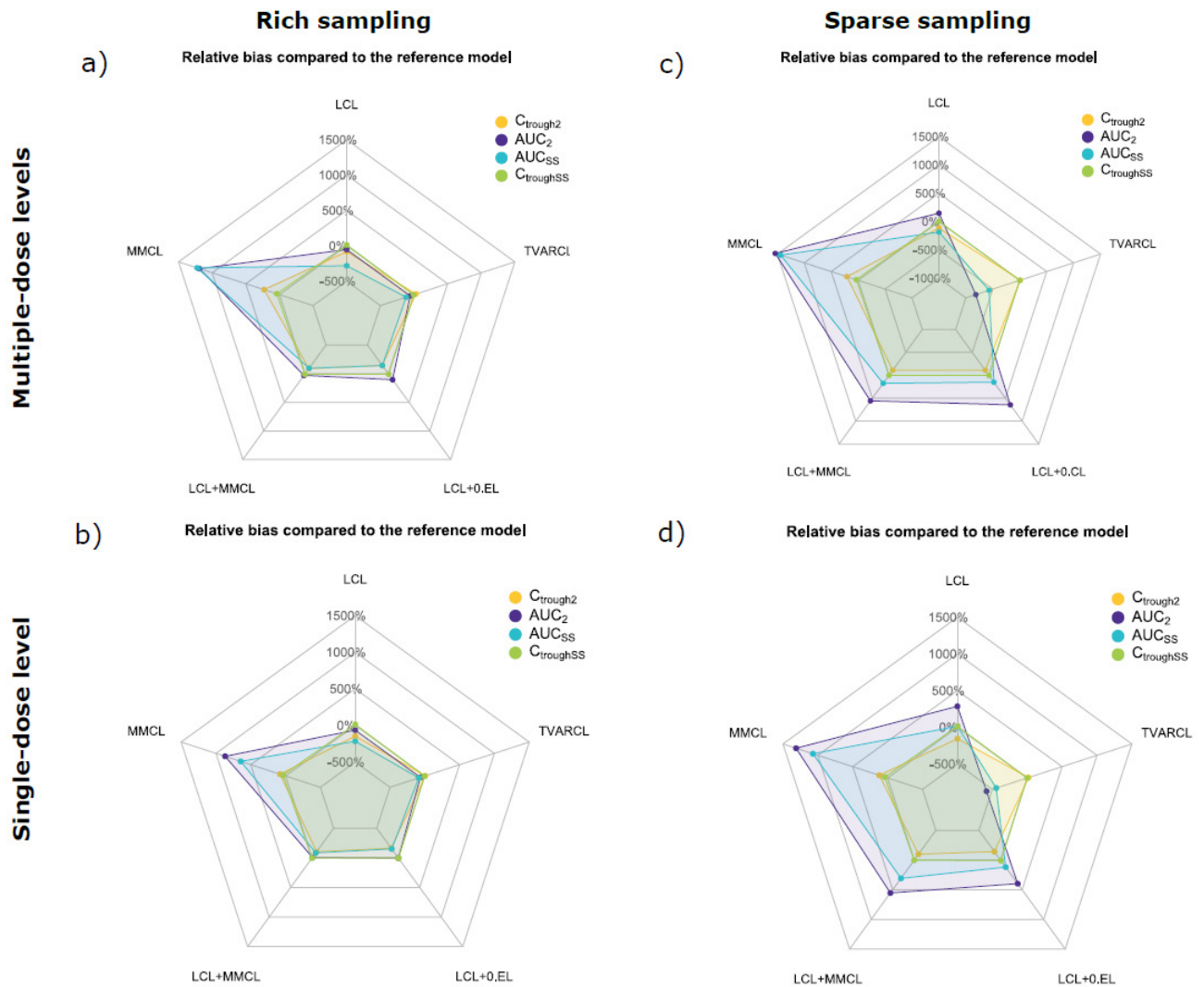
59 **Figure S5.** Accuracy in C_{\min} after the second dose and C_{\min} in steady state compared to reference MMCL
 60 + TVARCL model. (a) Study design A: multiple dose levels and rich sampling; (b) Study design B: single
 61 dose level and rich sampling; (c) Study design C: multiple dose levels and sparse sampling; (d) Study
 62 design D: single dose level and sparse sampling. 0.CL, zero-order clearance; LCL, linear clearance;
 63 MMCL, Michaelis-Menten clearance; RMSE, root mean squared error; TVARCL, time-varying linear
 64 clearance.



66 **Figure S6.** Accuracy in AUC after the second dose and AUC in steady state compared to reference
 67 MMCL + TVARCL model. (a) Study design A: multiple dose levels and rich sampling; (b) Study design B:
 68 single dose level and rich sampling; (c) Study design C: multiple dose levels and sparse sampling; (d)
 69 Study design D: single dose level and sparse sampling. 0.CL, zero-order clearance; LCL, linear clearance;
 70 MMCL, Michaelis-Menten clearance; RMSE, root mean squared error; TVARCL, time-varying linear
 71 clearance.



73 **Figure S7.** Relative bias in AUC and C_{trough} after the second dose and in steady state compared to
 74 reference MMCL+TVARCL model. (a) Study design A: multiple dose levels and rich sampling; (b) Study
 75 design B: single dose level and rich sampling; (c) Study design C: multiple dose levels and sparse
 76 sampling; (d) Study design D: single dose level and sparse sampling. 0.CL, zero-order clearance; LCL,
 77 linear clearance; MMCL, Michaelis-Menten clearance; TVARCL, time-varying linear clearance.



```
79  NONMEM model code

80  $PROBLEM Cetuximab time-varying linear + MM CL

81  $INPUT ID TIME AMT RATE CMT EVID MDV DV

82  $DATA dataset.csv IGNORE=#

83  $SUBROUTINE ADVAN6 TRANS1 TOL9

84  $MODEL NCOMP=2 COMP=(CENTRAL DEFOBS) COMP=(PERIPH)

85  $PK

86  TVCLL = THETA(1)

87  CLL = TVCLL*EXP(ETA(1))

88  TVV1 = THETA(2)

89  V1 = TVV1*EXP(ETA(2))

90  TVQ = THETA(3)

91  Q = TVQ*EXP(ETA(3))

92  TVV2 = THETA(4)

93  V2 = TVV2*EXP(ETA(4))

94  TVVM = THETA(5)

95  VMAX = TVVM*EXP(ETA(5))

96  TVKM = THETA(6)

97  KM = TVKM*EXP(ETA(6))

98  TT50 = THETA(7)

99  GAM = THETA(8)

100  TMAX = THETA(9)

101  TMETA = ETA(7)

102  S1 = V1

103  S2 = V2
```

```

104  K12=Q/V1
105  K21=Q/V2
106  K10=CLL/V1

107  $DES
108  C1 = A(1)/V1
109  C2 = A(2)/V2
110  DADT(1) = -K12*A(1)+K21*A(2)-(C1*VMAX/(KM+C1))-
111  (K10*EXP((TMAX+TMETA)*T**GAM)/(TT50**GAM+T**GAM))*A(1))
112  DADT(2) = K12*A(1)-K21*A(2)

113  $ERROR
114  DEL=0
115  IF(F.EQ.0) DEL=1
116  IPRED = LOG(F+DEL)
117  IRES = DV-IPRED
118  W = SQRT((THETA(10)*THETA(10))/((F+DEL)*(F+DEL))+THETA(11)*THETA(11))
119  IF (W.EQ.0) W = 1
120  IWRES = IRES/W
121  Y = IPRED+W*ERR(1)

122  $THETA (0.0001,0.013851) ; 1 CLL
123  $THETA (0.0001,3.706311) ; 2 V1
124  $THETA (0.0001,0.035420) ; 3 Q
125  $THETA (0.0001,3.078210) ; 4 V2
126  $THETA (0.0001,0.957218) ; 5 VMAX
127  $THETA (0.0001,10.69743) ; 6 KM
128  $THETA (0.0001, 168.000) ; 7 TT50
129  $THETA 1 FIX ; 8 GAM

```

130 \$THETA 0.1 ; 9 TMAX
131 \$THETA (0.0001,7.391201) ; 10 additive residual error
132 \$THETA (0.00001,0.24688) ; 11 proportional residual error

133 \$OMEGA 0.1485 ; 1 OM CLL
134 \$OMEGA 0.0926 ; 2 OM V1
135 \$OMEGA 0 FIX ; 3 OM Q
136 \$OMEGA 0.3906 ; 4 OM V2
137 \$OMEGA 0.1801 ; 5 OM VMAX
138 \$OMEGA 0 FIX ; 6 OM KM
139 \$OMEGA 0.09 ; 7 OM TMAX

140 \$SIGMA 1 FIX ; RUV as THETAs

141 \$ESTIMATION NOABORT SIGDIG=3 MAXEVAL=9999 PRINT=1 METHOD=1 INTERACTION
142 MSFO=runXXX.msf

143 \$COVARIANCE PRINT=E

144 \$TABLE ID TIME IPRED IRES IWRES CWRES NOPRINT ONEHEADER FILE=sdtabXXX

145 \$TABLE ID CLL V1 Q V2 VMAX KM TMAX TT50 GAM ETA1 ETA2 ETA3 ETA4 ETA5 ETA6 ETA7 NOAPPEND
146 NOPRINT ONEHEADER FILE=patabXXX

1
2
3
4
5
6

Supplementary Tables

Table S1. Proportion of runs (in %) that were completed with successful minimization for each study design.

TVARCL+MMCL (reference) model	LCL model	TVARCL model	MMCL model	LCL+MMCL model	LCL+0.EL model
Study design A					
90.0	98.5	95.0	64.0	66.5	86.5
Study design B					
89.5	90.0	97.5	55.0	47.5	70.0
Study design C					
87.0	99.5	98.5	63.0	58.0	82.5
Study design D					
82.5	97.0	97.5	54.5	39.5	62.5

0.EL, zero-order elimination; LCL, linear clearance; MMCL, nonlinear clearance; TVARCL, time-varying linear clearance.

Table S2. Bias in model parameter estimates for study designs with rich sampling (study designs A and B) and sparse sampling (study designs C and D).

	Study Design A						Study Design B					
	MMCL+TVARCL (Reference model)	LCL model	TVARCL model	MMCL model	LCL+MMCL model	LCL+0.EL model	MMCL+TVARCL (Reference model)	LCL model	TVARCL model	MMCL model	LCL+MMCL model	LCL+0.EL model
LCL, L/h	-0.000880	0.00280	-2.62	-	-0.00712	0.000250	-0.000950	0.00451	-2.62	-	-0.00842	0.00268
V ₁ , L	-0.00668	0.0107	3.63	4.60	0.0775	0.0889	-0.0004	0.07036	3.67	4.18	0.0666	0.0956
Q, L/h	0.000324	-0.00938	-3.62	-2.64	-0.00896	-0.0122	0.00039	-0.0142	-3.62	-2.63	-0.00505	-0.01407
V ₂ , L	0.125	2.64	3.41	133	1.058	1.83	0.10018	2.414	2.61	106.4	0.917	2.12
K _M , mg/L	24.3	-	-	94.2	109	-	172	-	-	52876160	55.3	-
V _{max} , mg/h	0.550	-	-	4.23	2.77	-	1.21	-	-	565542	2.00	-
ln(I _{max})	-0.0485	-	-3440	-	-	-	-0.660	-	-3440	-	-	-
T ₅₀ , weeks	1.29	-	1172	-	-	-	1.028	-	53340	-	-	-
γ	-	-	-11.8	-	-	-	-	-	-12.3	-	-	-
K ₀ , mg/h	-	-	-	-	-	-0.483	-	-	-	-	-	-0.667
η _{LCL} , CV%	-8.23	34.5	46.7	-	63.0	31.0	-3.65	34.9	-47.1	-	78.07	33.5
η _{V1} , CV%	-5.55	-7.84	-25.0	-8.60	9.105	10.15	-4.85	-7.18	-24.5	8.50	-8.29	-8.78
η _{V2} , CV%	-11.2	92.7	66.5	204	58.0	66.3	-21.7	115	74.2	196	50.10	86.5
η _{Vmax} , CV%	-7.33	-	-	7.47	19.1	-	21.3	-	-	19.2	6.62	-
η _{I_{max}} , CV%	24.3	-	134	-	-	-	28.1	-	89.8	-	-	-
η _{K0} , CV%	-	-	-	-	-	120	-	-	-	-	-	189
Additive RUV, mg/L	0.00343	5.34	4.20	-6.36	-3434	-7.64	0.0500	4.88	3.84	-7.508	-3434	-7.88
Proportional RUV, CV%	-0.01	-1300	49.7	-343975	-75.7	-344000	-0.0660	-1306	49.7	-344000	-75.8	-343976

	Study Design C						Study Design D					
	MMCL+TVARCL (Reference model)	LCL model	TVARCL model	MMCL model	LCL+MMCL model	LCL+0.EL model	MMCL+TVARCL (Reference model)	LCL model	TVARCL model	MMCL model	LCL+MMCL model	LCL+0.EL model
LCL, L/h	-0.000670	0.00278	-2.62	-	-0.00586	-0.000690	0.000359	0.00445	-2.62	-	-0.0084	0.00344
V ₁ , L	-0.0758	-0.0214	3.53	4.83	-0.0287	0.00284	-0.0517	0.0219	3.55	4.62	0.00334	0.0220
Q, L/h	0.0441	-0.00897	-3.51	-2.64	0.0182	-0.01505	0.0572	-0.0147	-3.42	-2.64	0.0357	-0.0102
V ₂ , L	0.500	2.95	4.58	144	1.084	1.75	0.382	2.606	3.67	126	0.6040	3.0201
K _M , mg/L	15176440	-	-	88.21	68.1	-	75520740	-	-	38967060	29.4	-
V _{max} , mg/h	52457	-	-	4.19	1.70	-	418775	-	-	529319	1.43	-
ln(I _{max})	-0.0832	-	-3440	-	-	-	-0.09037	-	-3440	-	-	-

T ₅₀ , weeks	5.99	-	72881	-	-	-	1.76	-	411901	-	-	-
γ	-	-	-11.6	-	-	-	-	-	12.1	-	-	-
K ₀ , mg/h	-	-	-	-	-	-0.374	-	-	-	-	-	-0.725
η _{LCL} , CV%	2.70	35.8	-41.9	-	52.2	30.77	0.897	35.6	-43.9	-	68.6	33.8
η _{V1} , CV%	-8.51	-11.6	-25.0	25.8	-10.86	-14.5	-7.43	-10.10	-24.2	37.5	-8.74	-12.5
η _{V2} , CV%	-6.15	85.8	59.7	203.0	54.2	64.3	3.86	108.6	65.9	33.6	43.2	82.04
η _{Vmax} , CV%	33.0	-	-	-8.75	32.07	-	86.1	-	-	198	-34.8	-
η _{Imax} , CV%	36.6	-	189	-	-	-	32.9	-	88.9	-	-	-
η _{K0} , CV%	-	-	-	-	-	134	-	-	-	-	-	218
Additive RUV, mg/L	-0.0386	4.83	3.76	-6.46	-3434	-8.051	0.0320	4.65	3.52	-7.58	-3434	-7.89
Proportional RUV, CV%	0.0355	-1306	49.7	-343975	-75.5	343975	-0.044	-1306	49.6	-343975	-75.5	-343976

0.EL, zero-order elimination; η, between-patient variability; γ, curve shape factor; K₀, zero-order rate constant of elimination from central compartment; K_M, Michaelis-Menten rate constant; LCL, linear clearance; I_{max}, maximum change in time-varying clearance; MMCL, Michaelis-Menten clearance; Q, intercompartmental exchange rate; RSE, relative standard error; RUV, residual unexplained variability; Shr, shrinkage; T₅₀, time at which clearance is halved; TVARCL, time-varying linear clearance; V₁, central volume of distribution; V₂, peripheral volume of distribution; V_{max}, maximum rate of saturable elimination.

Manuscript IV

Equity Ratio Statement

Title of the manuscript:

“Infliximab clearance decreases in the second and third trimesters of pregnancy in inflammatory bowel disease”

Journal United European Gastroenterology Journal

Volume 9, Issue 1, Pages 91-101 (2021)

Authorship Shared first author

Status Published

DOI: <https://doi.org/10.1177/2050640620964619>

Reprinted with permission from United European Gastroenterology Journal.

Own contribution

- Data set modification and checkout
- Modelling and simulation activities, including PK model development, model evaluation, and simulations
- Drafting of parts of the manuscript, in particular related to modelling and simulation activities, including methodology, results, interpretation of the modelling and simulation analysis results
- Creation of some figures and tables for the manuscript
- Involvement in adaptation of the manuscript according to the reviewers' and editor's comments, in particular related to the modelling and simulation analysis

Ana-Marija Grišić

(Doctoral candidate, shared first author)

Prof. Dr. Charlotte Kloft

(Supervisor)

Infliximab clearance decreases in the second and third trimesters of pregnancy in inflammatory bowel disease

United European Gastroenterology
 Journal
 0(0) 1–11
 © Author(s) 2020
 Article reuse guidelines:
 sagepub.com/journals-permissions
 DOI: 10.1177/2050640620964619
 journals.sagepub.com/home/ueg



Ana-Marija Grišić^{1,2,*}, Maria Dorn-Rasmussen^{3,*}, Bella Ungar⁴,
 Jørn Brynskov³, Johan F K F Ilvemark³, Nils Bolstad⁵,
 David J Warren⁵, Mark A Ainsworth³, Wilhelm Huisinga⁶,
 Shomron Ben-Horin⁴, Charlotte Kloft^{1,#} and
 Casper Steenholdt^{3,#}

Abstract

Background: Infliximab therapy during pregnancy in inflammatory bowel disease is challenged by a dilemma between maintaining adequate maternal disease control while minimizing fetal infliximab exposure. We investigated the effects of pregnancy on infliximab pharmacokinetics.

Methods: The study population comprised 23 retrospectively identified pregnancies. Patients with inflammatory bowel disease were generally in clinical remission at pregnancy conception (74%) and received steady infliximab maintenance therapy (5 mg/kg q8w $n = 17$; q6w $n = 4$; q10w $n = 1$; 10 mg/kg q8w $n = 1$). Trough blood samples had been obtained in the same patients prior to pregnancy ($n = 119$), the first trimester ($n = 16$), second trimester ($n = 18$), third trimester ($n = 7$), and post-pregnancy ($n = 12$). Data were analyzed using nonlinear mixed-effects population pharmacokinetic modelling.

Results: Dose-normalized infliximab concentrations were significantly higher during the second trimester (median 15 $\mu\text{g/mL/kg}$, interquartile range 10–21) compared to pre-pregnancy (7, 2–12; $p = 0.003$), the first trimester (9, 1–12; $p = 0.04$), or post-pregnancy (6, interquartile range 3–11; $p > 0.05$) in patients with inflammatory bowel disease. Similar trends were observed in the third trimester (13, 7–36; $p > 0.05$). A one-compartment model with linear elimination described the pharmacokinetics of infliximab (volume of distribution = 18.2 L; clearance 0.61 L/day). Maternal infliximab exposure was influenced by the second and third trimester of pregnancy and anti-infliximab antibodies, and not by pregnancy-imposed physiological changes in, for example, body weight or albumin. Infliximab clearance decreased significantly during the second and third trimesters by up to 15% as compared to pre- and post-pregnancy and the first trimester. The increased maternal infliximab exposure was weakly associated with lowered clinical disease activity. Pharmacokinetic model simulations of virtual patients indicated the increased maternal infliximab trough concentrations imposed by pregnancy will not completely counteract the decrease in infliximab concentration if therapy is paused in the third trimester.

Conclusion: Infliximab clearance decreases significantly in the second and third trimesters, leading to increasing maternal infliximab concentrations in any given regimen. Maternal infliximab levels may thus be maintained as constant in a de-intensified regimen by therapeutic drug monitoring guidance in inflammatory bowel disease.

¹Department of Clinical Pharmacy and Biochemistry, Institute of Pharmacy, Freie Universitaet Berlin, Berlin, Germany

²Graduate Research Training Program PharMetrX, Germany

³Department of Gastroenterology, Copenhagen University Hospital Herlev, Herlev, Denmark

⁴Department of Gastroenterology, Sheba Medical Center Tel Hashomer & Sackler School of Medicine, Tel-Aviv University, Ramat Gan, Israel

⁵Department of Medical Biochemistry, Oslo University Hospital, Oslo, Norway

⁶Institute of Mathematics, Universität Potsdam, Potsdam, Germany

*shared authorship

#shared authorship

Corresponding author:

Casper Steenholdt, Department of Gastroenterology, Copenhagen University Hospital, Herlev, Ringvej, 75 DK-2730, Denmark.
 Email: steenholdt@dadlnet.dk

Keywords

Infliximab, pharmacokinetics, IBD, pregnancy, population modelling, anti-TNF

Received: 5 July 2020; accepted: 16 September 2020

Key Summary

Summarize the established knowledge on this subject

- IFX during pregnancy is challenged by a dilemma between maintaining adequate maternal disease control while minimizing fetal drug exposure.
- Clinicians may refrain from administering IFX in the last part of pregnancy to lower the risk of imposing unknown effects of anti-TNF- α therapy on the fetus.
- International guidelines are conflicting regarding whether IFX should be paused in the third trimester.

What are the significant and/or new findings of this study?

- IFX CL significantly decreases in the second and third trimesters of pregnancy by up to 15%, resulting in increasing maternal circulating IFX levels.
- Maternal IFX exposure during pregnancy is affected by trimester and anti-IFX Abs (increasing IFX CL by 69%).
- Increased maternal IFX exposure during pregnancy correlated weakly with lower disease activity.
- Maternal IFX concentrations may be maintained at a constant level at a de-intensified therapeutic regimen in the second and third trimesters via a therapeutic drug monitoring guided-dose adjustments.

Introduction

Infliximab (IFX) therapy during pregnancy in patients with inflammatory bowel disease (IBD) is challenged by a dilemma between maintaining adequate maternal disease control and at the same time minimizing fetal IFX exposure. IFX is a monoclonal immunoglobulin (Ig) G1 antibody (Ab) and, along with endogenous IgG molecules, is actively transported from maternal to fetal circulation via placental neonatal Fc receptors (FcRn) expressed by syncytiotrophoblasts.^{1–3} This natural maternal-fetal transfer of immunoglobulins gives immunological support to the newborn and occurs with increasing efficiency over the pregnancy due to the upregulation of placental FcRn expression.^{4,5} As a result, IFX concentrations in infants, whose mothers have been exposed to IFX during pregnancy, are often supra-maternal and IFX can be detected for up to 1 year postpartum.^{6,7} IFX exposure of the fetus and newborn have not been associated with severe adverse outcomes for the child, and reported associations with lower birth weight, shorter gestational term, and increased risk of delivery by cesarean section may have been attributable to confounding by disease activity.^{8–12} However, pharmacological use during pregnancy is often done carefully and with extra safety precautions. Current European guidelines advocate pausing IFX in the third trimester whereas North

American guidelines recommend pausing in the last 6–10 weeks prior to delivery.^{13,14} Keeping this in mind, clinicians may refrain from administering IFX in the last part of pregnancy to reduce fetal IFX exposure. This proof-of-concept study aimed to elucidate, and subsequently quantify, potential effects of pregnancy per se on the pharmacokinetics (PK) of IFX in patients with IBD.

Methods

Study design

This was a retrospective study including IBD patients, irrespective of disease activity status, who had all received IFX therapy during pregnancy until 2018 at two tertiary IBD centers (Copenhagen University Hospital Herlev, Denmark, and Sheba Medical Center, Tel Aviv University, Israel). Included patients were required to have at least one bio-banked trough (C_{\min}) blood sample obtained during each pregnancy available for analysis. As part of the standard of care, patients had been evaluated by disease activity scorings (Harvey-Bradshaw Index (HBI) for Crohn's disease and Simple Clinical Colitis Activity Index or partial Mayo Score for ulcerative colitis), and with storage of trough blood samples drawn immediately prior to IFX infusions. As part of this study, IFX concentrations and

presence or absence of anti-IFX Abs were measured in all available bio-banked samples obtained while on IFX therapy during and before and/or after pregnancy in the same patients. All patients received steady IFX maintenance therapy at the time of conception (5 mg/kg q8w $n = 17$; q6w $n = 4$; q10w $n = 1$; 10 mg/kg q8w $n = 1$). The dosing regimen was not adjusted during pregnancy and all patients thus continued to receive IFX dosing based on their pre-pregnancy body weight.

IFX and anti-IFX Ab analyses

IFX concentrations and anti-IFX Abs were measured in bio-banked trough serum samples, which had been stored at -80°C . IFX was measured using a time-resolved fluorometric assay performed on the automated dissociation-enhanced lanthanide fluorescent immunoassay platform (AutoDELFIA; PerkinElmer, Turku, FIN), and with limit of detection (LOD) of $0.1 \mu\text{g/mL}$.¹⁵ Samples with IFX $\leq 5 \mu\text{g/mL}$ were assessed for anti-IFX Abs using an automated inhibition assay on the AutoDELFIA platform and with LOD 15 arbitrary units/L.¹⁵ All analyses were done simultaneously and blinded (Department of Medical Biochemistry, Oslo, Norway).

IFX PK model development and effects of covariates

Circulating IFX, anti-IFX Abs, and clinical data were analyzed using the population approach (i.e., nonlinear mixed-effects modelling) to quantify structural PK parameters (clearance (CL), volume of distribution (V_D), interpatient variabilities in PK parameters), and the impact of patient, pregnancy, and therapy-related factors on these PK parameters using the software programs NONMEM[®] (version 7.3, ICON, IRL), PsN (version 4.7.0), R (version 3.3), and RStudio (version 1.1.447).¹⁶ Before PK model development, statistical (Wilcoxon test) and graphical analyses were performed. For the purpose of modelling, IFX data were log transformed. Samples with IFX $< \text{LOD}$ were excluded (10% of samples).¹⁷ The model development strategy comprised the following steps:

1. Based on pre-pregnancy data, a fundamental PK model structure explaining the general IFX concentration-time profile (PK model I) was established, whereby PK parameters such as CL, V_D , and the impact of anti-IFX Abs as well as interpatient variability in PK were determined. In addition, pre-selected covariates (e.g., body weight, concomitant therapies, disease type, serum albumin concentration, thrombocyte count, and white blood cell count) were investigated for impact on CL, by

means of investigation of each single covariate separately and via forward addition. This approach allowed characterization of the PK in the population without a potential interference of pregnancy, so any potential effect of pregnancy could be investigated in the next step, and by using the totality of the data.

2. The PK model I was subsequently applied to the entire dataset (PK model II), and effects of pregnancy/trimester on PK model parameters was investigated as a covariate. In this step, the previously determined PK parameters were fixed, making the assumption that any differences in PK during/post pregnancy were due to pregnancy itself—an assumption deemed valid considering no dosing or other therapy-related adjustments had been made during pregnancy.
3. Based on the data availability (range of covariate values or number of patients per covariate category) and graphical and statistical analyses, re-assessment of potential effects of the pre-selected other covariates was performed. The effects of these on IFX PK were investigated by implementing them into the PK model II.
4. The final PK model II was applied to illustrate effects of pregnancy and anti-IFX Abs on the PK of IFX during pregnancy by model simulations, as detailed in the Supplementary Material.

Statistics

Descriptive data are presented as percentages for discrete variables, and for continuous variables as medians with ranges or mean with standard error of the mean (SEM). Maternal disease activity was reported as all available clinical disease activity scores recorded in each patient during ongoing IFX therapy from up to 1 year prior to conception and up to 1 year after delivery, and analyzed by non-paired analyses by Welch's unequal variances t -test. Dose-normalized IFX concentrations were used to adjust for body weight changes of the administered doses in the pregnancy (unit of IFX concentration: $\mu\text{g/mL/kg}$). Values $< \text{LOD}$ were set to zero. Missing data were excluded. As this was a mechanistic and exploratory proof-of-concept study and there are no relevant data available in this vulnerable population from other studies available at the time of study, formal sample size calculations had not been carried out. PK model simulations are detailed in the Supplementary Material. Basic statistical analyses were carried out in GraphPad Prism version 5 for Windows (GraphPad Software, CA, USA). Two-sided p values < 0.05 were considered significant.

Table 1. Characteristics of the study population.

Patient characteristics	
Diagnosis, <i>n</i> (%)	
Crohn's disease	14 (74)
Ulcerative colitis	5 (26)
Disease duration at IFX initiation (years), median (IQR)	6 (2–9)
Crohn's disease location, <i>n</i> (%)	
Ileal	0 (0)
Colonic	6 (43)
Ileocolonic	8 (57)
Isolated upper disease	0 (0)
Crohn's disease behavior, <i>n</i> (%)	
Non-stricturing, non-penetrating	5 (36)
Stricturing	4 (29)
Penetrating	5 (36)
Crohn's disease perianal disease, <i>n</i> (%)	6 (43)
Ulcerative colitis extent, <i>n</i> (%)	
Proctitis	0 (0)
Left sided	1 (20)
Extensive	4 (80)
Previous abdominal surgery, <i>n</i> (%)	3 (16)
Smoking, <i>n</i> (%)	0 (0)
Age at conception (years), median (IQR)	31 (27–34)
Clinical disease activity at last clinical visit before conception ^a	
Harvey-Bradshaw Index, median (IQR)	3 (2–5)
Simple Clinical Colitis Activity Index, median (IQR)	2.5 (0.0–5.5)
Number of pregnancies per patient, <i>n</i> (%)	
One pregnancy	16 (84)
Two pregnancies	2 (11)
Three pregnancies	1 (5)
IFX therapy during pregnancy, <i>n</i> (%)	
First trimester IFX therapy	23 (100)
Second trimester IFX therapy	20 (87)
Third trimester IFX therapy	7 (30)
Concomitant therapy during pregnancy, <i>n</i> (%)	
Thiopurines	3 (15)
Steroids systemic	1 (5)
Blood sample characteristics	
Trimester, <i>n</i> (%)	
Pre-pregnancy	119 (69)
First	16 (9)
Second	18 (11)
Third	7 (4)
Post-pregnancy	12 (7)
Anti-IFX Ab positive, <i>n</i> (%)	41 (30)
Albumin concentration (g/L), median (min-max)	37 (27–44)
C-reactive protein (mg/dL), median (min-max)	2.5 (0–128)
Thrombocyte count (10^9 cells/L), median (min-max)	349 (217–1283)
White blood cell count (10^9 cells/L), median (min-max)	5 (3.5–22)

^a<3 months from conception (median 26 days, IQR 5–52)

IFX: infliximab; Abs: antibodies; IQR: interquartile range.

Results

Study population

The study population comprised 23 pregnancies from 19 women (Table 1). Of these, 20 pregnancies resulted in healthy children assessed at 1 year after delivery, two pregnancies resulted in miscarriages, and one child was born with congenital abnormality (cleft soft palate and impaired intrauterine growth (2692 g)). Most patients were in clinical remission at conception of pregnancy (17 of 23; 74%) and most paused IFX therapy in the third trimester (16 of 23; 70%) (Table 1).

A total of 172 samples was available for PK analysis (Table 1). Samples were obtained prior to pregnancy ($n = 119$), in the first trimester ($n = 16$), second trimester ($n = 18$), third trimester ($n = 7$), or post-pregnancy ($n = 12$). The timing of sampling after the last IFX dosing covered a wide time interval as samples originated from both the induction and maintenance phases and from patients who received different dosing intervals (Figure 1(a) and (b)).

Maintenance phase IFX before, during, and after pregnancy

The graphical and statistical analysis revealed that samples obtained during pregnancy had significantly higher dose-normalized IFX concentrations compared to samples obtained from non-pregnancy periods (Figure 1(c)). Furthermore, anti-IFX Ab-positive samples had significantly lower dose-normalized IFX trough concentrations as compared to anti-IFX Ab-negative samples (Figure 1(d)). The frequency of anti-IFX Ab detection was similar ($p > 0.5$) in periods with or without pregnancy, indicating pregnancy is neither preventive nor predisposing to anti-IFX Ab development.

Maintenance phase IFX during trimesters of pregnancy

Having found that dose-normalized IFX concentrations increased during pregnancy, we next explored IFX concentrations during different trimesters (Figure 1(e)). Dose-normalized IFX was higher during the second trimester (median 15.0 $\mu\text{g}/\text{mL}/\text{kg}$, interquartile range (IQR) 9.8–20.5) compared to pre-

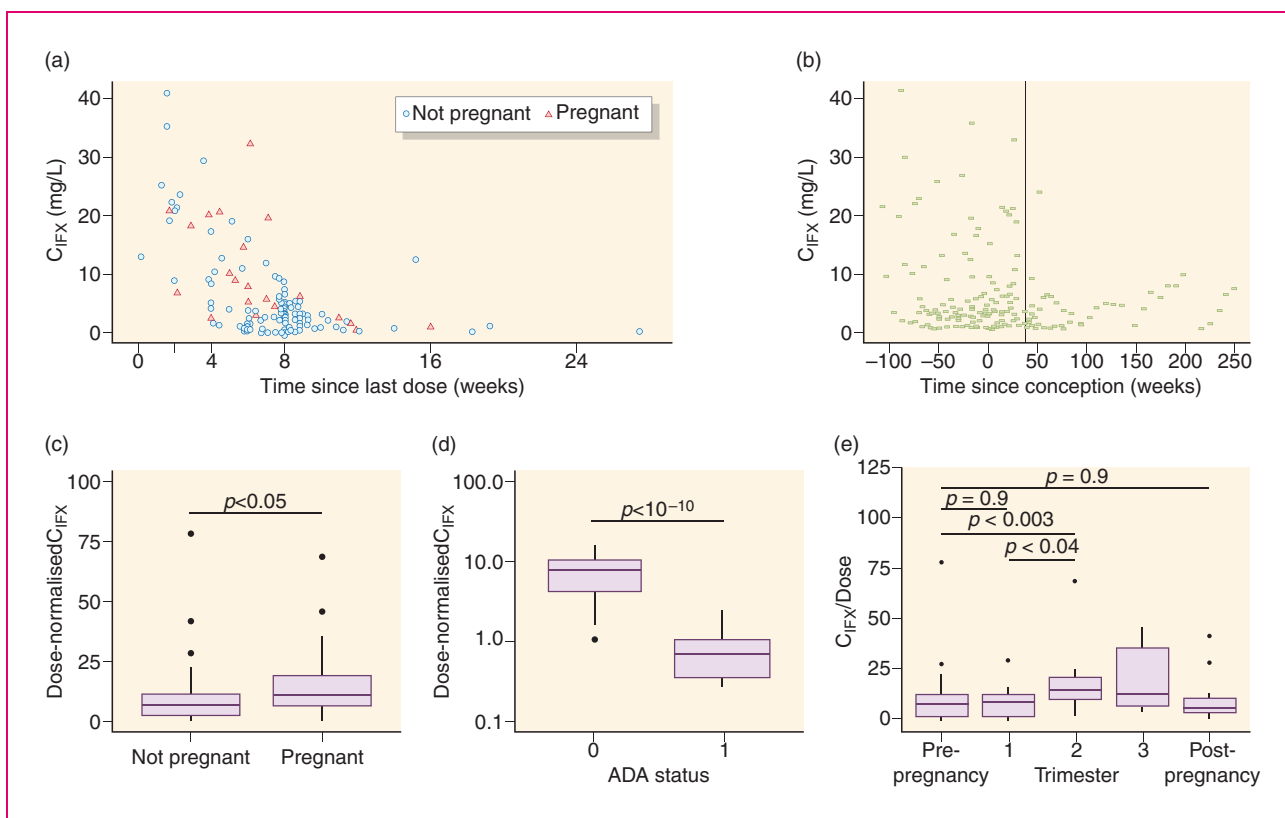


Figure 1. Exploratory graphical analysis of concentration of infliximab (IFX) (C_{IFX}) over time (a) since last dose, and (b) since conception. Effect of pregnancy and anti-IFX Ab (ADA) status on IFX exposure for dose-normalized maintenance phase IFX concentrations (C_{IFX}) (c) per pregnancy status, (d) per ADA status with 0 representing ADA- and 1 ADA+ samples, and (e) per trimester.

Table 2. Final pharmacokinetic model parameters.

Clearance, L/d (RSE%)	0.608 ^a (16) ^b
Volume of distribution, L (RSE%)	18.2 ^a (23) ^b
Effect of anti-IFX Abs on clearance ^c (RSE%)	0.685 ^a (24) ^b
Effect of second/third trimester on clearance ^c (RSE%)	-0.121 (56)
Interpatient variability in clearance, CV% (RSE%) (Shrinkage)	30.7 (28) (23)
Interpatient variability in volume of distribution, CV% (RSE%) (Shrinkage)	53.3 (30) (23)
Residual unexplained variability, µg/mL (RSE%) (Shrinkage)	0.371 (13) (6)

^aParameter value fixed to the final estimate from PK model I.

^bRSE from PK model I.

^cThe covariate effects on clearance were defined as: $CL = CL_{\text{typical}} * (1 + \text{effect of anti-IFX Abs on clearance}) * (1 + \text{effect of second/third trimester on clearance})$.

Abs: antibodies; CV: coefficient of variation; IFX: infliximab; RSE: relative standard error.

pregnancy (7.3, 2.0–11.6; $p = 0.003$), the first trimester (8.5, 1.4–11.5; $p = 0.04$), or post-pregnancy (5.9, IQR 3.3–11.1; $p > 0.05$). Similar trends were observed for the third trimester (13.0, 6.5–35.8; $p > 0.05$ compared to pre-pregnancy) despite the limited sample size. IFX concentrations were similar in pre- and post-pregnancy samples and first trimester samples ($p = 0.9$ and $p = 0.9$, respectively). These observations raised the question of whether IFX CL is decreased in the second and third trimesters, resulting in higher circulating IFX concentrations compared to the first trimester or periods without pregnancy.

Population PK modelling

Effects of pregnancy on IFX PK. The PK model I comprised one compartment with linear elimination. All parameters were estimated with high precision (relative standard error (RSE) <35%) and low shrinkage (<35%). The volume of distribution was 18.2 L and CL was 0.608 L/d with moderate interpatient variabilities of 51.2% and 40.7% coefficient of variation (CV), respectively (Table 2). None of the investigated covariates had significant impact on CL, and no covariates except anti-IFX Abs were thus maintained in PK model I.

As indicated by the observations above, PK modelling utilizing the entire dataset (PK model II) clearly demonstrated that IFX CL was significantly decreased by 12% in combined second to third trimesters of pregnancy compared to the first trimester, pre-, and post-pregnancy levels. Due to the low number of samples from the third trimester, the second and third trimester samples were initially combined. However, when

analyzing data from the second and third trimesters separately, IFX CL was found to additionally decrease in the third trimester to a final decrease of 15%. These trimester-specific effects were estimated with high imprecision (RSE > 50%), presumably due to the low number of samples available from the third trimester. The model did not detect changes in V_D in addition to the changes in CL over the pregnancy.

Effects of other variables on IFX PK. In addition to pregnancy status and trimester of pregnancy, anti-IFX Abs strongly influenced the PK of IFX. Hence, anti-IFX Abs detected in 30% of samples markedly increased IFX CL by 69% (Table 2).

Based on mechanistic plausibility, available patient and therapy-associated data (Table 1), and graphical and statistical analyses, further effects of selected covariates on IFX CL were explored; for example, body weight, concomitant therapies, disease type, serum albumin concentration, thrombocyte count, and white blood cell count. None of these factors influenced the PK of IFX (all $p > 0.1$). Thus, PK model II was considered the final PK population model. This final PK model described well both the typical PK profile and interpatient variability in PK, and it performed well in predicting the observed data as the 90% confidence intervals of the simulation range (the grey area in Figure 2) covered the observations, and with adequate matching of the corresponding 5th, median, and 95th percentile lines of observed and model-simulated data (Figure 2).

Disease activity

Having shown that IFX CL significantly decreases in the second and third trimesters of pregnancy and is accompanied by increased maternal IFX exposure, we next explored how these altered pharmacological conditions correlated with maternal disease activity. As illustrated in Figure 3(a), clinical disease activity in patients with Crohn's disease tended to decrease during pregnancy starting from the first trimester (HBI mean 2.8 (1.6–4.1), $p = 0.02$) and lasting throughout the second (3.7 (2.5–5.0) $p = 0.22$) and third trimesters (4.1 (1.7–6.6), $p = 0.60$), compared to pre-pregnancy activity (4.8 (3.6–5.9)). Following delivery, disease activity tended to increase in the first 3 months (6.5 (3.9–9.2), $p = 0.20$), after which it returned to pre-pregnancy scores (4.2 (3.0–5.4), $p = 0.46$). Similar trends were observed in the small number of patients with ulcerative colitis (Figure 3(b)).

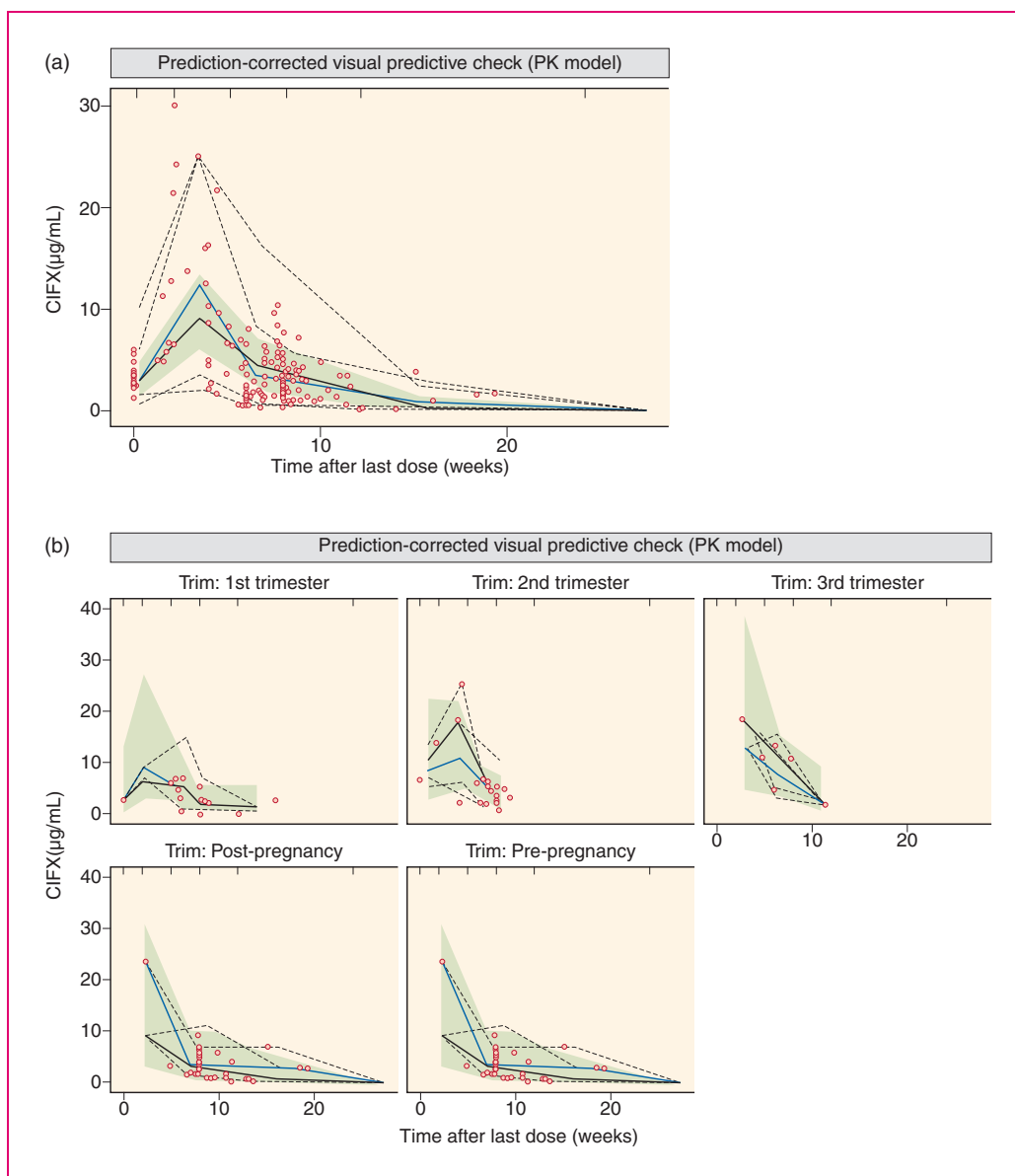


Figure 2. Prediction-corrected visual predictive check for the final pharmacokinetic (PK) model for all data (a) and per (non) pregnancy phase (b). Full lines are median and dashed lines are the fifth and 95th percentile of observations (black lines) and simulations (grey lines); the grey area denotes the 90% confidence interval around the median of the simulated data; dots denote observations.

PK model simulations

Lastly, we explored the extent to which the increased maternal IFX exposure arising from decreased IFX CL in the second and third trimesters counteracted the decline in IFX trough concentrations caused by pausing IFX throughout the entire third trimester, applied as a precautionary measure. Thence, in a separate exploratory analysis utilizing the final population PK model II, we simulated the theoretical effects of pausing IFX in the entire third trimester on the proportion attaining pre-defined IFX PK targets as points of reference (Figure

4). For simulation purposes, ‘standard’ patients treated with ‘standard’ IFX regimens were applied as detailed in the Supplementary Material. As shown in Table 3, pausing IFX in the third trimester in anti-IFX Ab-negative patients resulted in a notable reduction of the proportion of patients attaining the PK targets as compared to steady-state non-pregnant patients or patients having continued IFX treatments during the third trimester. However, only a small proportion of anti-IFX Ab-positive patients attained the PK targets irrespective of scenario, illustrating the profound negative effects of anti-IFX Abs on circulating IFX.

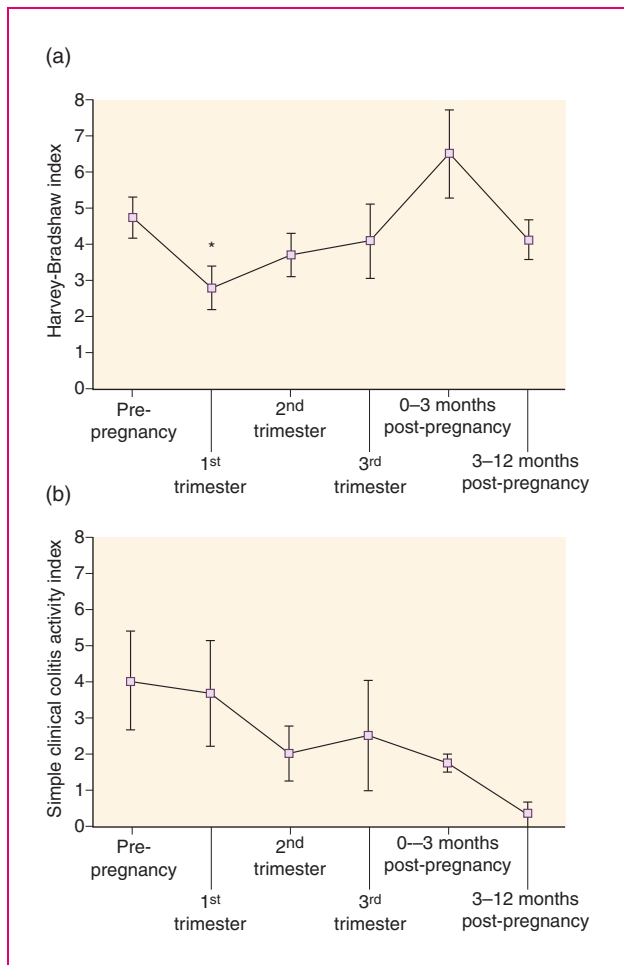


Figure 3. Clinical disease activity during ongoing infliximab (IFX) therapy from 1 year prior to pregnancy until 1 year after delivery in patients with (a) Crohn's disease ($n=15$ pregnancies) or (b) ulcerative colitis ($n=5$ pregnancies). Shown are mean with SEM. * $p<0.05$ as compared to pre-pregnancy.

Discussion

This is the first quantitative assessment using state-of-the-art population PK modelling of the effects of pregnancy on the PK of any monoclonal therapeutic Ab. In this proof-of-concept study, IFX CL was found to significantly decrease by 12% during the second and third trimesters of pregnancy in patients with IBD, and with a trend of additional decrease from the second to third trimester to a final of 15%. Maternal IFX exposure was influenced only by pregnancy and anti-IFX Abs (increasing IFX CL by 69%), and not by other patient-, disease-, or pregnancy-related characteristics including changes in body weight, V_D , or albumin. Our findings imply that pregnant IBD patients in the second and third trimesters have higher circulating IFX trough concentrations than in non-pregnant periods or the first trimester. Apart from effects on tumor necrosis

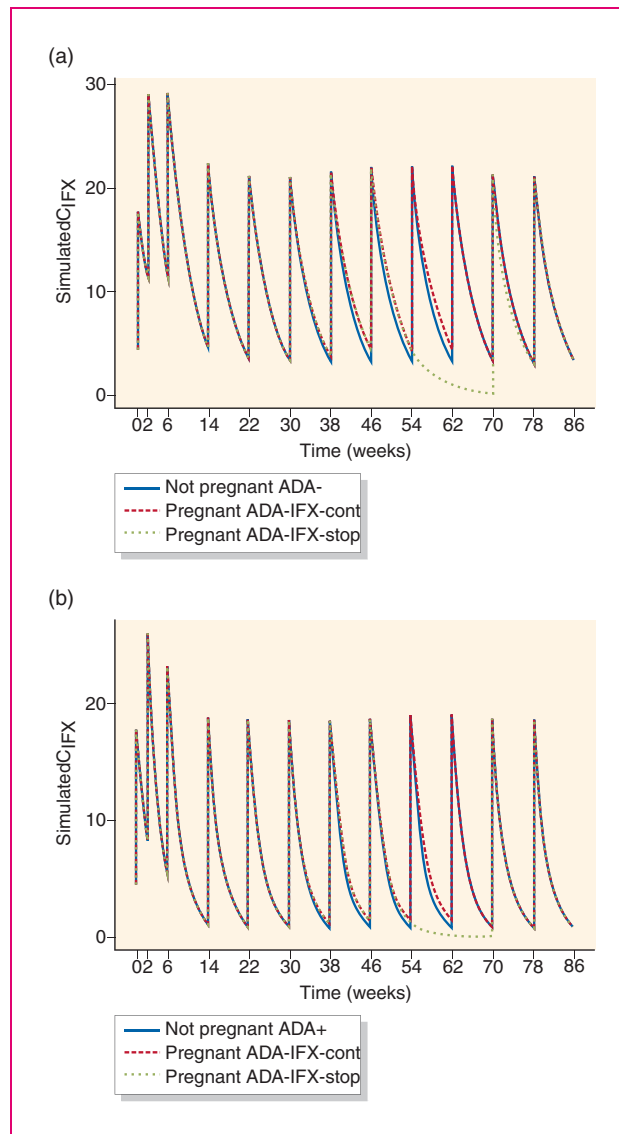


Figure 4. Pharmacokinetic (PK) model simulations of the impact of pregnancy, continuation of infliximab (IFX) in the third trimester, and anti-IFX antibodies on IFX concentration (C_{IFX})-time profiles for women for typical induction and maintenance IFX therapy (5 mg/kg, 65 kg body weight) in absence of pregnancy, and during pregnancy with discontinuation of IFX therapy in the third trimester, i.e., weeks 48–62 (IFX-stop) or without discontinuation (IFX-cont) (a) without anti-IFX antibody formation (ADA-) and (b) with anti-IFX antibody formation (ADA+). Time of conception was set to week 22 and time of delivery was week 62.

factor (TNF)-related processes in the fetus, the altered IFX CL during pregnancy may also have maternal implications as well as consequences for the maternal-fetal transfer of IFX, but these aspects were not examined.

Available observations have not indicated serious safety signals for anti-TNF therapies during

Table 3. Pharmacokinetic (PK) model simulations of attainment of PK targets of trough infliximab (IFX) concentrations of >3 µg/mL, >4 µg/mL, or >5 µg/mL for anti-IFX antibody negative (ADA-) or positive (ADA+) patients in case of safety pausing IFX therapy in the entire third trimester of pregnancy (IFX-stop); continuation of steady IFX maintenance therapy in the third trimester of pregnancy (IFX cont.); and non-pregnant patients receiving standard IFX maintenance therapy.

	Pregnant, IFX-stop in third trimester	Pregnant, IFX cont. in third trimester	Non-pregnant patients
ADA-	%n _{>3µg/mL} = 30	%n _{>3µg/mL} = 65	%n _{>3µg/mL} = 51
	%n _{4µg/mL} = 19	%n _{>4µg/mL} = 52	%n _{>4µg/mL} = 39
	%n _{>5µg/mL} = 11	%n _{>5µg/mL} = 41	%n _{>5µg/mL} = 28
ADA+	%n _{>3µg/mL} = 3	%n _{>3µg/mL} = 17	%n _{>3µg/mL} = 11
	%n _{>4µg/mL} = 1	%n _{>4µg/mL} = 9	%n _{>4µg/mL} = 5
	%n _{>5µg/mL} = 1	%n _{>5µg/mL} = 3	%n _{>5µg/mL} = 2

pregnancy, but clinicians nevertheless sometimes pause IFX therapy in the third trimester as an extra precaution to diminish fetal IFX exposure and as suggested by European guidelines.^{13,14} Hence, prospective cohort studies have demonstrated an inverse correlation between time from last IFX dose and IFX concentration in the umbilical cord, an infant-to-mother IFX concentration ratio of approximately 2, and a median time to complete infant IFX CL of ~7 months.^{6,18} A study used non-normalized raw IFX concentrations without PK modelling and indicated increased IFX levels over the pregnancy.¹⁹ Having determined that IFX CL decreases significantly in the second and third trimesters by up to 15%, we wanted to explore the relative impact of this effect on the ability to maintain IFX PK targets of >3–5 µg/mL if IFX therapy was paused throughout the entire third trimester.¹⁹ Even though these results should be interpreted with care as they originate from PK model simulations, they indicate the increased maternal IFX trough concentrations imposed by pregnancy will not completely counteract the decrease in IFX concentration if therapy is paused in the third trimester. Hence, if a constant maternal IFX concentration until the end of pregnancy is desired, dosing in the late second trimester or early third trimester is necessary. It is unknown whether a short period of sub-therapeutic IFX in the last part of pregnancy imposed by pausing therapy in the third trimester has clinical implications in form of increased risk of disease flare or anti-IFX Ab formation.^{8,11} A recent study indicated more steroid usage and a higher risk of preterm pregnancies when IFX was discontinued in the first or second trimesters.²⁰ Of note, the absolute decrease in IFX levels if therapy is paused in the second and third trimester will be lower than at a drug holiday of similar duration in non-pregnant

patients due to the decreased IFX CL. If IFX is continued in the last part of pregnancy, therapeutic drug monitoring can aid balancing a de-intensified dose regimen that secures a constant maternal drug level and thus avoids increasing IFX exposure of the fetus.

This study was not designed to examine the underlying mechanisms for the observed decrease in IFX CL during pregnancy. However, despite well-known changes in body composition, immunological state, and albumin concentrations, which could impact the PK of IFX during pregnancy, along with our study and another study indicated no influence of body weight, concomitant therapies, disease type, albumin, platelets, or leukocytes on maternal IFX CL.¹⁹

Our study has limitations. The cohort was relatively small and comprised mainly Crohn’s disease patients in clinical remission receiving steady IFX q8w maintenance therapy at pregnancy conception. The sample size was limited, especially during the third trimester, and only seven patients had samples available from pre-pregnancy, pregnancy, and post-pregnancy, implicating potential imprecision in the estimated PK differences between the second and third trimesters. Thus, our findings, especially for the third trimester, should be interpreted with care. However, nonlinear mixed-effects population PK modelling was used as this is a highly versatile approach when a sample size is low. This method analyses all data points simultaneously and allows describing the central tendency (“typical behavior”) in the population, as well as individual PK parameters/profiles by quantifying in addition to the central tendency the between- and within-patient variability. Clinical disease activity can be challenging to evaluate during pregnancy, and we did not have systematic endoscopic data obtained shortly prior to conception (median 289 days, IQR 224–492). Furthermore, the correlation between decreased IFX CL and lowered disease activity during pregnancy was weak and not matched to individual patients. Although only trough samples were included, availability of samples from both induction and maintenance phase, and different dosing regimens, rendered the data to be sufficiently informative for population PK modelling. The lack of detection of changes in V_D in addition to changes in CL is likely caused by the limited sample size combined with IFX predominantly being distributed in the circulation, which only increases to a small extent over the pregnancy. The latter is also most likely the explanation of our data being described by a one-compartment model, and others have also found this model appropriate.^{21–24} Of note, we used dose-normalized IFX concentrations to adjust for any changes in bodyweight. As the therapeutic threshold for IFX is not well defined, we included simulations of PK targets of 3–5 µg/mL.^{25–27} This study

investigated maternal implications of IFX therapy during pregnancy, and PK in the fetus or infant was not explored. Further studies on the effect of pregnancy on the kinetics of other biologics are warranted.

In conclusion, maternal IFX CL decreases significantly during the second and third trimesters, leading to increased maternal-fetal IFX trough levels at a constant therapeutic regimen. Therapeutic drug monitoring can aid balancing a de-intensified IFX regimen that secures constant maternal drug levels during pregnancy and at the same time avoids increasing IFX exposure of the fetus.

Note

The abstract was presented as a lecture presentation during Digestive Disease Week in San Diego, CA, 18–21 May 2019, *Gastroenterology* 156(6): Suppl 1:S–18.

Acknowledgements

The authors thank Professor Klaus Bendtzen for intellectual input and Rolf A Klaasen for technical assistance.

Author contributions

JB and CS conceptualized the study. MDR, BU, and JFI collected data. NB and DJW were responsible for IFX and anti-IFX Ab analyses. AMG, MDR, CS, and CK conducted and thoroughly discussed data analysis. CK and WH provided methodological support. AMG, MDR, and CS drafted the manuscript. All authors were involved in interpretation of results and critical revision of the manuscript. All authors approved the final version of the manuscript.

Conflicts of interest

Bella Ungar: consultation/lecturer fees from Takeda, Janssen, Neopharm and Abbvie. Nils Bolstad: speaker/consulting honoraria from Pfizer, Orion Pharma, Napp Pharmaceuticals, Takeda, Roche, Janssen, Novartis. Wilhelm Huisinga: grants from an industry consortium (AbbVie Deutschland GmbH & Co. KG, Boehringer Ingelheim Pharma GmbH & Co. KG, Grünenthal GmbH, F. Hoffmann-La Roche Ltd, Merck KGaA and SANOFI) supporting the PharMetrx PhD Program (www.pharmetrx.de). Shomron Ben-Horin: consulting and advisory board fees and/or research support from AbbVie, MSD, Janssen, Takeda and CellTrion. Jørn Brynskov: consultation and lecturer fees from Abbvie, Pfizer, Takeda, MSD, Janssen. Charlotte Kloft: grants from an industry consortium (AbbVie Deutschland GmbH & Co. KG, Boehringer Ingelheim Pharma GmbH & Co. KG, Grünenthal GmbH, F. Hoffmann-La Roche Ltd, Merck KGaA and SANOFI) supporting the PharMetrx PhD Program (www.pharmetrx.de), Diurnal Ltd and the Innovative Medicines Initiative-Joint Undertaking. Maria Dorn-Rasmussen, Ana-Marija Grišić, Johan F Ilvemark, David J Warren, Mark A

Ainsworth, and Casper Steenholdt have no interests to declare.

Ethics approval

The study was approved by the Danish Data Protection Agency (HGH-2016-008-04409) and The Regional Ethics Committee of Region Hovedstaden, Denmark (2012-58-0004; 4/2/2016), and by Sheba Medical Center Ethics Committee (5598/08; 15/2/2016; written informed consent obtained). The study was done in accordance with the 1975 Declaration of Helsinki.

Funding

The authors disclosed receipt of the following financial support for the research, authorship, and/or publication of this article: This work was supported by the Internationalisation Fund, Institute for Clinical Medicine, Faculty of Health and Medical Sciences, University of Copenhagen.


Guarantor

CS.

Informed consent

Written informed consent was obtained.

ORCID iD

Casper Steenholdt  <https://orcid.org/0000-0003-3898-4212>

Supplemental material

Supplemental material for this article is available online.

References

1. Roopenian DC and Akilesh S. FcRn: The neonatal Fc receptor comes of age. *Nature Rev Immunol* 2007; 7: 715–725.
2. Martins JP, Kennedy PJ, Santos HA, et al. A comprehensive review of the neonatal Fc receptor and its application in drug delivery. *Pharmacol Therap* 2016; 161: 22–39.
3. Wilcox CR, Holder B and Jones CE. Factors Affecting the FcRn-mediated transplacental transfer of antibodies and implications for vaccination in pregnancy. *Front Immunol* 2017; 8: 1294–1294.
4. Kane SV and Acquah LA. Placental transport of immunoglobulins: A clinical review for gastroenterologists who prescribe therapeutic monoclonal antibodies to women during conception and pregnancy. *Am J Gastroenterol* 2009; 104: 228–233.
5. Zelinkova Z, de Haar C, de Ridder L, et al. High intra-uterine exposure to infliximab following maternal anti-TNF treatment during pregnancy. *Alimentary Pharmacol Therap* 2011; 33: 1053–1058.
6. Julsgaard M, Christensen LA, Gibson PR, et al. Concentrations of adalimumab and infliximab in mothers and newborns, and effects on infection. *Gastroenterol* 2016; 151: 110–119.

7. Steenholdt C, Al-Khalaf M, Ainsworth MA, et al. Therapeutic infliximab drug level in a child born to a woman with ulcerative colitis treated until gestation week 31. *J Crohn Colitis* 2012; 6: 358–361.
8. de Lima A, Zelinkova Z, van der Ent C, et al. Tailored anti-TNF therapy during pregnancy in patients with IBD: Maternal and fetal safety. *Gut* 2016; 65: 1261–1268.
9. Shihab Z, Yeomans ND and De Cruz P. Anti-Tumour Necrosis Factor α therapies and inflammatory bowel disease pregnancy outcomes: A meta-analysis. *J Crohn Colitis* 2016; 10: 979–988.
10. Lichtenstein GR, Feagan BG, Mahadevan U, et al. Pregnancy outcomes reported during the 13-year TREAT registry: A descriptive report. *Am J Gastroenterol* 2018; 113: 1678–1688.
11. Luu M, Benzenine E, Doret M, et al. Continuous Anti-TNF α use throughout pregnancy: Possible complications for the mother but not for the fetus: A retrospective cohort on the French National Health Insurance Database (EVASION). *Am J Gastroenterol* 2018; 113: 1669–1677.
12. Bröms G, Kieler H, Ekblom A, et al. Anti-TNF treatment during pregnancy and birth outcomes: A population-based study from Denmark, Finland, and Sweden. *Pharmacoepidemiol Drug Safety* 2020; 29: 316–327.
13. van der Woude CJ, Ardizzone S, Bengtson MB, et al. The second European evidenced-based consensus on reproduction and pregnancy in inflammatory bowel disease. *J Crohn Colitis* 2015; 9: 107–124.
14. Mahadevan U, Robinson C, Bernasko N, et al. Inflammatory bowel disease in pregnancy clinical care pathway: A report from the American Gastroenterological Association IBD parenthood project working group. *Gastroenterol* 2019; 156: 1508–1524.
15. Jorgensen KK, Olsen IC, Goll GL, et al. Switching from originator infliximab to biosimilar CT-P13 compared with maintained treatment with originator infliximab (NOR-SWITCH): A 52-week, randomised, double-blind, non-inferiority trial. *Lancet* 2017; 389: 2304–2316.
16. Mould DR and Upton RN. Basic concepts in population modeling, simulation, and model-based drug development-part 2: Introduction to pharmacokinetic modeling methods. *CPT Pharmacomet Systems Pharmacol* 2013; 2: e38–e38.
17. Xu XS, Dunne A, Kimko H, et al. Impact of low percentage of data below the quantification limit on parameter estimates of pharmacokinetic models. *J Pharmacokinet Pharmacodynam* 2011; 38: 423–432.
18. Mahadevan U, Wolf DC, Dubinsky M, et al. Placental transfer of anti-tumor necrosis factor agents in pregnant patients with inflammatory bowel disease. *Clin Gastroenterol Hepatol* 2013; 11: 286–e24.
19. Seow CH, Leung Y, Vande Casteele N, et al. The effects of pregnancy on the pharmacokinetics of infliximab and adalimumab in inflammatory bowel disease. *Alimentary Pharmacol Therap* 2017; 45: 1329–1338.
20. Truta B, Leeds IL, Canner JK, et al. Early discontinuation of infliximab in pregnant women with inflammatory bowel disease. *Inflamm Bowel Dis* 2020; 26: 1110–1117.
21. Ternant D, Berkane Z, Picon L, et al. Assessment of the influence of inflammation and FCGR3A genotype on infliximab pharmacokinetics and time to relapse in patients with Crohn's disease. *Clin Pharmacokinet* 2015; 54: 551–562.
22. Ternant D, Passot C, Aubourg A, et al. Model-based therapeutic drug monitoring of infliximab using a single serum trough concentration. *Clin Pharmacokinet* 2018; 57: 1173–1184.
23. Petitcollin A, Brochard C, Siproudhis L, et al. Pharmacokinetic parameters of infliximab influence the rate of relapse after de-escalation in adults with inflammatory bowel diseases. *Clin Pharmacol Ther* 2019; 106: 605–615.
24. Dreesen E, Faelens R, Van Assche G, et al. Optimising infliximab induction dosing for patients with ulcerative colitis. *Br J Clin Pharmacol* 2019; 85: 782–795.
25. Vande Casteele N, Herfarth H, Katz J, et al. American Gastroenterological Association Institute technical review on the role of therapeutic drug monitoring in the management of inflammatory bowel diseases. *Gastroenterol* 2017; 153: 835–857.e6.
26. Gibson DJ, Ward MG, Rentsch C, et al. Review article: Determination of the therapeutic range for therapeutic drug monitoring of adalimumab and infliximab in patients with inflammatory bowel disease. *Alimentary Pharmacol Therap* 2020; 51: 612–628.
27. Steenholdt C, Bendtzen K, Brynskov J, et al. Optimizing treatment with TNF inhibitors in inflammatory bowel disease by monitoring drug levels and antidrug antibodies. *Inflamm Bowel Dis* 2016; 22: 1999–2015.

Supplementary Methods

IFX PK model simulations

The final population PK model II was applied to illustrate effects of pregnancy and anti-IFX Abs on the PK of IFX during pregnancy by model simulations. First, PK profiles for typical patients were simulated. Then, PK profiles for 6,000 virtual patients differing in anti-IFX Ab status, pregnancy status, and (dis)continuation of IFX in the 3rd trimester were simulated, including interpatient variability in PK parameters. The virtual patients were assigned to be anti-IFX Ab negative (ADA-) or anti-IFX Ab positive (ADA+), IFX dosing was set to 325 mg (corresponding to a 5 mg/kg dosing of a standard patient of 65 kg), and the IFX regimen comprised standard induction (i.e., infusions at weeks (w) 0, 2, and 6) and maintenance therapy (infusions every (q) 8w). Date of conception was set to week 22 (corresponding to timing of 2nd maintenance IFX infusion). As the therapeutic threshold for IFX is not well defined, the percentage of patients reaching different pre-defined PK targets of >3, >4, and >5 µg/mL at week 62 of IFX therapy corresponding to end of pregnancy, was compared relative to anti-IFX Ab status, pregnancy status, and IFX administration in the 3rd trimester.

Acknowledgements

Acknowledgements are not included in the electronic version of the dissertation for reasons of data protection.

Curriculum Vitae

According to the EU General Data Protection Regulation (GDPR) the Curriculum Vitae has been removed from the electronic version of the dissertation.

